Impacts of Hydrological Alterations in the Mekong Basin to the Tonle Sap Ecosystem

---

A thesis submitted in partial fulfilment of the requirements for the Degree of Doctor of Philosophy in Civil Engineering

By Mauricio Eduardo Arias

Department of Civil and Natural Resources Engineering

University of Canterbury

Christchurch, New Zealand

2013

ACKNOWLEDGEMENTS

I must say that I have truly enjoyed every single day of my PhD, and this is for the most part a reflection of the great people who have supported me throughout this journey. Foremost, I would like to thank my senior supervisor, Tom Cochrane, for giving me the chance to adventure into this project and for providing the ideal level of supervision I always hoped for. I would also like to thank the other members of my supervisory committee, Brian Caruso, Matti Kummu, Tim Killeen, and David Norton, who were extremely supportive through the different stages of my PhD. Although they were not part of the committee, Taber Hand and Thanapon Piman became great advisors, hosts, and friends. I'm also truly thankful to those that helped me in the field, especially Puthea Khon, Nith Chum, and Sok. Thanks also to those collaborators whose ideas and models have contributed to this thesis, including Jorma Koponen, Gordon Holtgrieve, Vittoria Elliott, and Hannu Lauri.

This thesis could not have been possible without the institutional support I received both in New Zealand and Cambodia. I would like to thank those at the University of Canterbury who put out with me throughout these years, especially my officemates, technical and administrative staff, and researchers of the HydroEco group. Thanks to Conservation International staff who welcomed me as one of their team members every time I went to Cambodia; much of what I learned and saw of the country was thanks to them. I would also like to thank the Cambodian Ministry of the Environment staff who gave me access and guided me in the core areas of the Tonle Sap Biosphere Reserve. Thanks also to the water and soils labs at Research Development International for accommodating my laboratory needs in Cambodia.

Financial support came from the University of Canterbury's International Doctoral Scholarship and the Critical Ecosystems Partnership Fund grant entitled "River at Risk:

Modelling and monitoring the potential impacts from large-scale disruptions to the hydrological cycles of the Mekong River Basin".

To Mariana, who has been part of this journey since the beginning and who has been with me even during the longest of days in the field. I have been blessed to find you, and your companionship and love have definitely made these some of the greatest years of my life.

Last but not least, I am most thankful to my family for their love, constant encouragement and most sincere advice. The years and distance apart have only made us stronger. Los quiero mucho y muy bien saben que todo esto es gracias a ustedes y dedicado a ustedes.

I would like to especially dedicate this thesis to my grandmother, Lucia, who always offered me all her devotion –and laughs – to her very last breath. I know you are proud of me, Abue.

SUMMARY

The Tonle Sap is the largest and most important natural wetland in Southeast Asia. It covers an area of more than 15,000 km^2 with a unique mosaic of natural and agricultural floodplain habitats that coexist with the largest fishery in the Mekong Basin. Accelerating hydropower development and climate change, however, are altering the Mekong's hydrology, which could negatively affect downstream ecosystems.

The Tonle Sap is facing a two-fold problem. First, the link between its hydrology and ecosystem properties is not well understood. Second, potential ecological changes caused by future hydrological disruptions related to hydropower and climate change are unknown. Thus, the main objective of this thesis was to quantify how alterations to the Mekong hydrology could affect the Tonle Sap ecosystem. The following studies were performed to addressed the objective: (1) an assessment of landscape patterns using geographical information and remote sensing tools; (2) an assessment of habitat patterns based on field surveys of water, vegetation, and soils; (3) ecosystem function modelling to simulate net primary production (NPP) as a function of water quantity, sediments, and habitat type; and (4) fauna habitat modelling linking the results from the assessment of landscape patterns to fauna species.

The assessment of landscape patterns revealed a distinct relationship between inundation and vegetation. Habitats in the Tonle Sap were divided into five groups based on annual flood duration, as well as physiognomic factors and human activity: (1) open water, (2) gallery forest, (3) seasonally flooded habitats, (4) transitional habitats, and (5) rainfed habitats. Large habitat shifts could occur as a result of hydropower development scenarios by the 2030s; areas optimal for gallery forest could decrease by 82% from baseline conditions, whereas areas of rainfed habitats could increase by 10-13 % (813-1061 km^2).

The assessment of habitat patterns demonstrated that despite the complexity and intense human use of this ecosystem, the flood-pulse is the underlying driver of habitat characteristics by (1) determining inundation depth and duration; (2) creating the main soils gradient; (3) limiting the area cleared for agriculture; (4) influencing vegetation structure and water quality; and (5) shaping the composition of plant species.

The ecosystem function model was used to estimate a reduction of 9-39% in annual NPP caused by different scenarios of hydropower development and/or climate change during 2032-2042. Cumulative impacts from hydropower would disrupt NPP to a greater extent than climate change.

The fauna habitat model revealed that species richness was greatest in the gallery forests and seasonally flooded habitats. Animals that permanently reside in or that rely on these habitats to complete essential life-history stages would be the most affected by future changes.

This thesis provides the first quantitative formulation that directly links fundamental components of the Tonle Sap ecosystem to its flood-pulse hydrology. It also provides a comprehensive assessment of the impacts of expected hydrological alterations. Hydropower is expected to bring more abrupt and distinct ecological alterations than climate change in future decades. Relative aerial changes to the gallery forests are expected to be greater than in other habitats. A decline of the Tonle Sap's ecosystem services will occur if appropriate measures are not implemented. These measures include mitigating hydropower alterations, conserving natural habitats in areas that are likely to remain hydrologically undisturbed, restoring natural habitats in projected areas for optimal growth, and optimizing agricultural practices in the floodplain. Research findings from this thesis focused on the Tonle Sap, but given the fundamental commonalities between this system and other large floodplains, the information presented is highly informative to other large flood-pulse driven systems around the globe.

Deputy Vice-Chancellor's Office
Postgraduate Office

UNIVERSITY OF CANTERBURY
Te Whare Wānanga o Waitaha
CHRISTCHURCH NEW ZEALAND

Co-Authorship Form

This form is to accompany the submission of any thesis that contains research reported in co-authored work that has been published, accepted for publication, or submitted for publication. A copy of this form should be included for each co-authored work that is included in the thesis. Completed forms should be included at the front (after the thesis abstract) of each copy of the thesis submitted for examination and library deposit.

Please indicate the chapter/section/pages of this thesis that are extracted from co-authored work and provide details of the publication or submission from the extract comes:

Chapter 3:
Arias, M.E., Cochrane, T.A., Piman, T., Kummu, M., Caruso, B., Killeen, T.J. (2012) Quantifying changes in flooding and habitats in the Tonle Sap Lake (Cambodia) caused by water infrastructure development and climate change in the Mekong Basin. Journal of Environmental Management 112 53-66.

Chapter 4:
Arias, M.E., Cochrane, T.A., Norton, D., Killeen, T.J., Khon, P., The flood pulse as the underlying driver of vegetation in the largest wetland and fishery of the Mekong Basin. AMBIO 42 (7) 864-876.

Chapter 5:
Arias, M.E., Cochrane, T.A., Kummu, M., Lauri, H., Koponen, J., Holtgrieve, G.W., Piman, T. (2014) Impacts of hydropower and climate change on drivers of ecological productivity of Southeast Asia's most important wetland. Ecological Modelling 272C 252-263, DOI: 0.1016/j.ecolmodel.2013.10.015.

Chapter 6:
Arias, M.E., Cochrane, T.A., Elliott, V. Modelling future changes of habitat and fauna of the Tonle Sap wetland of the Mekong. Environmental Conservation DOI:10.1017/S0376892913000283.

Please detail the nature and extent (%) of contribution by the candidate:
The candidate developed methodologies (80%), carried out data collections (100%), data analyses (100%), and led manuscripts' writing (80%). Overall, the candidate's contribution was 90%. Co-authors were involved mainly when developing methodologies and proofreading manuscripts, with the exception of M. Kummu, H. Lauri, and G.W. Holtgrieve who also provided data used for the model presented in chapter 5.

Certification by Co-authors:
If there is more than one co-author then a single co-author can sign on behalf of all
The undersigned certifies that:

- The above statement correctly reflects the nature and extent of the PhD candidate's contribution to this co-authored work
- In cases where the candidate was the lead author of the co-authored work he or she wrote the text

Name: *Thomas A. Cochrane* Signature: 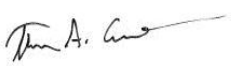 Date: 19/06/2013

LIST OF ACRONYMS

3D EIA: Three Dimensional Environmental Impact Assessment Model

ADB: Asian Development Bank

AGB: Above Ground Biomass

amsl: above mean sea level

ANOVA: Analysis of Variance

CCA: Canonical Corresponding Analysis

DBH: Diameter at Breast Height

DCA: Detrended Correspondence Analysis

DCCA: Detrended Correspondence Canonical Analysis

DEM: Digital Elevation Map

DO: Dissolved Oxygen

DSF: Decision Support Framework

ENSO: El Niño-Southern Oscillation

FAO: Food and Agricultural Organization

GCM: Global Circulation Model

GIS: Geographical Information System

HEC-ResSim: Hydrological Engineering Center Reservoir Simulation Model

IPCC: International Panel on Climate Change

IQQM: Integrated Quantity and Quality Model

ISIS: hydrodynamic model developed by HR Wallingford and Halcrow

JICA: Japanese International Cooperation Agency

LAI: Leaf Area Index

LULC: land use/land cover

MIKE: Water modelling software developed by the Danish Hydraulic Institute

MOWRAM: Cambodia Ministry of Water Resources and Meteorology

MRC: Mekong River Commission

NMS: Non-metric Multidimensional Scaling ordination method

NPP: Net Primary Production

PC: Principle Component

PCA: Principle Component Analysis

RDI: Research Development International-Cambodia

RUA: Royal University of Agriculture-Cambodia

SLURP: Land Use-based Runoff Processes

SRTM: Shuttle Rapid Topography Mission

SSC: Suspended Sediment Concentrations

SSD: Sum of Squares Differences

SWAT: Soil and Water Assessment Tool

TAMS: Tonle Area Management Scenarios

TP: Total Phosphorus

TSS: total suspended solids

UNESCO: United Nations Educational, Scientific and Cultural Organization

UTM: Universal Transverse Mercator geographic coordinate system

VIC: Variable Infiltration Capacity model

VMOD: Hydrological model developed by Environmental Impact Assessment Ltd.

WCD: World Commission on Dams

WGS: World Geodetic System

YHyM: University of Yamanashi distributed hydrological model

YSI: Yellow Springs Instrument Company of water quality sensors

TABLE OF CONTENTS

LIST OF FIGURES

LIST OF TABLES

CHAPTER 1: INTRODUCTION

1.1 Statement of Problem

The Tonle Sap Lake is regarded as "the Heart of Cambodia", an expression that goes far beyond its central location in the country. The Tonle Sap is the largest wetland in Southeast Asia, covering an area of 15,000 km^2 and storing a volume of 50-80 km^3 of water that flows from the Mekong River during the wet monsoon season via the world's largest freshwater flow reversal system (MRC, 2005). The annual flood-pulse in the Tonle Sap has shaped a unique mosaic of natural and agricultural floodplain habitats that was declared a UNESCO Biosphere Reserve – the only one of its kind in the country (UNESCO, 2010). These habitats coexist with the largest fishery in the Mekong, which provides most of the protein Cambodians consume. The dependency of Cambodia on the Tonle Sap dates back to the 9th to 15th centuries when the Khmer Empire dominated the region and established the largest preindustrial urban society supported by a complex agricultural and irrigation network (Day et al., 2012; Evans et al., 2007; Kummu, 2009). The hydrological, ecological, nutritional, and cultural value that the Tonle Sap provides to Cambodia is unquestionable, and it is arguably among the highest provided to a nation by a single natural system around the world.

Similarly, the Mekong River Basin – which drives the Tonle Sap's hydrology– is recognized internationally for its great value. The basin covers an area of 795,000 km^2, making it the largest in the Indo-Burma Peninsula and the 21st largest in the world (Costa-Cabral et al., 2007). The river travels nearly 4,800 km between the Tibetan Plateau in Yunnan Province (China) and the South of Vietnam (Figure 1.1), where an average of 475 $km^3\ yr^{-1}$ of water is discharged into the South China Sea (MRC, 2005). The Mekong ranks 12th and 8th among the largest rivers in the planet based on length and discharge, respectively (Costa-

Cabral et al., 2007). The basin is shared among six countries, of which Laos has the largest fraction (25%), followed by Thailand (23%), China (21%), Cambodia (20%), Vietnam (8%), and Myanmar (3%; MRC, 2005).

In addition to its physical and hydrological dimensions, the Mekong's cultural and biological resources are critical. The basin is home to more than 72 million people (Campbell, 2009), whose livelihoods and food security are primarily dependent upon the resources supported by the river (MRC, 2010a). The Mekong is part of one of the most significant hotspots in the planet because of the large number of endemic species and high fraction of remaining primary vegetation (Myers et al., 2000). Over 924 species of freshwater fishes have been recorded in the Mekong (Valbo-Jørgensen et al., 2009), a number that ranks the river as the world's 3rd most diverse after the Amazon and the Zaire rivers (Dudgeon, 2000). In terms of fisheries, the high annual fish catch (a rough estimate of 2.6 million tonnes in the Lower Mekong; Hortle, 2007) places the Mekong among the largest inland fisheries on the planet (Baran and Myschowoda, 2009).

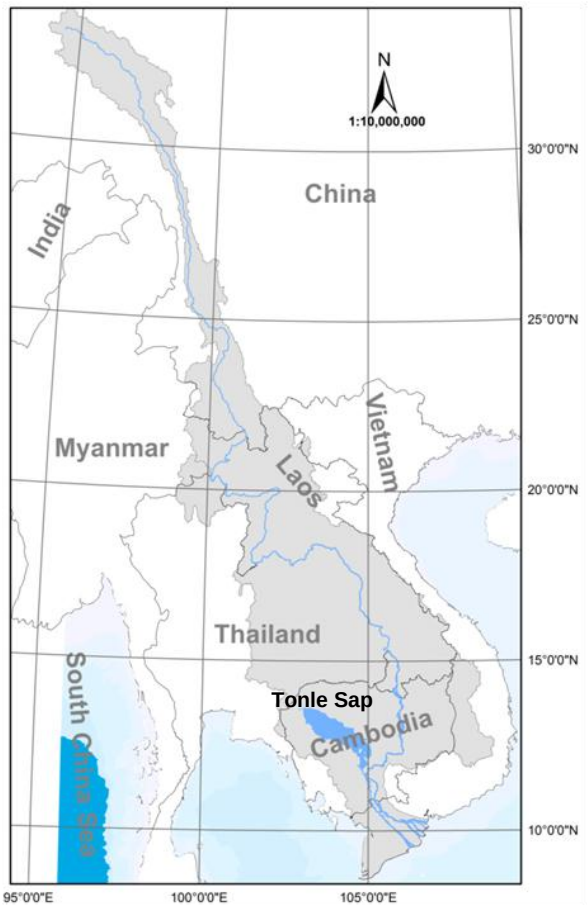

Figure 1.1. Overview map of the Mekong River Basin and the full inundation extent of the Tonle Sap.

As a result of civil conflict in the region, not much water infrastructure development took place in the Mekong until recent decades; nowadays, regional politics have become much more stable, the population and economies are growing, and energy demand is increasing. Hence, hydropower has become a very attractive electricity source for governments and private investors. Hydropower development in the Mekong has accelerated exponentially in the past decade, and once the proposed regional scheme is completed, the number of large hydropower projects could triple while the active storage could increase ten-fold (MRC, 2009; Kummu et al., 2010). In addition to hydropower, recent findings have demonstrated that the Mekong's climate has become more variable (Delgado et al., 2010; Räsänen et al., 2013), but despite multiple efforts to project future scenarios, additional impacts from climate change –besides accelerating ongoing disruptions– are still uncertain

(Kingston et al., 2011; Lauri et al., 2012). Even though these hydrological changes are not clear yet in the Tonle Sap, the escalating basin modifications will eventually bring significant disruptions to the Tonle Sap's flood-pulse in the upcoming decades (Kummu and Sarkkula, 2008; MRC, 2010; Västilä et al., 2010)

The Tonle Sap's surface hydrology and the flood-pulse phenomenon are well understood, but how the water cycle drives ecological structure and function has been poorly studied in situ, thus it has been hypothesized to function as in other large floodplains around the world. The Flood-Pulse Concept explains that the unimodal and predictable seasonal flood regime drives large floodplain ecosystems by selecting flood-tolerant species, controlling habitat quality, and driving nutrient cycles (Junk et al., 1989; Junk, 1997). Although this theory has been postulated based on observations in the Central Amazon floodplains, it has been suggested that the Flood-Pulse Concept could also explain the Tonle Sap's functioning despite the little scientific knowledge that has been published on this ecosystem (Kummu et al., 2006; Lamberts, 2006; Lamberts and Koponen, 2008). In order to fill this major research gap and test if the Flood-Pulse Concept actually applies to the Tonle Sap, it is crucial to first establish a quantitative relationship between flooding and vegetation characteristics.

The Tonle Sap is facing a two-fold problem: first, the link between the Tonle Sap's hydrology and ecosystem properties has not been established; second, the changes that the upcoming hydrological disruptions will bring to the Tonle Sap ecosystem are unknown. Given these two issues, an engineering approach aiming at *solving* these two problems simultaneously by applying science in a methodological way may prove to be a good strategy for the Tonle Sap.

1.2 Objectives

The main objective of this thesis was to quantify how alterations to the Mekong hydrology caused by hydropower and climate change will affect the Tonle Sap ecosystem. To answer this research question effectively, this thesis takes a holistic view and integrates multiple methodologies grouped into four components: (1) assessment of landscape patterns; (2) assessment of habitat patterns; (3) ecosystem function modelling; and (4) fauna habitat modelling. Each component has a distinct sub-objective, but results from some of the components served as feedback into the others to ultimately answer the main research question postulated (Figure 1.2). As a common approach, each of the components followed a two-step procedure: First, the historical/baseline relationship between hydrology and the ecosystem attribute was established. Second, this relationship was used to assess how future changes in the Mekong hydrology could alter the different aspects related to the Tonle Sap ecosystem.

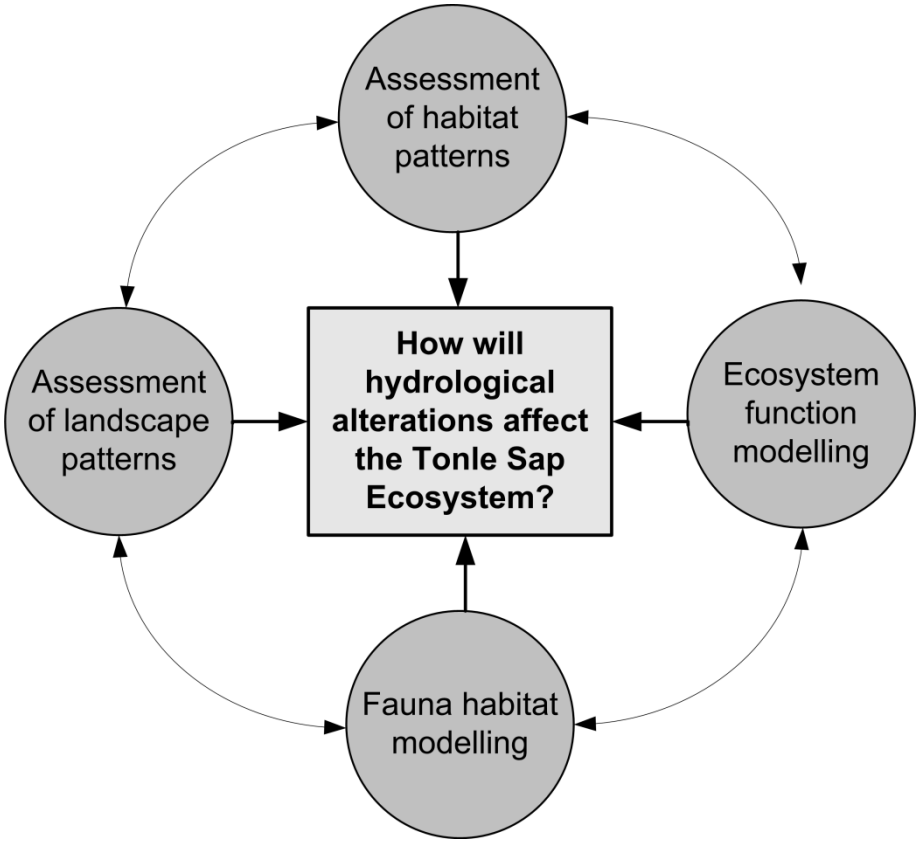

Figure 1.2. Four methodological approaches were used to address this thesis' research question. All components are interrelated and information derived from some of the components provided feedback into the others.

Assessment of landscape patterns: the objective of this component was to use geographical information and remote sensing tools to determine the landscape-scale relationship between inundation and vegetation and to assess how these patterns could shift in the future.

Assessment of habitat patterns: This component was conducted to characterize multiple field attributes of the Tonle Sap habitats –including vegetation, soils, and water quality – to establish a baseline relationship with local and landscape inundation patterns.

Ecosystem function modelling: this component used state-of-the-art numerical modelling in conjunction with information from the previous two components in order to quantify sedimentation and aquatic primary production as a function of environmental conditions and to project potential future changes.

Fauna habitat modelling: This component proposed a modelling framework to link the landscape-scale relationships from component (1) with information related to fauna habitat preference and usage, and thus providing a tool to quantify potential future changes in fauna.

1.3 Hypotheses

The research presented in this thesis lies upon two hypotheses that were explored through the different methodological components. The first hypothesis was that the Mekong's flood-pulse is the major driver of floodplain vegetation distribution and structure in the Tonle Sap. As it will be discussed in more detail in Chapter 2, observations in other large (sub-) tropical floodplains that experience unimodal annual flood pulses demonstrate a close relationship between spatial inundation patterns and vegetation, but up to date, no study has adequately tested this relationship for the Tonle Sap. This first hypothesis was verified through the landscape and the habitat assessments, in which remotely-sensed and field data were compared to historical and current inundation patterns.

The second hypothesis of this thesis was that modifications to the Mekong hydrology caused by hydropower and climate change could bring significant disruptions to the ecological structure and function of the Tonle Sap. The most obvious mechanism causing these disruptions is the reduction of the flood magnitude and the amount of sediments and nutrients delivered; nonetheless, there are other mechanisms that could be significant. For instance, disruptions may also result from shifts in the inner/outer edges of the floodplain that are likely to become permanently inundated/dry. Moreover, disruptions may occur as a result of spatial shifts in habitats, promoted by species likelihood to remain within the areas with a flood regime that they can tolerate. Although this second hypothesis cannot be verified empirically before hydrological alterations are evident, how hydrological alterations could modify the Tonle Sap ecosystem was demonstrated via modelling procedures in the landscape assessment, ecosystem function, and fauna components.

1.4 Thesis outline

Following the introduction, this thesis is divided into six chapters. Chapter 2 provides an overview of the scientific literature related to this study, starting with background information on the Tonle Sap hydrology and ecology, background on drivers of hydrological change (aka., hydropower and climate change), and a review of the methodologies used in this thesis. Chapter 3 describes the landscape assessment, in which GIS and remote sensing data were used to investigate large-scale patterns of inundation and vegetation. Chapter 4 describes the field studies that were carried out in order to establish relationships among habitat biophysical characteristics, including inundation patterns, water quality, vegetation, and soils. Chapter 5 describes the numerical modelling approach that was used to quantify sedimentation and primary productivity and their potential future changes. Chapter 6 presents a spatial modelling framework in which the information from the landscape assessment (Chapter 3) was linked to habitat-fauna relationships in order to quantify future impacts to fauna. Finally, Chapter 7 provides a summary of the thesis, the main conclusions, and a number of recommendations for future research and ecosystem management.

CHAPTER 2: BACKGROUND AND LITERATURE REVIEW

2.1 Introduction

This chapter describes essential background information on the Mekong and the Tonle Sap (sections 2.2-2.4), as well as relevant published literature associated with the main methodologies reported in this thesis (sections 2.5-2.7): landscape assessment using GIS and remote sensing tools, field assessment of floodplain habitat characteristics, and hydro-ecological modelling. Each of these three sections has two parts, one that describes published literature on tropical and subtropical floodplain wetlands, and a second one that describes the studies that have been carried out specifically in the Tonle Sap.

2.2 Hydrological features of the Tonle Sap

The Tonle Sap is a complex hydrological system, composed of a 2,600 km^2 permanent shallow lake, a 120 km long river (Tonle Sap River) that connects the lake to the Mekong, and a 12,876 km^2 floodplain covered with a mosaic of natural and agricultural habitats that the Mekong replenishes with water and sediments annually (Figure 2.1). The surface hydrology and flood-pulse in the Tonle Sap is driven by the Asian Monsoon regime, which brings approximately 65% of the total annual rainfall to the Mekong Basin between July and October (MRC, 2005). More than half of the annual flow into the Tonle Sap comes directly from the Mekong via the Tonle Sap River (53.5%), 34% from 11 tributaries in the Tonle Sap catchment, and 12.5% from rainfall precipitation (Kummu et al., 2013). During the dry season (October through May) the Tonle Sap River discharges a maximum of 11,345 $m^3 s^{-1}$ out from the lake towards the Mekong (Table 2.1). At the end of this period of "normal" flow, the lake reaches a minimum depth of less than 1.5 m and a surface water area less than 2,500 km^2. When the wet monsoon reaches the basin, the level of the Mekong River rises to a

higher level than the Tonle Sap, forcing the Tonle Sap River to reverse its flow towards the lake. This phenomenon causes the lake's water depth to increase by 5.6 - 9.0 m and its surface area by 7,517 - 12,876 km^2 (range of values depending on the year; Table 2.1). At the peak of the flood (between the end of September and the beginning of October), the total flood extends over 9,637 - 15,278 km^2. Flood duration varies proportionally to flood level throughout the floodplain, from a few days at the outer edge to 9-11 months in the gallery forest. The average flood duration over the entire floodplain is 5.4 ± 3.9 months per year (± standard deviation from historical mean; Table 2.1).

The hydrological processes governing the Tonle Sap have been explained through multiple numerical models (Johnston & Kummu, 2011). In terms of the basin's hydrology – including the Tonle Sap tributaries– at least six different models have been applied to the Mekong: Soil and Water Assessment Tool (Piman et al., 2013), Semi-distributed Land Use-based Runoff Processes (SLURP; Geoff Kite 2001), Variable Infiltration Capacity (Costa-Cabral et al., 2007), VMOD (Lauri et al. 2012), YHyM (Yoshimura et al., 2009) and MIKE SHE (Thompson et al., in press). There is much overlap in the data input among these models (as most come from the Mekong River Commission [MRC]), and in general all of the models were shown to accurately simulate the Mekong's hydrology. In terms of the Tonle Sap hydrodynamics, at least four models have been applied: ISIS (Piman et al., 2013), 3D EIA (Sarkkula et al., 2003; Västilä et al., 2010), MIKE 11 (Fujii et al., 2003), and a 2-D finite element model (Hai et al., 2008). Among all of these hydrology and hydrodynamic models, only those that are maintained by MRC (SWAT and ISIS) and the ones that were initially developed in cooperation with the Finnish Environment Institute (VMOD and 3D EIA) have been regularly updated and used for a number of studies. Even so, very little research has been done in linking any of these models to the ecology of the Tonle Sap.

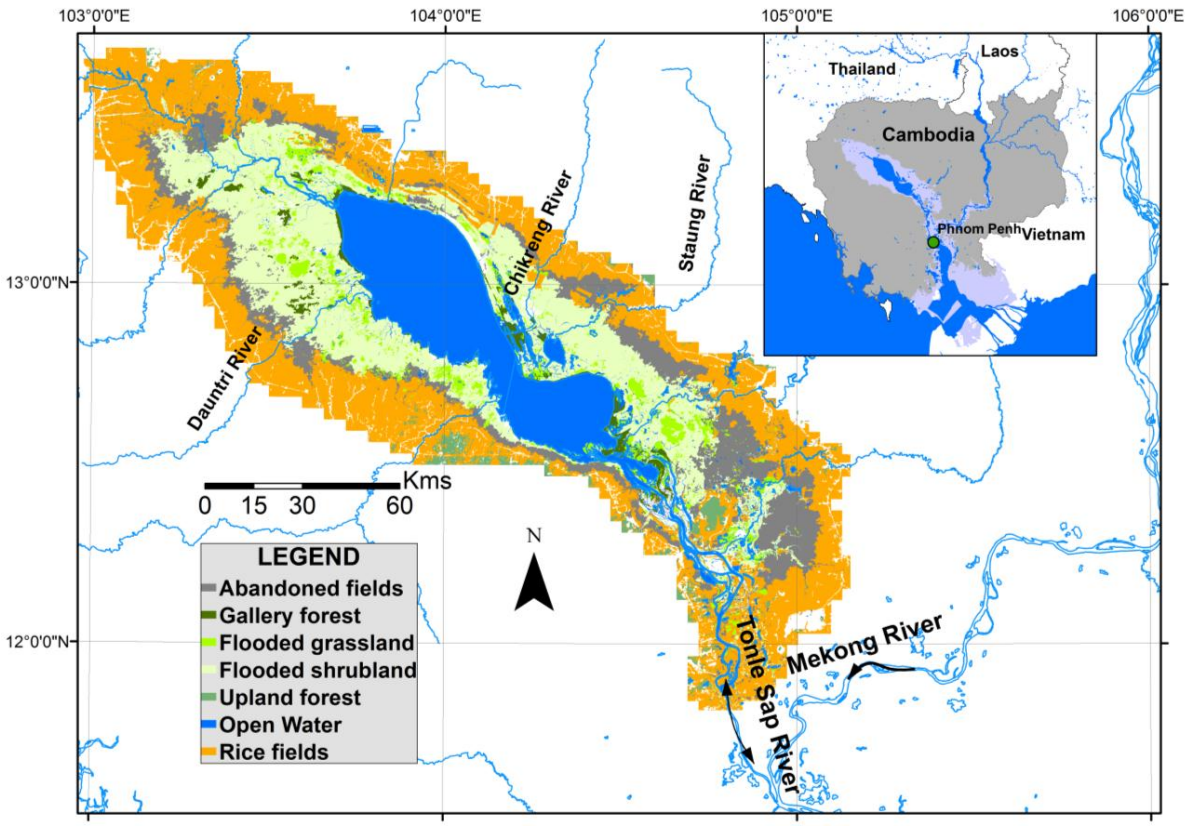

Figure 2.1. Overview map of the Tonle Sap system, highlighting its connection with the Mekong, the permanent open water, and the seasonally flooded habitats.

Table 2.1. Summary of Tonle Sap hydrological features (1997-2010).

Hydrological parameter	Hydro-year [a]:	1997	1998	1999	2000	2001	2002	2003	2004	2005	2006	2007	2008	2009	2010	Mean
Daily river flow [b] ($m^3 s^{-1}$)	Min	-8186	-5041	-8252	-10403	-9302	-8619	-7412	-8019	-8645	-11345	-7150	-7561	-	-	-8328
	Mean	-739	-373	-1375	-1509	-1119	-943	-352	-510	-391	-1724	-540	-647	-	-	-875
	Max	10361	5140	7978	8867	8953	8746	7624	8233	10051	8357	7938	7490	-	-	8385
Daily water level [c] (m)	Min	1.20	1.24	1.38	1.48	1.42	1.19	1.27	1.25	1.26	1.25	1.32	1.29	1.38	1.11	1.30
	Mean	5.28	4.41	3.48	5.41	5.96	5.45	5.44	3.92	4.65	4.55	4.79	4.44	4.97	4.75	4.79
	Max	9.29	6.86	8.97	10.36	9.89	10.10	8.26	9.20	9.29	10.20	8.98	8.70	9.23	7.73	9.20
	Max date	10/13	10/12	10/17	9/28	10/5	10/6	10/8	10/2	10/8	10/18	10/24	10/15	10/15	10/27	-
Water level change rates ($cm\ d^{-1}$)	Rising	5	3	4	5	6	6	5	5	6	7	4	5	4	5	5
	Receding	4	3	4	4	4	4	3	3	3	5	4	4	3	3	4
	Rise start	4/14	4/9	5/1	4/30	5/18	5/20	4/29	4/7	6/3	6/9	5/7	5/5	4/27	6/8	-
Flood extent [d] (km^2)	Min	2069	2120	2284	2402	2331	2061	2155	2131	2143	2131	2213	2178	2278	1968	2192
	Mean	7338	6123	4890	7519	8309	7572	7554	5473	6454	6324	6649	6172	6891	6595	6664
	Max	13481	9637	12950	15278	14478	14834	11805	13327	13475	15004	12966	12511	13368	10970	13347
Flood volume (km^3)	Min	1.4	1.4	1.6	1.8	1.7	1.3	1.5	1.4	1.5	1.4	1.5	1.5	1.6	1.2	2
	Mean	19.5	13.5	8.5	20.4	24.9	20.7	20.6	10.7	15.1	14.5	16.0	13.8	17.2	15.7	16
	Max	61.0	33.0	56.8	76.1	69.2	72.2	48.1	59.8	61.0	73.7	56.9	53.4	60.1	42.0	60
Flood duration (months) [e]	Mean	5.2	3.9	6.1	6.7	6.1	6.1	4.4	5.2	5.1	5.5	5.0	5.5	5.4	4.1	5.4
	SD	3.8	4.3	4.1	3.5	3.6	3.7	4.2	4.2	3.9	3.5	4.1	4.1	4.0	4.1	3.9

[a] Each hydro-year starts on May 1st of the calendar year and goes until April 30th following calendar year.
[b] Negative flows are out of the lake into the Mekong.
[c] Water levels at Kampong Luong above mean sea level in Hatien, data provided by MRC.
[d] Flood extent and volumes estimated from regression curves estimated by Kummu et al. (2013).
[e] Floodplain-wide estimate based on flood duration maps, see chapter 3.

2.3 Influence of the flood-pulse hydrology on the Tonle Sap habitats and ecology

The extreme seasonal inter-phase between flood and drought in the floodplain determines major habitat types, geochemical processes, ecological interactions, and human activities interplaying in the Tonle Sap. While the scientific understanding of this ecosystem is still far from optimal, it is possible to conceptualize how major physical, biological, and social components of this ecosystem interact with each other. This conceptual model is presented in a systems diagram in Figure 2.2; sections 2.2 through 2.4 describe the main components of this diagram in more detail, relating it to the state of the knowledge on the influence that hydrological processes have on the Tonle Sap ecology and how drivers of hydrological alterations could affect these interactions.

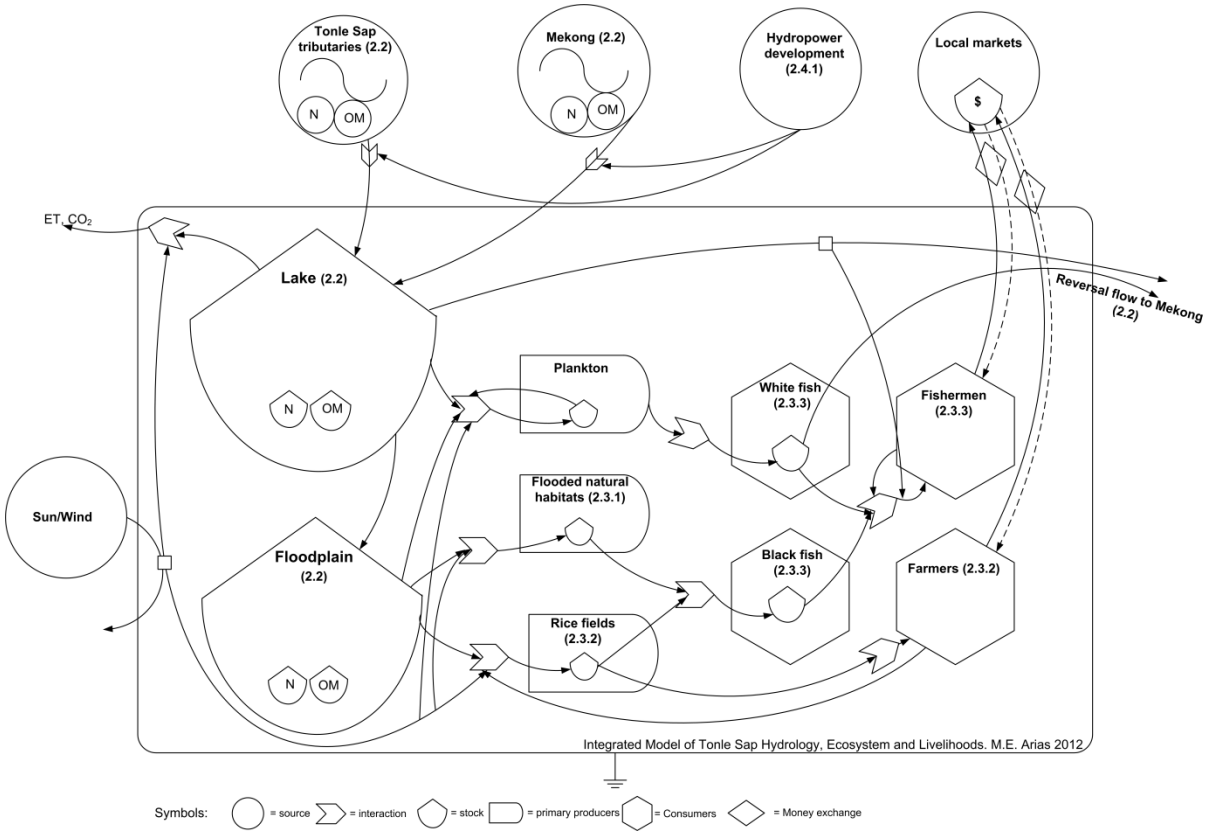

Figure 2.2. Conceptual systems diagram of the interaction between hydrology, ecosystem, and livelihoods in the Tonle Sap. Numbers in parenthesis refer to specific sections where components are described.

2.3.1 Natural habitats

The seasonal flooding in the Tonle Sap has shaped a unique vegetation gradient that varies in both species composition and canopy structure. McDonald et al. (1997) proposed a descriptive model of the vegetation gradient, dictated by a combination of flooding disturbance during the wet season and water stress during the dry season. This gradient starts with a narrow fringe of floating and submerged vegetation on the edges of the open water, including *Eichhornia crassipes* and *Polygonum barbatum.* Aquatic vegetation is followed by a rim of gallery forest dominated by tall (10-15 m) trees, including *Barringtonia acutangula* and *Diospyros cambodiana.* Further up from the gallery forest, vegetation height decreases rapidly to an average of 5-7 m and then gradually becomes dominated by shrubby species such as *Combretum trifoliatum* and *Cratoxylum pruniflorum*. This area of shrubs covers the largest fraction of the natural habitats, but why this area is covered with shrubs and not tall trees is not well understood. On the one hand, McDonald et al. (1997) suggested that shrubs dominate the area because of the extreme flood/draught conditions the floodplain is subject to: when the floodplain is not inundated, little water is available to plants except for areas near open water (hence the existence of gallery forest), but when the rainy season starts, the plants only have a few months to grow before they become submerged again. On the other hand, the most common belief is that shrub dominance is a result of human disturbance (Campbell et al. 2006; Araki et al. 2007): the floodplain has been inhabited and used by humans for centuries, and if it was not for their presence, most of the floodplain would be covered with forests. Thus far, neither of these two hypotheses has been proven, and despite the fact that both extreme flood/drought seasonality and human intervention are evident, what the primary driver of natural vegetation is throughout the floodplain remains an open question.

2.3.2 Rice habitats

Rice cultivation is a key component of the Tonle Sap ecosystem which is highly synchronized with the flood-pulse. Historically, one third of the floodplain has been used for rice (Bonheur and Lane, 2002), and a majority of the floodplain inhabitants (63 %) have depended on agriculture for their subsistence (Keskinen, 2006). Yet, the major constraint for rice farmers is flooding; what variety of rice is planted, where is planted, and when is planted, is dictated by the flooding regime. Given this constraint, there are mainly three types of rice that are used throughout the Tonle Sap: rainfed rice, floating rice, and recession rice (Hand, 2002; Nesbitt, 1997; Sarkkula et al., 2003). Rainfed or wet season is the dominant variety in the region. These paddies cover most of the outer edge of the floodplain where flooding reaches a maximum depth of 50 cm only during wet years; virtually all the floodplain that does not flood every year is currently used for this type of rice cultivation (See Chapter 3). Land preparation, seeding, and transplanting of rainfed paddies occurs in the first 4 months of the rainy season while harvesting occurs at the end of this season (Figure 2.3). Receding rice occurs in areas of the floodplain that flood up to 5 m for 4-7 months every year. It represents only about 10% of the cultivated part of the floodplain (Hellsten et al., 2003), and all cultivation stages happen within the 6 months when the flood recedes (December-May). Floating rice is planted in areas with similar flooding conditions as receding rice but during different times of the year. Floating rice fields used to represent a large fraction of the total cultivated area in the floodplain, but since the 1980s its area has been declining (Nesbitt, 1997; Sarkkula et al., 2003). This variety of rice is particularly susceptible to changes in hydrological factors (Nesbitt, 1997), and for instance, Sarkkula et al. (2003) found that the loss in floating rice fields during the late 1990s and early 2000s was correlated with an increase in annual maximum water level.

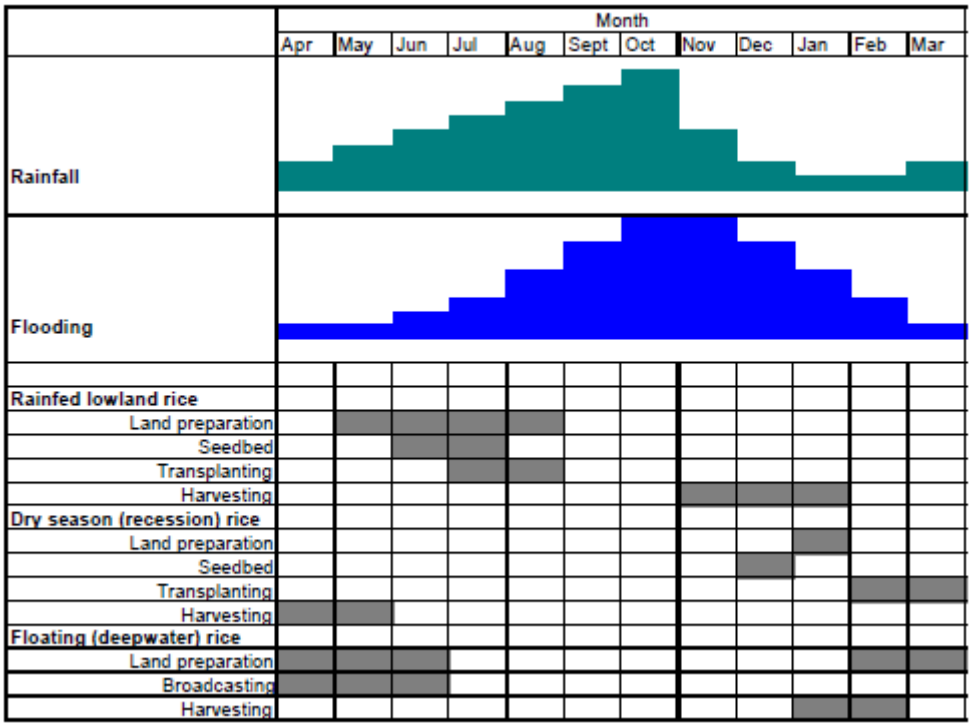

Figure 2.3. Rice cultivation practices synchronized with the flood pulse in the Tonle Sap. From Hellsten et al. (2003). No specific units provided for the rainfall and flooding graphs in the original source.

2.3.3 Fish

The flood-pulse is one of the main factors responsible for the large fish production and species diversity of the Tonle Sap. Based on consumption surveys, 199,204 tons yr^{-1} of fresh fish are caught from non-commercial fishing, which accounts for a floodplain-wide yield of 130 kg ha^{-1} yr^{-1} and 75% of the animal protein consumed in the region (Hortle, 2007 after Ahmed et al., 1998). Moreover, 167 species of fish have been recorded on the lake (Valbo-Jørgensen et al., 2009), and their life histories are highly dependent upon the flood-pulse. Because of this dependency, fish of the Tonle Sap have been broadly classified into 3 classes: black fish, white fish, and grey fish. Black fish are permanent residents of the floodplain and include species in the Channidae family (snakeheads), as well as *Clarias batrachus* (walking catfish) and *Anabas testudineus* (Climbing perch; Lim et al., 1999). These fish are adapted to low dissolved oxygen and high temperature conditions that develop in shallow water habitats,

and some species are even capable of breeding atmospheric oxygen, crawl above ground and survive buried in the soil (Valbo-Jørgensen et al., 2009). White fish are migratory species that inhabit the Tonle Sap during the wet season and include large species in the Pangasiidae family and the small species in the Cyprinidae family, which represents a large fraction of the fish catch in the region (Lim et al., 1999). These species breed further upstream in the Mekong system, and their larvae flow down into the Tonle Sap as the flood starts every year. White fish feed in the floodplain for the remainder of the flooding season, and leave the system once the Tonle Sap River flows into the Mekong in later October/early November. Grey fish are an intermediate group that have the ability to withstand low dissolved oxygen conditions in the floodplain but that depend on permanent water bodies for their survival during the dry season. This group includes species in the Ambassidae, Cyprinidae, and Belonidae families (Valbo-Jørgensen et al., 2009). Beyond this broad classification, little has been published about the Tonle Sap fish ecology.

2.3.4 Other fauna

Other fauna besides fish are highly depended on the flood-pulse for habitat, feeding, and reproduction. The state of the knowledge on non-fish fauna is limited, but recent studies have revealed interesting patterns in relation to the flood-pulse. Zooplankton and zoobenthos play a key role as the primary consumers of the aquatic foodweb, and the greatest density of these organisms have been found in the seasonally flooded habitats (Tanaka and Ohtaka, 2009). Water snakes also live in these areas, and their reproduction cycle is synchronized with the flood-pulse so that the gestation period of most species occurs at the end of the dry season (Brooks et al., 2009). Birds have received the most attention and monitoring efforts among fauna of the Tonle Sap because several colonies represent significant fractions of their global population (Campbell et al., 2006). Most species live in the natural seasonally flooded habitats and have fish or water snakes as their primary food source, thus it is expected that the

flood-pulse is a highly influential factor in their life histories. Large mammals are absent in the Tonle Sap except for domestic water buffalo that are allowed to freely roam through the grasslands and abandoned fields during the dry season. In short, even though the information on hydro-ecological aspects of fauna is very scarce, there is a strong indication that the flood-pulse plays a fundamental role for most living organisms in this ecosystem.

2.4 Drivers of change and future scenarios

The hydrology of the Mekong and the Tonle Sap is changing. Hydropower and climate change have been identified as the most important threats, and therefore, it is important to understand how these two factors have influenced and will probably continue to influence seasonality and long-term hydrological patterns in the Mekong and thus affect the Tonle Sap ecosystem.

2.4.1 Hydropower development

While the worldwide boom for hydropower development peaked in the 1970s (WCD, 2000), the Mekong remained relatively untapped for another two decades. Prior to 1991, only 9 dams with a active storage of 7.9 km^3existed in the entire basin, most of them in remote tributaries in Thailand (MRC, 2009a). Between 1991 and 1995 four dams were built (Manwan in China, Pak Mun in Thailand, O Chum 2 in Vietnam, and Xeset in Lao), increasing the active storage capacity by 0.4 km^3. Despite this small increase, there is evidence altererations to the Mekong hydrology during this period, mainly observed as an increase in dry season water levels and more frequent water level fluctuations at the stations closest downstream from the Manwan and the Pak Mun (Cochrane et al., in preparation). Between 1996 and 2005, at least another 9 dams were constructed, most notably the Dachaoshan in the Upper Mekong in China and the Yali in Vietnam. Although previous studies found that there was a significant increase in the dry season flows of the Mekong

during this period (Li & He, 2008; Campbell, 2007), this was attributed to climate patterns and not to hydropower. From 2005 to 2010 at least 14 dams were commissioned, which increased the active reservoir storage capacity from 1.5 to 19.3 km^3. Most of these dams were built in the Vietnamese highlands in the Sesan, Sre Pok, and Sekong (3Ss) sub-basin, plus another 3 dams that were built north of Vientiane in Lao (including the Nam Ngum 2).

Although it appears that hydropower development in the Mekong had caught up with the rest of the world, the dam construction boom is just starting in the Lower Mekong (Figure 2.4; Table 2.2). The total hydropower production potential in the Mekong Basin is 106,104 MW (King et al., 2007), most of which is actually in the upper Mekong in China (64,728 MW). Yet, all of the existing and under construction dams in the upper Mekong account for 14,800 MW (Räsänen et al., 2012), while the proposed development in the Lower Mekong accounts for 22,667 MW (MRC, 2009b). A large fraction (65%) of the proposed hydropower capacity is concentrated in 12 run-of-river dams on the mainstem of the lower Mekong River, which have been extremely controversial due to their potential impacts on fisheries (Grumbine & Xu, 2011; Grumbine et al., 2012). Despite the focus of the media on the 12 run-of-river dams, a much greater number of dams and active storage is under construction or planned in the Mekong tributaries, in particular the 3Ss, where a total of 42 dams with 26 km^3 of active storage are planned or under construction.

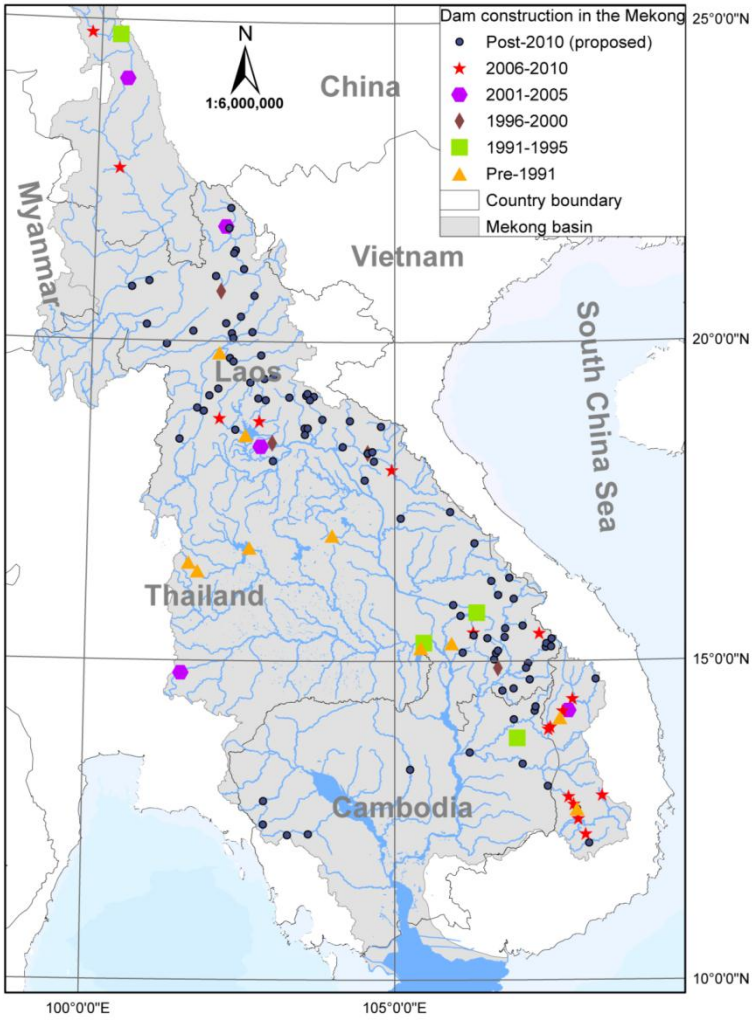

Figure 2.4. Map of commissioned and proposed hydropower project in the Mekong basin. Data from MRC (2009).

Table 2.2. Summary of hydropower development in the Mekong. Information from King et al. (2007), MRC (2009a), and Räsänen et al. (2012) after ADB (2004).

		Existing projects (2012)			Proposed and under construction		
Location	Potential capacity (MW)	Active storage (km^3)	Capacity (MW)	Number	Active storage (km^3)	Capacity (MW)	Number
Upper Mekong (China)	64728	10.7	7800	4	12.6	7000	2
Lower Mekong	41376	23.7	7018	44	60.5	22667	92
Mekong River Basin	106104	47.4	14818	48	83.7	29667	94

Future changes in the Mekong's hydrology caused by dam development have been quantified through numerical models. MRC used the Integrated Quantity and Quality Model (IQQM) –part of the MRC's Decision Support Framework (DSF)– to assess future scenarios up to 2060 that also included irrigation and water supply demands (MRC, 2011; Piman et al., 2013). This model projected that in the short term (5 years from the present) there could be a large (40-60%) increase in the dry season flows of the upper basin as a result of hydropower, but this change could be dissipated in the foreseeable and long-term scenarios (+20 years from present) as a result of an increase in irrigation demand. Despite the MRC-DSF's comprehensiveness, its scope has not so far included detailed information on dam/reservoir configuration and operations, and therefore, more detailed studies have been carried out in selected sub-basins where most of the hydropower development is occurring. For instance, Räsänen et al. (2012) studied the hydrological impacts of the Chinese dam cascade in the Upper Mekong using the hydrological model VMOD and a reservoir cascade optimization model. Their main findings were that the completion of the Chinese dam cascade will increase the dry season river discharge in Northern Thailand by 34-155%, and will decrease the wet season discharge by 29-36%. A different study focused on the 3Ss used the hydrological model SWAT in combination with the dam operation and routing model HEC-ResSim (Piman et al., 2012). This study found that the proposed development could increase the 3Ss contribution to the Mekong's discharge by 63% during the dry season and decrease it by 22% during the wet season. This study concluded that hydropower development in the 3Ss will have a much greater impact on hydrology than the Lower Mekong run-of-river dams and rather similar in magnitude to what is occurring with the Upper Mekong development in China.

2.4.2 Climate Change

In order to understand the ongoing and future changes in the Mekong's climate, it is crucial to first recognize the regional meteorological patterns that govern the basin's climate. It is well known that the Mekong's climate and hydrology seasonality is driven by the Asian monsoon (Costa-Cabral et al., 2007; MRC, 2005; Takeuchi, 2008), which brings the majority of the annual rainfall within four months (see section 2.2). Rainfall patterns, however, vary throughout the basin: the greatest rainfall is in the highlands of Southern Lao and in the Cardamoms Mountains in Cambodia, and the lowest is in the Upper Mekong (Figure 2.5). The Mekong basin falls in the boundary between the Indian and the East Asian monsoon regimes, but it appears as if the latter plays a greater role in determining rainfall and river discharge (Delgado et al., 2012). Inter-decadal fluctuations in the Asian monsoon and the Mekong climate are correlated to the El Niño-Southern Oscillation (ENSO; Delgado et al. 2012; Räsänen & Kummu, 2013); consequently, El Niño periods (e.g., 1982-3, 1997-8, 2002-3, and 2004-5) have corresponded to years of lower than normal flows, whereas La Niña periods (e.g., 1984-5, 2000-2001) corresponded to years of higher than normal flows (Räsänen & Kummu, 2013).

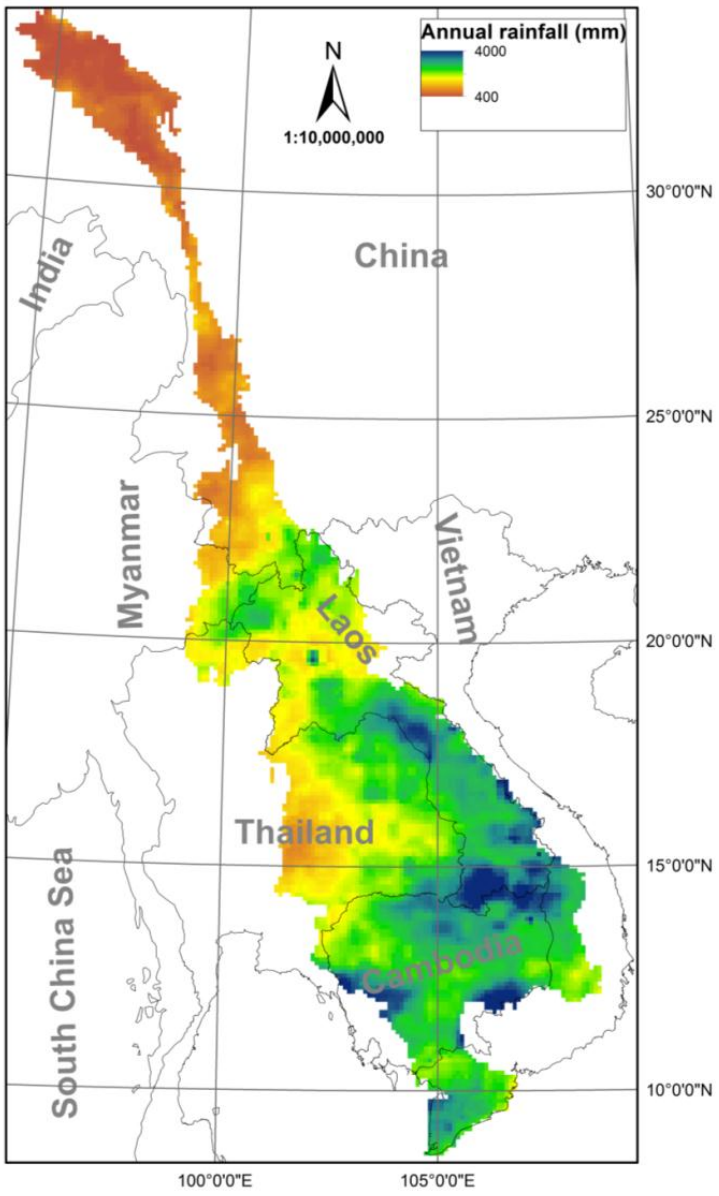

Figure 2.5. Annual rainfall patterns in the Mekong. Data from MRC.

A few studies have recently discovered extreme periods of drought and flood in the past, and most importantly, it has been demonstrated that the climate and hydrology of the Mekong started changing abnormally during the last century. Buckley et al. (2010) constructed a drought severity index of the early monsoon for the period between 1250 and 2008. They found that the Lower Mekong region experienced long and extreme droughts between periods of intense monsoons in the 13th and 14th centuries, which match the era when the Angkor Empire collapsed. Räsänen et al. (2013) revisited this drought severity

chronology and used it as a proxy for a long-term statistical analysis of changes in the Mekong hydrology. The main and most striking finding from this study was that the variability in hydrometeorology data has been much greater after the 1950s than what it was observed in the 600 years prior. More specifically, the years 2000 and 2001 were ranked as the wettest years in the entire time series (1300-2005), whereas the years 1992, 1993, and 1998 were ranked 1st, 2nd and 5th driest years. Räsänen et al. (2013) findings corroborated what Delgado et al. (2010) had concluded from analysing the time series at 4 stations along the Lower Mekong (Vientiane, Thakek, Pakse, and Kratie). An interesting finding from this study was that not much change has occurred in terms of average discharges, but instead, a significant increase in the frequency of extreme (both high and low) floods was observed in the past four decades.

Interestingly, projecting potential future climate changes has been a greater focus of research than observed past climate changes in the Mekong (e.g., Lauri et al., 2012; Västilä et al., 2010; Kingston et al., 2011; Eastham et al., 2008; Anthony et al., 2008). Most future climate change studies use projections from Global Circulation Models (GCMs), despite that the International Panel for Climate Change (IPCC) has stated that GCMs projections of the South Asian monsoon are equivocal (Ashfaq et al., 2009; IPCC, 2007). Kingston et al. (2011) first looked at the uncertainty in the Mekong hydrology predictions associated with the use of seven GCMs. This study found that GCM projections agreed with respect to an eventual increase in potential evapotranspiration and weakening snowmelt contribution, but GCMs disagreed with regards to rainfall precipitation. A more recent study looked at 2 different climate change scenarios simulated with 5 different GCMs (Lauri et al., 2012), and this study actually found that the variability among GCMs could be greater than the variability among different climate change scenarios. Moreover, this study analyzed the effects of hydropower and climate change combined, and it was concluded that hydropower could bring greater

magnitude changes than climate change in the upcoming 2 decades. Ashfaq et al. (2009) used a different approach from the GCMs to simulate the South Asian monsoon. Their nested climate model results fit well with observed data, and in general they found that there will probably be a weakening of the monsoon leading to a net reduction in precipitation during this century.

2.5 Landscape assessment methods

Studies relating hydrology and vegetation of large wetlands often emphasise on landscape patterns that drive ecosystem structure and function. However, field data collection with sufficient spatial coverage and resolution to study landscape patterns is difficult and cost-limited. This is even more pronounced in tropical wetlands, where access is very limited, wildlife may impose a threat to humans, willing personnel are seldom well-trained, and budgets are very limited. At the same time, GIS and remote sensing technology has progressed greatly in the past few decades, making landscape assessments in large and isolated wetlands feasible. This section summarizes a number of studies that have used GIS and remote sensing tools to study linkages between hydrology and vegetation in large wetlands. The first part describes multiple studies on large wetlands around the tropics and subtropics, whereas the second part describes the studies that have been carried out in the Tonle Sap.

2.5.1 Large tropical wetlands

Examples of studies of landscape interactions between the hydrology and floodplain vegetation exist for wetlands similar in nature to the Tonle Sap, including the Okavango Delta in Botswana, the Amazon and Orinoco basins in South America, the wet-dry tropics in Australia, and Florida's Everglades in the United States, among others. Murray-Hudson et al. (2009) studied how changes in the hydrological regime of the Okavango due to potential

future scenarios of climate change and development could impact vegetation cover. Flooding frequency and duration were determined from a hydrological model, and these features were then assigned to functional groups related to the existing habitat/vegetation cover. A baseline map was developed from the flooding/vegetation relationships and then this was compared to the resulting vegetation cover simulated from the probability maps for future scenarios. In a different study of the Okavango, Milzow et al. (2010) investigated how vegetation cover could change as a response to hydrological future scenarios by linking the results from a groundwater model to a vegetation cover map. Vegetation types were found to have distinct histograms of depth to groundwater level, so predictions of vegetation cover were based on the assumption that each vegetation type would maintain the same depth to groundwater histogram in the long-term. Wittmann et al. (2002, 2004, 2006) classified forest types according to the flooding regime in Amazon floodplain forest in Brazil and found clear differences in the canopy structure and species distribution as a result of flood height and duration. Moreover, Ward et al. (2012) used Landsat and MODIS images to investigate seasonal dynamics of inundation, turbidity, and aquatic vegetation in the wet-dry tropics of Australia. Despite the limitations encountered by cloud cover, this study established statistical relationships between remote sensing and field data that could be used for long-term monitoring. In order to overcome cloud cover limitation, studies in the large South American floodplains have used radar data to map seasonal inundation extent (Hamilton et al. 2002, 2004.). Despite the large spatial resolution of the data used (27 km), this was sufficient to create good water level-flood extent relationships in these large floodplains. In the Everglades National Park (USA), vegetation communities were found to be distributed along hydrological gradients represented by percent time of inundation and mean water depth (Todd et al., 2010). The resulting vegetation classification rules were then linked to a water depth model driven by rainfall inputs in order to investigate potential changes in vegetation

cover due to climate change (Todd et al., 2011). Without necessarily inferring a relationship between vegetation and hydrology, other studies have used remote sensing to map ecosystem coverage and structure of large floodplains and wetlands (e.g., Simard et al., 2006; Odunuga & Oyebande, 2007; MacAlister & Mahaxay, 2009; Harvey & Hill, 2001).

In short, GIS and remote sensing tools have become widely used in landscape studies of hydrological and vegetation patterns in large wetlands. These tools provide large spatial coverage and refine resolution that would be extremely difficult to capture with field collection methods on their own. There are, however, challenges that have been faced in using these tools in tropical wetlands, mostly related to cloud cover, and different strategies have been applied to overcome this issue. For vegetation inference, most studies have used existing vegetation cover maps, which are normally developed from a combination of satellite observations, aerial photographs, and field verification. For hydrological inference, two major approaches have been explored, one is using radar data that is not affected by cloud cover, and the other is mapping inundation patterns as a function of water level records and digital elevation maps.

2.5.2 Landscape assessments of the Tonle Sap

Some of the research challenges that are faced in large tropical wetlands are also applicable to the Tonle Sap; hence GIS and remote sensing have also become one of the main research tools in environmental management and impact assessment of this wetland in recent years. For instance, Kummu & Sarkkula (2008) assessed how changes in the Mekong River as a response to hydropower would affect the flood pulse characteristics of the Tonle Sap. This study found that the area of open water could increase by 17-40% as a response to higher water levels during the dry season, which would ultimately result in the permanent inundation

of all the area of gallery forest. The study also found that the area of seasonally inundated floodplain could decrease by 7-16% due to the decline in water level during the wet season.

A more recent analysis was carried out by MRC (2010) in which impacts from eight different water infrastructure development scenarios in the Tonle Sap were considered. The study concluded that there could be a reduction of flood depth during the wet season of over 0.5 m and an increase of water level during the dry season of 0.2-0.6 m. These changes could reduce the flooded area by 400-900 km^2. Consequently, flooded areas covered by forests could be reduced by 22-100 km^2, grasslands by 50-150 km^2, and rice fields by 300-630 km^2.

Other studies in the Tonle Sap have used remote sensing data to infer the present status of flooding and vegetation. Fujii et al. (2003) estimate inundation area and storage volume of the Tonle Sap and the rest of the Cambodian floodplain during 1999-2003 using a series of Radarsat images in order to construct a water balance and to verify their hydrodynamic model. Milne and Tapley (2004) used Airsat data to classify vegetation and flooding of a region in the northwest of the Tonle Sap (Siem Reap Province). Furthermore, Benger (2007, 2009) reported on a classification of satellite images to determine vegetation distributions and hydrological patterns. Most recently, Van Trung et al. (2012) analyzed seasonal variation in vegetation cover associated with water levels. They used both radar data (PALSAR) and optical data (MODIS) to establish a statistical relationship between water level and the change of remotely sensed signature within the main land cover types in the floodplain.

In short, GIS and remote sensing have become the most popular tools for landscape and environmental impact assessments in the Tonle Sap. However, the literature review reveals that there are a number of crucial aspects that are missing from the existing investigations. First, field verification has not been carried out. Second, historical and inter-annual variation in inundation and vegetation patterns has not been assessed. Third, potential vegetation shifts as a response to hydrological changes have not been acknowledged.

2.6 Field assessment of floodplain habitat characteristics

Despite the great benefits that GIS and remote sensing tools bring to the study of hydrological and vegetation patterns, field observations remain an essential method. Field observations are key in demonstrating statistical relationships among hydrological and habitat characteristics, as well as in verifying remotely-sensed data and numerical models. In order to identify the most important factors relating hydrology to vegetation, this section reviews studies of large tropical wetlands that have used field-based observations to establish relationships between hydrological indicators, vegetation, and other habitat characteristics such as soils and water quality.

2.6.1 Field studies in large wetlands

Field studies linking hydrological indicators and habitats have been carried out in some of the large wetlands that share similar hydrological and ecological characteristics with the Tonle Sap. Research in the Central Amazon floodplains found that the most influential factors determining vegetation distribution and composition are: water level, flood duration, physical stability (sedimentation and erosion), succession, water chemistry, soils, and human impact (Junk & Piedade, 1997; Worbes, 1997; Parolin et al., 2004). For instance, Ferreira and Stohlgren (1999) found strong negative linear regressions (r^2 = 0.68) between tree species richness and water level/flood duration. They used the non-metric multidimensional scaling (NMS) ordination method and found significant differences in tree species composition along a gradient highly correlated with water level and flood duration. In the Okavango Delta, plant species composition was also found to be driven by flooding (Murray-Hudson 2009; Murray-Hudson et al., 2011). These studies used two different ordination methods –NMS and canonical corresponding analysis (CCA) – to related plant species composition to the flooding gradient. Both methods suggested that flooding frequency was a strong predictor of

herbaceous plants distribution. The "Wet-dry tropics" in the Northern Territory of Australia has a strong flooding seasonality responsible for floodplain vegetation patterns (Finlayson, 2005; Warfe et al., 2011). Bowman and McDonough (1991) found that tree stem density and species richness in a floodplain the Wet-dry tropics follow skewed unimodal responses along a hydrological gradient. This study also found that soils characteristics such as clay fraction and carbon content varied along the hydrological gradient. Despite geographical differences between Cambodia and the Central Amazon, the Okavango, and the Australian Wet-dry tropics, the interaction between flooding and habitat patterns in these large floodplains is expected to also occur in the Tonle Sap.

2.6.2 Field studies of floodplain habitats in the Tonle Sap

Field expeditions into the floodplain were pioneered by French researchers in the 1960-1970s, who provided general descriptions of the area, a rough vegetation map from a sedimentology study, and preliminary lists of plants encountered in the floodplain (Carbonnel and Guiscafre, 1963; Hellsten et al., 2003; McDonald et al., 1997; Rollet, 1972). A field campaign was not documented again until the mid-1990s when McDonald et al. (1997) surveyed an extensive area of the floodplain with the goal of defining the core zones of the UNESCO Biosphere Reserve. This campaign identified a total of 233 plant species – the largest inventory of plants observed in the region to date – divided into three visibly evident vegetation types: gallery forest, shrubland, and aquatic herbaceous vegetation.

Hellsten et al. (2003) carried out a field campaign in July of 2002 with the goal of determining the link between the floodplain habitats and the system's hydrology. Descriptive observations on soils, vegetation cover, dominant species, invasive species, and water depth were made at 30 locations visited. Little conclusive information about the linkage between vegetation-hydrology was derived from these field observations because – as they stated – information about general ecology of the Tonle Sap was missing. Instead, the information

collected during this field campaign was used to formulate a model to be used in an environmental impact assessment. This model indicated that flood depth played a key role in habitat health, fish production, and rice agriculture.

Araki et al. (2007) conducted a field survey that resulted in a much more quantitative analysis than previous studies. They surveyed a total of 67, 100 m^2 plots within 4km distance upland from the open lake edge in the Phnom Krom region (Siem Reap Province). They identified species, measured maximum stem diameter and height, and calculated distance to lakeshore from each plot. Results from a two-way indicator species analysis indicated that their survey plots were adequately classified into seven classes based only on species composition: cultivated fields, fallow fields, shrub, tall shrub, scrub, open forest, and closed forest. Moreover, a detrended correspondence analysis (DCA) was carried between the species data and a number of plot characteristics. A distinct pattern was found between the distance to the edge of the open lake and the height of vegetation, with minimum vegetation height of 0.3 m at 4.1 km from the lake shore (cultivated field) to a maximum height of 13.8 m at 0.6 km from the lake shore (closed forest). Mean density of plant species was found to have a maximum of 15.9 species per 100 m^2 at intermediate inundation (tall scrub), and decreased both towards the edge of the lake (8 species per 100 m^2 in forest plots) and farther upland (11.2 species per 100 m^2 in cultivated plots). This study concluded that human impacts are the main cause of forest degradation in the Tonle Sap, and that the so-called closed forest – which experienced the largest flood duration and deepest flood height – was the only class that did not suffer much disturbance. Furthermore, the study concluded that the floodplain dominant species, *Barringtonia acutangula*, would cover a much greater extent if the studied area was protected from human impacts. Despite the scientifically-sound and replicable methodology of this study, a major downside was that it only covered a very small, non-protected area of the floodplain that is highly visited.

2.6.3 Water quality monitoring in the Tonle Sap

Water quality is a key component of floodplain wetland systems that reflect the influence that environmental conditions can have on the biota. A selected number of field efforts have sporadically measured different water quality parameters in the Tonle Sap, and in general, these studies show that water quality varies substantially with time and space. However, there is not a single monitoring effort that on its own has comprehensively addressed all sources of variability in water quality.

The longest and most persistent monitoring effort has been compiled by the MRC (Campbell et al. 2006; Campbell et al. 2009). This dataset has revealed a distinct seasonal trend in nutrients (Total Phosphorus and Nitrates) and suspended solids; normally, concentrations increase during the early dry season, peak during April-May, and then decline as more water comes into the system. The most complicated issue with this dataset is that it only includes one location in the open water at Kampong Luong (one of the largest floating villages on the lake with approximately 3,000 people) where the influence of wastewater may not reflect the natural trends in water quality throughout the lake.

The first study that monitored water quality in different locations was Lamberts (2001). Monthly measurements of DO, temperature, electrical conductivity, and pH were taken at 7 different habitats adjacent to Siem Reap Province. Lamberts (2001) found that these water quality parameters showed distinct patterns associated with the habitat type and the phase of flooding.

Sarkkula et al. (2003) carried out a 2-year monitoring program at different locations throughout the open water, the floodplain, and tributaries. This study led to the postulation of several hypotheses and generalizations related to the water quality of the Tonle Sap. First, they hypothesized that the lake was naturally mesotrophic and that primary production was Phosphorus-limited the majority of the time. They also concluded that the open water was

typically well oxygenated, in contrast to the floodplain, which was highly hypoxic during the flooding season. Finally, Sarkkula et al. (2003) stated that the sediments from the Mekong were the most important source of Phosphorus, hence any changes to the Mekong suspended sediment load could influence the productivity of the lake.

The most recent water quality study in the Tonle Sap consisted of a 2-year continuous monitoring (subhourly) of turbidity, DO, conductivity, temperature, and fluorescence in the open water, the floodplain, and in the Mekong River (Irvine et al., 2011). The observations from this study complemented the previous work by Lamberts (2001) and Sarkkula et al. (2003) through a much stronger analytical and statistical methodology. For instance, this study found that temperature, conductivity, and DO were significantly correlated to water level. No significant long-term trends were found; yet, a significant seasonal trend in conductivity was found, suggesting that this parameter is a good indicator of seasonal change in water sources and flow characteristics.

This section presented a number of studies in which the strong influence of hydrological indicators on habitat characteristics of large wetlands in the tropics have been demonstrated through field observations. This influence is normally first depicted by water levels and flood duration, but other factors such as sedimentation, erosion, vegetation succession, water chemistry, soils, and human impact – which are also driven by the hydrology – should also be measured to fully understand the hydrology-habitat interaction. Although a few studies in the Tonle Sap have made selected observations on these aspects, the information available is insufficient to comprehensively explain how hydrological patterns drive habitat characteristics. Major deficiencies of most field studies to date include: lack of direct measurements of hydrological indicators, limited spatial coverage, and minimal statistical inference.

2.7 Hydro-ecological models of large (sub-) tropical floodplain wetlands

Hydro-ecological models are defined here as computer models in which biological and chemical properties of ecosystems are dependent on physical properties of water. This group of models can be classified in multiple ways according to the exactness of results, level of system's detail, time and space dependency, and linearity, among others (Jørgensen and Bendoricchio, 2001). This section summarizes the scientific literature in a refined selection of models of large wetlands in the tropics and sub-tropics in which hydrology and hydrodynamics are used to predict different ecological properties and functions, including primary production, habitat cover, fish production, and animal populations.

2.7.1 Case studies of large tropical wetlands models

Multiple approaches are used to simulate the interaction between ecological and hydrological properties of large tropical wetlands. When data are limited, one approach is to simulate responses at high trophic levels as a direct function of hydrology, disregarding interactions with primary producers. For instance, Linhoss et al. (2012) used this approach to simulate fish populations as a function of flood pulse in the Okavango Delta. In contrast to the data limited approach above, detailed information on multiple trophic levels have been used to simulate the energy exchange within foodwebs in the Everglades in the USA (Brown et al., 2006) and the Upper Paraná River in Brazil (Angelini and Agostinho, 2005). Another approach consists in simulating the interaction among compartments of water, sediments, and primary producers. Models of this kind can represent wetlands as single geographic units with multiple compartments as Weber et al. (1996) did for a floodplain in the Amazon; they can also be represented as spatially-explicit systems of links and nodes as Kuper et al. (2003) did for the Niger River Delta, or as spatially-distributed models where variables are represented by layers of pixel-based information covering the spatial extend of the

ecosystem. Examples of the later type of spatially explicit models exist for the Mississippi Delta and for the Everglades (Fitz and Trimble, 2006; Reyes et al., 2000). A further step in hydro-ecological models is the integration of hydrology and primary production with higher trophic levels. These type of models requires detailed ecological data that are insufficient for most large tropical wetlands, hence these models have been primarily developed for the Everglades (DeAngelis et al., 1998; Gaff et al., 2000).

2.7.2 Hydro-Ecological Models of the Tonle Sap

A number of hydrodynamic models have been applied to the Tonle Sap (see section 2.2 above), but due to the lack of comprehensive information relating water and ecological features of this wetland, the applicability and linkage of these models to ecological questions remains limited. The first model integrating water and ecological features was the Tonle Area Management Scenarios (TAMS) presented by Hand (2002). TAMS is a dynamic model simulated with the software Stella, which uses systems theory and energy balance to relate changes in flood pulse, human population and resources management to productivity and nutritional value. TAMS, however, was developed as an educational and dialogue tool to enhance understanding of the Tonle Sap as a system, it was not intended to provide quantitative projections, in particular because very little scientific information on the system was published at the time. TAMS has been more recently revisited and a web based interfaced was developed to promote its educational and dialogue capabilities (http://mekongriver.info/tams).

More recently, Kum (2012) used similar systems dynamics principles to simulate the impacts of Mekong flow modifications to the Tonle Sap fisheries. Kum's model was a refinement from TAMS in the sense that it used monitored hydrological, nutrient, and fish catch data and more elaborate relationships among water flows, limiting nutrients (assumed

to be Phosphorus), plankton, fish, and fisheries. The simulations were carried using the software VenSim, a different computer program for systems dynamic models. Different components of the model were calibrated against actual observations and subject to sensitivity analysis via Monte Carlo simulations. Kum (2012) concluded that sub-meter changes in water level caused by hydropower could reduce peak loads of TP, which could then have a significant impact on fish stocks with a subsequent loss of 61-87% in the profitability of the dai fisheries.

Among the few numerical models applied to the Tonle Sap, the 3D EIA is the only one with peer-reviewed results linking hydrological and ecological processes (Lamberts & Koponen, 2008; Holtgrieve et al., 2013). The 3D EIA is a spatially distributed model that computes hydrodynamics, sediment processes, water quality, and aquatic primary production as a function of terrain elevation, atmospheric conditions, habitat type, and boundary flows and concentrations. The model platform has been in development since the 1970s and its Tonle Sap application was initially created in the early 2000s (Sarkkula et al., 2003). This first version was dedicated to water movement and sediment processes, both of which were successfully calibrated and validated (Kummu et al., 2008). A primary production component was later added to the model, but the parameters required for these computations have not been fully characterized with in-situ field observations. Moreover, a sensitivity analysis was presented for 2 parameters that influence primary production (Lamberts & Koponen, 2008), but there are actually at least 7 other parameters that have a direct effect on primary production and thus a more comprehensive sensitivity test is needed.

In short, this section described some of the most common modelling approaches for hydro-ecological interactions in large wetlands and how they are related to what has been done in the Tonle Sap. In general, the complexity of a model depends primarily on the information available on each system and the type of output expected. Only 3 such models

have been applied to the Tonle Sap, and although they vary greatly in approach and complexity, the three are certainly limited by data availability. Among these 3 models, the 3D EIA is the most complex; yet, it is also the only one with spatially explicit inputs/outputs, and the only one that has been subject to peer-review. Therefore, this model promises to be a robust approach at modelling the impacts of hydrological change on the ecological function Tonle Sap habitats.

2.8 Chapter summary

This chapter provided a literature review to contextualize the problem and methodology used in this thesis. The first part of the chapter described the state of the knowledge on the hydrology and the ecology of the Tonle Sap, focusing on how the flood-pulse hydrology drives most processes in both natural and agricultural habitats. The next section described the main drivers of hydrological alterations in the Mekong, namely hydropower and climate change. Recent studies have found that the Mekong hydrology has already been abnormally changing for at least four decades, and even though changes caused by hydropower are not so evident in the Lower Mekong yet, this driver is the one expected to bring the most significant alterations to seasonal patterns in future decades. The remaining parts of the chapter described the literature associated with the main methodological approaches used in this thesis, focusing on studies of wetlands with similar dimensions and characteristics as the Tonle Sap. A selected number of studies have been carried out in the Tonle Sap itself, but the information derived from those studies is far from sufficient to objectively quantify the hydrology-ecosystem interaction and how that could change in the future. Specifically, the literature review revealed major knowledge gaps in the following areas that this thesis will address:

- Field verification of GIS and remote sensing data;

- historical and inter-annual variation in landscape inundation and vegetation patterns;
- potential vegetation shifts as a response to hydrological changes;
- field measurements of hydrological indicators;
- extensive spatial coverage and variation;
- statistical inference;
- integration of water quality, soils, and human impact in the hydrology-habitat relationship;
- calibration and validation of hydro-ecological models;
- sensitivity of ecological function model outputs to input parameters.

CHAPTER 3: LANDSCAPE ASSESSMENT OF FLOODING AND HABITATS

3.1 Introduction

One of the main impediments to a full understanding of the hydrology-ecology interaction in the Tonle Sap is the absence of published data on habitats, primary production, and human interactions (Kummu et al. 2006; Lamberts 2006; Lamberts & Koponen 2008). Comprehensive field surveys of habitat characteristics in relation to the flooding regime and human disturbance may ultimately help to fill this knowledge gap, but this will be more effective and meaningful if it is guided by a landscape (or regional scale) assessment that incorporates existing hydrological, GIS, and remote sensing datasets.

Although similarities can be elucidated between other floodplains around the world and the Tonle Sap, the uniqueness of this ecosystem requires an in-depth analysis of the landscape interactions between hydrology, human use, and dominant habitats. The objectives of this chapter are thus to establish how the historical flooding regime has shaped landscape patterns of habitats in the Tonle Sap, examine how they might shift as a result of hydrological changes, and discuss implications on future natural resource management and conservation efforts.

3.2 Methods

3.2.1 Input Data

A record of water levels from 1986 to 2010 was used to quantify the recent flooding history of the lake. Water levels are monitored daily since 1996 at Kampong Loung (N12° 34.598

E104° 12.472; 0.6-0.7 m above mean sea level [amsl]; Figure 3.1) by the Cambodia Ministry of Water Resources and Meteorology (MOWRAM) and MRC. Water levels prior to 1996 were derived from records at Prek Dam (Figure 3.1) on the Tonle Sap river using a linear regression as proposed by Inomata and Fukami (2008). The term *water level* throughout this chapter refers to water surface elevation amsl, whereas the term *water depth* refers to the difference between water level and terrain elevation. The dataset was classified into hydrological years, which are considered to start on May 1st of the corresponding calendar year and end on April 30th of the following calendar year. Descriptive statistics of daily levels were compiled for each month, with 30 day moving averages estimated to examine temporal trends. Summary data from 1997, 1998, and 2000 were used to represent historical average, dry, and wet hydrological years, respectively. These hydrological years have been previously used to represent the full range of historical water level variability (Sarkkula et al. 2003; MRC 2010). Wet years occur at an approximate frequency of once every decade as calculated from the dataset and as suggested by other wet years in recent times (1991 and 2011).

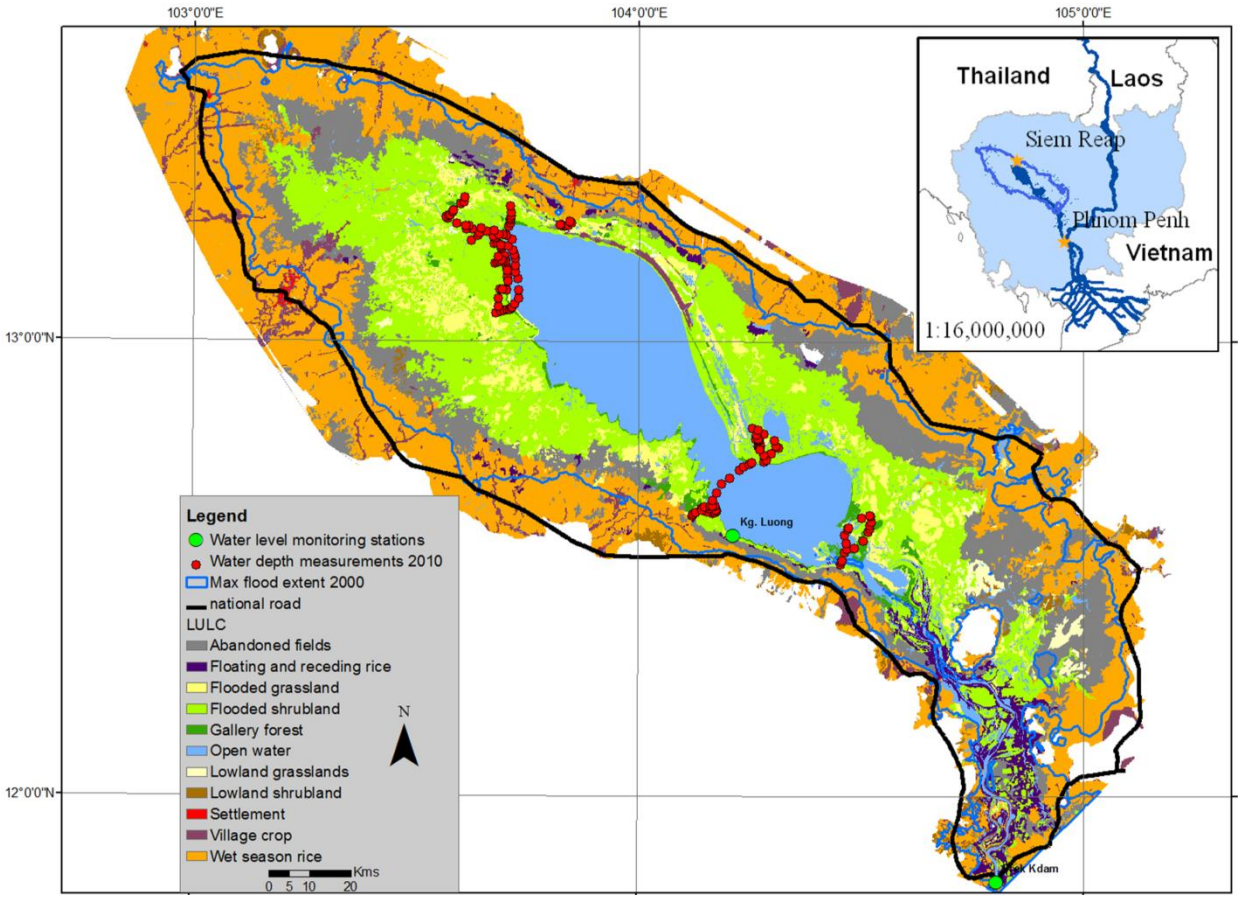

Figure 3.1. Overview map of the Tonle Sap with major LULC (land use/land cover) classes from JICA (1999) below 15 amsl (above mean sea level) and water depth measurements.

Scenarios of future flooding regimes in the Tonle Sap were derived from water level projections at Kampong Loung from two different basin-wide modelling efforts (Table 3.1). The first set of scenarios is based on the MRC-DSF, which simulated the impacts from water infrastructure development (hydropower, irrigation, and water supply) on the Lower Mekong Basin represented by multiple scenarios of progressive stages from 2015 to 2060 (MRC, 2011; Piman et al., 2013). Two climate change (CC) scenarios represented changes in the Tonle Sap hydrology for the 2030-40s estimated with a set of models coordinated by the Water Resources & Development Research Group at Aalto University (Västilä et al., 2010; Figure 3.1). Climate change scenarios in this chapter are based on simulations of the IPCC A2 emissions scenario from the downscaled ECHAM4 Global Circulation Model (GCM),

which predicts a mean basin-wide increase of 1-2°C in temperature and 4% in total rainfall (Västilä et al., 2010). None of the model scenarios evaluated in this chapter includes combined impacts from hydropower and/or multiple climate change GCMs, factors which add a greater level of complexity and variability; these additional factors, however, are considered and discussed in Chapter 5 of this thesis. Model results were analyzed for 3 hydrological years representing average, dry, and wet conditions. Mean monthly changes in depth from baseline conditions were estimated for each model scenario and this difference was then applied to the 1997 (average), 1998 (dry), and 2000 (wet) monthly observed averages.

Table 3.1. Summary of model future scenarios used in this study.

Scenario Name	Scenario Acronym	Approx impact year	Description	Source
Upper Mekong Dams	UMD	2015	Impacts on baseline hydrology (1985-2000) from dams cascade in the Upper Mekong in China	MRC (2011)
20Y water resources infrastructure development	2030DEV	2030	UMD scenario plus 25 dams in the Lower Mekong Basin (LMB), irrigation and water supply projects to 2008, and 11 mainstream dams, tributary dams, irrigation and water supply projects planned to 2030	MRC (2011)
50Y water resources infrastructure development	2060DEV	2060	Impacts on baseline hydrology (1985-2000) from full potential of water resources development in the LMB	MRC (2011)
Climate change 2030s	2030CC	2030s	Impacts on hydrology of the MRB up to the 2030s as a result of changes in temperature and precipitation caused by climate change as modelled from the downscaled ECHAM4 GCM under SRES A2 emissions scenario	Västilä et al. (2010)
Climate change 2040s	2040CC	2040s	Same as above but until 2040s	Västilä et al. (2010)

A number of digital elevation models (DEMs) have been used to support studies on the Tonle Sap (e.g., Eloheimo et al., 2002; Kite, 2001; Milne and Tapley, 2004). Kummu and Sarkkula (2008) prepared a DEM derived primarily from an actual topographic survey carried by Certeza Surveing Co. in 1964 and from bathymetry measurements from the 1999 MRC Hydrographic Atlas. For areas not covered by either dataset, the DEM includes information

from the Shuttle Rapid Topography Mission (SRTM). The original DEM covered an area of 27,232 km^2, an elevation range of 0-112 m amsl, and had a horizontal raster grid resolution of 100 m by 100 m. For purposes of this study, the DEM was modified to exclude terrain elevations higher than 15 m amsl, decreasing the study area to 21,123 km^2. The threshold elevation of 15 amsl was chosen because it is higher than the historical lake's highest daily record (10.36 m) and inclusive of all future water level predictions reviewed. The DEM was reprojected to WGS 1984 UTM Zone 48N, which was the default coordinate system used for all GIS datasets in this thesis.

3.2.2 GIS-based flood maps

Maps representing flood depth, extent, and duration at different temporal scales were derived from combining the DEM with water level records. This was carried out within a flood mapping toolbox in ArcGIS created with a model builder visual interface (See Appendix A). First, water depth maps were created for the median monthly water elevations. This was done by subtracting the DEM elevation values from a one-value raster representing the median water elevation for each month, which were converted to a two dimensional map showing the extent of inundated terrain. These maps were then stacked for each hydrological year to estimate the number of months that each raster pixel remained flooded (See GIS-based flood map step in Figure 3.2). Flood duration maps were created to represent years of historical/baseline conditions (1997, 1998, and 2000) as well as for the future scenarios. Flood duration maps were estimated in units of months, and thus each of the 13 distinct categories (representing annual inundation of 0 to 12 months) are hereafter referred as flood zones.

Satellite images from 2000 to 2010 were used to identify spatial flooding patterns in the Tonle Sap and to validate the flood extent maps. 8 day composite, 250 m resolution MODIS

images from the satellite Terra (MOD09Q1) were selected for the analysis. MOD09Q1 images are composed of two spectral bands, one covering green and red wavelengths and the other covering near infrared. Two images per year were processed: one near the end of the dry season (May) and one near the end of the wet season (October) when the lake is at near minimum and maximum levels of inundation and pixel quality from cloud cover is negligible (or acceptable for an 8-day composite).

Image processing began with a convolution median filter with a 3 by 3 pixel window applied to reduce image noise, followed by a principal component transformation to eliminate correlation between the two image bands. The transformed images were classified using an unsupervised classification method, which iteratively clustered pixels into 4-10 classes using a 5% change threshold to be met within 10 iterations. Once the images were automatically classified, they were reviewed to identify the pixels classes that corresponded to flooded terrain and open water.

Flood extent from the GIS modelling procedure was validated with the MODIS classified images. Maps were created using average water levels for the 8 day when the MODIS images were captured. Flood extent maps were then clipped to match the extent of the MODIS images, and then the area of overlap between the two datasets was calculated. The percent relative difference between the two datasets was estimated as follows:

$$\%_{\text{difference}} = 100\% \times \frac{Area_{\text{largest}} - Area_{\text{overlap}}}{Area_{\text{largest}}} \tag{3.1}$$

Where $Area_{largest}$ is the largest flooded area between each pair of MODIS-based and GIS-based maps, and $Area_{overlap}$ is the flooded area identical to each pair.

The GIS-based flood maps were compared to daily depth maps with actual water depth measurements taken during 2010 in the early dry season (January-February) and the wet

season (October). Measurements were taken throughout the floodplain in areas accessible by boat using a Dr Lange HT 1 probe and/or a Speedtech Instruments water depth probe. The location of each depth measurement was recorded with a Garmin Legend GPS handheld device. Location and depth measurements were then converted into an ArcGIS point feature shape file (Figure 3.1) and overlaid on water depth maps created for the specific dates of field measurements. The difference between field measurements and depth maps values were calculated to further validate the accuracy of the flood mapping procedure presented in this chapter.

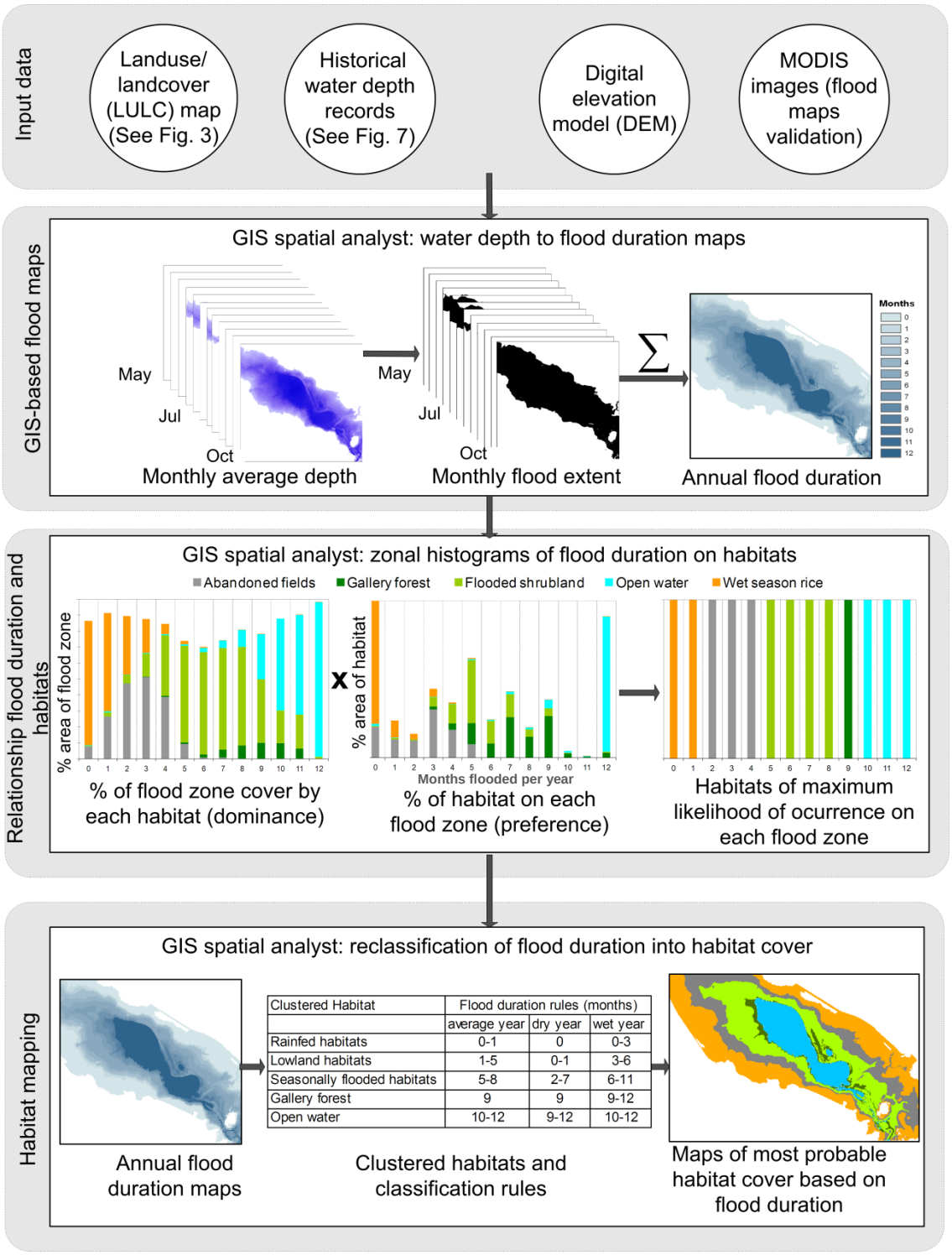

Clustered Habitat	Flood duration rules (months)		
	average year	dry year	wet year
Rainfed habitats	0-1	0	0-3
Lowland habitats	1-5	0-1	3-6
Seasonally flooded habitats	5-8	2-7	6-11
Gallery forest	9	9	9-12
Open water	10-12	9-12	10-12

Figure 3.2. Schematic of assessment and mapping approach used in this study. Input data (DEM and water depth records, section 3.2.1) are used to create GIS-based flood maps (section 3.2.2), which are then combined with a LULC (land use/land cover) map (JICA 1999) to create relationships between flood duration and habitats (section 3.2.5). The flood duration-habitat rules are then used to predict future habitat as a result of basin wide hydrological changes (section 3.2.6)

3.2.3 Tonle Sap habitats

Historical cover of habitats on the Tonle Sap was derived from Cambodia's country-wide land use/land cover (LULC) map developed by the Japanese International Cooperation Agency (JICA, 1999). This dataset was created using SPOT and Landsat images from the late 1990s (Sarkkula et al., 2003; Kummu and Sarkkula, 2008). Although no ground-truthing was done for the dataset due to the political instability of Cambodia at the time, it was later shown to provide good estimates of the actual vegetation cover throughout the floodplain (Hellsten et al., 2003). The LULC map has a 30 m by 30 m grid resolution, and includes 27 different classes within the area studied. Most of the minor classes were excluded or merged onto larger classes, so that only those classes that covered more than 1% of the total area below 15 meter amsl were included in the analysis (Figure 3.1). Merging of classes was only done on two occasions in which the nomenclature and location implied very little functional difference between the classes. Merged classes included village crops (composed of field crops, garden crops, orchard, paddy fields with villages, swidden agriculture, and village garden crop), and open water (composed of the Tonle Sap permanent lake and Boeng Chmar, a smaller lake permanently connected to the larger lake).

3.2.4 Historical (1996-2005) habitat cover change

Habitat cover change in the Tonle Sap during post-war times was investigated using two different LULC maps compiled from aerial imagery approximately one decade apart. The first dataset is the JICA (1999) LULC map described in section 3.2.3, and the second dataset (FA 2005) was classified by the Cambodian Fisheries Administration based on 1:5000 aerial imagery captured in 2004-2005 (Eng and Ouch, 2006; PASCO-FINNMAP CONSORTIUM, 2005). Once geographical projections and extents were coordinated, the classification nomenclature was harmonized according to recent field observations and with the

terminology that is commonly used to describe the Tonle Sap habitats and/or LULC classes. Finally, area coverage of each LULC class was calculated and compared between the two maps.

3.2.5 Relationship between flooding and habitats

The historical interaction between flooding and floodplain habitats was assessed with GIS by overlaying the flood duration maps on the LULC map and then calculating the histogram of flood zones on habitats using spatial analyst tools (See relationship flooding and habitats in Figure 3.2). These histograms can be expressed in a matrix form as follows:

$$\overline{\boldsymbol{Y}_t} = \begin{bmatrix} x_{0,1} & x_{0,2} \dots & x_{0,j} \\ x_{1,1} & x_{2,2} \dots & x_{2,j} \\ \vdots & \vdots & \vdots \\ x_{k,1} & x_{k,2} \dots & x_{k,j} \end{bmatrix} \tag{3.2}$$

where $\overline{\boldsymbol{Y}_t}$ is the matrix representing the histogram for the year *t* (average, dry, or wet), and the element $x_{k,j}$ represents the area covered by the flood zone *k* on the habitat *j*. Flood zone *k* has 13 distinct categories, which represent annual zones of 0 to 12 months of inundation within the Tonle Sap, and habitat j has 10 categories representing the habitats from Figure 3.1. The resulting histograms were then normalized in two ways to infer two different properties of the Tonle Sap habitats in relation to flood duration: dominance and preference. Dominance refers to the distribution of habitats within each flood zone, and it can be derived from the histogram in Eq. 3.2 by dividing each matrix element by the total area covered by their corresponding flood zone:

$$\overline{\boldsymbol{dominance_t}} = \frac{\overline{\boldsymbol{Y_t}}}{\sum_{i=1}^{j} x_{k,j}} \tag{3.3}$$

Preference refers to the distribution of each specific habitat among all flood zones. It was derived by dividing all elements of the matrix $\overline{\boldsymbol{Y_t}}$ by the total area covered by their corresponding habitat:

$$\overline{\boldsymbol{preference_t}} = \frac{\overline{Y_t}}{\sum_{i=0}^{k} x_{k,j}} \quad (3.4)$$

These two properties were then used to select the habitat of maximum likelihood of occurrence within each flood zone by simply applying a scalar multiplication between the matrices and finding the greatest element for each row of the resulting matrix:

$$\overline{\boldsymbol{Max\ likehood_t}} = \overline{\boldsymbol{dominance_t}} \cdot \overline{\boldsymbol{preference_t}} \quad (3.5)$$

3.2.6 Habitat mapping

A model habitat map for the baseline hydrological years was created by applying classification rules to the flood duration maps based on the maximum likelihood of habitat occurrence within each flood zone (See habitat mapping step in Figure 3.2). It is assumed that the spatial distribution of habitats is a response to long-term decadal flooding conditions rather than changes occurring on an annual basis; therefore, the classification rules were applied over a map that summarized flood duration values from average, dry, and wet hydrological years. Once the range of flood duration values was determined, each raster pixel was directly assigned a habitat class that best fit the results from Eq. 3.5. LULC classes that yielded very similar flood duration values were merged into a habitat group with unique distribution of flood duration. To assess the validity of the habitat modelling approach, the baseline modelled map was overlaid onto the original JICA (1999) map. Areas of habitat overlap and shifts from one habitat to another were then estimated. Modelled map accuracy was calculated as the percent of overlap area ($\%_{\text{overlap}}$) between habitats from JICA (1999; $Area_{\text{original}}$) and the model baseline map:

$$\%_{\text{overlap}} = 100\% \times \frac{Area_{\text{overlap}}}{Area_{\text{original}}} \quad (3.6)$$

Future shifts in habitat cover were assessed by applying the classification rules derived from the baseline data to the flood duration maps associated with the different scenarios from

basin-wide models (Table 3.1). Future impacts were assessed by determining the change in habitat cover relative to the model habitat map for the baseline scenario.

3.3 Results

3.3.1 Water levels and flood maps

The 1986-2010 water depth records at Kampong Loung show a clear annual flood pulsing behaviour with variable water levels during the wet season and consistent levels during the dry season (Figure 3.3). The year 1998 was the driest in the period of record, with a maximum monthly average water level reaching only 6.7 m, whereas 2000 was the wettest year with a maximum monthly average water level of 10.2 m. Water levels during 1997 were representative of the annual central tendencies for the period of record. The minimum and maximum monthly average water levels in 1997 were 1.5 and 9.1 respectively, compared to 1.6 and 8.9 for the entire period.

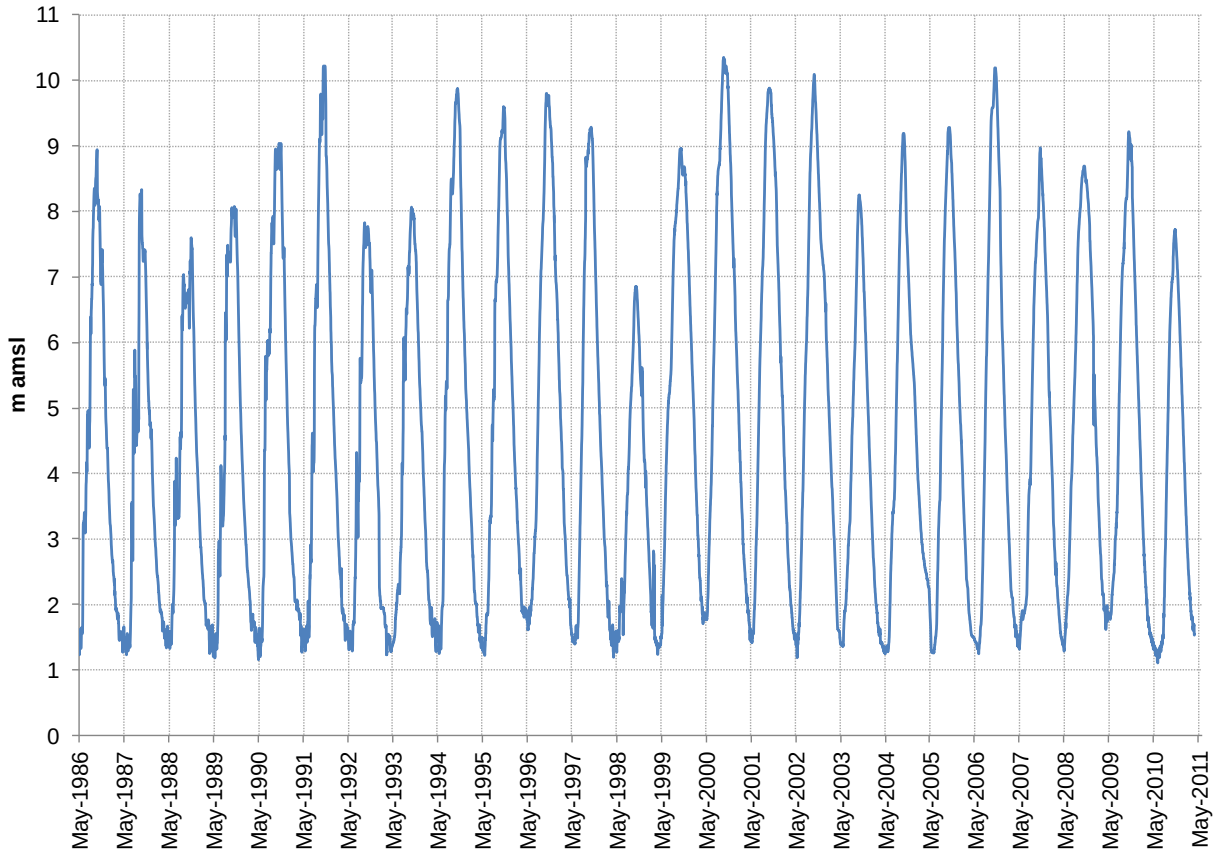

Figure 3.3. Tonle Sap water level hydrograph at Kampong Loung 1986-2010 in m amsl (above mean sea level). Records prior to 1996 were estimated from Prek Dam station on the Tonle Sap River. Data provided by MRC.

The impact of future infrastructure development and climate change scenarios on Tonle Sap water levels were studied for a range of hydrological conditions. Hydrographs from the two 2030 scenarios are compared to the observed monthly averages in Figure 3.4. The hydrographs show that there is a progression of water level changes from the wet year (least impacted) to the dry year (most impacted). During wet years, very little change is expected as a result of climate change and a slight decrease during the rainy season (July through September) is expected as a result of water infrastructure development. During average years, mean water levels in October and November increase by 0.50 m as a response to climate change, but decrease by 0.35 m during the same months due to infrastructure development. The largest changes occur during dry years. As a result of climate change, water levels remain the same during the low water months of April and May, but increase by 0.2-0.75 m

during the rest of the year. As a result of infrastructure development, water levels increase by 0.2-0.4 m from April to June and decrease up to 0.5 m from August through January.

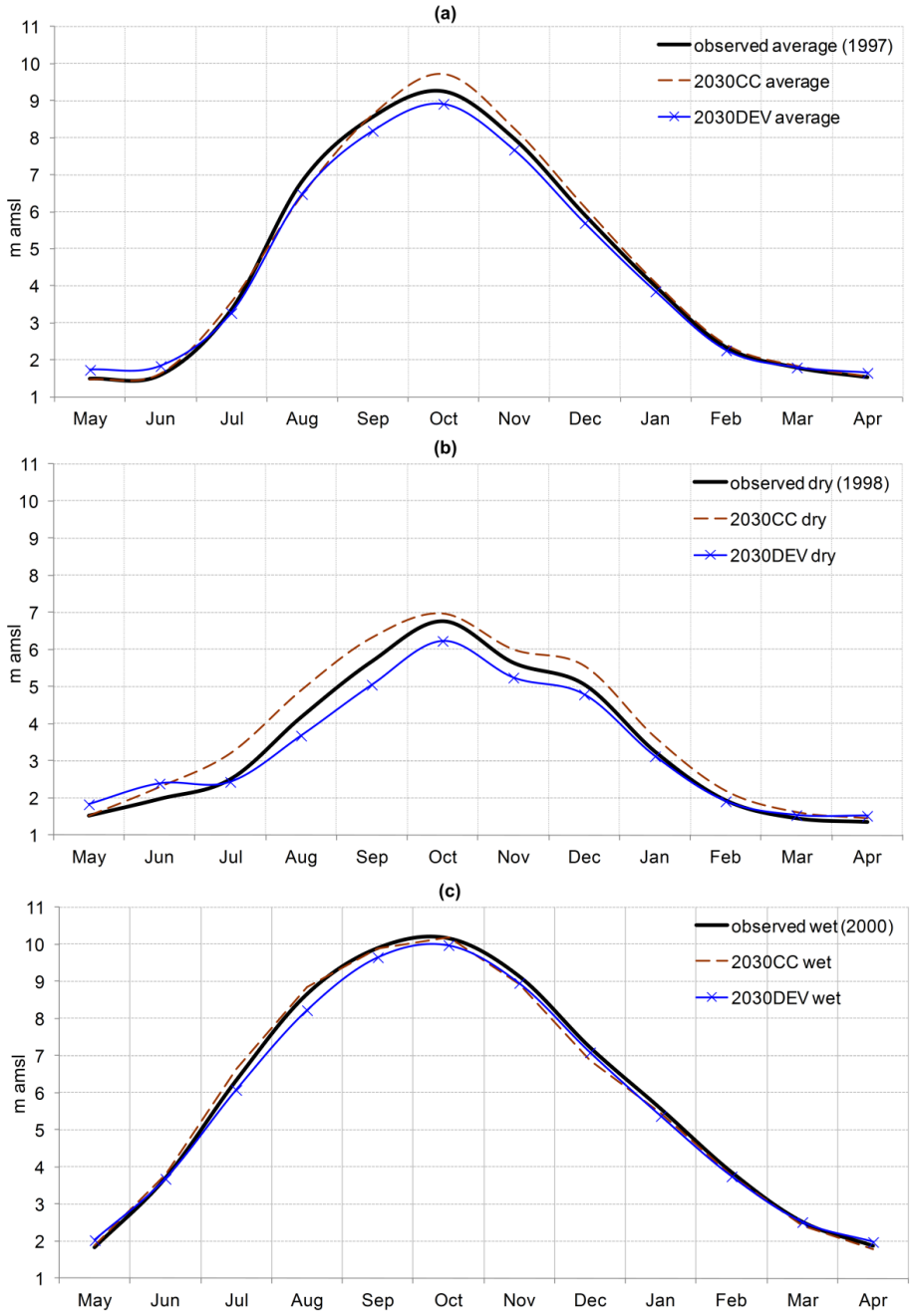

Figure 3.4. Comparison of mean monthly water level at Kampong Loung for historical observed records and model predictions for an (a) average year, (b) dry year, and (c) wet year. 2030CC = climate change scenario for 2030s; 2030DEV = water resources infrastructure development scenario for the 2030s. See Table 3.1 for description of scenarios.

Maps of inundation extent derived from 2000-2010 classified MODIS satellite images show that maximum extent of inundation varied from 12,000 to 15,000 km^2 during the wet season and between 2,500 and 2,800 km^2 during the dry season (Table 3.2). The results from this classification are consistent with the time series of water level records at Kampong Loung; greatest variability of inundation area was found during the peak of the wet season, and little variation occurred during the dry season. The largest inundation extent occurred in the wet seasons of 2000 to 2002 (average of 14,473 km^2), the period in which the highest water levels were also recorded. Following this period, the maximum inundation extent averaged 12,930 and never reached 14,000 km^2.

The GIS-based flood maps were validated for flood extent and water depth. Errors from the flood extent validation ranged from 7.6 to 18.8%, with a mean value of 11.7 ± 3.5% for the 16 sets of maps/images analyzed (Table 3.2). Validation of water depth was based on 140 measurements made between February and October 2010. Depth differences (field measurements minus flood map depth) ranged from -1.7 to 2.4m, with a mean difference of 0.4 ± 0.8 m (9.1 ± 40%). Overall, the tendency of the GIS-based flood maps was to underestimate the actual measurements; 91 of the measurements were underestimated by 0.8 m on average, whereas 37 of the measurements were overestimated by 0.6 m on average.

Table 3.2. Comparison of flooded area estimates from MODIS imagery classification and GIS-based maps. Area estimates in units of km^2 and water level in m amsl.

Date	MODIS flood extent (km^2)	Water level at Kampong Loung (m amsl)	GIS-model flood extent (km^2)	Area$_{overlap}$ (km^2)	% $_{difference}$
		Dry season			
2000-05-08	2841	1.80	3072	2716	11.6
2001-04-15	2751	1.84	3096	2662	14.0
2002-05-25	2580	1.47	2433	2396	7.13
2003-06-02	2605	1.69	3003	2556	14.9
2004-05-16	2579	1.34	2281	2246	12.9
2005-05-01	2841	1.98	3177	2579	18.8
2006-05-01	2667	1.48	2442	2396	10.2
2007-05-17	2626	1.73	3029	2574	15.0
		Wet season			
2000-10-23	14763	10.11	14030	13649	7.6
2001-10-08	14392	9.86	13792	13267	7.8
2002-10-16	14264	9.59	13103	12818	10.1
2003-10-24	12037	7.87	10863	10051	16.5
2004-10-23	12264	7.90	10894	10672	13.0
2005-10-16	13026	9.16	12665	11972	8.1
2006-10-24	13180	9.12	12624	11941	9.4
2007-10-16	12404	8.80	12300	11177	9.9
				Mean ± SD	11.7 ± 3.5

Floodplain-wide changes in annual flood duration were calculated from the GIS-based flood maps. The overall flood extent is expected to decrease by 196-710 km^2 (range depending on scenario) as a result of water infrastructure development and to increase by 1000 km^2 as a result of climate change for an average year (Figure 3.5a). A similar trend was estimated for a dry year (Figure 3.5b), with an overall decrease of flood extent by 513-681 km^2 as a result of infrastructure development and a minor increase as a result of climate change (75-225 km^2). For simulations of the wet year, total flood extent remained relatively constant for the different scenarios, but substantial area shifts were observed within the flood zones (Figure 3.5c).

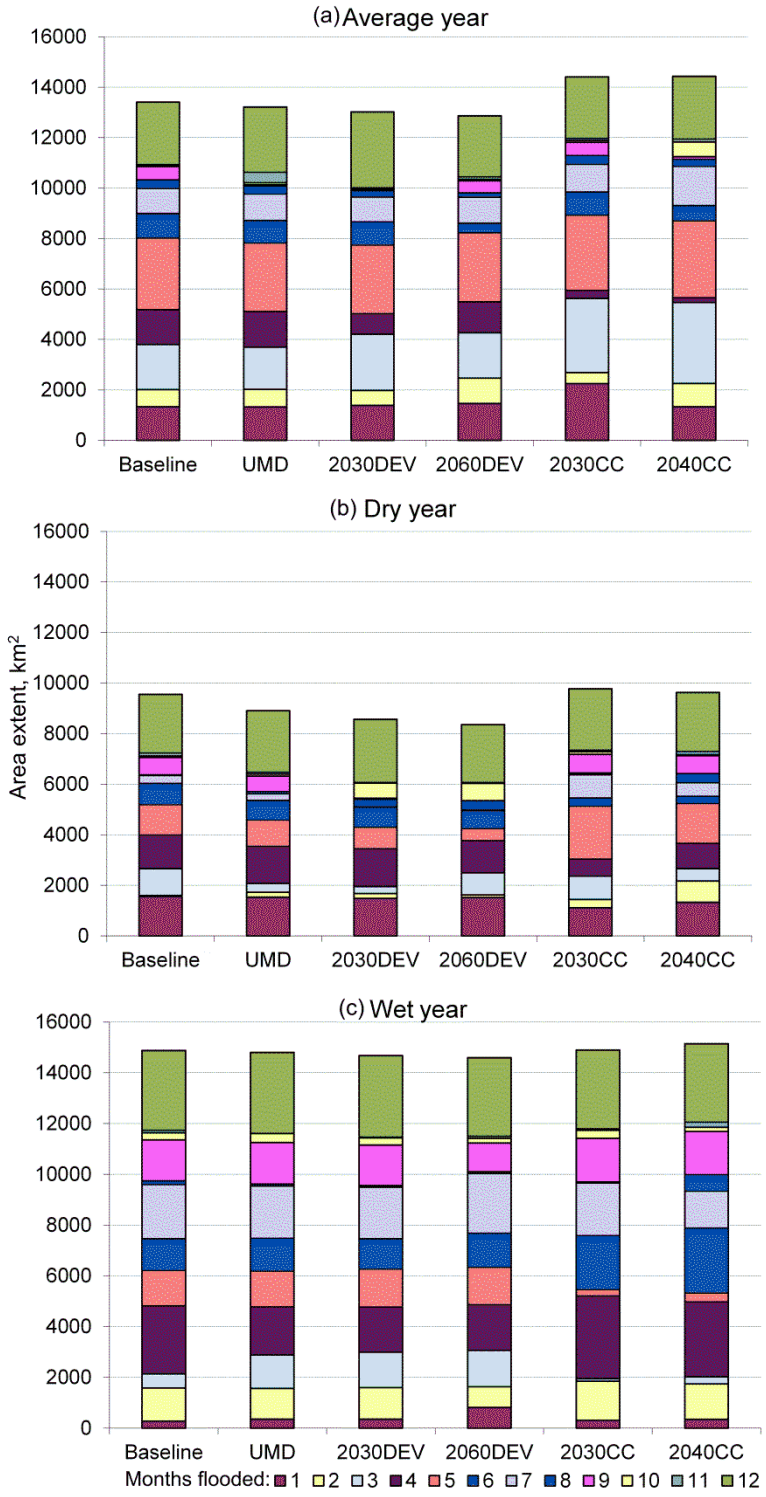

Figure 3.5. Annual flood duration (months) extent during an (a) average year, (b) dry year, and (c) wet year. Legend series in units of months. UMD = Upper Mekong Dams; 2030DEV = water resources infrastructure development scenario for the 2030s; 2060DEV = water resources infrastructure development scenario for the 2060s; 2030CC = climate change scenario for the 2030s; 2040CC = climate change scenario for the 2040s. Refer to Table 3.1 for description of scenarios.

3.3.2 Historical (1996-2005) habitat change

A comparison of two land cover maps representing the years of 1996 (JICA) and 2005 (FA) revealed differences only in the upper area of the floodplain and in areas covered by small classes such as settlements, floating/receding rice, and gallery forest (Figure 3.6). The largest shifts in LULC classes were an increase of wet season rice fields (+18%), which occurred mainly as a result of a reduction of abandoned fields (-18%) and floating/receding rice fields (-63%). The areas classified as settlements increased by 146%, and the area classified as gallery forest increased by 46%. Total area covered by flooded shrubland and open water (nearly 40% of the studied area) remained mostly unchanged.

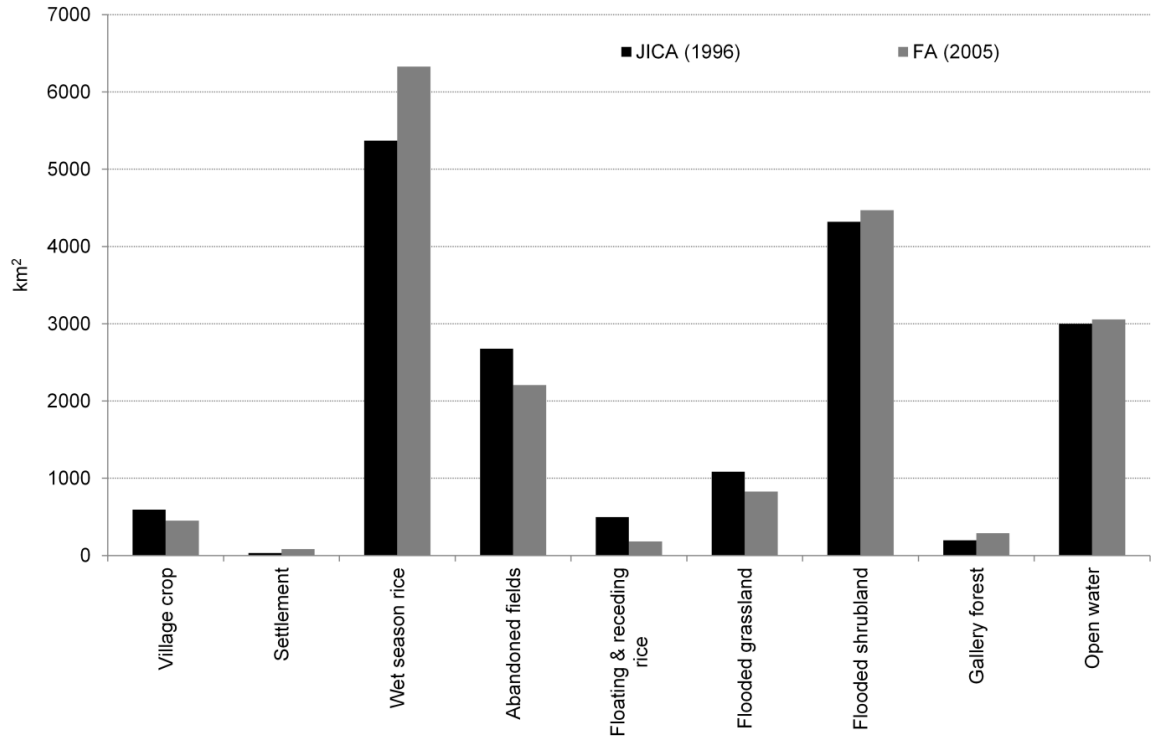

Figure 3.6. Change in selected habitat types interpreted from land use/land cover classes between JICA (1996) and FA (2005).

3.3.3 Relationship between flooding and habitats

To examine the dominant habitats within each flood zone, histograms of flood duration area extent on habitat types were normalized by the total area of each flood zone (Eq. 3.3; Figure

3.7). During the average year, wet season rice covered 62-78 % of the floodplain area inundated for 1 month or less. Abandoned fields covered 47-51% of the area flooded 2-3 months. The 4 month flood zone appeared to be co-dominated by abandoned fields (39%) and flooded shrubland (38%). The area flooded 5-8 months was covered mainly with flooded shrubland (61%) and flooded grasslands (16%). These two histograms followed very similar patterns, yet the magnitude of flooded shrubland was greater for all flood zones where both habitats were present. The 9 month flood zone appeared to be a transition zone covered with flooded shrubland (40%), open water (28%), flooded grassland (12%), and gallery forest (10%). Finally, open water covered 58-97% of the area flooded 10-12 months. Although the area extent histograms for dry and wet years have different magnitudes, their general patterns and distributions are similar as to the ones for the average year.

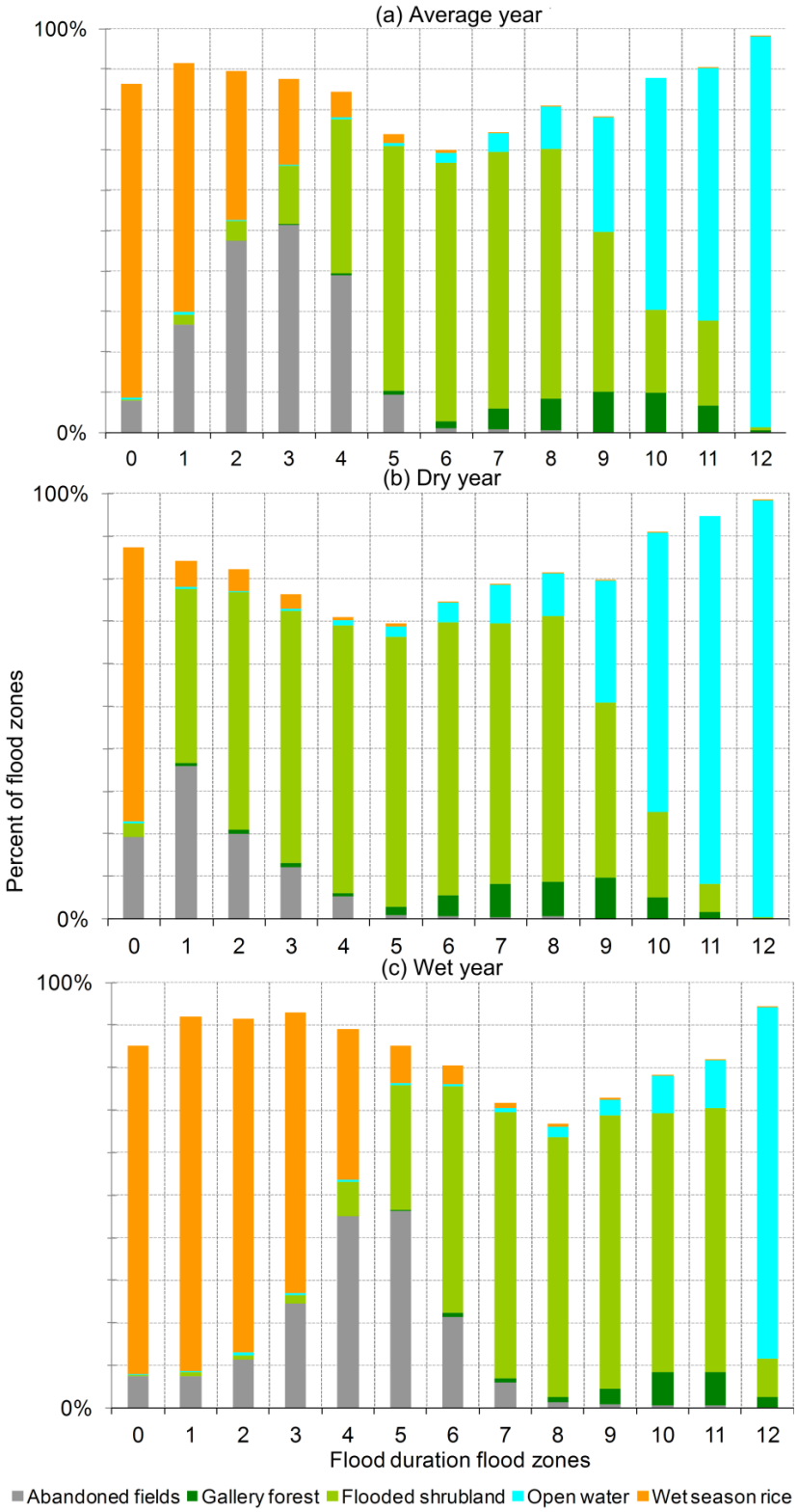

Figure 3.7. Flood duration (months) zone dominance (i.e., percent of flood zone area covered by each habitat) during hydrological (a) average, (b) dry, and (c) wet years. Histograms do not add to 100% since only habitats that covered largest area are shown.

Habitat preference for distinct flood zones was quantified by normalizing histograms of flood duration areal extent by the total area of each habitat (Eq. 3.4; Figure 3.8). Wet season rice, lowland shrubland and village crops occur mainly in the outer portion of the floodplain where natural flooding from the Tonle Sap only occurs once every decade. Abandoned fields covered a distinct area of the floodplain, with 31% of the habitat flooded 3 months during the average year, 74% experiencing no flooding during the dry year, and 40% experiencing 4 months of flooding during the wet year. Flooded grasslands and flooded shrublands experienced almost identical flooding regimes: 40% of their cover floods 5 months during the average year, 19-26% floods 4-5 months during the dry year, and 31-38% floods 7 months during the wet year. Optimum flooding for gallery forest was 9 months for average and dry years and 12 months for wet years, with 26-35% of all gallery forest occurring in this zone. As its name implies, 86-93% of the open water habitat experienced year-long inundation during all historical conditions.

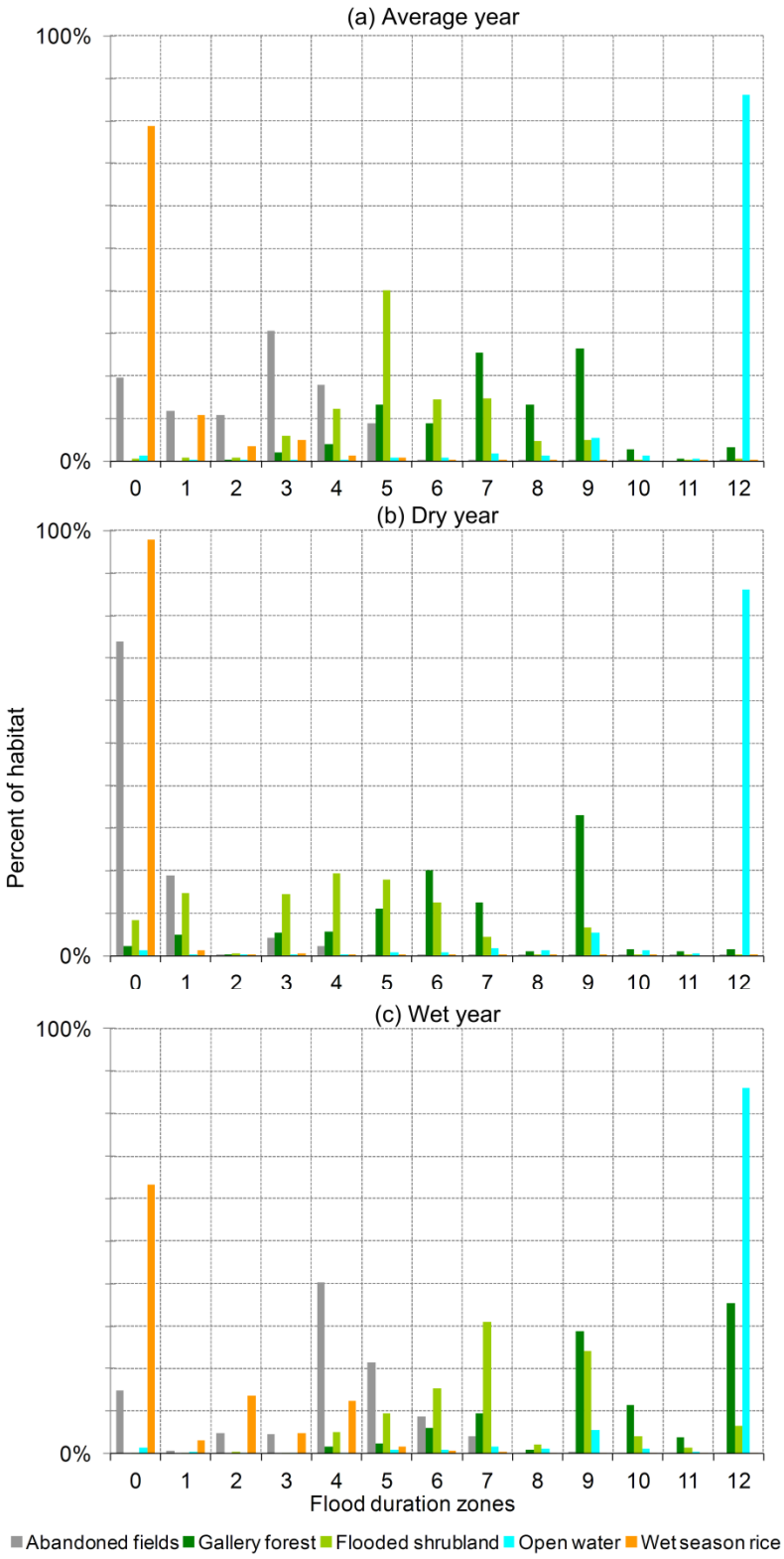

Figure 3.8. Habitat preference (i.e., percent of habitat extent covered by each flood duration (months) zone) during hydrological (a) average, (b) dry, and (c) wet years. Only habitats that covered greatest areas are shown.

Based on the dominance and preference analysis, five habitat groups with distinct distribution of flood duration conditions were defined: rainfed habitats, transitional habitats, seasonally flooded habitats, gallery forest, and open water (Table 3.3). Rainfed habitats included wet season rice, village crops, and lowland shrubland, defined by flood duration of 0-1, 0, and 0-3 months during average, dry, and wet years, respectively. Transitional habitats was defined as the area flooded for 1-5, 0-1, and 3-6 months during average, dry, and wet years, respectively, and it included abandoned fields, lowland grassland, and floating and receding rice. Seasonally flooded habitats included flooded shrubland and flooded grassland. This group was defined by flood duration of 5-8, 2-7, and 6-11 months during the average, dry, and wet years, respectively. Gallery forest was left as a single habitat since it dominated the transitional area between the seasonally flooded habitats and the open water (flood duration of 9 months during average and dry years and 9-12 months in a wet year). Open water was classified as the areas flooded for 10-12, 9-12, and 10-12 months during average, dry, and wet years, respectively. The baseline cover map derived from these flood duration rules was in good agreement (that is, a large area of overlap) with the spatial distribution of habitats from JICA (1999; Table 3.3).

Table 3.3. Flood duration rules used for modelling habitat cover and validation results. LULC = land use/land cover. Overlap refers to the area of agreement between the original and the simulated maps.

Habitat groups	LULC class(es)	Months of annual flood duration			Cover area (km^2)			% Overlap
		average year	dry year	wet year	Original	Model	Overlap	
Rainfed habitats	Wet season rice, village crops, lowland shrubland	0-1	0	0-3	8,641	8,386	6,999	81
Transitional habitats	Abandoned fields, floating and receding rice, lowland grassland	1-5	0-1	3-6	3,658	4,744	2,327	64
Seasonally flooded habitats	Flooded shrubland, flooded grassland	5-8	2-7	6-11	5,409	4,787	3,873	72
Gallery forest	Gallery forest	9	9	9-12	197	657	51	26
Open water	Open water	10-12	9-12	10-12	3,027	2,550	2,431	80
				Total	21,067	21,067	15,682	74

Flood duration rules defining each of the 5 habitat groups (Table 3.3) were then used to simulate the most likely changes in habitat due to potential future scenarios of water infrastructure development and climate change. Area extent and the percent difference with respect to the baseline cover map were calculated for each of the habitat groups (Table 3.4). Area of rainfed habitats could increase by 10-14% for all water infrastructure development scenarios and could decrease by up to 5% for the climate change scenarios. Area of transitional habitats could decrease up to 6% as a result of both infrastructure development and climate change scenarios. Area of seasonally flooded habitats could decrease by up to 22% as a result of infrastructure development, but could increase slightly as a result of climate change. The area most suitable for gallery forest could decreases by up to 83% as a result of development and up to 69% as a result of the 2040 climate change scenario. Maps displaying these results show clear habitat shifts as a result of future scenarios (Figure 3.9); alterations due to water infrastructure development show a large shift from gallery forest to open water, from seasonally flooded habitats to transitional habitats, and from transitional to rainfed habitats. Climate change scenarios also showed a large expansion of the open lake for

the 2040 scenario. Other notable shifts for the climate change scenarios were seasonally flooded habitats shift to gallery forest, transitional habitats shift to seasonally flooded habitats, and rainfed habitats shift to transitional habitats.

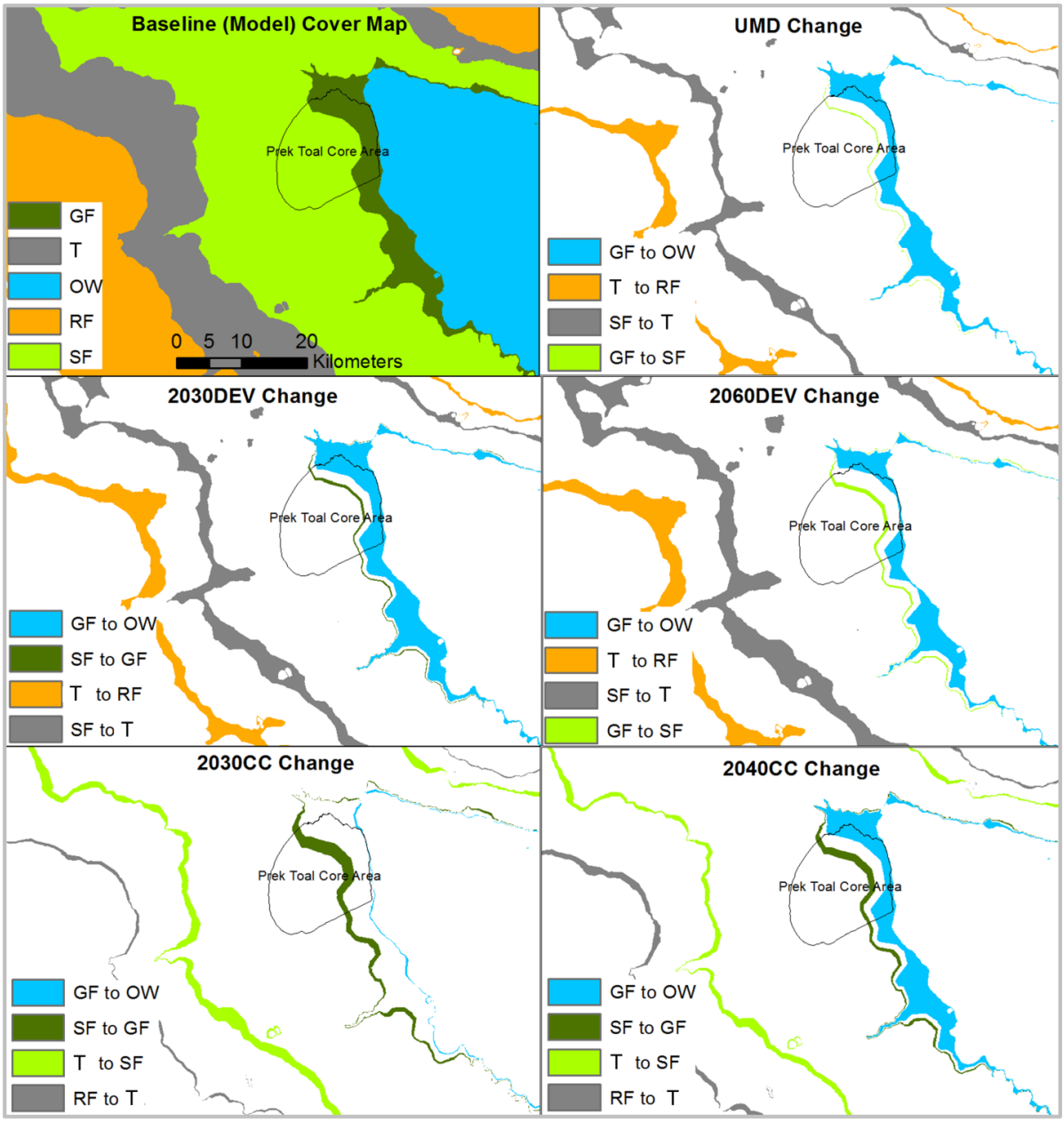

Figure 3.9. Shifts in habitat cover from the baseline model map in area around Prek Toal, the largest core area of the UNESCO Biosphere Reserve. RF = rainfed habitats, T = transitional habitats, SF = seasonally flooded habitats, GF = gallery forest, and OW = open water.

Table 3.4. Area change from baseline (modelled) habitat cover as a response to different future scenarios.

Model scenario	Rainfed habitats		Transitional habitats		Seasonally flooded habitats		Gallery forest		Open water	
	km^2	%	km^2	%	km^2	%	km^2	%	km^2	%
UMD	813	10	-189	-4	-612	-13	-537	-82	525	21
2030DEV	1061	13	-281	-6	-810	-17	-536	-82	567	22
2060DEV	1215	14	-133	-3	-1041	-22	-495	-75	454	18
2030CC	-201	-2	-265	-6	339	7	84	13	42	2
2040CC	-384	-5	84	2	219	5	-451	-69	531	21

3.4 Discussion

3.4.1 Historical changes in water levels, flood extent, and LULC

The changes in water level and flood extent in the Tonle Sap calculated in this study are consistent with findings from previous studies (Fujii et al. 2003; MRC 2005; Inomata & Fukami, 2008; Kummu & Sarkkula, 2008), which revealed little change in recent past decades in water levels and flood extent (hence, flood duration). Some of the cited studies have analyzed longer time series at stations in the Tonle Sap and Mekong Rivers, and their results show that the years used to represent recent historical conditions for the Tonle Sap (1997, 1998, and 2000) are appropriate. Recently, Räsänen et al. (2013) confirmed the significance of these hydrological years by pointing out that 1998/2000 are among the 10 driest/wettest years in more than seven centuries.

Despite the limited water level time series available at Kampong Loung, it appears as if decadal patterns of extreme events are influenced by ENSO patterns as it has been suggested for the entire Lower Mekong (Delgado et al., 2012; Räsänen & Kummu, 2013); extreme floods match strong La Niña years whereas droughts match years of strong El Niño. This linkage between regional and local climate patterns could be useful in studying long-term historical and future climate change in the absence of local long-term hydrological data. Other approaches to overcome the data limitation could be to expand the regression

relationships with other stations with longer historical records (Inomata and Fukami, 2008), or to use other long-term hydrological indicators such as sediment or tree cores (Buckley et al., 2010; Day et al., 2011). This later approach has already been studied for the Mekong River at Stung Treng (Räsänen et al., 2013).

A broad comparison of the two classified floodplain-wide land cover maps (1996 and 2005) revealed expected changes in habitats that followed documented land use modifications in the floodplain. The expansion of village crops and conventional rice paddies can be explained by the economic expansion and population growth following the end of a long period of civil conflict. Abandonment of floating rice fields has occurred since the late 1970s (Hand, 2002; Nesbitt, 1997; Sarkkula et al., 2003), and the results of our analysis suggest that some of the abandoned fields have more recently been cropped again for conventional rice paddies. An unexpected finding was the expansion of the area classified as gallery forest. Nearly all the area classified as gallery forest in FA (2005) was previously classified by JICA (1999) as either shrublands or grasslands, suggesting that the change in habitat of this small area (yet largest in terms of standing biomass per unit area) has occurred either as an unlikely example of natural succession occurring over short time scales, or as the result of different classification criteria and erroneous interpretation of the remote sensing data. The intention of this historical habitat change evaluation was to acknowledge the changes that might have occurred in the floodplain during a period when no significant changes in flooding regime occurred. Changes in the outer portions of the floodplain – covered primarily with agricultural fields – were expected, as flooding is not as dramatic in this area and it could be more easily regulated than areas closer to the lake. On the contrary, a larger portion of the floodplain, where seasonal flooding is much more prominent, has experienced much smaller habitat shifts. These observations suggest that flooding has played

a major role in the habitat distribution of the floodplain, primarily by preventing agriculture in areas where flooding is too deep and lasts too long.

3.4.2 Future changes in water level and flood duration

Moderate changes in average monthly water levels were projected by the MRC-DSF and Aalto's modelling schemes. Water infrastructure development is expected to shrink the flood-pulse magnitude by raising water levels during the dry season while reducing water levels during the wet season. Climate change will result in slightly higher water levels during the start of the wet season and moderately higher levels during its peak. Overall, more pronounced changes are expected during dry years than during wet years. Although slightly different trends, both models predicted water level changes of similar magnitude, implying that their input databases and modelling frameworks are similar and hence their results are comparable. This was not the case with previous modelling efforts, which showed large discrepancies and predicted much larger changes as a result of climate change (Eastham et al., 2008) than as a result of water infrastructure development (WB, 2004). In short, the water level changes predicted by the models used in this study seem to provide a higher level of confidence than previous predictions, transferring less uncertainty to subsequent predicted habitat changes.

Regarding hydropower, it is worth mentioning that the MRC model scenarios did not include detailed analysis of impacts from dams on Mekong tributaries such as the 3Ss, which contribute a large fraction of the mean annual Mekong River flow. Development of the 3Ss full hydropower capacity will have a similar impact on water flows than the hydropower scheme of the Upper Mekong Basin in China (Piman et al., 2012). This overlooked factor will subsequently alter the water levels in the Tonle Sap to a greater extent than current estimates. With regard to climate change, the scenarios presented in this chapter do not fully

represent differences among IPCC scenarios and GCMs, factors which have been suggested to bring the most variability to future projections of Mekong's hydrology (Lauri et al., 2012). These factors, however, are incorporated and discussed in Chapter 5.

Changes in annual flood extent and duration are slightly more pronounced than changes in monthly water levels. Overall, water infrastructure development is expected to reduce the flood extent by up to 1,200 km^2, while climate change scenarios are expected to increase the flood extent by up to 1,000 km^2. The greatest changes from baseline conditions will probably occur during average years, whereas wet years will probably experience the least changes. The trends and magnitude of flood duration estimated in this study are in agreement with the ones from Västilä et al. (2010) and MRC (2011). The areas that are likely to be affected the most are those at the fringe of the open water, with flood duration of 9-10 months, and half way between the open water and the edge of the floodplain, which is flooded approximately 4 months of the year. Overall, extensive changes – in the order of 100-1,000 km^2 – are expected in the spatial distribution of flood duration as a result of sub-meter changes in water levels, a magnified effect that would be expected in a floodplain as large and as flat as the Tonle Sap. The magnitude of these spatial changes in flood duration highlights the importance of this assessment to the overall understanding of the hydrological and ecological changes in the Tonle Sap, and it also suggests that a similar magnification of disruptions may occur in other large floodplains with comparable dimensions and biophysical conditions.

3.4.3 Modelling approach

A large fraction of landscape-scale vegetation patterns was explained solely as a function of flood duration, which is extremely useful to isolate and quantify future ecological impacts as a result of hydrological alterations. A considerable amount of work has been done on the hydrology of the Tonle Sap and the Mekong, and this chapter demonstrates how to link

hydrological and ecological changes using empirical, in situ observations. Although the model developed in this study was based on a classification rule scheme, it used a robust methodology that considered the full range of historical hydrological conditions as well as the full distribution of habitats through the Tonle Sap landscape. The five hydrologically-distinct habitat groups take into account both the adaptation of each habitat to flooding (i.e., optimal or preferred hydrological conditions for each habitat; Figure 3.8), as well as the competition among habitats for a single flood zone (i.e., dominance of habitats on flood duration zones; Figure 3.7). Although this chapter presents results for groups of habitats that have a common flood duration regime, an extra procedure has been added to this approach to distinguish between habitats of equal flood duration by considering the historical habitat cover; basically, if there are no changes in flood duration between historical/baseline and future conditions, the original habitat type in the baseline map is assumed to remain. Conversely, if there is a shift in the flood duration for a specific area, it is reclassified to the most widespread habitat within the group with common flood duration. This additional procedure is incorporated in the analysis of Chapters 5 and 6.

Nonetheless, the modelling approach has a number of limitations. First, the model uses an empirical approach to relate hydrological patterns to vegetation, and therefore, future projections are assumed to be shifts to existing habitat groups without considering the possibility of new ones to emerge. Moreover, the approach does not take into account habitat succession, as there are no documented observations on how this concept applies to the Tonle Sap ecosystem. Therefore, projected maps represent snapshots of the floodplain's habitat cover once hydrological alterations from future scenarios persist for sufficient time for habitats to establish. Although each of the future scenarios have a corresponding tentative decade for when they are likely to occur, this refers to the hydrological simulations, and all that can be stated with regards to habitat cover is that shifts would occur years after the

hydrological alterations. Furthermore, some of the classes from the JICA (1999) map were too small and/or determined by human use, and therefore they were not accurately estimated as a function of flood duration alone. For instance, the optimal area for gallery forest simulated was considerably larger than what was classified by JICA (1999) or FA (2005). One reason for the mismatch could be because this small habitat is surrounded by open water and seasonally flooded habitats, both of which cover extensive areas that strongly influenced the dominance flood duration relationship. Another reason could be that the gallery forest is the most intact section of the seasonally flooded gradient, and the unique vegetation structure of this habitat is an artefact of restricted human use in comparison to sections further upland. Furthermore, very similar hydrological conditions were found between flooded shrublands and grasslands, yet these two habitats have distinct vegetation species and structure. Field observations elucidate answers to these two anomalies, as it appears that gallery forest, flooded shrubland, and flooded grassland are part of a compositional gradient rather than distinct habitat types; gallery forest and flooded shrublands share similar vegetation composition, and the distinction between these two and seasonally flooded grasslands could be related to recent fire and cattle grazing (see Chapter 4). While subsequent chapters and ongoing research address the limitations summarized above, the methodology and results from this chapter present a simple and comprehensive model that could be used as a research and large scale management tool for the Tonle Sap.

3.4.4 Habitat cover changes

Large shifts in habitat cover could occur as a result of future scenarios of water infrastructure development and climate change. Although there have not been other attempts to model future habitat cover change on the Tonle Sap, the results of this assessment are in agreement with trends of potential impacts to the Tonle Sap ecosystem documented by others (Kummu & Sarkkula, 2008; MRC, 2010; MRC, 2011); water infrastructure development reduces the

spatial extent of seasonally flooded habitats and gallery forests while favouring rainfed/irrigated agricultural areas. These changes in habitat cover could have large implications to the overall functioning and productivity of the Tonle Sap ecosystem; forests and shrublands have the greatest standing biomass per unit area, hence these habitats provide a major role in sediment deposition, nutrient cycling, periphyton growth, primary production, fish food and refuge. This subject is related to impacts to ecological function and it will be quantified and described in more detail in Chapter 5.

Habitat shifts resulting from the development scenarios are substantial and that a large magnitude of the expected changes could begin happening soon as a result of the definite future scenario. Hence, it is crucial to begin monitoring environmental changes through field and remote sensing observations. Other studies have shown how remote sensing data can be used to assess inundation and vegetation changes in the Tonle Sap (e.g., Benger, 2007; Fujii et al., 2003; Milne and Tapley, 2004; Van Trung et al., 2012); yet, historical changes have not been previously quantified. Habitat cover shifts solely as a result of climate change showed a different picture than water infrastructure development scenarios, especially with respect to the rainfed habitats and seasonally flooded habitats. The estimated changes for the gallery forest and the open water, however, are similar to the development scenarios, with a net increase in open water area. Overall, the magnitude of shifts resulting from climate change was found to be smaller than those from water infrastructure development scenarios. This finding should not undermine the potential impacts from climate change, but it should instead promote more detailed and robust modelling of cumulative impact scenarios as it is shown in Chapter 5.

Regardless of which future scenario could bring more significant shifts, natural resources managers and authorities in Cambodia have little or no control over the drivers of these changes, and the choices that they are faced with have more to do with the

implementation of management strategies that would lead the floodplain towards a smoother transition that minimizes impacts to the ecosystem services historically provided by the Tonle Sap. By taking into account the potential habitat shifts, Tonle Sap managers could guide how and where to focus present and future efforts on habitat conservation and/or restoration. Based on the results of this assessment, habitat conservation and restoration should take place in areas most suitable for natural habitats (aka., grasslands, shrublands, and gallery forests) and least useful for rice cultivation under future hydrological regimes. A non-trivial fraction of the current grasslands, shrublands, and gallery forest could be replaced by permanent water and rice fields in the near future; yet, this study shows that a large area of the floodplain will probably be subject to the appropriate flooding conditions to support these habitats, mainly in areas that flood 5-9 months in average years, at least 2 months in dry years, and at least 6 months during wet years. It is important that conservation of these areas become a priority to ensure that the Tonle Sap ecosystem reaches a maximum potential of productivity in the future.

3.5 Chapter conclusions

This chapter combined hydrological and geographical information to establish the relationship between inundation and vegetation patterns in the Tonle Sap and to quantify how these patterns could shift as a result of disruptions from water infrastructure development and climate change in the Mekong. The results indicate that landscape-scale spatial distribution of habitats in the Tonle Sap is largely driven by flood duration patterns; humans are secondary drivers of change. Flooding alters habitats in the Tonle Sap first by delimiting the area where agriculture (primarily rice) takes place in the floodplain; cultivated areas are restricted mainly to the outer part of the floodplain where unregulated flooding only occurs for a few days in wet years. Within the non-cultivated areas of the floodplain, plant species are distributed

according to their tolerance to the flooding regime, water stress during the dry season, and human use.

Maps of LULC and inundation patterns were used to develop a set of rules to project habitat type based on their dominance and preference of flood duration zones. These flood duration rules were able to map five distinct habitat groups: (1) open water, (2) gallery forest, (3) seasonally flooded habitats, (4) transitional habitats, and (5) rainfed habitats. The accuracy of the mapping tools presented in this chapter were validated against field and remote sensing observations, decreasing the degree of uncertainty associated with this type of spatial analysis and subsequent projections. However, the flood duration rules were not able to discern habitats with small areal coverage and/or with common flood duration patterns. Therefore, an additional step that takes into account historical LULC was added to the procedure and is incorporated to the analyses of subsequent chapters.

Flood duration rules were combined with water level projections to quantify changes in habitats as a result of future scenarios of basin-wide hydrological change. Water infrastructure development would lead to the expansion of rainfed habitats, while decreasing the area covered by seasonally flooded habitats. In contrast, the climate change scenarios considered could enhance the optimum conditions for seasonally flooded habitats, but only to a small extent. Despite contrasting results, both sets of future scenarios (development and climate change) agreed on the increase of open water area and a net reduction of the optimum area for gallery forest. Therefore, combined scenarios of hydropower development with climate change are expected to result in shifts of even greater magnitude. These large shifts could have major implications to the Tonle Sap ecosystem, including changes in sedimentation, nutrient cycling, vegetation structure, primary production, fauna, and livelihoods. Some of these potential impacts are addressed in greater detail in the subsequent chapters.

Despite the magnitude of potential habitat shifts, local authorities and managers have very limited possibilities to control basin-wide drivers of change. Therefore, their role should focus on implementing protocols to monitor environmental/ecosystem changes, informing stakeholders about observed and potential impacts, and promoting ecosystem protection and restoration of areas most suitable for natural floodplain habitats in the near future.

CHAPTER 4: UNDERLYING DRIVERS OF HABITAT CHARACTERISTICS

4.1 Introduction

Little is known about the Tonle Sap as an ecosystem. Data on essential components such as sediments, biogeochemical cycles, vegetation characteristics, primary production, and fish ecology are scarce (Kummu et al., 2006; Lamberts, 2006). Even though the historical natural flood regime of the Mekong River is changing as a result of water resources infrastructure development and climate change, how these changes will affect the Tonle Sap ecosystem is not well understood. Some studies have already explored this issue with limited data (Arias et al., 2012; Kummu and Sarkkula, 2008; MRC, 2010b), but their findings have concentrated mainly on spatial habitat cover changes but little with regard to habitat characteristics. While these large-scale investigations are important to understand landscape patterns and their future changes, research and environmental impact assessments in the Tonle Sap and the Mekong will not go much further without quantitative observations linking the hydrology to other key ecological components such as soils, vegetation, and water quality.

Considering the absence of quantitative field data describing the Tonle Sap habitats, the main objective of this chapter is to identify the main drivers of habitat characteristics in the Tonle Sap floodplain. Focusing on observations collected directly in the field, the following questions are addressed:

1. What is the relationship among hydrological indicators, including water depth, flood frequency, annual flood duration, and soil moisture?
2. What is the influence of hydrological indicators on soils, human use, water quality, and current vegetation patterns?

3. What is the influence of hydrological indicators, soils, and human use on plant species composition?

4. How could habitat characteristics change with ongoing hydrological disruptions?

To answer these questions, field work was carried out in a number of sites that cover the full range of flood regimes and habitats in this wetland. The research questions were explored through bivariate and multivariate statistical procedures among the hydrological and habitat characteristics quantified.

4.2 Methods

4.2.1 Field sites description

Field surveys were undertaken in three distinct areas around the lake (Figure 4.1), providing a good representation of the different natural and agricultural habitats that exist in the floodplain and covering all 5 provinces surrounding the lake (Kampong Chnnang, Pursat, Battambang, Siem Reap, and Kampong Thom). The study areas were chosen because they are under protection by the Cambodia Ministry of the Environment or Conservation International –Cambodia, both of whom facilitated logistics and field guidance. Two of the sampling areas, Stung Sen and Prek Toal, included core zones of the UNESCO Tonle Sap Biosphere reserve (Hellsten et al., 2003; McDonald et al., 1997). The other study area, Kampong Prak, lies within the Biosphere reserve buffer zone in Pursat Province.

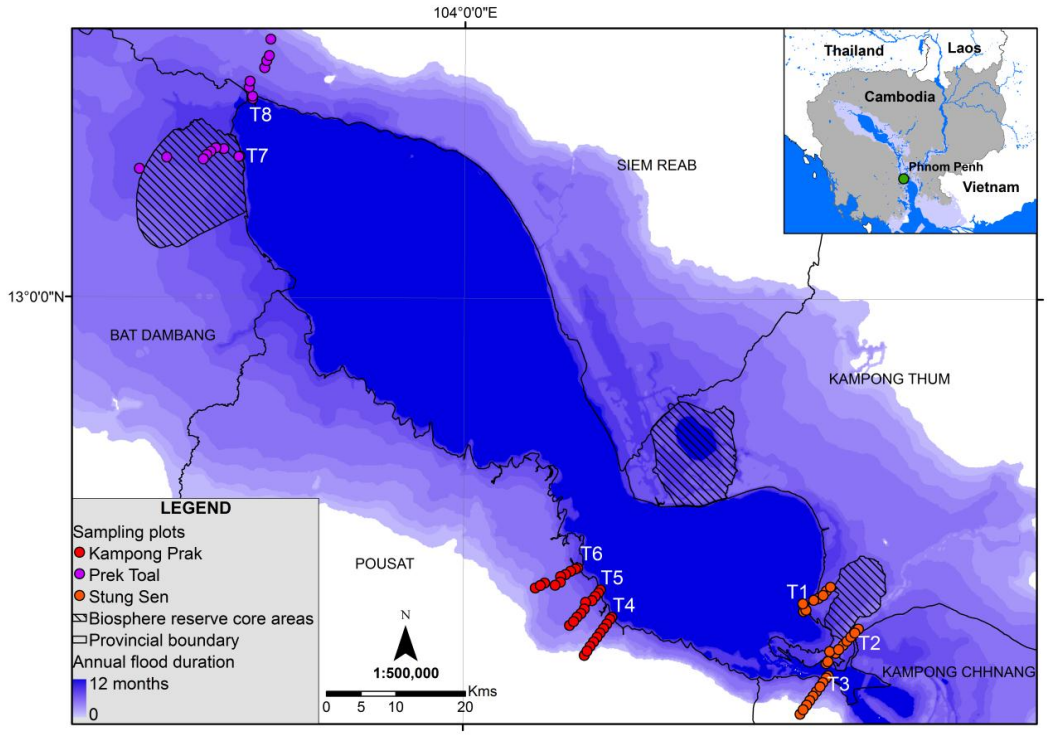

Figure 4.1. Sampling plot locations along survey transects T1-T8 overlaid on an average annual flood duration grid.

4.2.2 Data collection procedure

A total of eight transects were surveyed across the floodplain in the 3 study areas described above. 3 transects were surveyed in both Stung Sen and Kampong Prak, and 2 transects were surveyed in Prek Toal, where access during the dry season proved to be extremely difficult. Each transect started at the edge of the lake and followed the elevation gradient to cover the largest range of flooding conditions and vegetation communities (Figure 4.1). Overall, seventy seven 100 m^2 plots were measured in transects covering a distance of 5 to 15 kilometres, with field work carried out between March 2011 and March 2012.

Information on water regime, soil characteristics, vegetation, water quality, and human use were collected for each plot. Accompanying survey data included a general description of the area, GPS coordinates, present land use/land cover (LULC) according to classes defined in existing maps (JICA, 1999) and previous studies (Araki et al., 2007; Hellsten et al., 2003; McDonald et al., 1997), water depth, and photographs facing all four cardinal points.

An index of human use was determined based on evidence of wood extraction, evidence of recent fire in vegetation and soils, and presence of cattle. Surface soils (< 30 cm) were described according to the Food and Agricultural Organization soil description guidelines (FAO, 2006). Soil moisture and pH were measured in the field using handheld probes, and in addition, soil composite samples (500 g) from horizons A and B were collected in plastic bags for laboratory analyses. Particle size, pH, colour, electrical conductivity, and nutrients were analyzed at Research Development International-Cambodia (RDI) near Phnom Penh. Soil moisture and organic matter were analyzed at the Faculty of Agronomy of the Royal University of Agriculture (RUA) in Phnom Penh. Soil moisture was determined by weight difference after drying the samples at 105°C for at least 24 hours. Organic matter was estimated by the ignition loss method (weight loss of the soil after putting the samples in a muffle furnace at 600°C for 5-6 hours). Particle size fraction was determined using a hydrometer. pH and electrical conductivity were measured on a 1:5 by mass solution of soil to distilled water using an YSI handheld digital probe. Soil colour was recorded for dry and wet samples using standard Munsell colour charts. Nitrogen and potassium were analyzed using LaMotte colorimetric tests.

For vegetation sampling, plants were classified as either canopy or understory based on a diameter at breast height (DBH) threshold of 3.2 cm (equal to a 10 cm circumference). At the canopy level, all trees, lianas, and large shrubs within the 100 m^2 plot were identified, DBH recorded, one wood core per species extracted, and maximum height per species estimated using a tangent height gauge. Canopy cover was measured with a canopy densiometer at the centre of the plot facing each cardinal point. For measurements of the understory and ground vegetation cover, three 1 m^2 quadrants were randomly located within the larger plot. Understory cover was measured by placing the canopy densitometer at ground level, and ground vegetation cover was based on a visual estimate. All understory and ground

plants on the 3 quadrants were identified, and measurements per species included: diameter at ground level, height, stems count or ground coverage, and wet weight using an analogue ±10 g scale. Cover and biomass of standing litter in the 1 m^2 quadrants were also measured to provide an indicator of the litter available to the aquatic phase just before flooding. Selected samples of the harvested vegetation and litter were taken to RUA to determine moisture content. Plants were given unique identities in the field using a reference guide compiled from names, photographs and descriptions from previous field visits, and from previous work by Dy Phon (2000), McDonald et al. (1997), and Davidson (2006). Plant specimens were pressed and taken back to Phnom Penh where they were identified and stored at the National Herbarium of Cambodia at the Royal University of Phnom Penh. 10 of the 88 plant species encountered were not identified to the species level, and therefore a unique id (using the family name when known) was used for subsequent analyzes.

The vegetation information collected in the field was used to estimate above ground biomass (AGB) per unit area. AGB of woody vegetation at the canopy level (trees, lianas, and large shrubs) was estimated with an allometric equation for tropical dry forest (Chave et al., 2005), which estimates AGB as a function of wood density, tree height, and DBH. AGB for understory vegetation was estimated from direct harvest of most quadrants and allometric equations in other occasions. No allometric relationships for understory plants existed for the Tonle Sap, so these were developed from 242 harvested samples. One equation was developed for shrubs as a function of diameter, height, and wood density, and for herbaceous vegetation as a function of vegetation coverage and height (See Appendix B).

Water quality was assessed at the peak of the wet season in September-October 2012 at the same locations where vegetation and soils were surveyed during the dry season. Temperature, specific conductance (as a measure of conductivity corrected for temperature), pH, DO concentration, and DO saturation were measured with an YSI Pro Plus handheld

digital probe with a 4 m long sonde; measurements were taken at depths of 0.5, 1, 2, 3, and 4 m. In addition, water samples were collected at half of the total depth with a 1 L PVC sampler that allowed water to flow through before it was closed at the correct depth (Figure 4.2). Three samples were collected on each site, one in a 300 mL bottle for total suspended solids (TSS), one in a 100 mL bottle for Nitrate (NO_3^-) analysis, and another one in a 100 mL acid-washed bottle containing 2 drops of Hydrochloric acid solution for Total Phosphorus (TP) and Ammonia (NH_3) analysis. One duplicate and one blank (Deionised water) were bottled at random times in each of the three sites. Samples were taken to the water laboratory at RDI for analytical processing within 3 days of collection. TSS was determined by filtering the full content of the 300 mL bottle through a fibre glass filter with a 0.45μm pore size and then drying the filter for 24 hours at 105°C. NO_3^- was analysed with an ion chromatographer. A sample was prepared for TP by carrying an acid persulfate digestion (APHA/AWWA/WEF, 2005). TP and NH_3 were analysed in a DR/2400 Hach spectrophotometer using the methods described in HACH (2003). All analytical procedures in the laboratory used standard calibration procedures and additional duplicates/controls for quality assurance/quality control.

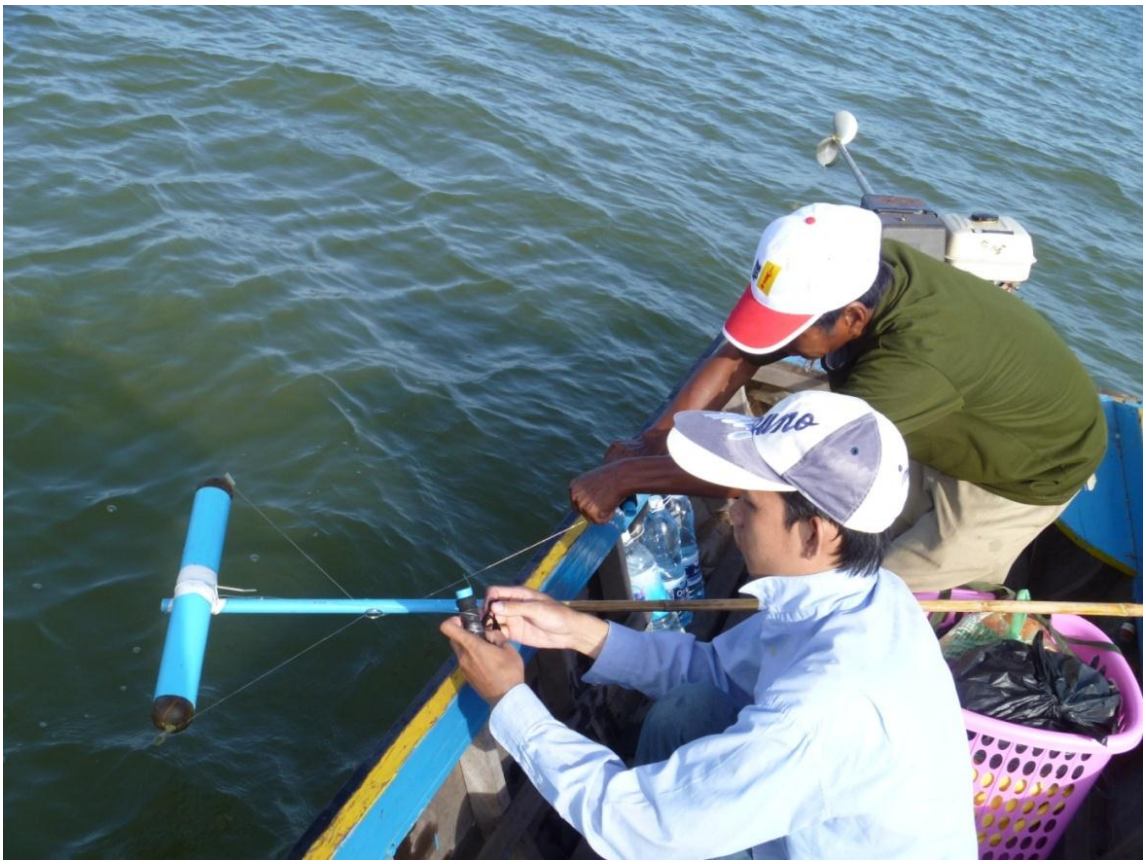

Figure 4.2. Research assistant using the water sampler.

4.2.3 Hydrological data

Mean annual flood duration, flood frequency, and maximum water depth were used as surrogates of hydrological conditions for establishing relationships to soil, human use, and vegetation. Records of daily water level since 1997 exist at Kampong Luong (N12° 34.598 E104° 12.472). There is a strong linear relationship between water levels at Kampong Luong and water levels in the Tonle Sap River at Prek Kdam (40 km away from Phnom Penh; Inomata and Fukami, 2008), and we used this relationship to extend the Kampong Luong time series back to 1986. The hydrological patterns observed during 1997, 1998, and 2000 represent well the average, dry, and wet conditions, respectively, of the contemporary water level patterns (See Chapters 2 and 3; Kummu and Sarkkula, 2008). Water levels were used in combination with a digital elevation map with a 100 m horizontal resolution to create maps of annual flood duration (number of days per year with standing water) and flood frequency

(fraction of years when flooding occurs). A detailed methodology of how flood duration and frequency maps were created and validated is provided in Chapter 3. These hydrological parameters were then determined for each survey plot by overlaying the GPS coordinates on the maps and matching the flood duration and frequency values to the survey points using GIS zonal statistics tools. Moreover, water depth was measured directly on each of the survey plots with a Dr Lange HT 1 probe and/or a Speedtech Instruments water depth probe within 23 days of the peak of the wet season in October 2011. Records at Kampong Luong were used to correct the field measurements to represent the maximum water level during the season, with a maximum difference of 51 cm (only 5% of the maximum water depth, 9.92m). Water levels during the 2011 wet season were similar to levels from 2000, the largest ever measured on the lake.

4.2.4 Statistical analyses

Prior to carrying out any statistical inferences, measured datasets were checked for normality using histograms, qq plots, and the Shapiro-Wilk test. To fulfil normality conditions a square-root transformation was applied to AGB, height, litter cover, ground cover, understory cover, canopy cover, species richness, and soil pH data. In order to explore the relationship among hydrological indicators, linear relationships among hydrological indicators (flood duration, flood frequency, maximum water level) and soil moisture were evaluated with Pearson correlation coefficients (r) using pairwise comparisons. Depth-weighted averages of water quality variables were calculated for each location, and these averages and the soil variables were also compared to hydrological indicators using Pearson correlations. Moreover, water quality and soil variables were standardized and two different sets of principle components (PCs) were calculated to determine the main gradients of variance among these variables and their relationship with flooding. Along with the PCs, the relative weighting that each variable has on them is calculated; the greater the magnitude of this score, the greater the association

between the variable and the PC. Negative weighting values imply an inverse relationship. Furthermore, the impact of clearance (presence of recent crops and fire) on vegetation structure (height, canopy cover, and AGB) and its spatial distribution along the flooding gradient were examined using analysis of variance (ANOVA). The role of hydrology and soils in predicting vegetation structure was evaluated with linear models for all possible interactions among flood duration and soil PCs. The linear models were compared according to the predictability (r^2 coefficients) and the model's certainty (p-value). Plots outside the seasonal floodplain (permanent lake and village crops not flooded during the 2011 wet season) were excluded from both the ANOVA and the linear models of vegetation. The relationship between habitats and water quality was explored in 2 different ways. First, profiles of the parameters measured at multiple depths were plotted to provide general descriptions with respect to each habitat. Second, the two largest water quality PCs were used to create boxplots for each habitat. Homogeneity of variance among habitats was tested with the Barlett's test, which examines the probability that the groups in question came from populations with equal variance (Bartlett, 1937). If the variance homogeneity assumption was valid, difference in means among habitats was explored with pairwise ANOVA comparisons. All statistical analyses were done using the software R 2.13.1 (http://www.r-project.org/).

The influence of flood duration, soils PCs, and human use on plant species composition was analyzed using two ordination techniques: Detrended Correspondence Analysis (DCA) and Detrended Correspondence Canonical Analysis (DCCA). DCA is an indirect gradient technique in which the underlying structure of the plant species composition is extracted and compared with environmental gradients; in contrast, DCCA is a direct gradient technique in which the axes of plant species composition variation are constraint by selected environmental variables (Ter Braak, 1986). Similarities in the results from the DCA and DCCA imply that the intrinsic variance in plant species composition is caused by the

measured environmental variables. Both techniques were applied using the software CANOCO (Lepš and Šmilauer, 2003) with the same input data: one matrix of species presence/absence per plot, and another matrix with measured environmental variables from each plot. The predictability of these techniques was assessed via Eigenvalues of plot scores (a measure of how much variation is explained along the gradient axes in standard deviation units), species-environment correlations (linear correlations between the environmental gradients and the species composition axes), and interset correlations (linear correlations between the environmental data and the plot scores of plant species; Ter Braak, 1986). The environmental variables were analyzed in two different groups: one with flood duration, soils PC's, and human use (a value between 0 and 3 based on the presence of fire, agriculture, and/or cattle), and another with biological-based variables (AGB, height, litter cover, ground cover, understory cover, canopy cover, and species richness). Plots outside the seasonal floodplain and plots with only one plant species were excluded from the analyses as they formed outliers in the ordinations.

4.3 Results

In order to provide a general description of hydrological patterns, soil characteristics, and vegetation communities along the flooding gradient, diagrams of transect elevation profiles and a summary table were prepared (Figures B1-B2; Table 4.1). All the transects started at an elevation of approximately 1.5 m amsl (measured at Hatien, Vietnam), which is the mean water surface elevation during the dry season, and the highest elevation surveyed was 11.5 m amsl, well above the maximum water level recorded (10.3 m amsl). The average terrain slope was 0.06%, varying from 0.01% to 0.14%. %. In general, greater habitat and plant species variation was associated with steeper slopes, while transects with flattest terrain had the most contiguous stands of seasonally flooded trees and shrubs. At elevations below 2 m amsl (flood duration between 8 and 10 months annually), soils were predominantly sandy clays

and habitats include aquatic grasslands and gallery forest with little understory coverage (open forest) and a moderate number of plant species (average 3-5 per 100 m^2). Between 2 and 5 m amsl (flood duration 5-8 months per year) soils were mainly clays, and habitats included closed forest with understory, shrublands, and grasslands with an average of 4-6 species per 100 m^2. 4 of the 5 seasonally flooded grasslands had evidence of fire in recent years. Between 5 and 9 m amsl, (flood duration 1-5 months per year), soils ranged from clay loams to loams, and vegetation gradually transitioned into a mosaic of natural and agricultural habitats, with tall shrublands, floating and recession rice fields, and abandoned rice fields. Because of the mixed habitat types and human uses, this region had the most variation in species richness, with 9 ± 2 species per 100 m^2 in tall shrublands to 3 ± 2 per 100 m2 in the abandoned fields. Above 9 m amsl, natural flooding from the Tonle Sap lasts a maximum of 1 month annually, and it remains dry for at least 3 in every 10 years. Therefore, this upper part is dominated by conventional rice paddies and village crops that cannot tolerate long and deep flooding; rainfall and irrigation are the primary means of water for agriculture in this region. Soils in this area had a sandy loam texture and land use was dominated by conventional rice paddies and village crops were mainly flood intolerant varieties such as citrus, mangos, cashews, and sugar palm. Photographs of some of the sites representing the habitats described in this paragraph are shown in Figure 4.3 and detailed information collected on each location is provided in Appendix B.

ANOVA tests showed that there are no significant differences in canopy height, canopy cover, or aboveground biomass among the 3 survey sites (Stung Sen, Kampong Prak, and Prek Toal). There appears to be differences in species richness at the 95% confidence level between Stung Sen (2.1 ± 0.6) and Kampong Prak (2.6 ± 0.8), but species richness in Prek Toal (2.2 ± 0.6) was not significantly different from the other two. Overall, 25 of the 88

plant species encountered were present in all 3 regions, and another 15 were found in at least two sites.

Table 4.1. Mean and standard deviation (in parenthesis) of computed flood duration and field observations for each habitat. See Appendix B for detail information collected at specific locations and full names of plant species.

Habitat	n	Flood duration (days)	Water max depth (m)	Soil Moisture (%)	Clay (%)	Sand (%)	Soils organic matter (%)	Species richness	Code for key plant species	Ground cover (%)	Canopy cover (%)	Max height (m)	total AGB[a] (kg/m^2)	*Clearance*[b]
Open water	2	335 (43)	9.5 (0.2)	49 (1)	33 (4)	56 (5)	1.7 (0)	0 (0)	NA	0 (0)	0 (0)	0 (0)	0 (0)	NA
Aquatic grassland	4	277 (35)	8.9 (0.3)	33 (13)	41 (5)	31 (9)	10.3 (3.9)	3 (2)	*Brachi*	70 (5)	3 (5)	1.7 (0.6)	0.9 (0.3)	0
Open forest	8	240 (48)	8.4 (0.6)	30 (7)	46 (9)	38 (11)	10.2 (5.0)	5 (2)	*Barrin*	35 (28)	30 (31)	8.2 (4.4)	2.3 (1.7)	3
Closed forest	19	229 (46)	7.6 (0.7)	24 (10)	49 (8)	31 (11)	8.5 (2.1)	6 (2)	*Barrin*	20 (12)	63 (23)	11.2 (3.9)	3.1 (3.1)	4
Shrubland	12	210 (40)	6.9 (0.8)	21 (7)	54 (14)	32 (12)	11.4 (4.0)	4 (2)	*Vitex*	23 (10)	58 (16)	4.4 (1.7)	1.4 (1.9)	4
Grassland	6	208 (12)	8.0 (0.3)	24 (8)	50 (9)	32 (13)	9.0 (3.1)	5 (2)	*Mimosa*	46 (25)	13 (11)	3.4 (3.7)	0.6 (0.4)	5
Tall shrubland	12	149 (26)	5.2 (1.2)	16 (6)	34 (11)	44 (11)	9.4 (2.6)	9 (2)	*Hymeno*	19 (8)	61 (14)	6.6 (2.1)	2.0 (1.4)	3
Receding rice	2	137 (13)	5.3 (0.3)	26 (1)	30 (13)	56 (12)	5.8 (4.7)	8 (0)	*Orysat*	55 (1)	0 (0)	3.4 (4.0)	0.7 (0.1)	2
Floating rice	3	110 (23)	4.4 (0.7)	14 (7)	36 (18)	47 (14)	5.5 (4.0)	4 (4)	*Orysat*	5 (8)	0 (0)	0.3 (0.3)	0.0 (0.0)	3
Abandoned field	3	69 (20)	2.6 (0.8)	6 (1)	21 (5)	45 (11)	4.3 (2.5)	3 (2)	*Cyndac*	27 (17)	0 (0)	1.2 (0.9)	0.4 (0.5)	0
Village crop	2	24 (33)	0.0 (0.0)	4 (0)	5 (0)	80 (0)	2.2 (2.5)	4 (0)	*Cocos*	22 (32)	36 (51)	13.6 (6.2)	14.7 (14.1)	2
Wet season rice	4	10 (17)	0.8 (0.9)	4 (1)	12 (4)	55 (21)	2.3 (1.8)	1 (0)	*Orysat*	6 (6)	1 (3)	0.0 (0.0)	0.0 (0.1)	4

[a] AGB: Above ground biomass

[b] Number of plots where clearance (fire or agriculture) was observed

Figure 4.3. Photographs of different habitats visited. From left to right, top to bottom: Aquatic grasslands, gallery forest, shrubland, grassland, tall shrubland, floating rice field, abandoned field, wet rice field, village crop.

4.3.1 Relationship among hydrological indicators

As expected, there is strong correlation among different hydrological indicators in the lake. Analysis of maximum water depth, mean annual flood duration, flood frequency, and dry season soil moisture revealed significant ($p \leq 0.001$) correlations for all plausible one-to-one relationships (Table 4.2). The strongest correlation was between maximum water depth and flood duration ($r = 0.88$). Flood frequency had the lowest correlation to the other hydrological parameters (0.55-0.61), mainly because most of the wetland area floods every year and the distribution of flood frequency values is quite skewed. Given the strong relationship among the three hydrological indicators, subsequent analyses are presented only for mean annual flood duration, which is the variable that most directly represents seasonal flooding patterns.

Table 4.2. Pairwise Pearson correlation coefficients (r) among hydrological indicators. $p \leq 0.001$ for all correlations.

	Max water depth	Flood frequency	Soil moisture
Flood duration	0.88	0.61	0.71
Max water depth	-	0.59	0.79
Flood frequency	-	-	0.55

4.3.2 Influence of annual flood duration on soils and water quality

Nine of the soils parameters analyzed were found to be significantly correlated with flood duration (Table 4.3). Strongest correlations ($p \leq 0.001$) were found with clay content (0.56), electrical conductivity (0.70), sand content (-0.48), and mottles content (0.40). The variability among all of the 16 soil variables was summarised via a Principle Component Analysis (PCA), which explained 64% of the variance into four PCs (Table 4.4). The 1st PC explained 24% of the variance among all soils data and showed a strong correlation with flood duration ($r = 0.73$, $p \leq 0.001$). The soil attributes with the strongest weightings on the 1st PC were: clay content, sand content, organic content, electrical conductivity, and soil moisture. Moreover, the 2nd, 3rd, and 4th PCs explained 19, 12, and 9 % of the soils data variance, respectively, and

although the 2nd and 3rd PCs were also significantly correlated to flood duration, the relationships were much weaker and less significant than for the 1st PC.

Table 4.3. Pair-wise Pearson correlation coefficients (r) between soil and water quality parameters and flood duration

	Parameter	Pearson's r
Soils	Clay content	0.56***
	Plant available water	0.21
	pH	0.22
	N content	0.18
	Sand content	-0.48***
	Colour dry soil	0.24*
	K content	-0.32**
	Soil electrical conductivity	0.70***
	Organic matter content	0.36**
	Silt content	-0.18
	Colour wet soil	0.23*
	Moisture content	0.71***
	A horizon depth	0.09
	Organic layer depth	-0.16
	Mottles content	0.40***
Water	DO concentration	0.13
	Water electrical conductivity	0.70***
	pH	0.67***
	Total Phosphorus	0.17
	Ammonia (NH3-N)	-0.11
	Temperature	-0.30**
	Total suspended solids	-0.10
	Nitrate (NO3-N)	0.37***

*: $p \leq 0.05$; **: $p \leq 0.01$; ***: $p \leq 0.001$.

Table 4.4. Principle components (PC) of soil properties and their relationship to flood duration. The first three components are significantly correlated to flood duration and their largest variable scores are for clay content, plant available water, and pH, respectively. The greater the magnitude of the PC score, the greater the association between the variable and the corresponding PC. Negative weighting values imply an inverse relationship.

	1st PC	2nd PC	3rd PC	4th PC
Standard deviation	1.90	1.68	1.37	1.15
Cumulative variance proportion	0.24	0.43	0.55	0.64
Pearson's r coefficient with flood duration	0.73***	0.24*	0.28*	-0.08
PC scores				
Clay content	0.49	0.02	0.05	-0.13
Plant available water	0.15	0.50	-0.25	0.13
pH	-0.06	0.25	0.47	-0.16
N content	0.07	0.09	0.22	0.62
Sand content	-0.40	-0.33	0.14	-0.05
Colour dry soil	-0.16	0.37	0.16	-0.32
K content	-0.09	0.14	-0.43	-0.16
Electrical conductivity	0.35	0.15	0.12	-0.37
Organic matter content	0.36	-0.11	0.09	0.01
Silt content	-0.14	0.45	-0.27	0.26
Colour wet soil	-0.17	0.36	0.30	-0.21
Moisture content	0.35	0.01	0.30	0.29
A horizon depth	-0.01	-0.06	0.24	-0.13
Organic layer depth	0.10	-0.23	-0.21	-0.22
Mottles content	0.33	-0.02	-0.25	-0.14

*: $p \leq 0.05$; ***: $p \leq 0.001$.

Four of the nine water quality parameters analyzed were found to be significantly correlated with flood duration (Table 4.3). Strongest correlations ($p \leq 0.001$) were found with electrical conductivity (0.70), pH (0.67), and Nitrate (0.37). A separate PCA was done for water quality, which summarized 83% of the data variance into four PCs (Table 4.5). The 1st PC explained 30% of the variance in water quality, it had strongest weighting on DO, and it was slightly correlated to flood duration ($r = 0.25$, $p \leq 0.05$). Moreover, the 2nd PC explained 25% of the variance and it was strongly correlated to flood duration ($r = 0.71$, $p \leq 0.001$). The variables with the strongest weighting on the 2nd PC were conductivity and pH.

Table 4.5. Principle components (PC) of water quality parameters and their relationship to flood duration. The greater the magnitude of the PC score, the greater the association between the variable and the corresponding PC. Negative weighting values imply an inverse relationship.

	1st PC	2nd PC	3rd PC	4th PC
Standard deviation	1.561	1.401	1.128	0.939
Cumulative variance proportion	0.304	0.550	0.709	0.819
Pearson's r coefficient with flood duration	0.25*	0.71***	-0.18	-0.02
PC scores				
DO concentration	0.515	-0.025	0.407	0.124
Conductivity (specific conductance)	0.040	0.656	-0.172	0.219
pH	0.355	0.548	0.098	0.158
Total Phosphorus	0.260	0.096	-0.560	-0.329
Ammonia (NH3-N)	0.003	-0.223	-0.489	0.813
Temperature	0.377	-0.239	0.342	0.288
Total suspended solids	0.415	-0.389	-0.270	-0.159
Nitrate (NO3-N)	0.474	0.041	-0.228	-0.186

*: $p \leq 0.05$; ***: $p \leq 0.001$.

4.3.3 Influence of annual flood duration on human use

The difference in the mean flood duration between cleared and non-cleared plots was significant ($p \leq 0.001$). Vegetation clearance occurred preferentially in areas that flood on average 5 ± 2 months per year, whereas areas that flood for longer time (7 ± 2 months per year) were predominantly used for selected wood harvesting and complete vegetation clearance was thus rare.

4.3.4 Influence of annual flood duration and soils on vegetation structure and species richness

Mean annual flood duration and soil properties play a significant role in determining canopy height, canopy cover and AGB (Table 4.6). However, statistical models yielded low to moderate r^2 coefficients. Among response variables, canopy height showed the most significant r^2 coefficients, while AGB yielded the least significant relationships. The strongest r^2 came from the model of canopy height as a response of flood duration, and the

2nd, 3rd, and 4th PC of soils (r^2 = 0.593). The 1st PC of soils was excluded from this analysis because of its high correlation with flood duration.

Table 4.6. Coefficient of determination (r^2) of the linear relationships of canopy cover, aboveground biomass (AGB), and canopy height as a function of flood duration and principle components (PC) of soils.

Factors used for the linear statistical model				Coefficient of determination (r^2)		
Flood Duration	2nd PC	3rd PC	4th PC	Canopy height	Canopy cover	AGB
x				0.256***	0.103**	0.129**
x	x			0.262**	-	0.139*
x		x		0.392***	0.291***	-
x			x	0.261***	-	0.154*
x	x	x		0.414***	0.365***	0.236*
x		x	x	0.450***	0.347***	0.332***
x	x	x	x	0.593***	0.459**	0.410**

*: $p \leq 0.05$; **: $p \leq 0.01$; ***: $p \leq 0.001$.

Plots of vegetation characteristics as a response of annual flood duration suggest that the underlying relationship between vegetation and flood duration is complex (Figure 4.4). The mean and standard deviation of canopy height tended to increase with flood duration, with a maximum of 8.4 ± 4.3 m at plots flooded 6-7 months annually (Figure 4.4a). Species richness followed a unimodal trend, with a maximum number of species occurring in plots flooded 3-4 months annually, and then decreasing towards both drier and wetter plots (Figure 4.4b). A very similar unimodal pattern was followed by the presence of the most abundant trees and shrubs in the floodplain, with the main difference being that the occurrence of these species clearly peaked in plots flooded 7 months annually (Figure 4.4c). A detailed account of species richness at each location is provided in Appendix B.

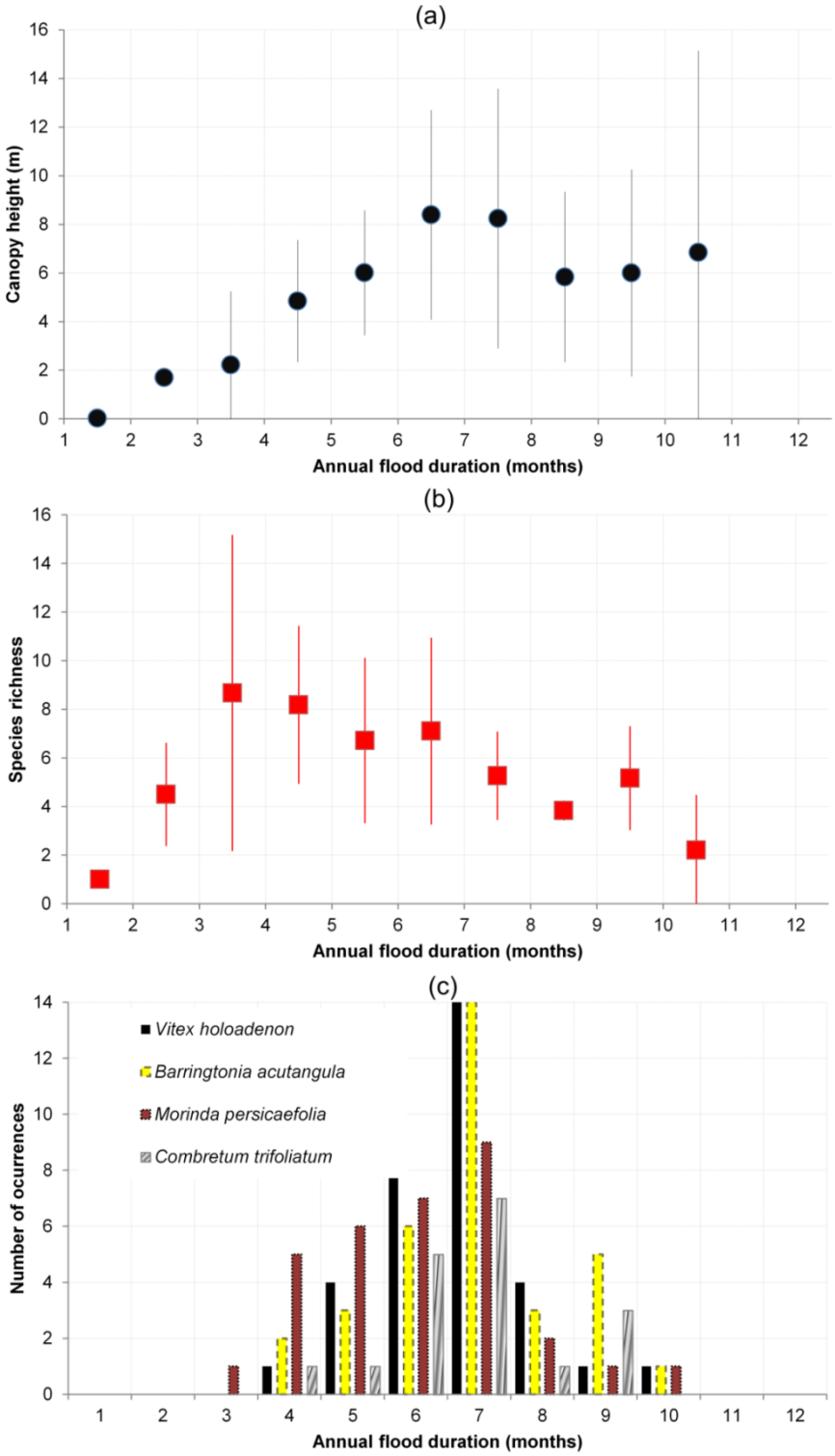

Figure 4.4. Response of vegetation characteristics to annual flood duration. Error bars in (a) and (b) represent 1 standard deviation from the mean value. Histograms in (c) depict the most abundant plant species in the survey. See appendices for detail information collected at each location.

4.3.5 Influence of annual flood duration and other drivers on plant species composition

Strong correlations (0.87 and 0.80) between the 1st and 2nd axes of the DCA and the DCCA suggest that the variables analyzed were good descriptors of the intrinsic variance in species composition. For the environmental variables (annual flood duration, soil PCs, and human use), the strongest correlations with the 1st gradient axis we found with flood duration (0.68 and 0.84 in the DCA and the DCCA, respectively; Table 4.7). The 1st axis is thus considered a good representation of seasonal flooding patterns in the floodplain. Species-environment correlations with the 1st axis were 0.75 and 0.92 in the DCA and the DCCA, respectively. For the biological variables, good interset correlations were found between the 1st axis and litter cover, subcanopy cover, and herbs AGB. Species-environment correlations for the 1st axis were 0.84 and 0.92 in the DCA and the DCCA, respectively. Species-environment correlations with the 2nd axis were 0.72 and 0.82, while the Eigenvalues were 0.41 and 0.35 in the DCA and DCCA, respectively.

Table 4.7. Summary of detrended correspondence analysis for non-constrained (DCA) and constrained (DCCA) presence/absence of plant species.

		1st Axis		2nd Axis	
Environmental variables		DCA	DCCA	DCA	DCCA
Correlation between axes site scores		0.80		0.87	
Eigenvalues[a]		0.41	0.55	0.72	0.16
Species-environment correlations[b]		0.75	0.92	0.54	0.61
% variance species-environment[c]		25.6	49.2	14.8	13.8
Interset correlations[d]:	Flood duration	0.68	0.84	0.15	-0.12
	Human use	-0.04	0.01	0.19	0.16
	Soils 1st PC[e]	0.57	0.68	0.19	-0.02
	Soils 2nd PC	0.18	0.20	-0.06	-0.05
	Soils 3rd PC	0.47	0.62	0.41	0.34
	Soils 4th PC	-0.07	-0.24	-0.04	0.13
Biological variables		DCA	DCCA	DCA	DCCA
Correlation between axes site scores		0.93		0.73	
Eigenvalues		0.72	0.54	0.41	0.35
Species-environment correlations		0.84	0.92	0.72	0.82
% variance species-environment		24.7	25	14.6	21.7
Interset correlations:	litter cover	-0.62	-0.65	-0.14	-0.20
	ground cover	0.28	0.31	0.24	0.10
	understory cover	-0.64	-0.73	0.12	0.11
	Canopy cover	-0.73	-0.83	0.08	0.08
	AGB[f]				
	canopy	-0.05	-0.17	0.38	0.42
	AGB shrubs	-0.52	-0.47	-0.22	-0.28
	AGB herbs	0.64	0.76	0.13	-0.06
	Vegetation height	-0.41	-0.52	0.39	0.36
	Species richness	-0.48	-0.38	-0.37	-0.58

[a] a measure of how much variation is explained along the gradient axes, in standard deviation units.
[b] linear correlations between the environmental gradients and the species composition axes
[c] % of variance on species composition caused by the environmental gradient along each axis
[d] linear correlations between the environmental data and the plot scores of plant species.
[e] Principal component
[f] Above ground biomass

The influence of annual flood duration and human use on the composition of plant species was also examined via an ordination diagram (Figure 4.5), which shows the position of the species along the two main DCCA axes as well as the vectors representing the direction and magnitude of variation in annual flood duration and human use. The 1st axis

represents a flooding gradient that explained 49.2 % of variance in plant species composition. Human use is represented in the 2nd axis and only explained 13.8% of the variance in plant species composition.

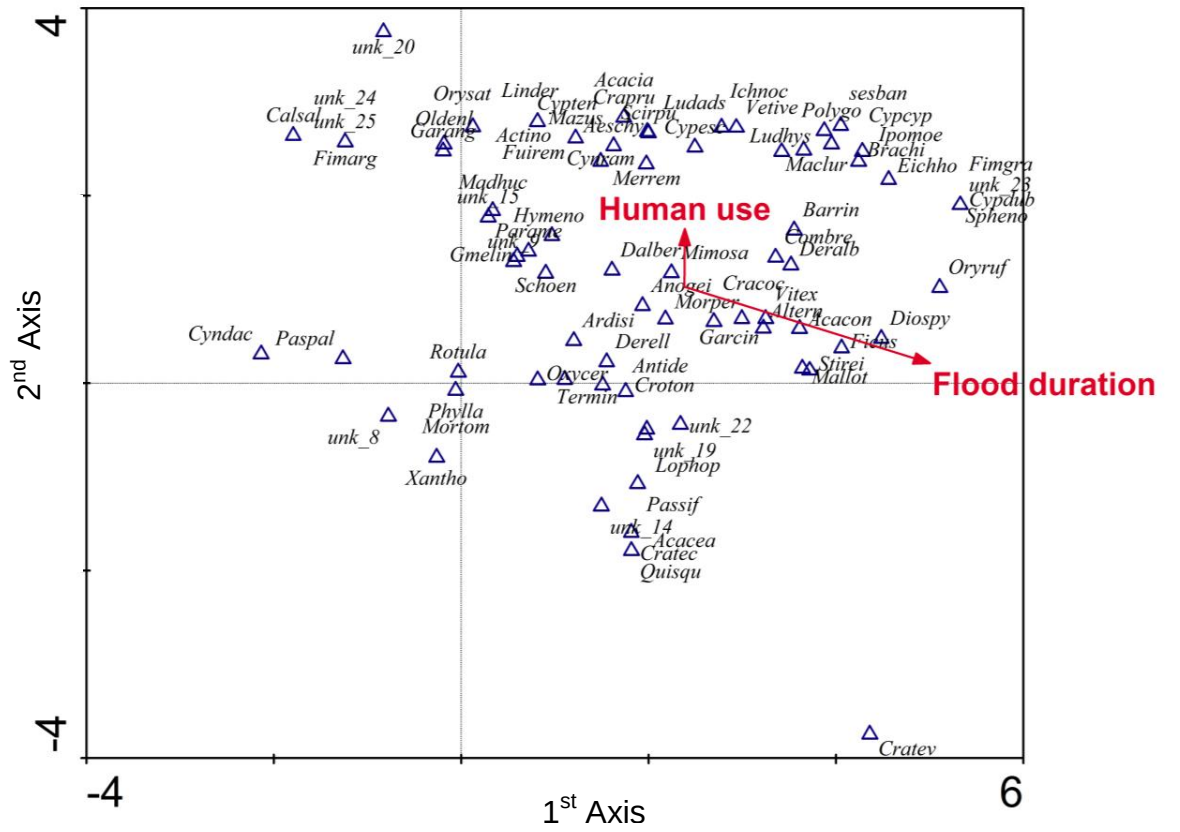

Figure 4.5. Ordination diagram of Detrended Corresponding Canonical Analysis (DCCA) of plant species composition with flood duration and human use. The 1st axis is strongly correlated to flood duration and explains 49% of the variation in plant species composition. See Appendix B for a list of the scientific names associated with the species codes

4.3.6 Relationship between habitats and water quality

Vertical profiles of water quality according to habitats revealed both commonalities and differences across parameters (Figure 4.6). DO concentration was high at the surface water (0.5m depth) and decreased with depth in all habitats; however, the rate of oxygen depletion with depth was different among habitats: vertical differences were smallest at the open water (5.5 to 7 mg/L) and greatest in the floating rice and abandoned fields (0 to 7.5 mg/L). Temperature profiles followed similar patterns as DO, with the least vertical variation in the open water (28.9-29.5°C) and maximum in the floating rice fields (27.6-30.8°C). pH profiles

show the least vertical variation within each habitat; yet, there is a clear difference among habitats, with open water consistently having near neutral values (7.14-7.50) and receding rice and abandoned fields the most acidic (5.78-6.19). Conductivity had high and constant profiles in the open water, forest, and grassland plots (82-96 $\mu S\ cm^{-1}$), but values decreased in the shrubland habitats (30-85 $\mu S\ cm^{-1}$) and rice fields (18-60 $\mu S\ cm^{-1}$).

The relationship between water quality and habitats was also examined by comparing the difference in the two largest water quality PCs with respect to habitats. This was done graphically via boxplots (Figure 4.7) and statistically by comparing variances and means. The 1^{st} PC (mostly related to DO) showed a significant difference in the variance within habitats (Bartlett's test $p < 0.05$), and therefore ANOVA comparisons were not valid. In contrast, the 2^{nd} PC, which is strongly correlated to flood duration and mostly related with conductivity, showed no significant difference in variance (Bartlett's test $p = 0.175$), and significant differences among means. Based on a pairwise comparison of means, three significantly distinct groups of habitats according to the 2^{nd} PC were found: one composed of wet season rice, receding rice, and abandoned fields, another composed of closed forest and open water, and tall shrubs as one on its own.

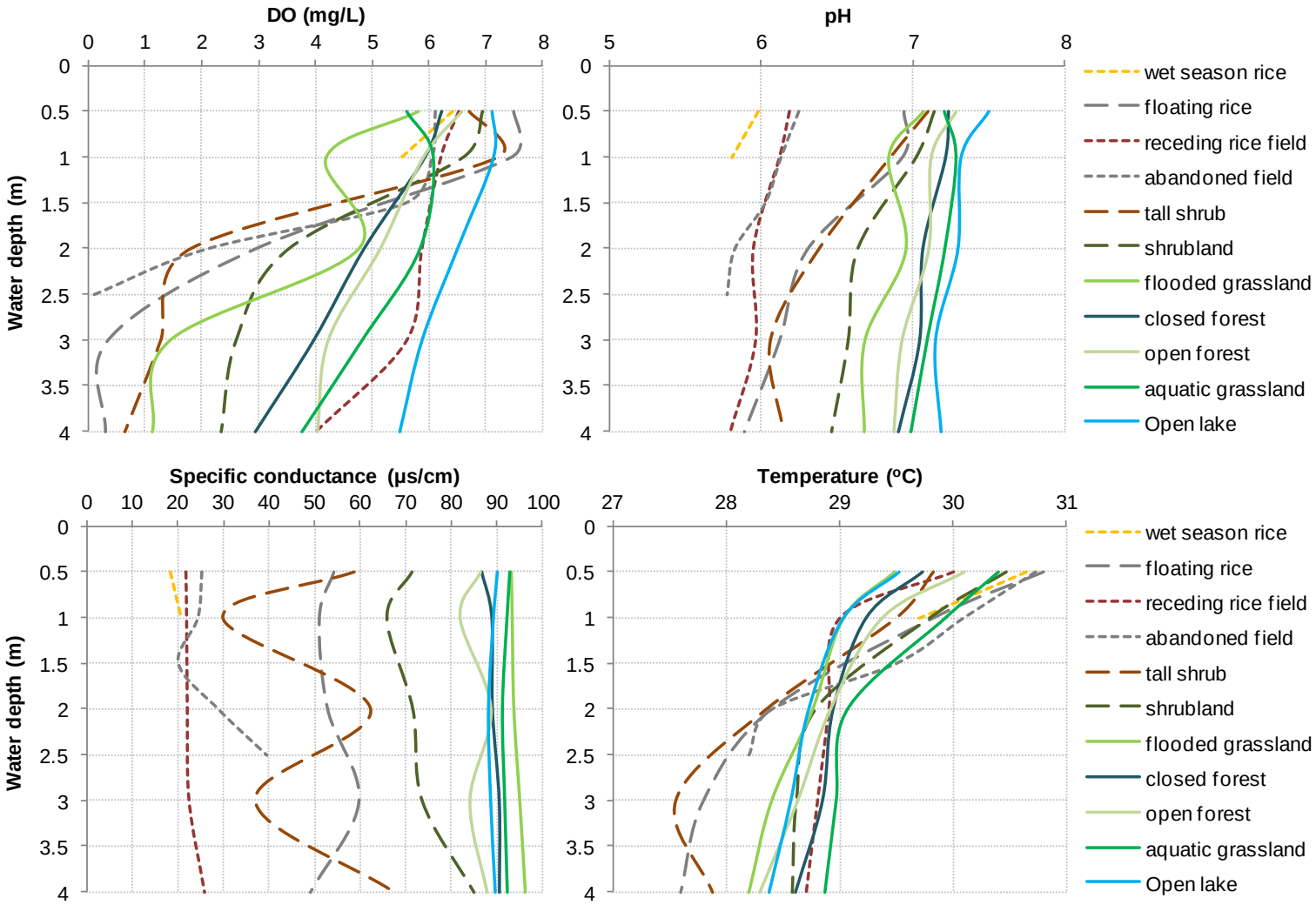

Figure 4.6. Vertical profiles of selected water quality parameters according to habitat type.

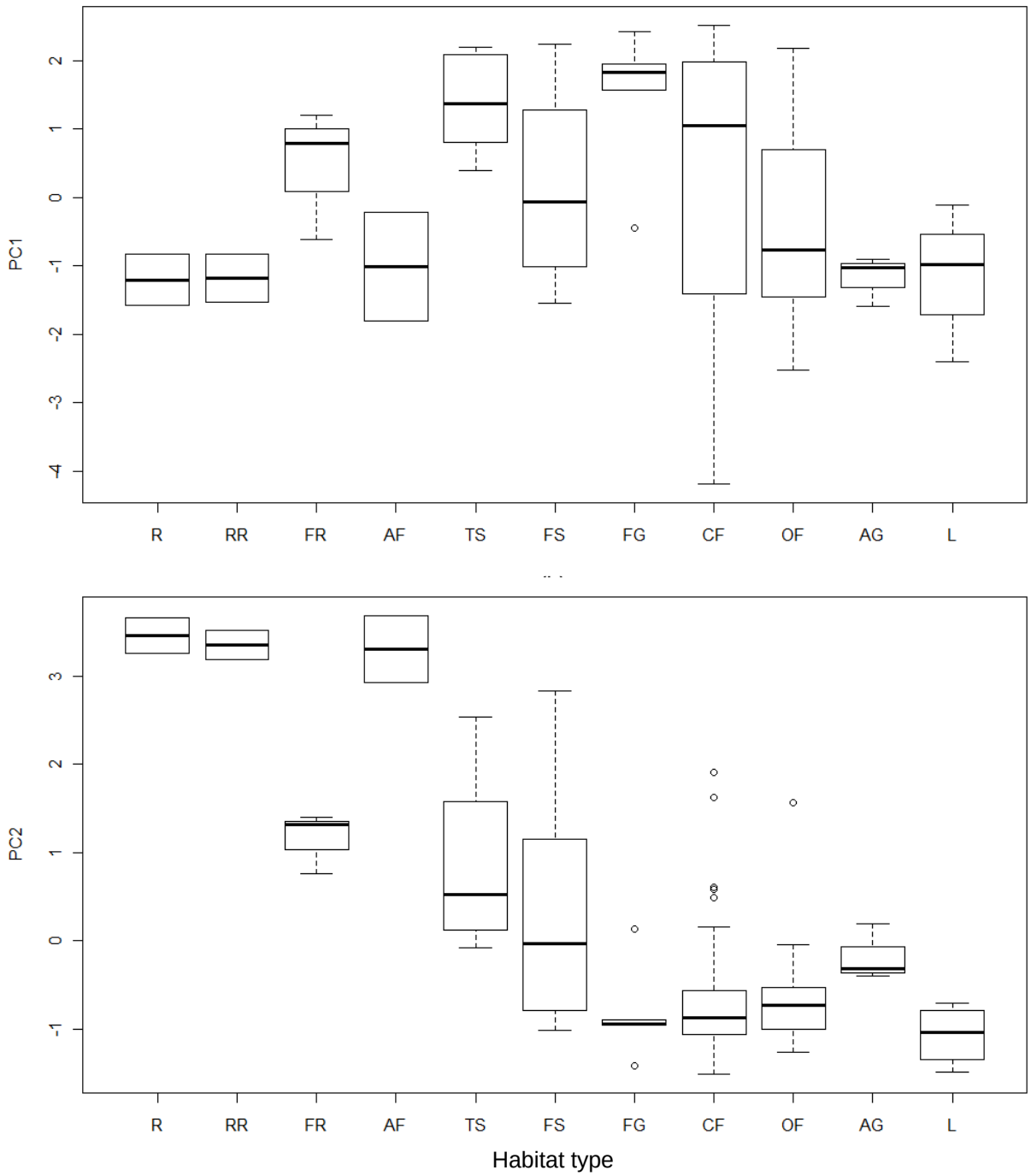

Figure 4.7. Boxplots of the 2 largest principle components (PCs) of water quality with respect to habitat type. Rectangles represent 25th and 75th percentiles, bold horizontal line represents the 50th percentile, thin horizontal lines beyond the rectangles are sample spread, and circles are outliers. (a) 1st PC has the greatest weighting on DO and (b) 2nd PC has greatest weighting on pH and specific conductance. Both components are significantly correlated with flood duration. L = open water; AG = aquatic grasslands; OF = open forest; CF = closed forest; FG = flooded grassland; FS = flooded shrubland; TS = tall shrubland; FR = floating rice; AF = abandoned field; RR = receding rice; R = wet season rice.

4.4 Discussion

Most of what is written about the Tonle Sap's habitats and their characteristics is based on either conceptual models or highly localized observations. The information previously reported was valuable in scoping this study, but did not clearly characterise habitats and their main drivers. In this chapter, a comprehensive habitat characterisation was presented with statistical evidence that key parameters are linked to hydrological indicators and human use.

Water depth and annual flood duration provided the most discerning information on hydrological conditions within each plot, whereas flood frequency provided the least because most plots are inundated every year. This parameter, however, is the main factor distinguishing conventional rice paddies and village crops from the rest of the habitats that flood every year. Annual flood duration was responsible for the greatest variance among soil characteristics, a relationship consistent with other large tropical wetlands (Bowman and McDonough, 1991; Furch, 1997; Mubyana et al., 2003).

The conversion of natural vegetation by fire and human use also was correlated to flood duration. In seasonally flooded habitats, inundated for at least 7 months every year, vegetation clearance occurred mainly due to fires in grasslands, whereas agriculture was the principal factor in areas flooded for less than 5 months annually. Fires are known to occur in the floodplain during the dry season and they probably start both naturally and intentionally (Campbell et al., 2006). Whichever the cause, the opening of these areas creates an opportunity for uses such as water buffalo grazing and rice paddies, which subsequently reduce the chances of the natural re-vegetation of burned areas. It is important to note that the Tonle Sap is a unique ecosystem where seasonal flooding limits human use; nearly 6000 km^2 of floodplain are covered with natural vegetation, and if there was no seasonal flooding, all of this area would have been converted to rice paddies centuries ago.

Flood duration was found to be closely related to vegetation structure and species richness. Data summarized in Table 4.1 reveal patterns of species richness, canopy cover, and maximum height along the flooding gradient; yet, these relationships show complex responses to flooding (Figure 4.4; Table 4.6). Vegetation communities and species in other large tropical wetlands have been shown to be non-uniformly distributed along the hydrological regime (Foti et al., 2012; Milzow et al., 2010; Todd et al., 2010), and this could be a fundamental factor in the resulting nonlinear relationships between vegetation properties and hydrology. I infer that the complexity of vegetation properties in the Tonle Sap is strongly influenced by the interplay between human use and hydrology.

Soil attributes, including clay content, sand content, and organic matter content, were associated with particular habitats, which is consistent with preliminary observations of the Tonle Sap (Hellsten et al., 2003) and general patterns observed in the Amazon (Cochrane and Cochrane, 2010). The variation in these soil attributes was found to be correlated with flood duration, and it is thus inferred that the hydrological gradient is one of the primary mechanisms linking soils with vegetation. There are also feedback mechanisms in which vegetation influence soils in the long term, including suspended sediment trapping and litter fall, but more studies are needed to evaluate the significance of these processes. Ecohydrological processes (aka., the cycle of water through the soil, plants, and the atmosphere) have also been shown to be intrinsically related to habitat characteristics (Foti et al., 2012), but this is a subject completely unexplored in the Tonle Sap.

Spatial patterns in water quality during the wet season were also linked to the flooding and habitat gradients. In general, the patterns observed in this study complement the observations that Lamberts (2001) made at a much smaller number of sites. Although this study measured additional parameters from those measured by Lamberts (2001), in particular TSS, NO_3^{-2}, NH_3 and TP, the spatial variation among these variables during the wet season

was not as apparent as those variables directly measured in the field. Concentrations of these four parameters were overall extremely low, so there is a high possibility that laboratory analytical resolution and detection limits were not accurate enough for the assessment of spatial variation in the wet season.

The majority of the variance in water quality in this study was summarized into a few components, the two largest of which were linked to flooding. The 1st water quality PC was related to DO, but this gradient was only slightly correlated to flood duration. This occurred mainly because DO has a large diurnal range that depends on aquatic metabolism and atmospheric exchange (Holtgrieve et al., 2010; Odum, 1956). Daily DO fluctuations have been already documented in the Tonle Sap (Holtgrieve et al., 2013; Irvine et al., 2011; Sarkkula et al., 2003); hence, this study did not consider diurnal changes and instead focused on determining large scale spatial variation during one specific season. On the other hand, the second largest water quality PC (mostly related to conductivity and pH) was strongly correlated to flood duration. The spatial variation in conductivity and dissolved minerals in floodplain wetlands is thought to be influenced by river inputs, whereas patterns in pH are thought to be linked to changes in carbon cycling (Furch and Junk, 1997a, 1997b; Mackay et al., 2011). A strong correlation between conductivity and water levels was also found in the Tonle Sap at different seasons (Irvine et al., 2011), suggesting that this parameter is indeed primarily determined by the source of water and therefore it could be a good candidate for continuous monitoring of both water quality and water source changes.

Results from the ordination analyses showed that average annual flood duration was the best descriptor of plant species composition among non-biological environmental variables, whereas canopy cover and herbaceous AGB were the best descriptors among biological variables. In addition to illustrating the influential role of flood duration in plant species composition, the results from the ordination analyses point out that there is a selected number

of environmental and biological variables that best describe the spatial distribution of plant species through the Tonle Sap, including annual flood duration, maximum annual water depth, clay content, sand content, Potassium soil content, canopy cover, litter cover, and herbaceous AGB.

4.4.1 Implications of a disrupted hydrological regime

The ongoing development in the Mekong Basin would affect the Tonle Sap's flood-pulse by decreasing the extent of maximum flooding and increasing the extent of the permanent lake (Arias et al., 2012; Kummu and Sarkkula, 2008; MRC, 2010b). Expected alterations in the Mekong will probably increase the dry season water levels by 80-90cm and reduce wet season levels by 40-50cm (See chapter 5). Because of the extremely flat terrain, the reduced seasonal water level fluctuation could cause horizontal shifts of more than 500 m horizontally (Figure 4.8). This modified flood gradient will probably change soil, vegetation, and water quality patterns in the long term. Changes in texture, moisture, and organic content of floodplain soils are expected. Nearly all of the forests in the coastal zone, which have the largest biomass and canopy cover of all seasonally flooded habitats, could be permanently inundated. Due to the reduction in seasonal flood extent, land clearance will be favoured, thus reducing the buffer between the agricultural boundary and natural habitats. The loading and flushing effect of the Mekong flood-pulse on water quality may become less apparent, and even though the area of well oxygenated open water could increase, good water quality in this area will be confronted by the growing influence of human waste and agricultural runoff.

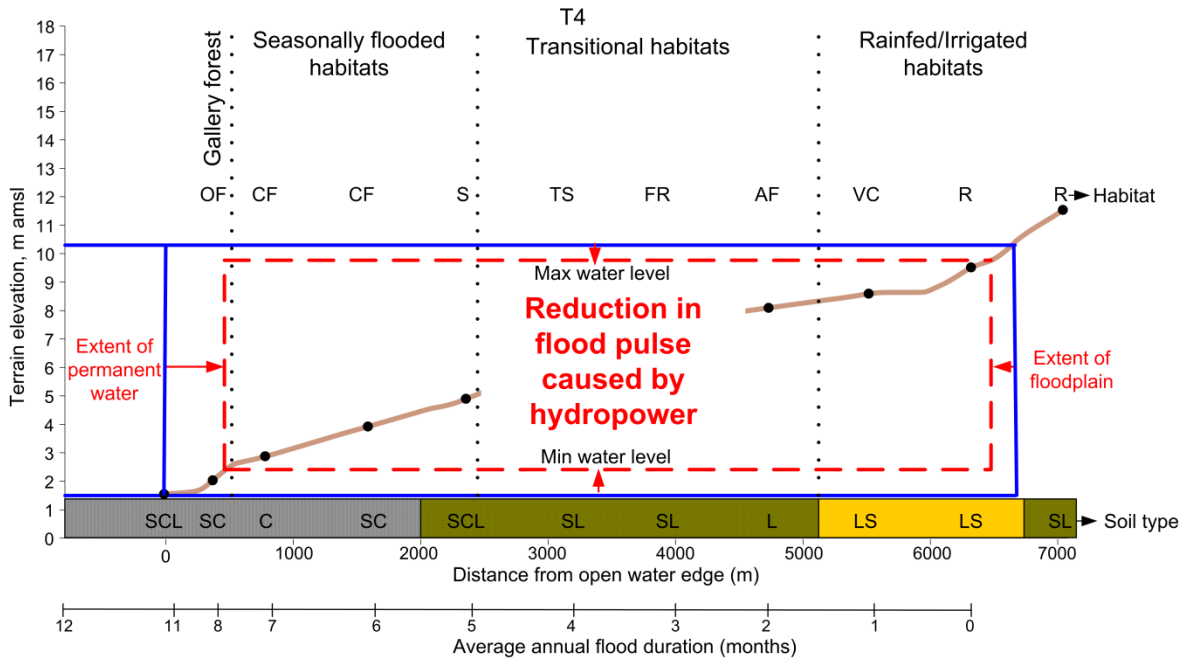

Figure 4.8. Projected changes from hydropower in annual minimum and maximum water level and flood extent on elevation profile of transect T4. Blue lines indicate the historical min/max water levels and flood extend, whereas the red dotted lines indicate the projected conditions under a future hydropower scenario. The brown line is terrain elevation , black dots are sampling plot locations, and capital letters represent habitat or soil types. Habitat groups based on flood duration (Arias et al., (2012) and changes in water levels based on maximum hydropower potential in the Mekong Basin (Lauri et al., 2012). C = clay; SC = sandy clay; SCL = sandy clay loam; SL = sandy loam; L = loam; LS = loamy sand; OF = open forest; CF = closed forest; S = flooded shrubland; TS = tall shrubland; FR = floating rice; AF = abandoned field; VC = village crop; R = wet season rice.

4.5 Chapter conclusions

In summary, the results from this chapter show that despite the complexity and intense human use of this ecosystem, the flood-pulse is the underlying driver of habitat characteristics by determining the depth and duration of inundation, creating the main gradient of soils, limiting the area cleared for agriculture, influencing vegetation structure and water quality, and shaping the composition of plant species. The physiological adaptations and life histories of the floodplain's natural vegetation are largely unknown and further research on this subject would greatly improve our knowledge on the ecohydrology of this wetland.

Strong linear relationships among all hydrological indicators suggested that the main gradient the floodplain is subject to is driven by the flood-pulse from the Mekong. A

significant relationship was found between this hydrological gradient and soils characteristics, in particular clay content, sand content, soil moisture, and organic matter. These variables are linked to the hydrology through multiple processes that should be subject to further studies in the Tonle Sap, including sedimentation, soil moisture dynamics, transpiration, and litter fall/decomposition.

Human use is a widespread and influential factor in habitat characteristics. Seasonally flooded shrublands and grasslands occurred in areas of similar hydrological conditions; yet, most grasslands surveyed had been recently burned, suggesting that this might be an important factor distinguishing these two habitats. However, human use is only a secondary factor, since it is highly influenced by flooding. Vegetation clearance was found primarily in areas where hydrological patterns are appropriate for rice cultivation, implying that if it was not for the intensity of flooding, rice paddies would cover a greater fraction of the floodplain. Moreover, spatial variation in water quality, in particular electrical conductivity and pH, were correlated with flood duration and habitat type. Even though this study only addressed a non-temporal dimension in water quality, a comprehensive review of all studies that have addressed temporal variation should be carried out in conjunction with this chapter's results in order to inform management institutions about effective monitoring schemes that incorporate both spatial and temporal dimensions.

Distinct patterns in vegetation characteristics as a function of flood duration were found, but these patterns were predominantly unimodal, with maximum values at a region of intermediate disturbance where the non-flooded phase is long enough to promote the growth of natural rooted vegetation, but where the water during the flooded phase is too deep for rice cultivation. These field-based observations are key to understanding how the hydrology drives this ecosystem, because they provide the fundamental relationship between physical and biological parameters needed for further field and numerical studies.

Ordination analyses revealed that annual flood duration, maximum annual water depth, clay content, sand content, Potassium soil content, canopy cover, litter cover, and herbaceous AGB were the best predictors of plant species composition. It is recommended that further studies prioritize some of these variables while expanding the number and area of sampling locations.

CHAPTER 5: MODELLING IMPACTS OF HYDROPOWER AND CLIMATE CHANGE ON ECOLOGICAL PRODUCTIVITY DRIVERS

5.1 Introduction

Large tropical floodplains with unimodal and predictable hydrology are typically described following the flood-pulse concept (Junk et al., 1989), which states that geochemical and biological processes are dictated by the seasonal pulse of water. Recent studies on the water chemistry, vegetation, soils and fauna all suggest that the Tonle Sap acts like a classic flood-pulse ecosystem (e.g., Brooks et al., 2009; Irvine et al., 2011). It is therefore expected that changes in the flood-pulse should have a direct effect on physical and chemical properties of the ecosystem, which subsequently would impact primary and secondary productivity (including fisheries). These connections have not been comprehensively studied in the Tonle Sap, but given the imminent transformations that the drivers of productivity are undergoing, it is crucial to use available empirical evidence in conjunction with numerical models to examine resulting changes in productivity.

The purpose of this chapter is to quantify future changes in the Tonle Sap sedimentation and net primary production (NPP) that could result from hydropower development and climate change in the Mekong Basin using the 3D EIA model. Comprehensive and published field measurements of floodplain vegetation and aquatic productivity are used to calibrate the model, a detailed sensitivity analysis is done, and future scenarios of hydrology and habitat cover based on published information of climate change and hydropower development in the Mekong Basin are used to predict sedimentation and NPP changes.

5.2 Methods

This section describes the different procedures that were carried out to achieve the goal of this chapter. First, the approach that was used to connect the different modelling components is introduced. This is then followed by a description of the 3D EIA model and the equations that drive NPP. After this, the land use/land cover maps and its associated parameters are described. Finally, procedures used in the calibration, validation, sensitivity analysis, and simulation scenarios are presented.

5.2.1 Modelling approach

Multiple data sources and models were used to simulate daily NPP throughout the Tonle Sap in order to properly consider the complexity of the system (Figure 5.1). The baseline hydrology of the Mekong Basin and modifications to water flows caused by hydropower and climate change were simulated using the distributed model VMOD (Lauri et al., 2012). Simulated daily flows were then routed through the Lower Mekong floodplains using the 2D application of the EIA model, which estimated the hydrodynamics driving the Tonle Sap, including water levels and the flow reversal in the river (Västilä et al., 2010). The changes in water level at Tonle Sap were then used in combination with a digital elevation map to estimate changes in flood duration and habitat cover using the GIS-based model described in Chapter 3 (referred here as PULSEHAB). These maps and the river flows were then used as inputs to the Tonle Sap 3D EIA model, which resulted in daily estimations of spatially distributed sedimentation and NPP.

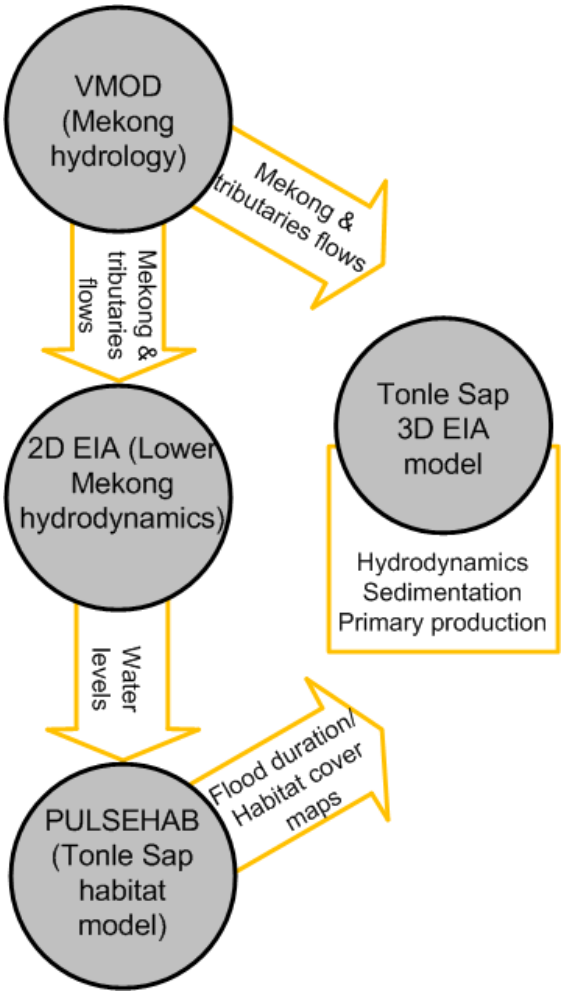

Figure 5.1. Modelling approaches used to estimate impacts on sedimentation and primary production.

5.2.2 3D EIA model description and input data

The 3D EIA is a distributed, three dimensional, and multi-layer model that computes hydrodynamics, sediment movement and NPP (Koponen et al., 2010a; Koponen et al., 2010b; Sarkkula et al., 2010). A summary of the 3D EIA model is provided describing the most relevant processes driving NPP (Figure 5.2). The Tonle Sap system is primarily driven by 3 external sources: sunlight, which is responsible for biological activity, and the Mekong River and Tonle Sap tributaries, which are the main sources of water and sediment. The Tonle Sap "Great Lake" has an aquatic and a terrestrial phase (represented by the inundated area and floodplain in Figure 5.2) that exchange the area according to the time of the year. Different processes occur on each of these phases that contribute to NPP. During the terrestrial phase,

rooted vegetation uses the floodplain area and uptake nutrients from the soil. Upon flooding, a fraction of the biomass accreted by the seasonally flooded vegetation enters the aquatic phase, and at the same time, plankton production takes place as a function of nutrients, light availability, and water depth.

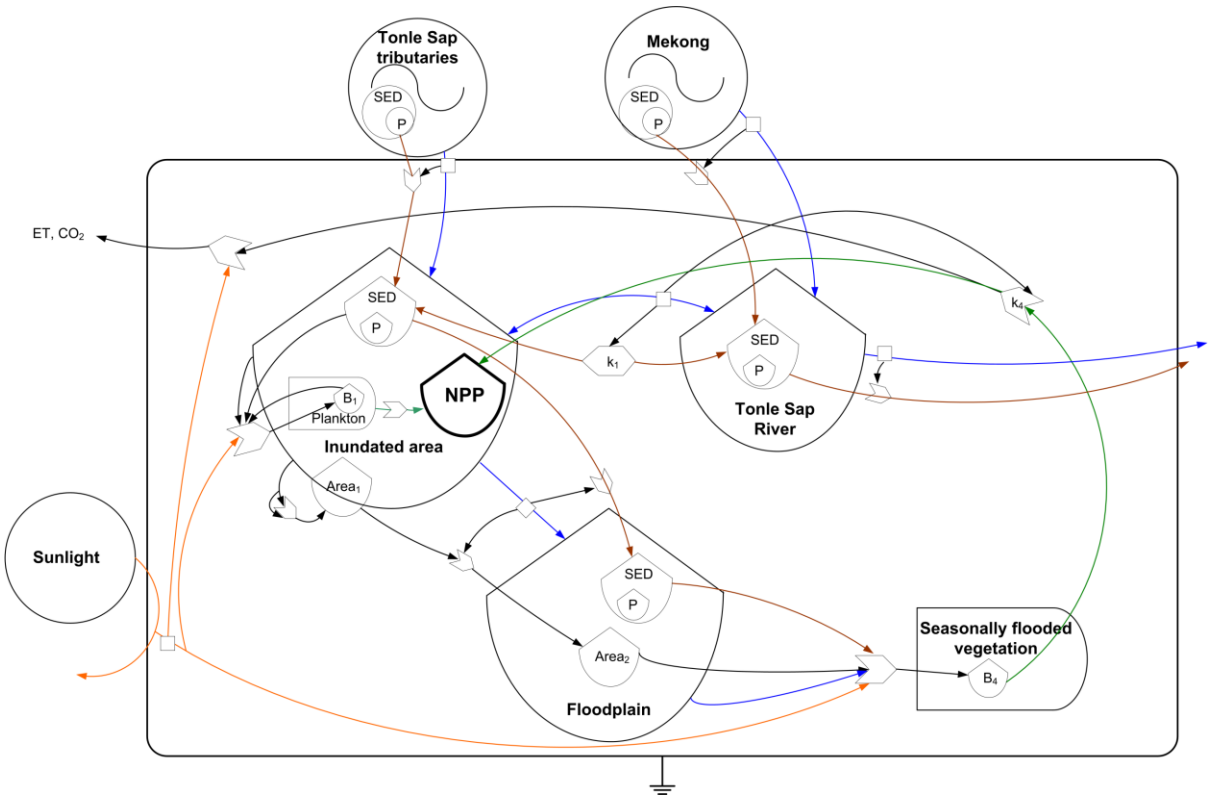

Figure 5.2. Systems diagram representing main factors and processes driving aquatic net primary production (NPP) in the 3D EIA model. SED = sediments, P = Phosphorus, B = biomass, $Area_1$ = extent of aquatic phase, $Area_2$ = extent of terrestrial phase.

Water movement through the lake and floodplain is represented by the simplified Navier-Stokes (eq. 5.1) and the continuity equation (eq. 5.2):

$$\rho \frac{d\vec{v}}{dt} = \rho \frac{\partial \vec{v}}{\partial t} + \rho \vec{v} \circ \nabla \vec{v} = -\nabla p + \rho \vec{g} \circ \bar{\bar{I}} - 2\rho \vec{\omega} \times \vec{v} + \rho \upsilon^m \nabla^2 \vec{v} \quad (5.1)$$

$$\rho \frac{\partial \vec{v}}{\partial t} + \nabla \cdot (\rho \vec{v}) = 0 \quad (5.2)$$

Where $\vec{v}$ is the instantaneous flow velocity vector, ρ is the instantaneous density of water, p is the instantaneous pressure, $\vec{g}$ is the gravity acceleration vector, $\bar{\bar{I}}$ is the unit matrix of the coordinate system, $\vec{\omega}$ is the angular velocity vector of earth's rotation, $\upsilon^m$is the kinematic

molecular viscosity of water, t is time, ∇ is the gradient operator, $\nabla\cdot$ is the divergence operator, and ∇^2 is the LaPlace operator. The model solves the equations numerically using a finite difference method; calculations are carried out in 1 km^2 horizontal grid cells and a maximum of 14 vertical layers. The model uses water flows at the 14 main tributaries of the Tonle Sap (including the Tonle Sap River) as boundary conditions. Water level records from 1996 to 2005 at Kampong Luong were used to validate the model hydrodynamics.

The 3D EIA model calculates the amount of sediment transported, deposited, and eroded throughout the floodplain as a function of hydrodynamics, terrain, and LULC. Sediment quantities and processes are a key component of the model because they control turbidity and bioavailable phosphorus (P). The Mekong (via the Tonle Sap river) is the largest source of sediment in the lake and floodplain (Kummu et al., 2008), and suspended sediment concentrations (SSC) are correlated to water flows, despite the complex flow reversal system (Figure 5.3). In general, SSC out of the Tonle Sap is fairly low and constant (0-50 mg/L), but once the Mekong starts flowing into the Tonle Sap, SSC rises proportionally to water flows; SSC then gradually decreases and it reaches minimum values soon after water starts flowing out of the lake. SSC in/out of the Tonle Sap were characterized with monthly measurements from 1993 to 2001 (Sarkkula et al., 2003), which were used to create a polynomial regression relating SSC to water flow. Long term net sedimentation has been validated with estimates from sediment cores in the open lake (Kummu et al., 2008).

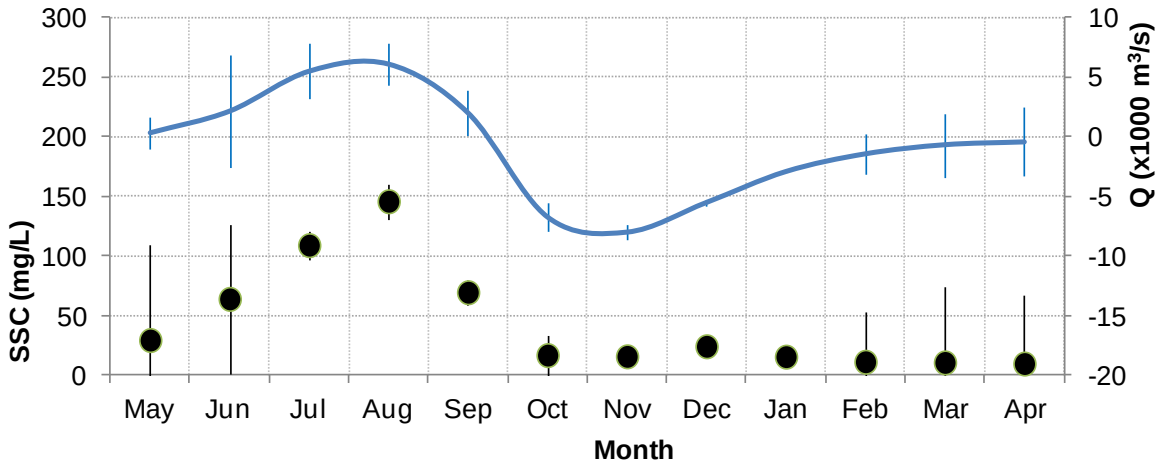

Figure 5.3. Relationship between suspended sediment concentration (SSC) and water flows (Q) at Prek Kdam in the Tonle Sap River.

The model assumes that P is the limiting nutrient for NPP throughout the year. This assumption has not been tested experimentally, but based on measured nutrient concentrations and seldom blue-green algae blooms (except during the dry season), it is unlikely that nitrogen limits NPP year-round. Both SSC and bottom sediments are assumed to have constant P concentrations, P_{SSC} and P_{SED}, which were characterized with field measurements (Koponen et al., 2010b). SSC and P, in combination with recent sediments accumulated at the bottom (SED, g m^{-2}), water depth at a given vertical layer (h_b), and vegetation height (h_{veg}) were used to estimate the amount of P available for plankton and for rooted vegetation for each grid cell (Koponen et al., 2010b):

$$P_{plankton} = [P_{SSC} * SSC] + [P_{SED} * (SED/h_b)] \quad (5.3)$$

$$P_{veg} = P_{SED} * \left(SED/h_{veg}\right) \quad (5.4)$$

NPP by phytoplankton, periphyton, and seasonally flooded rooted vegetation comprise total ecosystem NPP. The model calculates the hourly contribution of each of these three components for each grid cell as a function of water depth, euphotic depth, and $P_{plankton}$. Euphotic depth (ZE) is defined as the water depth at which solar light does not limit plankton

NPP. ZE was set to be equivalent to the secchi disk depth (D_{secchi}), which was found to decrease exponentially from the maximum secchi disk observed depth ($D_{secchimax}$) as a function of SSC concentration (Koponen et al., 2010b):

$$ZE \cong D_{secchi} = D_{secchimax} e^{-0.054 * SSC} \tag{5.5}$$

To link $P_{plankton}$ to NPP, a nutrient dependent growth coefficient, $A_{plankton}$, was calculated:

$$A_{plankton} = 1 - PP_{SED} + \left[PP_{SED} * (1 + P_k/P_{AV}) * \left(P_{plankton}/\{P_{plankton} + P_k\}\right)\right] \tag{5.6}$$

Phytoplankton is defined as the autotrophic plankton community in the water column, and its contribution to NPP is estimated as a function of a volumetric phytoplankton productivity rate (PPY, in units of mg $m^{-3}hr^{-1}$), the surface area of the grid cell (SA, in m^2), and daily exposure time (ET; Koponen et al., 2010b):

$$NPP_{phyto} = PPY_{phyto} * SA * ZE * ET * A_{plankton} \tag{5.7}$$

Periphyton is defined as the autotrophic plankton community attached to submerged bottom sediments and vegetation. The model assumes that periphyton has a growth rate so that its maximum contribution to NPP is only reached after 14 days of submersion (Koponen et al., 2010b):

$$NPP_{peri} = PPY_{peri} * SA * ET * AD * A_{plankton} * (ZE/Z_{max}) * e^{-\beta(t_w - T)/T} \tag{5.8}$$

where PPY_{peri} is the areal periphyton productivity rate (mg $m^{-2}hr^{-1}$), AD is the grid density area (dimensionless), Z_{max} is the water depth (m), β is the periphyton growth exponent (assumed to be $3d^{-1}$), t_w is the wetting time (days), T is the growth time scale (14 days), and all other terms as defined previously. AD was assumed to be equivalent to the leaf area index (LAI), and whenever ZE exceeded Z_{max}, the area exposed to sunlight at the bottom of the grid cell was also available for periphyton.

Rooted vegetation in the floodplain grows at a constant rate during the terrestrial phase (aka., $Z_{max} = 0$) as a function of the available P in the floodplain (Koponen et al., 2010b):

$$A_{veg} = 1 - PP_{SED} + \left[PP_{SED} * (1 + P_k/P_{AV}) * \left(P_{veg}/\{P_{veg} + P_k\}\right)\right] \quad (5.9)$$

$$Z_{max} = 0 \rightarrow NPP_{veg} = PPY_{veg} * SA * A_{vegetation} \quad (5.10)$$

where A_{veg} is the nutrient dependent growth coefficient for rooted vegetation and PPY_{veg} is the areal rooted vegetation productivity (mg $hr^{-1}m^{-2}$). Once a grid cell becomes flooded, rooted vegetation stops growing and a small fraction of PPY_{veg}eventually becomes part of the aquatic phase NPP after decomposition.

5.2.3 Land use /Land cover (LULC) maps and parameters

The LULC map published by JICA (1999) was used to represent observed historical cover conditions. Simulated baseline conditions and future scenarios used habitat cover maps from PULSEHAB as the LULC map in the 3D EIA model. As it was pointed out in Chapter 3, these maps classified the floodplain into 5 habitat groups based on their spatial preference and dominance of annual flood duration zones. Habitats with common flood duration patterns were then distinguished from each other by considering the historical cover; if there were no changes in flood duration between historical/baseline and future conditions, the historical habitat type was assumed to remain. Conversely, if there was a shift in flood duration, the area was reclassified to the habitat type that dominates the new flood duration zone. This was done whenever a particular area shifted to flood duration zones corresponding to rainfed habitats, transitional habitats, or seasonally flooded habitats, cases in which the LULC was reclassified to wet season rice, abandoned fields, or flooded shrublands, respectively. Table 5.1 describes how these specific rules were applied to the habitat maps. Overall, each of the maps used in this chapter include 10 different classes that cover most of the floodplain and permanent water. Each LULC class is associated with 9 parameters which affect

hydrodynamics, sedimentation, and NPP (Table 5.2). Three parameters (h_{veg}, vegetation cover, LAI) were estimated from field measurements in 2011-2012 taken in all 5 provinces surrounding the Tonle Sap (See Chapter 4). LAI was approximated from vegetation cover estimates (as a measure of canopy gap fraction) and the solar zenith angle with the expression described by Breda (2003):

$$LAI = \ln\big(P(\theta)\big)\cos(\theta)\,/G(\theta) \tag{5.11}$$

Where $P(\theta)$ is the canopy gap fraction, θ is the zenith angle of view (a function of longitude, latitude, and time of the day), and $G(\theta)$ is the fraction of foliage projected to the plane normal to θ (estimated with the procedure and assumptions described by Wilson, 1963).

The remaining parameters (vegetation drag, aeration, sediment oxygen demand, PPY_{veg}, PPY_{peri}, and PPY_{phyto}) were estimated using published values from other large tropical floodplains (Lamberts and Koponen, 2008; Sarkkula and Koponen, 2010).

Table 5.1. Rules applied to habitat cover maps derived from flood duration rules in order to map specific land use/land cover (LULC)

Historical map habitat group	Historical LULC	Change flood duration rule to:				
		Rainfed habitats	Transitional habitats	Seasonally flooded habitats	Gallery forest	Open water
		Resulting LULC:				
Rainfed habitats	R	R	AF	FS	GF	OW
	VC	VC	AF	FS	GF	OW
	LS	LS	AF	FS	GF	OW
Transitional habitats	AF	R	AF	FS	GF	OW
	TR	R	TR	FS	GF	OW
	LG	R	LG	FS	GF	OW
Seasonally flooded habitats	FS	R	AF	FS	GF	OW
	FG	R	AF	FG	GF	OW
Gallery forest	GF	R	AF	FS	GF	OW
Open water	OW	R	AF	FS	GF	OW

R = wet season rice; VC = village crop; LS = lowland shrubland; AF = abandoned fields; TR = floating and receding rice fields; LG = lowland grassland; FS = flooded shrubland; FG = flooded grassland; GF = gallery forest; OW = open water.

Table 5.2. EIA model parameters associated with land use/ land cover classes

land use/land cover class	h_{veg} [a] (m)	surface cover (%)	Vegetation drag	sediment O_2 demand (mg $m^2 d^{-1}$)	Aeration	PPY_{peri} [b] (mgC $m^2 h^{-1}$)	LAI[c] (m^2 m^{-2})	PPY_{phyto} [d] (mgC $m^3 h^{-1}$)	PPY_{veg} [e] (mgC $m^2 h^{-1}$)
Wet season rice	0.1	0.1	0.3	1.2	0.3	109.9	2.5	64.4	114
Floating and receding rice	0.3	0.1	0.3	1.2	0.3	109.9	3.4	64.4	114
Village crops	13.6	0.36	0.3	1.2	0.3	109.9	5.7	64.4	114
flooded grassland	3.4	0.47	0.3	1	0.9	109.9	6.2	64.4	114
abandoned fields	1.2	0.27	0.3	1	0.9	109.9	4.7	64.4	114
lowland grassland	3.4	0.47	0.3	1	0.9	109.9	6.2	64.4	114
flooded shrublands	5.5	0.75	0.6	1.4	0.2	109.9	6.4	64.4	114
tall shrublands	6.6	0.74	0.6	1.4	0.2	109.9	7.3	64.4	114
Gallery forest	8.3	0.68	0.5	1.1	0.1	109.9	6.8	64.4	114
Open water	0	0	0	0	1	17.0	6.0	151.0	114
All others	0.1	0.1	0.3	1.2	0.3	109.9	2.5	64.4	114

[a]vegetation height;
[b]Periphyton productivity rate;
[c]Leaf area index;
[d]Phytoplankton productivity rate;
[e]Terrestrial production rate.

5.2.4 EIA model calibration and validation

The Tonle Sap 3D EIA model has already been calibrated and validated for water levels, water volume, and sedimentation (Sarkkula, et al., 2003; Kummu et al., 2008). This chapter revisited the water level validation by comparing model estimates from the baseline scenario (hab_bl in Table 5.3) with observed daily water levels. In addition, primary productivity rates were calibrated and validated with the primary production field estimates presented by Holtgrieve et al. (2013). The 234 oxygen metabolism measurements were randomly split into two datasets, one for calibration and one for validation. The model was calibrated by adjusting PPY_{peri}, and PPY_{phyto} so that the sum of squares differences (SSD) between the simulated and measured NPP was minimized. Once the model was calibrated, SSD was calculated with the validation dataset. Calibration and validation were assessed based on the normalized SSD (SSD divided by the number of observation) and the average percent difference between the observed and simulated values.

5.2.5 Simulation scenarios

Simulations of baseline historical conditions and eleven future scenarios of hydropower development and/or climate change were carried out (Table 5.3). The baseline historical simulations were run with a combination of 2 LULC maps (the historical JICA 1999 LULC and the baseline land cover from PULSEHAB), and 2 sets of tributary flows (historical observations and simulated). All the simulated tributaries flows and land cover maps from PULSEHAB were derived from projections made with the VMOD Mekong basin-wide model (Lauri et al., 2012). Climate change was represented with the downscaled A1b scenario simulated by 5 different global circulation models (GCMs). Although downscaled results also exist for the B1 scenario, Lauri et al. (2012) showed that the discharge variability in Kratie among the five A1b simulations is inclusive of the B1 results. Baseline simulations were run for 11-23 years, whereas all future simulations were run for 10 years.

SSC from tributaries were the same in the climate change scenario as in the baseline, but in the hydropower scenarios the sediment loads from the Mekong Basin (upstream from Tonle Sap River) and Tonle Sap tributaries (Stung Sen, Sangker, and Pursat) with proposed dams were reduced according to the dam trapping efficiencies estimated by Kummu et al. (2010).

Comparisons among scenarios were done for the following parameters: water levels, maximum annual flood extent, annual flood duration, LULC classes/habitat cover area extent, net sedimentation, and total lake/floodplain NPP. Water level comparisons to historical measurements were done in the same way as in Chapter 3, by estimating the mean monthly water level residuals between future scenarios and the baseline scenario (hab_bl). The delta factors estimated were then compared to the monthly water levels for the historical observations representing average, dry, and wet years. Flood duration and flood extent were also compared using these 3 hydrological representative years. Net sedimentation and NPP were analyzed annually and monthly for all simulated years.

Table 5.3. Summary of 3D EIA simulation scenarios. See Lauri et al (2012) for details on the global circulation models (GCMs) used.

Scenario name	Scenario description	Climate change impact	Hydropower Impact
hab_bl	Simulated baseline conditions (1982-2005).	N	N
hab_bl+rv	baseline conditions (1982-2005) affected by hydropower development. Also used to test model's sensitivity to sediment reduction.	N	Y
mpA	2030s A1b climate change scenario from the MPI-ECHAM5 GCM without development plans.	Y	N
ccA	2030s A1b climate change scenario from the CCCMA-CGCM3.1 GCM without development plans.	Y	N
cnA	2030s A1b climate change scenario from the CNRM-CM3 GCM without development plans.	Y	N
giA	2030s A1b climate change scenario from the GISS-AOM GCM without development plans.	Y	N
ncA	2030s A1b climate change scenario from the NCAR-CCSM3 GCM without development plans.	Y	N
ccA+rv	2030s A1b climate change scenario from the CCCMA-CGCM3.1 GCM with hydropower development.	Y	Y
cnA+rv	2030s A1b climate change scenario from the CNRM-CM3 GCM with hydropower development.	Y	Y
giA+rv	2030s A1b climate change scenario from the GISS-AOM GCM with hydropower development.	Y	Y
mpA+rv	2030s A1b climate change scenario from the MPI-ECHAM5 GCM with hydropower development.	Y	Y
ncA+rv	2030s A1b climate change scenario from the NCAR-CCSM3 GCM with hydropower development.	Y	Y

5.2.6 Sensitivity analysis

A sensitivity analysis was done on 9 parameters that influence NPP (listed in Table 5.7). The procedure followed a combined Latin-hypercube and one-factor-at-a-time sampling, method in which each of the parameters is sampled multiple times, simulations carried with each of the sampled values, and then the overall impact of each parameter on the model output calculated (van Griensven et al., 2006). The baseline scenario (simulated from 1997 to 2001)

was run 91 times in which each of the 9 parameters was varied within the range of plausible values. Total NPP was then estimated and linear regressions were fit between NPP and each of the 9 parameters to assess model sensitivity. Furthermore, a local sensitivity test was carried out on the assumed reduction in sediment loads applied to the hydropower scenarios by simulating the hab_bl+rv scenario with adjusted sediment loads from the tributaries corresponding to 0, 50, and 150% of the default sediment load reduction.

5.3 Results

5.3.1 EIA model calibration and validation

Simulations with the EIA model baseline scenario (hab_bl) show a good representation of the observed daily water levels at the lake (Figure 5.4). Overall, the Pearson correlation coefficient (r) between observed and simulated water levels was 0.972. At mid to high observed water levels (greater than 5 m asl.), the simulations are very accurate and there is an even distribution between overestimated and underestimated water levels. At low water levels (< 3 m), however, there was a tendency for the model to overpredict water levels.

Measured NPP was 0.89 ± 0.53 gC m^{-2} d^{-1} (Holtgrieve et al., 2013), while the 3D EIA model predicted 0.52 ± 0.13 gC m^{-2} d^{-1} for the same locations and dates of the measurements. For the calibration dataset, the normalized SSD was 0.41 and the average match was 81 ± 48 %. For the validation dataset, the normalized SSD was 0.38 and the average match was 76 ± 46 %. Although these NPP calibration and validation results are not optimal, the fact that the two sets of NPP values are derived from completely different theorical approaches (field-based estimates come from an oxygen metabolism approach whereas the 3D EIA model is based on plankton growth) needs to be considered. Limitations and uncertainties associated with different approaches to estimate aquatic primary production has been long discussed in

the literature (Hall and Moll, 1975), and the fact that these is reasonable level of agreement in the NPP comparison is a compelling finding.

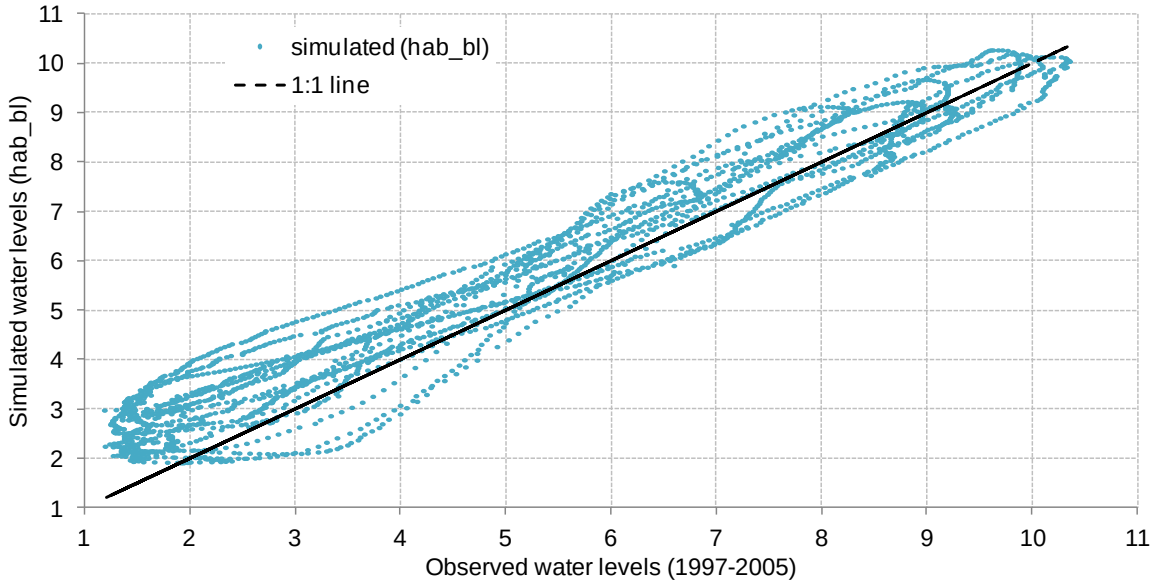

Figure 5.4. Comparison of observed and simulated daily water levels for 1997 to 2005.

5.3.2 Water level changes future scenarios

The simulation of the 5 GCMs of the A1b climate change scenario resulted in an uncertainty envelope around the observed water level hydrographs of representative hydrological years (Figure 5.5a-c; Table 5.4). Largest uncertainty is expected in dry years for the months of October through December, with changes of -0.66 to +0.70 m from baseline conditions; in contrast, smallest changes and uncertainty are expected during wet years, with changes of -0.41 to + 0.32 m during the same months. Hydropower development simulations resulted in more prominent changes, mainly a reduction of water levels during the wet season and an increase during the dry season (Figure 5.5d-e). Disruptions caused by hydropower would be most intense during dry years, with higher water levels during the dry season in May-June (+ 0.87 ± 0.17 m), and lower water levels at the peak of the wet season in October (- 0.4 ± 0.5 m).

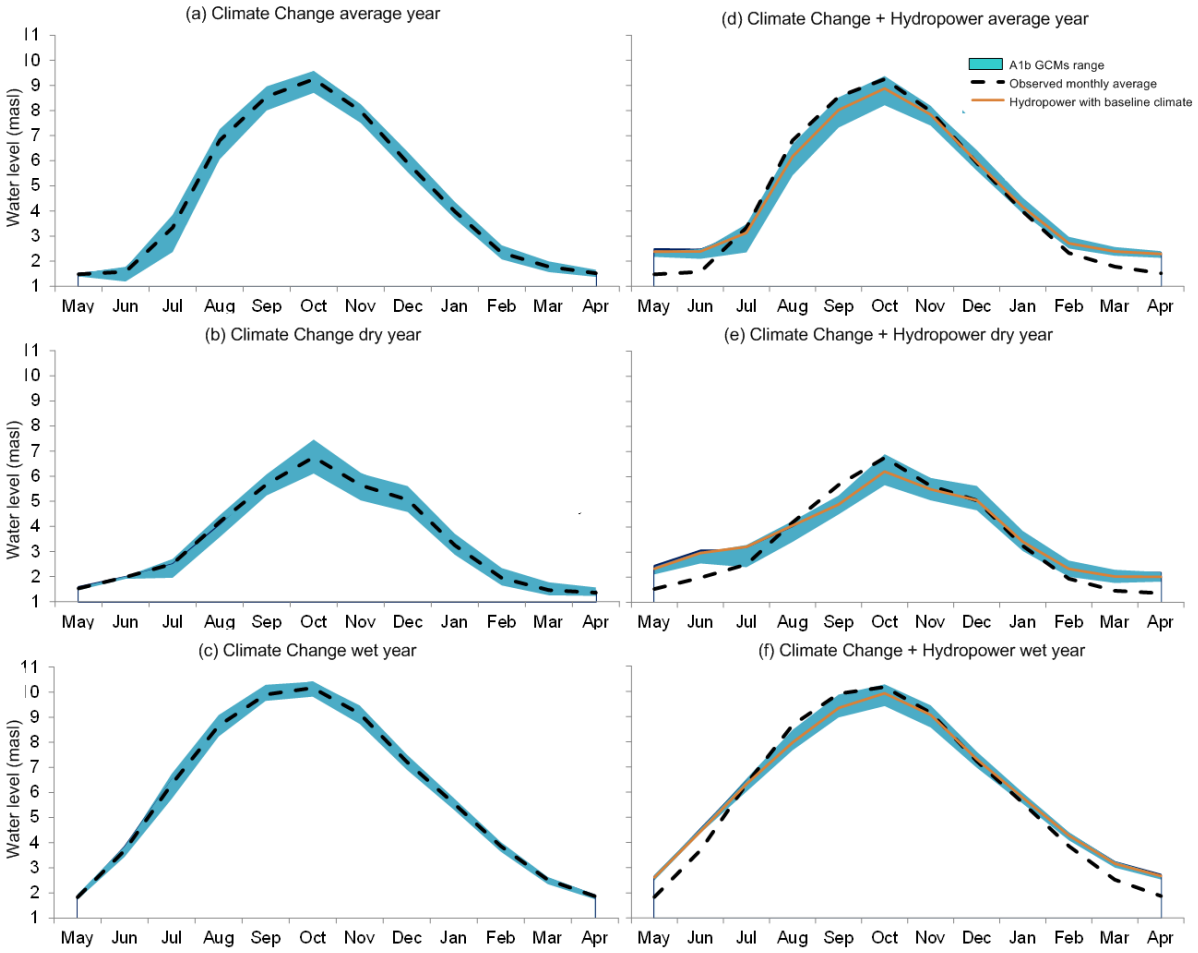

Figure 5.5. Impact of climate change and hydropower on monthly average water levels of 3 representative hydrological years in the Tonle Sap. Climate change could increase uncertainty whereas hydropower could dampen water level fluctuation.

Table 5.4. Changes in monthly water level caused by climate change and hydropower during 3 representative hydrological years in the Tonle Sap.

Month	hab_ bl	hab_ bl+rv	mpA	ccA	cnA	giA	ncA	mpA +rv	ccA +rv	cnA +rv	giA +rv	ncA +rv
	masl	*Change from bl (m)*										
Average year												
May	2.61	0.90	0.03	0.04	-0.09	-0.01	0.04	1.01	0.87	0.69	0.90	0.90
Jun	3.01	0.81	0.08	0.16	-0.39	0.14	0.20	0.89	0.83	0.51	0.88	0.90
Jul	5.68	-0.21	-0.26	0.51	-0.97	0.11	0.21	-0.42	0.14	-0.99	-0.15	-0.07
Aug	7.78	-0.64	-0.42	0.45	-0.75	-0.06	0.09	-1.01	-0.14	-1.39	-0.65	-0.51
Sep	9.46	-0.53	-0.21	0.41	-0.55	-0.20	0.23	-0.75	-0.03	-1.23	-0.74	-0.21
Oct	9.44	-0.38	0.01	0.33	-0.54	-0.15	0.32	-0.38	0.13	-1.04	-0.59	0.03
Nov	8.24	-0.14	0.05	0.25	-0.47	-0.09	0.28	-0.12	0.21	-0.58	-0.27	0.16
Dec	6.99	0.05	0.11	0.21	-0.37	-0.08	0.44	0.18	0.35	-0.30	-0.04	0.52
Jan	5.76	0.18	0.11	0.17	-0.29	-0.07	0.39	0.29	0.39	-0.08	0.11	0.55
Feb	4.69	0.38	0.08	0.12	-0.26	-0.09	0.30	0.46	0.51	0.18	0.32	0.64
Mar	3.77	0.61	0.04	0.07	-0.21	-0.09	0.21	0.67	0.69	0.44	0.54	0.79
Apr	3.03	0.77	0.02	0.04	-0.15	-0.06	0.14	0.81	0.81	0.61	0.72	0.88
Dry year												
May	2.56	0.81	0.06	0.03	-0.07	-0.01	0.05	0.93	0.79	0.58	0.78	0.85
Jun	2.44	0.98	0.01	0.03	-0.07	-0.01	0.03	1.09	1.00	0.57	1.00	1.01
Jul	3.64	0.70	-0.34	0.19	-0.56	-0.01	-0.01	0.57	0.77	-0.11	0.67	0.65
Aug	5.73	-0.12	-0.51	0.26	-0.61	-0.11	-0.13	-0.38	0.06	-0.77	-0.19	-0.19
Sep	8.06	-0.79	-0.20	0.40	-0.45	-0.22	0.12	-0.88	-0.43	-1.18	-0.95	-0.67
Oct	8.40	-0.55	0.37	0.70	-0.66	-0.26	0.48	-0.18	0.14	-1.09	-0.86	-0.02
Nov	7.47	-0.14	0.33	0.50	-0.61	-0.23	0.46	0.14	0.31	-0.58	-0.39	0.31
Dec	6.50	0.01	0.20	0.29	-0.49	-0.16	0.55	0.23	0.30	-0.39	-0.17	0.58
Jan	5.38	0.17	0.14	0.20	-0.38	-0.13	0.46	0.33	0.35	-0.21	0.04	0.59
Feb	4.36	0.39	0.12	0.16	-0.29	-0.09	0.40	0.53	0.53	0.08	0.30	0.72
Mar	3.50	0.57	0.09	0.12	-0.20	-0.06	0.31	0.73	0.70	0.31	0.53	0.84
Apr	2.86	0.65	0.06	0.07	-0.13	-0.04	0.21	0.82	0.78	0.46	0.64	0.84
Wet year												
May	2.75	0.78	0.04	0.06	-0.10	0.00	0.12	0.82	0.80	0.66	0.78	0.89
Jun	2.90	0.74	0.04	0.12	-0.26	0.15	0.16	0.81	0.83	0.68	0.84	0.86
Jul	4.80	-0.01	-0.17	0.41	-0.59	0.15	0.21	-0.05	0.21	-0.31	0.09	0.12
Aug	7.47	-0.69	-0.40	0.43	-0.43	-0.01	0.16	-0.97	-0.19	-1.00	-0.67	-0.40
Sep	9.96	-0.57	-0.21	0.39	-0.25	-0.10	0.23	-0.77	-0.03	-0.94	-0.74	-0.21
Oct	9.66	-0.25	0.01	0.24	-0.35	-0.06	0.27	-0.24	0.11	-0.76	-0.39	0.09
Nov	8.72	-0.08	0.16	0.32	-0.41	-0.03	0.25	0.09	0.30	-0.58	-0.14	0.20
Dec	7.19	0.08	0.14	0.29	-0.32	-0.05	0.20	0.23	0.38	-0.26	0.02	0.29
Jan	5.80	0.21	0.10	0.21	-0.25	-0.05	0.15	0.30	0.41	-0.03	0.16	0.35
Feb	4.67	0.41	0.07	0.17	-0.22	-0.05	0.12	0.49	0.55	0.23	0.37	0.51
Mar	3.73	0.64	0.05	0.12	-0.17	-0.05	0.08	0.71	0.73	0.48	0.60	0.70
Apr	3.00	0.80	0.04	0.07	-0.12	-0.04	0.05	0.85	0.84	0.66	0.76	0.83

5.3.3 Changes in flood duration and habitat cover under future scenarios

As a response to climate change alone, the uncertainty associated with water level projections led to an inconclusive net change in maximum flood extent. This is demonstrated, for instance, by the color bands in the outer parts of the floodplain in Figure 5.6c-d, which occur wherever there was flood duration differences among future scenarios. However, cumulative scenarios of climate change and hydropower show a tendency to reduce the maximum flood extent by 529 ± 619 km^2 (5 ± 6%; Figure 5.6d). Although the relative change in flood extent is small and variable depending on scenario, patterns in annual flood duration could change drastically. The area of the floodplain that would be most affected under cumulative scenarios is where flood duration is 9 months in average and dry years; this area will be reduced by 33 ± 42 %.

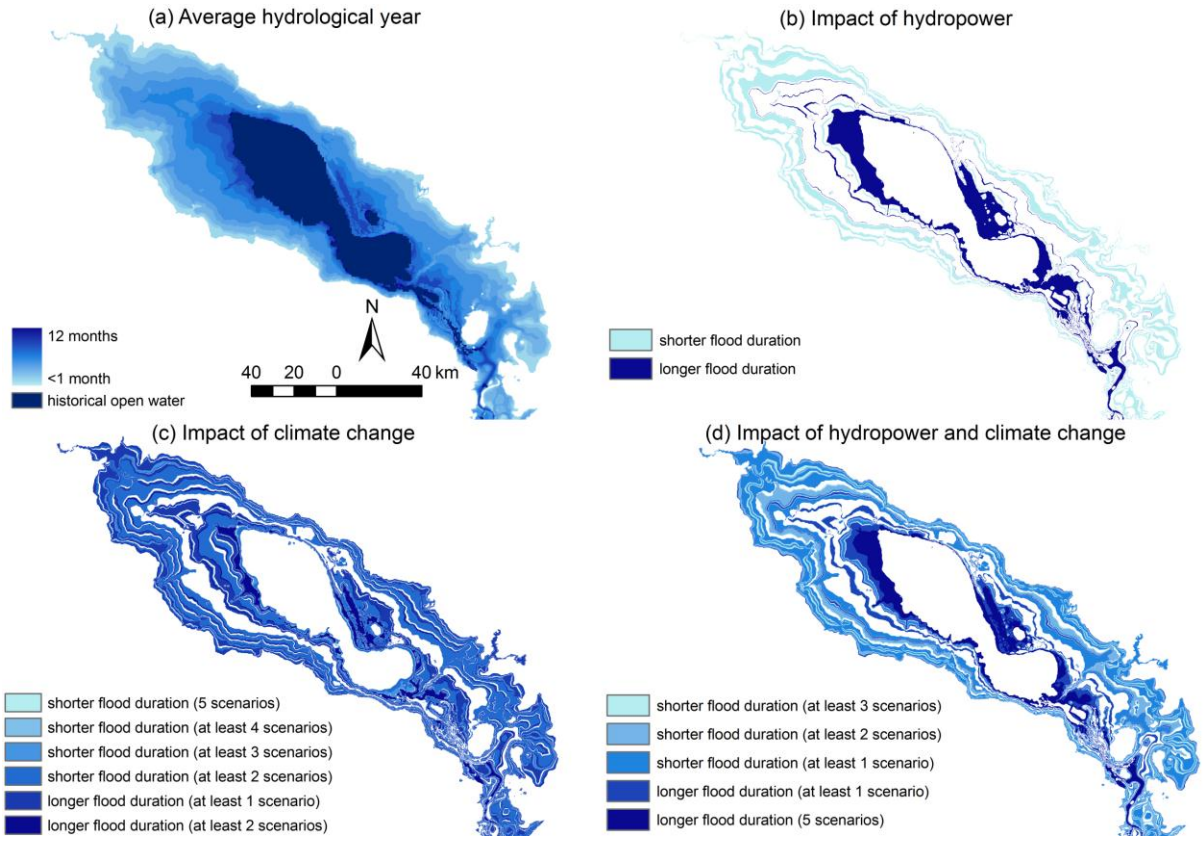

Figure 5.6. Changes in spatial distribution of annual flood duration and increase in the permanent lake area during an average hydrological year.

Small changes in water level, flood extent, and flood duration will probably result in substantial changes in the optimal area for some of the most representative habitats in the Tonle Sap (Table 5.5). As a response to climate change, the open water could expand by 362 ± 266 km^2 (14 ± 10 %), while the gallery forest could shrink by 400 ± 205 km^2 (63 ± 31 %). As a response to hydropower and climate change combined more drastic changes are expected. Open water and rainfed/irrigated rice could expand by 883 ± 76 km^2 (35 ± 3 %) and 1184 ± 375 km^2 (16 ± 5 %), respectively. Overall, the optimal area for seasonally flooded habitats will decrease; gallery forest by 261 ± 175 km^2 (40 ± 27 %), flooded shrublands by 492 ± 212 km^2 (13 ± 5 %), and flooded grasslands by 108 ± 28 km^2 (12 ± 3 %).

Table 5.5. Expected shifts in aerial extent of the most representative habitats of the Tonle Sap. The largest shift in aerial extent is expected to occur in the irrigated rice and abandoned fields, but the largest relative changes is expected to occur in the gallery forest and open water. See Table 5.2 for scenarios description.

	Rainfed / Irrigated rice		Flooded grasslands		Abandoned fields		Flooded Shrublands		Gallery forest		Open water	
Scenario	Total area in model (km^2)											
Baseline	7511		866		4440		3921		657		2550	
	Changes from baseline											
	km^2	%	km^2	%	km^2	%	km^2	%	km^2	%	km^2	%
ccA	-479	-6	35	4	98	2	403	10	-476	-72	496	19
cnA	989	13	-76	-9	-149	-3	-594	-15	-40	-6	-111	-4
giA	4.9	0	-58	-7	624	14	-473	-12	-544	-83	460	18
mpA	843	11	4.5	1	-1036	-23	281	7	-437	-66	444	17
ncA	-185	-2	12.5	1	-155	-3	403	10	-503	-77	523	20
hab_bl+rv	1259	17	-126	-15	-1249	-28	-526	-13	-143	-22	893	35
ccA+rv	639	9	-118	-14	-854	-19	-360	-9	-130	-20	910	36
cnA+rv	1646	22	-97	-11	-880	-20	-870	-22	-492	-75	742	29
giA+rv	1284	17	-57	-7	-1234	-28	-267	-7	-482	-73	861	34
mpA+rv	1434	19	-131	-15	-1434	-32	-541	-14	-158	-24	943	37
ncA+rv	843	11	-123	-14	-1020	-23	-387	-10	-164	-25	949	37

5.3.4 Changes in sediments

The estimated annual average net sedimentation in the floodplain and open water combined is 3.28 ± 0.93 million tons, or 765 ± 203 g m^{-2}. Assuming a bulk sediment density of 1.6 g/cm^3, this is equivalent to 0.48 ± 0.13 mm yr^{-1} , which is consistent with contemporary sedimentation rates estimated from sediment cores (Kummu et al., 2008; Penny et al., 2005). Net sedimentation seasonal fluctuation follows the same patterns as incoming suspended sediments, with negligible sedimentation occurring from April to July, and with 70% of the annual total occurring between August and October (Figure 5.7a). Minor seasonal changes are expected as a result of climate change scenario A1b, and overall, this scenario could result in a small annual change (Table 5.6). Much greater changes are expected as a response of hydropower (Figure 5.7b); in both types of scenarios (hydropower scenario alone and combined with climate change), an annual reduction of more than 50% in net sedimentation is expected (Table 5.6).

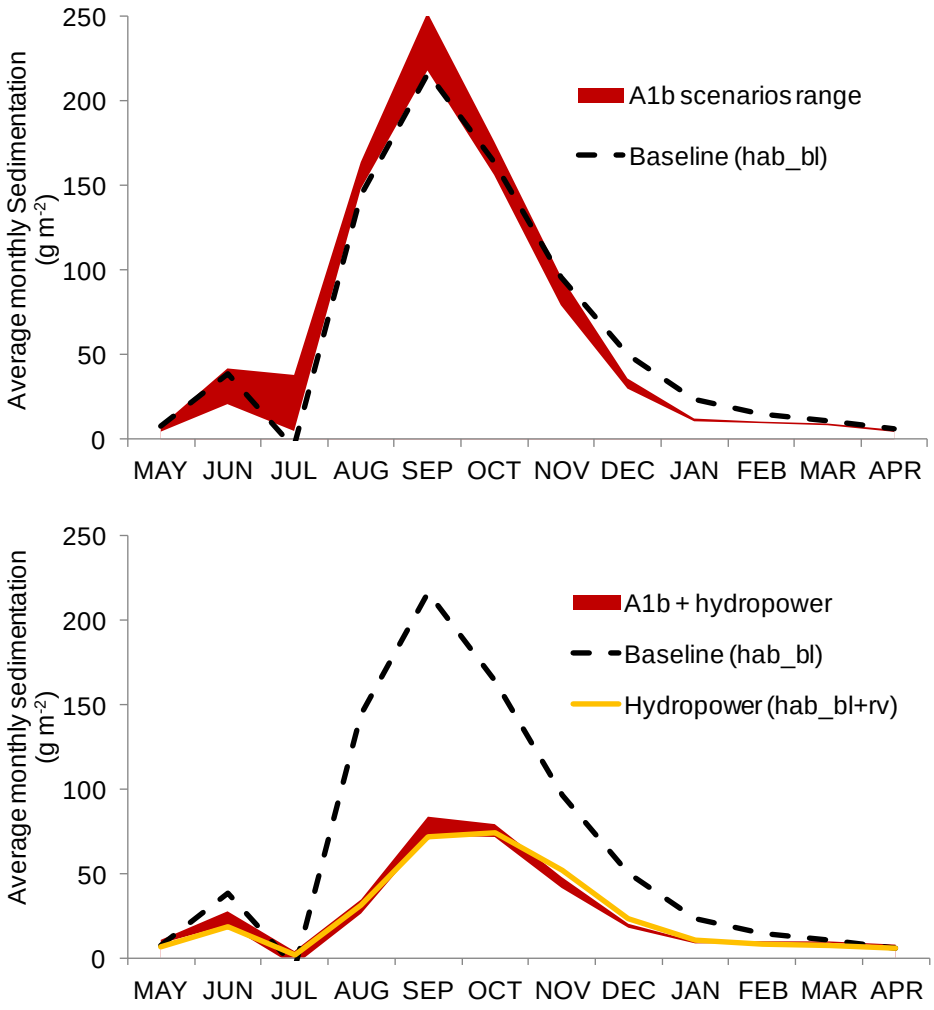

Figure 5.7. Average monthly sedimentation in the lake and floodplain is expected to decrease primarily as a response to hydropower.

5.3.5 Changes in primary production

The baseline annual average NPP was 1.07 ± 0.06 million tons C (or 707 ± 264 gC m^{-2}) in the open water and 3.67 ± 0.61 million tons C (or 772 ± 190 gC m^{-2}) in the floodplain. Average monthly estimates show that under all future scenarios NPP could decline (Figure 5.8). A total annual reduction of 31% occurs as a result of hydropower, 9-15% reduction as a result of climate change, and 33-39% reduction as the combined effect of climate change and hydropower (Table 5.6).

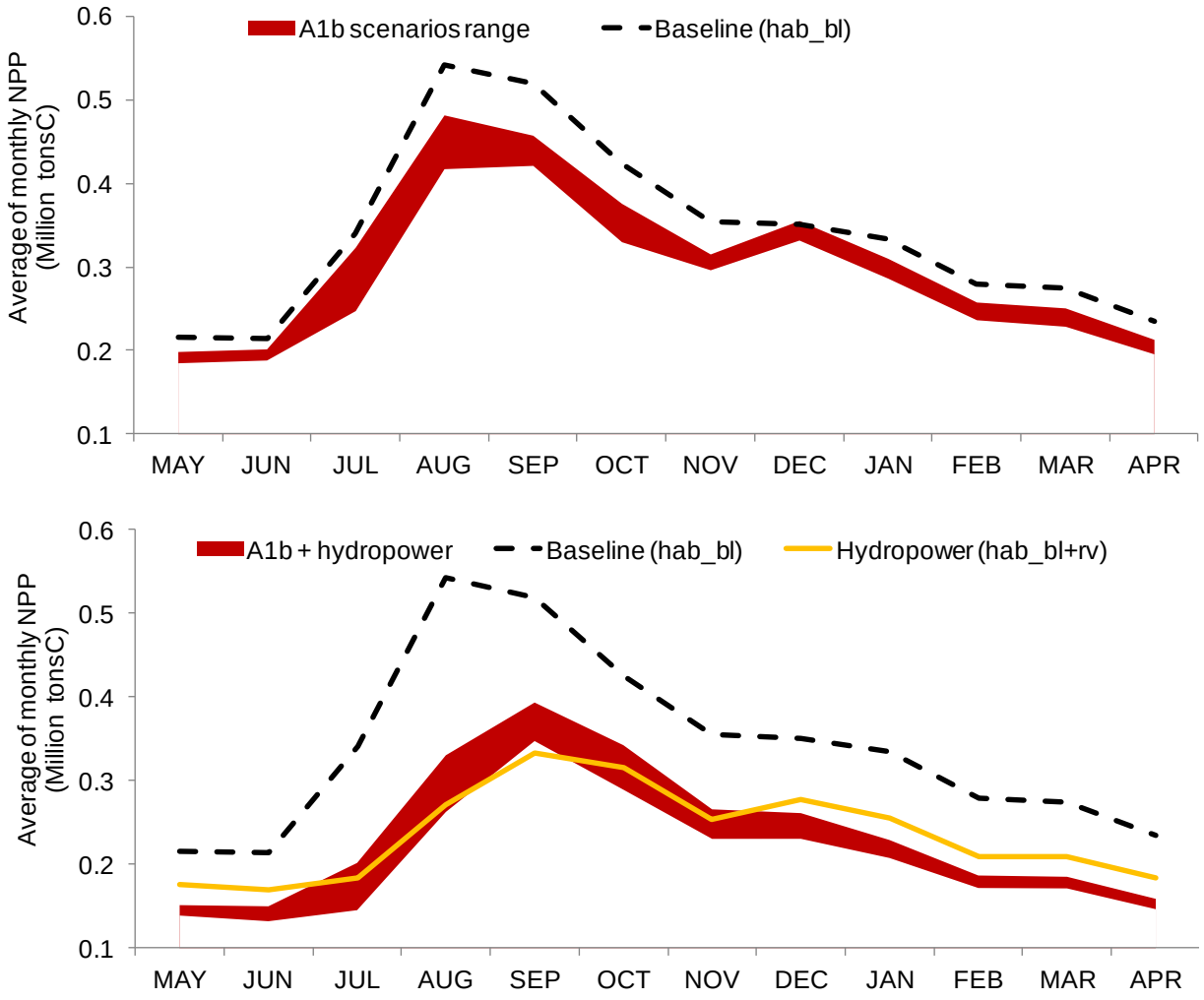

Figure 5.8. Average monthly net primary production (NPP) in the Tonle Sap lake and floodplain.

Table 5.6. Total annual changes in sedimentation and net primary production. Values ranges (±) represent standard variation among different years.

Unit	baseline (hab_bl) amount	climate change (A1b)	% change	Hydropower (hab_bl+rv)	% change	A1b + hydropower	% change
			Net sedimentation				
g m^{-2}	765 ± 203	781±157	+2	309 ± 52	-60	319 ± 65	-57
10^6 ton	3.3 ± 0.9	3.3 ± 0.7	-1	1.5 ± 0.3	-53	1.4 ± 0.3	-35
			Net primary production				
gC m^{-2}	979 ± 52	857 ± 20	-12	567 ± 153	-42	657 ± 31	-34
10^6 tonC	4.1 ± 0.2	3.6 ± 0.6	-13	2.8 ± 0.1	-31	2.7 ± 0.2	-35

5.3.6 Sensitivity analysis

Results of the sensitivity analysis suggest that the 3D EIA estimates of NPP are highly predictable and stable as a response to changes in vegetation characteristics, plankton productivity, water quality, and soil quality (Table 5.7). NPP was most sensitive to $D_{secchimax}$, which caused an NPP increase of 23% with a 50% increase in the input parameter, and PPY_{phyto}, which cause an NPP increase of 19% as a result of 50% increase in the input parameter (see last column in Table 5.7). The model was least sensitive to P_{SED}, with only a 1% increase in NPP as a response to a 50% increase in this parameter.

Table 5.7. Sensitivity of total floodplain and lake net primary production (NPP) to model parameters.

Model parameter (x)	Range values tested	Linear regression	Default value[a]	% change in NPP caused by a 50% increase from the default value
$D_{secchimax}$ [b]	0-370	NPP = 3.01E+01x + 9.22E+03	250	23%
PPY_{phyto} [c]	0-300	NPP = 4.46E+01x + 7.98E+03	110	19%
LAI[d]	1-10	NPP = 8.75E+02x + 1.26E+04	6.1	15%
PPY_{peri} [e]	0-300	NPP = 3.05E+01x + 1.08E+04	103	11%
P_{SSC} [f]	0.0001-0.01	NPP = 6.83E+05x + 1.37E+04	0.004	8%
PPY_{veg} [g]	0-360	NPP =1.65E+01x + 1.50E+04	114	6%
vegetation coverage	0.01-0.9	NPP = 2.31E+01x + 1.55E+04	66	5%
h_{veg} [h]	0-18	NPP = -2.81E+02x + 1.82E+04	6.2	-5%
P_{SED} [i]	0.001-0.007	NPP = 2.10E+06x + 2.87E+04	0.0002	1%

[a] Default value represents floodplain wide average, see Table 1 for values used in specific land use/Land cover classes;
[b] Secchi disk max depth(cm);
[c] Phytoplankton productivity rate (mgC h^{-1} m^{-3});
[d] Leaf area index (m^2 m^{-2});
[e] Periphyton productivity rate (mgC $h^{-1}m^{-2}$);
[f] Bioavailable P in suspended sediments (%);
[g] Terrestrial production rates (mgC h^{-1} m^{-2});
[h] vegetation height (m);
[I] Bioavailable P in bottom sediment (%).

Sediment trapping in upstream reservoirs was found to be a significant factor in determining net sedimentation (Table 5.8). If hydropower dams in the Mekong and Tonle Sap tributaries are assumed to not trap sediments, the net sedimentation in the floodplain would be 176 ± 65 g yr^{-1} m^{-2}. On the contrary, if the proposed dams are assumed to trap a fraction of the incoming sediments according to the estimates by Kummu et al. (2010), the average net sedimentation in the floodplain would be reduced by 41.6 ± 7.7%. Variation in the sediment reduction factors would result in a proportional variation in floodplain net sedimentation (aka., a 50% decrease/increase in the trapping efficiency yields a 50% decrease/increase in floodplain annual net sedimentation). Even though these estimates suggest a direct relationship between sediment trapping in reservoirs upstream and net sedimentation in the Tonle Sap downstream, it

should be acknowledged that only sediment processes within the Tonle Sap system and not in the Mekong River channel were taken into account. Sediment erosion and deposition along the Mekong are significant (Darby et al., 2010; Walling, 2009), and these processes could play an important role in the amount and timing of sediment transported in and out of the Tonle Sap.

Table 5.8. Sensitivity of floodplain annual net sedimentation to dam suspended sediment trapping.

	No sediment trapping	50% of default	Default sediment trapping	150% of default
Net sedimentation (g yr^{-1} m^{-2})	176 ± 65	135 ± 51	103 ± 42	70 ± 31
Change in sedimentation (%)	-	-23.1 ± 6.6%	-41.6 ± 7.7%	-60.6 ± 8.9%

5.4 Discussion

The results of this chapter suggest that ongoing and future modifications in the Mekong Basin caused by hydropower and climate change are likely to create a chain of effects leading to an eventual decrease in NPP. Projected changes in water levels and flood duration caused by hydropower were found to match estimates from previous modelling efforts (described in Chapter 2 and Johnston and Kummu, 2011), which reported water level changes up to +0.6 m and -0.75 m during the dry and wet seasons, respectively. Water level alterations caused by climate change are in agreement with those presented by Västilä et al. (2010), showing discrepancies in monthly average values among climate change simulations without a single direction in the magnitude of changes. Water levels and flood duration changes could eventually shift LULC/habitat cover, in particular at the inner/outer floodplain boundaries. Previous studies (Arias et al., 2012; Kummu and Sarkkula, 2008) also showed that these areas are the most vulnerable to changes in water levels and flood duration, but the refinements made in the present

study have permitted projections associated with specific LULC classes (e.g., grasslands and shrublands within the seasonally flooded habitats). Results from the baseline simulations were found to be in good agreement with observed sedimentation rates (Kummu et al., 2008; Penny et al., 2005) and aquatic productivity (Holtgrieve et al., 2013).

The sensitivity analysis revealed that the 3D EIA model is not disproportionately sensitive to any of the input parameters tested. In other words, model outputs changed linearly and proportionally to variation in model's input parameters. The results of this sensitivity analysis are useful in pointing out those parameters with the greatest influence on NPP and that should be the priority of further research. For instance, secchi disk max depth ($D_{secchimax}$) and bioavailable P in suspended sediments (P_{SSC}) have been previously measured (Sarkkula, et al., 2003; Koehnken, 2012), but the model's assumption of stationary and uniform conditions should be further tested. Although plankton productivity rates were estimated based on oxygen metabolism measurements at a reduced number of locations (Holtgrieve et al., 2013), the contribution from specific primary producers (phytoplankton vs. periphyton) and differences in rates depending on habitat remain unknown. Also, the role of floodplain vegetation, in particular with regards to LAI and production rates, has not been well documented.

5.4.1 Hydrology, sediments, and LULC are the drivers of change

The flood-pulse from the Mekong is expected to be dampened with ongoing development, reducing the peaks of sediment flows and reducing the extent of the floodplain. In addition, sediments are also major drivers of NPP by replenishing the lake and floodplain with nutrients; yet, the sediment load is projected to decrease due to reservoir trapping (e.g. Kummu et al 2010), and this could subsequently decrease floodplain-wide net sedimentation by 42%. Reservoir

trapping could also modify sediment characteristics (e.g., particle size distribution and nutrient content), but the extent of these potential changes needs further investigation. Furthermore, modifications to the annual flood duration throughout the floodplain could expand the area of permanent water and reduce the extent of seasonally flooded natural habitats; this will modify floodplain vegetation characteristics (e.g., LAI and canopy height) that play an important role in the floodplain's NPP. The mechanisms by which water, sediments, nutrients, and terrestrial productivity limit NPP are unknown and should be subject to further research in order to improve future predictions. However, observations of floodplain vegetation, soils, water quality, and aquatic organisms indicate that spatial and temporal patterns of these environmental attributes in the Tonle Sap are highly influenced by the seasonal inundation cycle (e.g., Arias et al., 2013.; Brooks et al., 2009; Irvine et al., 2011). This follows the the general principles described by the Flood-Pulse Concept observed in other large tropical floodplains, suggesting that the ecological principles underlying the 3D EIA model are valid.

5.4.2 Hydropower is a more immediate threat to the Tonle Sap ecosystem than climate change

Results from this chapter suggest that climate change in the next decades could bring greater seasonal uncertainty, but not substantial changes to the average seasonal trends. Other studies have found that inter-annual variation in the basin's hydrology has been intensifying for at least three decades (Delgado et al., 2012; Räsänen et al., 2013), but whether this is directly caused by climate change or caused by a long-term climate cycle is still a subject of discussion. The 10 year long simulations that comprised the future scenarios in this chapter were not long enough to fully address the inter-annual variability issue, and thus this should be considered in future research.

Paleolimnological evidence suggests that sedimentation and primary production have varied at longer temporal scales (Day et al., 2011; Penny, 2006), which implies that the Tonle Sap ecosystem has indeed been impacted by past climate and environmental changes. However, the changes that the Tonle Sap hydrology is currently facing are much faster than any other that the system has experienced before and therefore an abrupt transition in ecosystem function could occur in the upcoming decades.

This is the first study that assesses the cumulative impact of hydropower and climate change on the ecological function of the Tonle Sap. The main outcome of this comparison is that the seasonal impacts from hydropower overrule those from climate change. This finding complements the results from Chapter 3 (which evaluated impacts from multiple infrastructure development scenarios separately from climate change) as well as the hydrological assessment of cumulative impacts for the entire Mekong Basin (Lauri et al., 2012). Even though the hydropower scenario used in this chapter and in Lauri et al. (2012) represents a large number of dams that are only at the planned stage, the recent development trends imply that most of the hydropower potential in the basin could eventually be exploited (Grumbine and Xu, 2011; MRC, 2011). Nonetheless, information about the location and operation of planned dams is seldom publicly available, and therefore there is a moderate degree of uncertainty associated with studies that use multiple hydropower scenarios. Modifications to the location and operation of planned dams, however, has significant effects on the level of hydrological disturbance (Piman et al., 2012), as well as on the level of alterations to the ecosystem services provided at the watershed and regional scales (Arias et al., 2011; Ziv et al., 2012). With good regional planning and coordination, guided hydropower development could bring an opportunity for developers,

governments, scientists, and conservationists to create sustainable solutions that optimize electricity generation along with ecological and nutritional values.

5.4.3 Changes in primary production could alter ecosystem function and livelihoods

The changes in the primary production and the other environmental drivers assessed in this chapter could bring significant disruptions to the ecosystem services that the Tonle Sap provides to local livelihoods and the lower Mekong region. Other studies have made a direct link between the basin's future disruptions (mainly hydropower) and the impact on fish migrations and food security (Orr et al., 2012; Ziv et al., 2012). In this chapter, this potential threat is emphasized by showing that the drivers of ecological productivity of the most important wetland ecosystem in the Mekong Basin are highly vulnerable to ongoing disruptions.

Holtgrieve et al. (2013) points out that aquatic primary production of the Tonle Sap is within the typical range for tropical lakes; when the contribution from the floodplain is accounted for, average NPP is 2.63 ± 0.13 gC $m^{-2}d^{-1}$, nearly identical to the global average productivity reported by Melack (1976). The average NPP from the Tonle Sap, however, supports one of the largest harvests of freshwater organisms in the planet, which suggests that a high fraction of aquatic NPP is entering the food web (as much as 69%), and/or there is significant inputs of allochthonous organic matter (Holtgrieve et al., 2013). A reduction in NPP from decreased sedimentation combined with lower allochthonous inputs due to reduced flooding means the basal resources to support fish production will be diminished in the future, potentially compromising the entire foodweb and the society that it supports.

5.5 Chapter conclusions

The 3D EIA model was used to estimate water levels, flood duration, sedimentation, and aquatic net primary production in the Tonle Sap. Published field observations were used to characterize, calibrate, and validate the different components of this model. Estimates of baseline scenarios show good agreement with historical water levels and primary production observations. The model was moderately sensitive to sediment inputs and their role in limiting euphotic depth. Hence, further research on sediment processes is needed.

Future sedimentation and NPP projections were carried out for the most probable scenarios of basin-wide cumulative impacts from climate change and hydropower development. It is concluded that hydropower development will probably bring more imminent disruptions than climate change. As a response to maximum hydropower capacity, seasonal fluctuation of water level and flood extent could decrease, sediments could be trapped, and the area of gallery forest and other natural habitats could be permanently flooded or converted to agriculture. It is important, however, to recognize that the effects of hydropower development will be seen rather gradually in the upcoming decades and that there is some level of uncertainty associated with the number, location, and operation of hydropower projects. When hydropower and climate change are analyzed together, future scenarios show that the cumulative effect would be of similar magnitude as the hydropower scenario alone, but a range of uncertainty is added to the overall reduction of natural habitats, sedimentation, and NPP.

CHAPTER 6: MODELLING IMPACTS TO FAUNA HABITATS

6.1 Introduction

Spatial distribution models of wetland species in the tropics are limited to those areas were appropriate biological monitoring has been carried out (Rodríguez, 2003). The Everglades, for example, is the best studied wetland in the (sub-) tropics (Junk et al., 2006), and spatial models of distribution of multiple aquatic and terrestrial animals have been developed (DeAngelis et al., 1998; Gaff et al., 2000). These models, however, represent complex biophysical and foodweb interactions that were only understood after decades of monitoring and research.

In contrast, the Tonle Sap in Cambodia remains one of the least explored large wetlands in the world (Junk et al., 2006; Parolin and Wittmann, 2010). Knowledge on ecological properties and interactions in the Tonle Sap is limited (Lamberts 2006; Kummu et al. 2006), yet this wetland is facing ecological changes as a result of imminent disruptions to its hydrology. Hydrological changes in the Mekong Basin caused by hydropower and climate change will result in a modified flood-pulse, mainly by reducing seasonal water level variability while increasing inter-annual uncertainty. These hydrological changes could in turn result in permanent modification of habitats (See Chapter 3).

Both anecdotic and scientific evidence suggest that fauna in the Tonle Sap are highly depended on habitat type and their characteristics (Davidson, 2006; Bonheur & Lane, 2002). For instance, migratory fish species access the seasonally flooded habitats to feed during the wet season, while resident fish species inhabit these areas throughout their life cycles (Valbo-

Jørgensen et al., 2009). Moreover, an assembly of 7 species of water snakes –which are subject to the largest snake harvest in the planet–, are permanent residents of the gallery forests and adjacent habitats (Brooks et al., 2009). Some fish species of the Tonle Sap are reliant on the nutrient-rich habitats made available during the flood pulse aquatic phase to complete their life-cycles, others require the refugial ponds created by the inundation of the habitat to survive the dry season. Various endangered bird species inhabit the Tonle Sap, and most of these have particular habitat preferences; for example, grey-headed fish-eagles (*Ichthyophaga ichthyaetus*) are typically found in forested areas (Tingay et al., 2010), whereas Bengal floricans (*Houbaropsis bengalensis*) are predominantly found in grasslands (Gray et al., 2009). The close linkage of these species to their habitats and the restrictions that this imposes suggests that flooding and distribution of habitats in the Tonle Sap is crucial for maintaining biological productivity and biodiversity.

The Tonle Sap is home to a large human population that subsists on the wetland's resources. Based on a 1998 survey, 1.2 million people inhabited the Tonle Sap and nearly 70% of them were subsistence farmers and fishermen (Keskinen, 2006). The population grew to 1.7 million by 2008, and although the greatest growth rates occurred in the urban areas, the majority of the population are still dependent on agriculture and fishing (Keskinen et al., 2011). The vast majority of the protein that the Tonle Sap inhabitants eat comes directly from fish and other aquatic organisms harvested in the open lake and inundated habitats (Hortle, 2007 after Ahmed et al., 1998). Moreover, agricultural fields –mainly rice paddies– are an integral component of the Tonle Sap that represent nearly one third of the wetland area. Human activities are thus an important factor of the Tonle Sap ecosystem, which imposes the greatest challenge to fauna conservation. In addition to changes in habitat resulting from future hydrological changes, any

conservation management planning will need to incorporate an understanding of how hydrological changes will affect human activities on and around the wetland.

The importance of the Tonle Sap for biodiversity and livelihoods has recently drawn significant international and regional conservation efforts in recent decades. In 1997, UNESCO established the Tonle Sap as Cambodia's only Biosphere Reserve (UNESCO, 2010), and the government created the Tonle Sap Authority agency in 2007 to coordinate management, conservation, and development plans at the ministerial level (Keskinen and Varis, 2012). Moreover, several international conservation organizations, including Wildlife Conservation Society, Conservation International, World Wildlife Fund, and Flora and Fauna International have established monitoring and conservation programs in the Tonle Sap and adjacent ecosystems.

It is essential that these conservation efforts consider spatial planning in an adaptive and dynamic way, particularly under the inevitable scenarios of rapid and imminent changes in hydrology and population. Given that physical function of the Tonle Sap wetland is well understood, but biological data are limited, development of a spatial modelling framework is a logical way to simulate potential scenarios of change under established relationships between fauna and biophysical properties. Such a framework would not only guide spatial conservation planning, but it would also facilitate communication to stakeholders of the impact of future hydrological changes on fauna.

The main objective of this chapter is to quantify the projected impacts of hydrology-driven changes to fauna in the Tonle Sap. First, a database of key animal species and associated habitat usage is presented. A modelling framework to link this database with projected changes in

hydrology and habitats is then introduced. Finally, I highlight how this analysis should be incorporated in spatial conservation planning in the region.

6.2 Methods

The modelling framework presented in this chapter uses available biophysical and fauna characteristic datasets and geo-processing algorithms to create maps of fauna habitat suitability and potential future changes (Figure 6.1). Spatial analysis to create habitat maps was carried-out as described in Chapter 3. A DEM with a 100 m horizontal resolution and a vertical range of 0-15 m asl was derived from bathymetry and topography surveys in the open water and a majority of the floodplain, and complemented with data from the SRTM in the upland regions (Kummu & Sarkkula, 2008). Historical daily water levels in the open water were obtained from MRC. The (JICA, 1999) LULC map was used as a surrogated of historical habitats and land use. Baseline and projected hydrology under future scenario of hydropower development and climate were derived from the VMOD basin-wide hydrological model (Lauri et al., 2012). A hydrodynamic model was used to route water through the Lower Mekong floodplains and to determine water levels on the Tonle Sap (See Chapter 5).

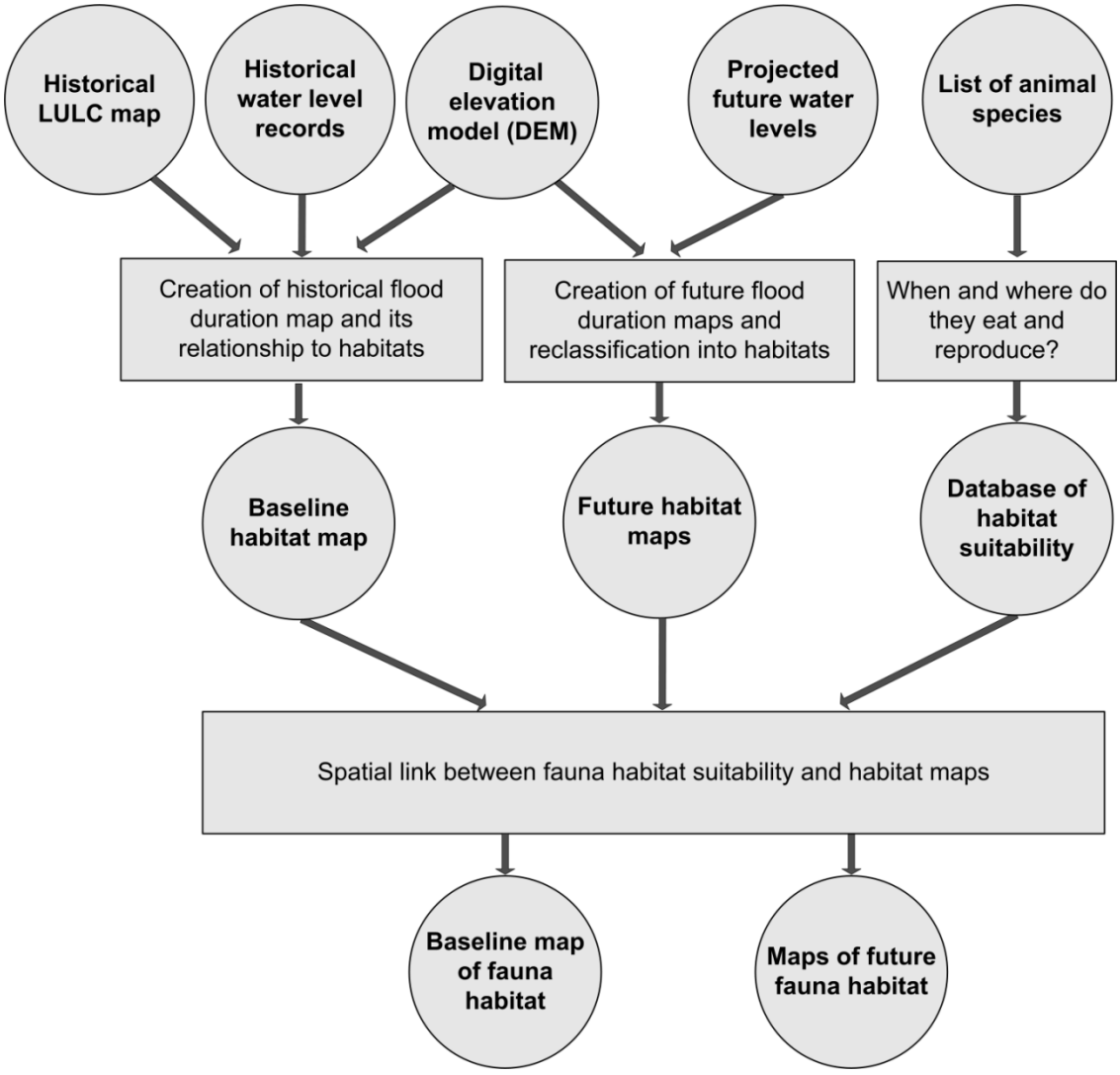

Figure 6.1. Process flow of modelling framework for mapping likely fauna habitat.

Information on fauna was extracted from publications that reported species-specific habitat preference or usage, as well as feeding, and breeding habits. Published studies with required information for the analysis were only available for a selected group of animals, including fishes (Lamberts, 2001; Lim et al., 1999), water snakes (Brooks et al., 2009), Bengal Florican (Gray et al., 2009), Grey-Headed Fish-Eagle (Tingay et al., 2010), and aquatic invertebrates (Tanaka and Ohtaka, 2009). Data for other species were inferred from syntheses of the Tonle Sap biodiversity

and general available life-history characteristics (Campbell et al. 2006; Davidson 2006; Bonheur & Lane 2002). Seven categories of information were gathered for each species, including diet, breeding time (month or season), breeding location, and likely location during each of the four seasons dictated by the water regime: rising season (June-August), wet season (September-November), receding season (December-February), and dry season (March-May). Species were also labelled (yes or no) according to their conservation, ecological, and nutritional value. Conservation value was assigned to those species whose global populations are either threatened or whose local population is a significant fraction of the world's population. Ecological value was assigned to those species that are either at the bottom of the foodweb, because they facilitate the transfer of energy from producers to higher trophic levels (Porter, 1996), or species at the top of the foodweb because of their potential effect on the entire food web as keystone predators (Abrams et al., 1996). Nutritional value was assigned to those species that are sought as food source by local human populations.

The DEM and historical water level records were combined to create maps of annual flood duration (See chapter 3 for the detailed methodology). LULC classes were associated with spatial patterns of flood duration, and this relationship was used to define 5 habitat groups according to historical flood patterns: open water, gallery forests, seasonally flooded habitats (composed of shrublands and grasslands), transitional habitats (composed of abandoned fields, floating/receding rice, and lowland grasslands), and rainfed/agricultural habitats (composed of wet season rice, village crops, and lowland shublands). If there were no changes in the flood duration, the original land use was assumed to remain. If there was a change in the flood duration for a specific area, the area was reclassified to the most common LULC class within the new habitat group.

Changes to the historical water levels caused by hydropower and climate change were used to estimate flood duration and habitat maps for the future scenarios described in Chapter 5. Previous chapters have already evaluated the level of impact and uncertainty associated with different future scenarios of water infrastructure development and climate change on flood patterns and habitats, and therefore it was deemed not necessary to analyze these multiple scenarios again. Instead, this chapter focuses on two hydropower scenarios (definite future from Chapter 3 and maximum hydropower capacity [hab_bl+rv] from Chapter 5). The first scenario represents the definite future conditions for ac. 2015 and it considers 47 hydropower dams plus irrigation and water supply demand (Piman et al. 2013). This scenario would increase average water levels during the driest months (April and May) by 10 cm and decrease water levels during the wettest months (October and September) by 19 cm. The second scenario represents the maximum hydropower capacity in the Mekong Basin according to the MRC hydropower database (MRC 2009), which includes 126 dams. This scenario would raise average water levels during the driest months by 79 cm and decrease water levels during the wettest months by 51 cm.

When comparing a future scenario to the baseline LULC map, short and long term changes were considered according to the expected adaptability of vegetation to the new hydrological conditions. In the short term, little adaptability is expected, thus this is represented by the fraction of the current LULC that will remain unchanged by hydrological disruptions. This approach is similar to the spatial analysis presented by Kummu & Sarkkula (2008). In the long term, habitats are expected to adapt to the hydrological conditions in a similar manner as the current ones do, thus long term potential habitat shifts are represented using a maximum likelihood approach following the concepts presented in Chapter 3. There will likely be a transition phase between the short and long term instead of an abrupt one, however there are no

data on vegetation succession in the Tonle Sap that would allow us to simulate gradual shifts dynamically (aka., varying in time).

The habitat maps were linked to the fauna database by first determining the habitats that each animal species is likely to use in any given season based on feeding and breeding habits. If several species were found to occupy identical habitats, they were analyzed together as one functional group. Total potential habitat area for each species/functional group was estimated for the baseline scenario and for the two dimensions of the hydropower scenarios (aka., short and long term). Comparison between the baseline scenario and the hydropower scenario was expressed numerically as percent changes from the baseline scenario, and spatially through maps displaying the potential area lost or gain by each species.

6.3 Results

6.3.1 Species database generalities and spatial distribution

A list of 61 animal species with documented nutritional, conservation, and/or ecological value is presented in Appendix C. This list includes 13 species of fish, 10 reptiles, 16 birds, 10 mammals, and 12 invertebrates. From this list, 23 species were found to have high nutritional value (mainly fishes and water snakes), 35 species were found to have high conservation value, and 23 had a high ecological value. Clearly, some species were accounted for more than one category; 20 were actually found to have high value of two categories, and only two species, *Cylindrophis ruffus* (Red-tailed pipe snake) and *Canis aureus* (Asiatic jackal), were found to have high values for the three categories. While *Cylindrophis ruffus* are commonly seen in the Tonle Sap, *Canis aureus* have not been observed in the area for more than one decade (Campbell et al. 2006).

A count of species present in each of the habitats highlights what areas of the Tonle Sap are most important for maintaining species diversity (Figure 6.2). Areas covered with gallery forests, closely followed by flooded shrublands and grasslands, were found to provide habitat to the greatest number of species. Open water provides habitat mainly to fish and aquatic invertebrates. No animals were found to use transitional habitats (lowland grasslands, abandoned fields, floating and receding rice) exclusively; most of the animals using these areas are migrating species of fish and birds that spread throughout multiple habitats during their seasonal stay in the Tonle Sap. Finally, rainfed/irrigated habitats (village crops, lowland shrublands, and wet season rice) have been rarely documented to provide habitat to wildlife in the Tonle Sap.

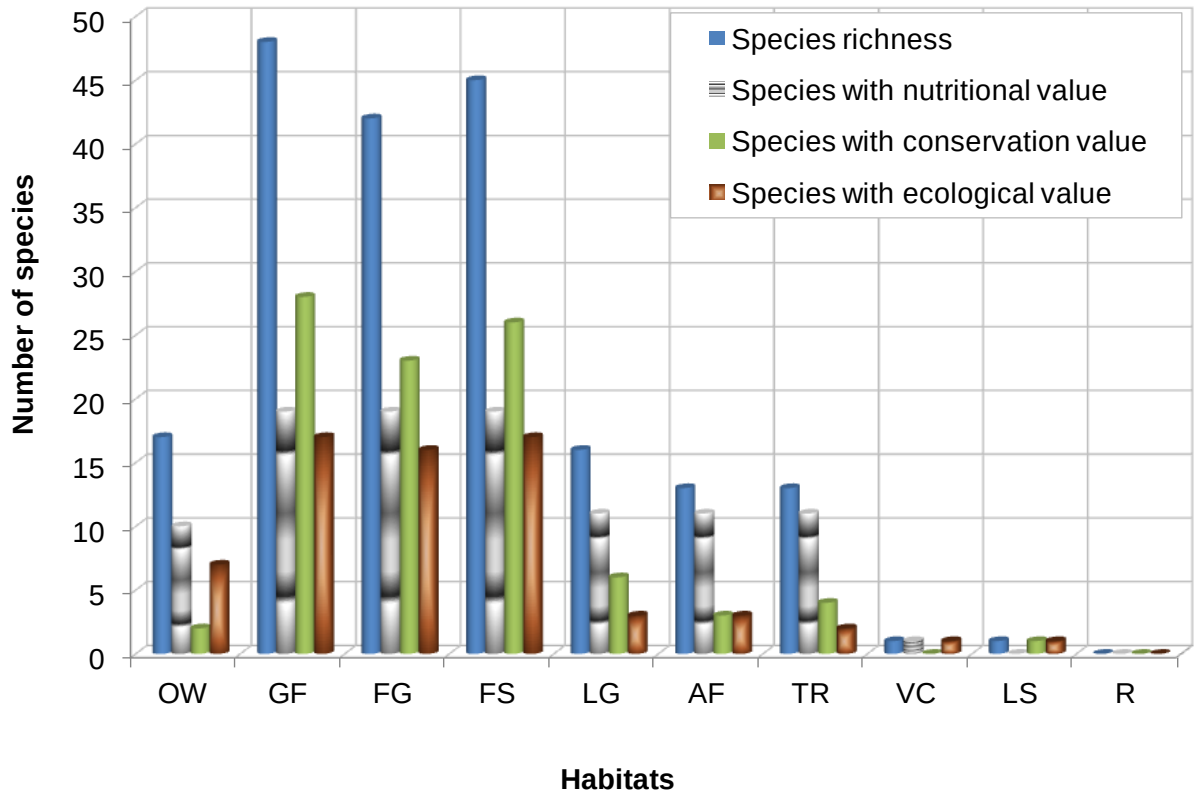

Figure 6.2. Distribution of fauna species throughout the Tonle Sap. Length of annual flood duration decreases from left to right. OW = open water, GF = gallery forest, FG = seasonally flooded grasslands, FS = seasonally flooded shrublands, LG = lowland grasslands, AF = abandoned fields, TR = transitional zone rice (floating and recession rice), VC = village crops, LS = lowland shrublands, and R = rainfed/irrigated rice.

6.3.2 Changes under future scenarios

Ongoing hydropower development in the Mekong basin could result in flooding shifts that are likely to modify the spatial distribution of habitats throughout the Tonle Sap (Figure 6.3). The flood pulse, or the regular seasonal water level variation, is expected to decrease as a result of higher water levels during the dry season and lower water levels during the wet season, thus homogenizing the annual cycle. Because of the extremely flat terrain, sub-meter water level changes would result in disproportionally large changes in spatial flooding patterns. As a result of this, 19% (2,820 km^2) of the 15,097 km^2 study area could be subject to permanent habitat changes. These changes, however, will not be evenly distributed across the Tonle Sap; areas at the boundaries of the seasonally flooded habitats are expected to be the most vulnerable to changes. Therefore, some of the habitats will be subject to greater shifts than others (Table 6.1). For instance, the expansion of the open water by 518-895 km^2 (+20-35% from baseline) will permanently inundate all of the current gallery forest, making this area permanent open water. However, other areas suitable for gallery forest, under adequate inundation patterns, will develop in other parts of the Tonle Sap as a result of hydrological change. Areas feasible for gallery forest regrowth in the long-term will be 138 and 505 km^2 for the definite future and the maximum hydropower scenarios, respectively. Furthermore, the reduction of maximum flood extent will enlarge the area feasible for rain-fed/irrigated rice by 854-1,259 km^2, which is an increase of 38-56% from the baseline area and consequent loss of habitat for alternative uses.

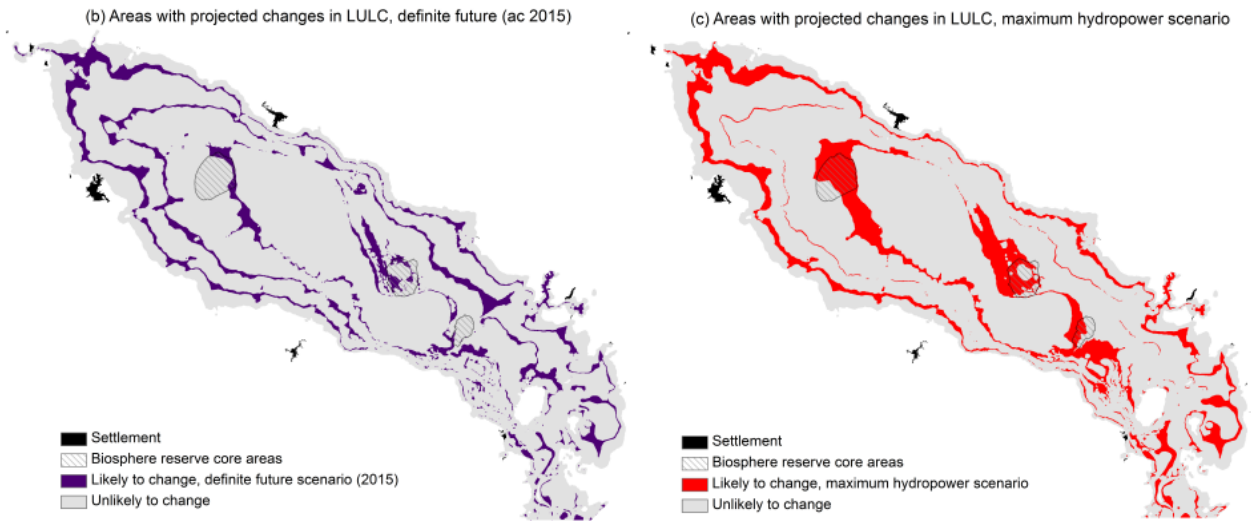

Figure 6.3. Changes in future habitat cover as a result of hydropower. See Chapter 3 and 5 for a detail description of these two scenarios.

Table 6.1. Changes in potential habitat area caused by hydrological disruptions from future hydropower scenario. Area values in km^2.

		Definite future				Maximum hydropower scenario			
Habitat	Baseline Area	area short term	Long area term	Short term change (%)	Long term change (%)	Short term area	Long term area	Short term change (%)	Long term change (%)
	a	b	C	(b-a)/a	(c-a)/a	d	e	(d-a)/a	(e-a)/a
Open water	2550	3068	3068	+20	+20	3445	3445	+35	+35
Gallery forest	657	138	138	-79	-79	0	505	-100	-23
Flooded grasslands	866	807	807	-7	-7	753	759	-13	-12
Flooded shrubland	3921	3325	3325	-15	-15	3290	3386	-16	-14
Abandoned fields	4440	3591	4187	-19	-6	4336	3109	-2	-30
Floating and receding rice	220	199	224	-9	+2	0	180	-100	-18
Lowland grasslands	85	71	105	-17	+24	77	55	-17	-35
Wet season rice	2231	3085	3085	+38	+38	3489	3489	+56	+56
Village crops	97	118	118	+22	+22	126	126	+30	+30
Lowland shrubland	13	13	20	0	+62	0	23	-100	+82

6.3.3 Changes in habitat of specific fauna groups

Analysis of spatial habitat patterns for specific animal species revealed that future hydrological disruptions caused by hydropower could result in a net loss of habitat in both the short and long terms (Table 6.2; Figure 6.4). The most affected animals will probably be those that are known to use gallery forests as their primary habitat, such as the primates *Macaca fascicularis* and *Semnopithicus cristatus*, whose populations are already severely depressed in the wetland. Species, such as the Bengal Florican that are habitat specialists and thus have a restricted range will be significantly impacted by even small loss or shifts in the habitat types. Animals that are known to use multiple habitats will be the least vulnerable, however, this does not account for the required use by many species of particular habitats to complete specific stages of their life-cycle. For instance, large waterbirds rely on the gallery forest for nesting, but feed on a variety of other habitats where they can find their prey. A similar situation applies to both migratory and non-migratory fishes that use different habitats throughout the year. Nevertheless, habitat changes will probably have a negative impact on various species particularly in the short-term. Due to an overall predicted reduction in the flood pulse, most animals could experience a greater impact in the short-term than in the long-term because the combination of permanent inundation of some areas of the floodplain and drying of others will homogenize the system and cause rapid changes in habitat type.

Many of the terrestrial and aquatic species are reliant on the gallery forest to complete stages of their life-history, either on an annual basis or during their development (Appendix Table C1). Although the overall loss of habitat is low, the loss of the essential breeding or feeding habitat will negatively affect the life history of most species. For instance, the non-

migratory snakeheads (Channidae family), which have a very high nutritional value, spawn in the gallery forests that flood in June and July (Lim et al., 1999). With the predicted hydrological changes, most of these forests would be permanently inundated, which could result in complete loss of spawning grounds or changes to the reproduction patterns of Channidae. Although there is future potential for new areas to be recruited to gallery forest habitat in the long-term, loss of habitat will probably occur much more rapidly than habitat gains, and consequently having detrimental effects on the fauna of the lake.

Table 6.2. Habitat area of representative fauna groups in baseline and future hydropower scenarios. All area values in km^2. OW = open water, GF = gallery forest, FG = seasonally flooded grasslands, FS = seasonally flooded shrublands, LG = lowland grasslands, AF = abandoned fields, TR = transitional zone rice (floating and recession rice), VC = village crops, and LS = lowland shrublands.

Common name/Group	Species	Habitats used	Baseline area used	Definite future				Maximum hydropower scenario			
				Short term area	Long term area	Short term change (%)	Long term change (%)	Short term area	Long term area	Short term change (%)	Long term change (%)
			a	c	b	(c-a)/a	(b-a)/a	e	d	(e-a)/a	(d-a)/a
Hairy-nosed Otter	*Lutra sumatrana*	GF, FS	4578	3808	3525	-17	-23	3290	3892	-28	-15
Long-tailed Macaque	*Macaca fascicularis*	GF	657	518	505	-21	-23	0	505	-100	-23
Cyprinids	*Henicorhynchus spp., Cirrhinus microlepis, Osteochilus spp., Cyclocheilichthys enoplos, Dangila spp.*	OW, GF, FS, FG, AF, TR, LS	12653	10681	11854	-16	-6	9917	11439	-22	-10
Snakeheads	*Channa striata, Channa micropeltes, Channa lucius*	OW, GF, FS, FG, AF, TR, LS	12653	10681	11854	-16	-6	9917	11439	-22	-10
Water snakes	*E. enhydris, E. Longicaude, H. buccata, E. Bocourti, E. Tentaculatus, X. Piscator, C. Ruffus*	GF, FS, FG	5443	3808	3525	-30	-35	4043	4651	-26	-15
Grey-headed Fish-eagle	*Ichthyophaga ichthyaetus*	GF, FS, FG	5443	3808	3525	-30	-35	4043	4651	-26	-15
Bengal Florican	*Houbaropsis bengalensis*	FG, LG	866	877	911	+1	+5	753	814	-13	-6

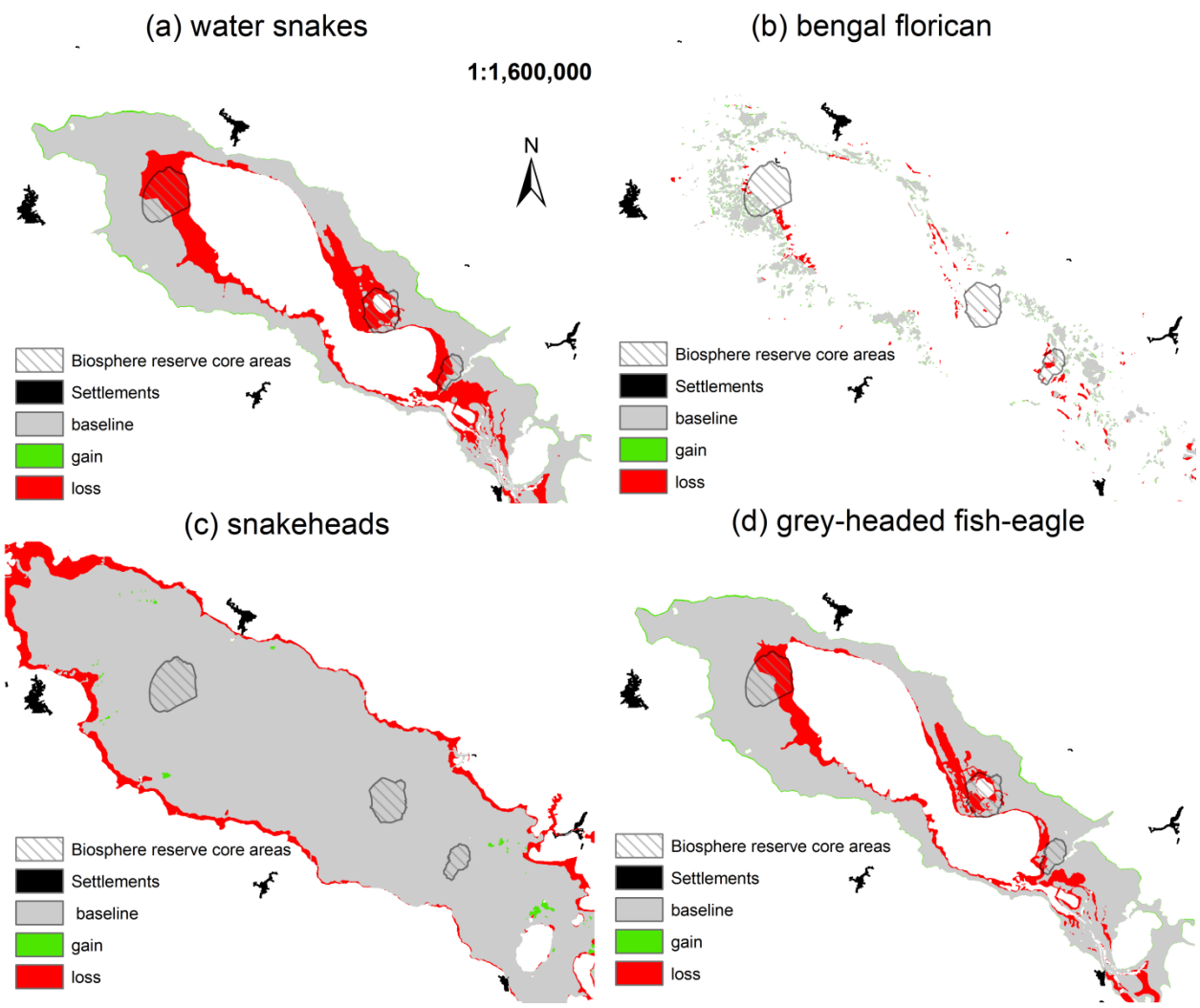

Figure 6.4. Potential habitat for representative animals and the expected gain/loss from full hydropower development in the Mekong basin.

6.4 Discussion

6.4.1 Life history according to the flood-pulse

Life histories and agricultural practices are synchronous with the flood-pulse seasonality (Figure 6.5 and Section 2.2.1). During the dry season in March-May, water levels can reach as low as 1.5 m as water drains out of the Tonle Sap and water only remains in the open water/permanent lake area. At this time, domestic water buffalo also roam through the floodplain grasslands. Permanent residents, including many aquatic fish, snake species, and waterbirds breed at this time, while migratory fish breed outside the Tonle Sap in upstream tributaries and then return from the Mekong and tributaries at the start of June, driven by the flow reversal into the Tonle Sap. The rising season typically begins in June when the Tonle Sap starts receiving water from the Mekong. Seasonally flooded habitats become inundated; hence multiple plant species fruit at this time. The start of the wet season in September is dictated by a sharp decrease and eventual flow reversal of the Tonle Sap River; water levels reach a maximum of 9 m asl and the Great Lake is formed. Fish dispersal is at its maximum during this season; hence large-scale fishing activities are low. Some carnivorous species like *C. ruffus* and *A. melanogaster* breed during the wet season, presumably because of an increased supply of prey (fish and water snakes). The receding season starts in November and is dictated by a gradual reduction in water levels and out flow of the Tonle Sap. Migratory fish flow out of the system with the river discharge, while northern wintering birds immigrate.

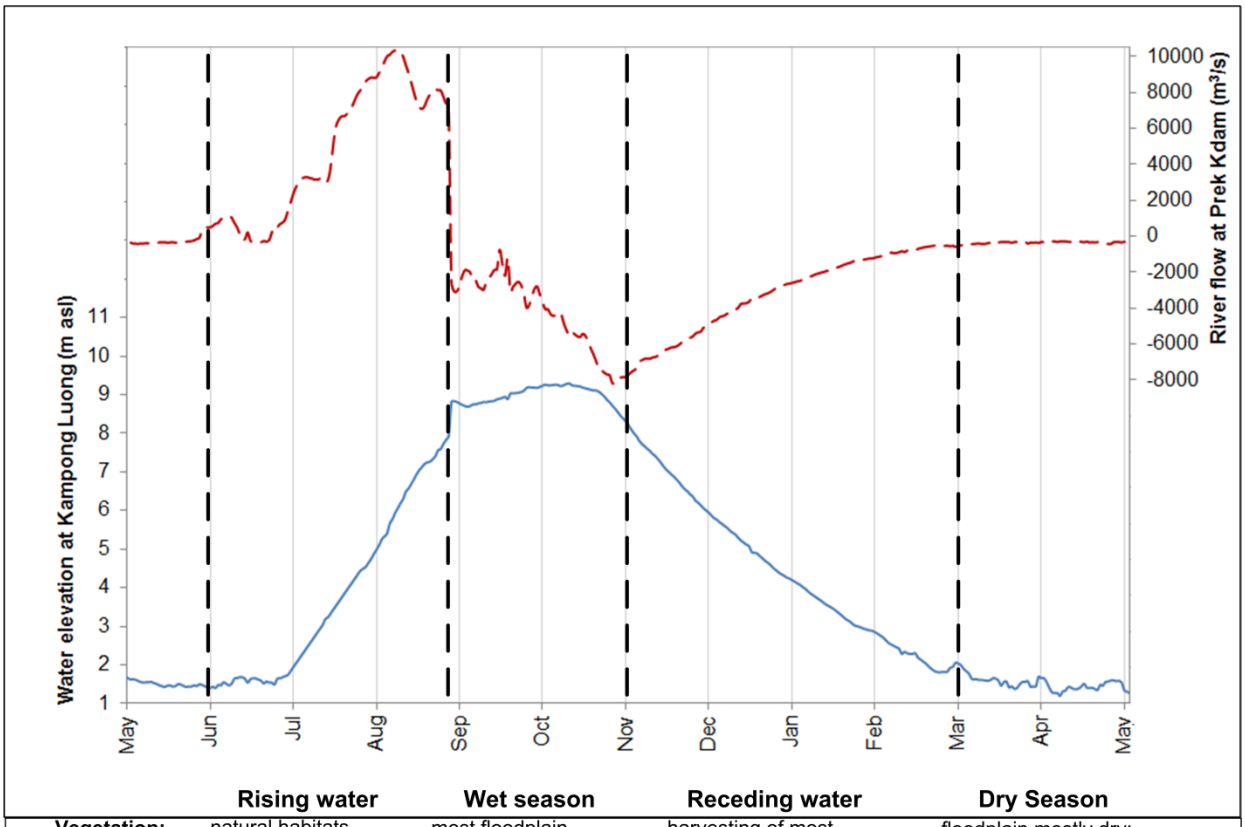

	Rising water	Wet season	Receding water	Dry Season
Vegetation:	-natural habitats flooded; plants fruiting	-most floodplain submerged	-harvesting of most varieties of rice; export of plant litter to the Mekong	-floodplain mostly dry; flowers blooming
Plankton:		-Lowest concentration of phytoplankton; *A. granulata* dominates		-*Cyanophyta* algae dominates
Fish:	-white fish inmigration; snakeheads breeding in floodplain	-Fish dispersal throughout the floodplain	-outmigration of white fish	-white and grey fish breeding in permanent water bodies
Water snakes:		-*C. Ruffus* breeding		-Homalopids and *X. piscator* breeding
Birds:		-*A.melanogaster* breeding	-inmigration of wintering birds; Breeding of permanent residents (e.g., *H. bengalensis, L. dubius, P. philippensis*)	-Outmigration of wintering birds; Breeding of permanent residents (e.g., *H. bengalensis, L. dubius, P. philippensis*)
Water buffalo:	-preparing paddies for rainfed and floating rice	-In villages	-preparing paddies for receding rice	-grazing throughout the floodplain

Figure 6.5. Major biological life history events in the Tonle Sap are synchronized with the flood pulse. See text and database for sources of information.

6.4.2 Disruptions could alter ecological interactions

The Tonle Sap is undergoing environmental changes that have not been experienced in more than 4,000 years when the system first became flood-pulsed. Before the early Holocene, the Tonle Sap functioned as a lacustrine system, with very little seasonality, high sedimentation rates, and organic matter loading from algae predominantly (Day et al., 2011; Penny, 2006). However, marked changes in the polen type and C:N ratio of sediment cores suggest that the hydrological shift during the Holocene brought drastic changes to the surrounding biota and their influence on aquatic productivity (Day et al., 2011; Penny, 2006). Although the ongoing hydrological alteration is not as dramatic as what occurred during the Holocene, this is an indication that biological changes should be expected as a response to ongoing disruptions.

With the expected weakening of the flood-pulse, the area of seasonally flooded forests, shrublands, and grasslands will be reduced. In addition to the decrease of shelter and food sources, the reduction of these habitats imply that fauna may become more concentrated, modifying population dynamics and prey-predator interactions. However, very little is known about the current status of the Tonle Sap foodweb and its adaptability to new environmental conditions, thus it is difficult to specify and quantify potential foodweb modifications. Furthermore, the buffer between natural habitats and agricultural land will probably be smaller. The reduced buffer could impose further risks to wildlife by means of further habitat loss and direct hunting. Villages and urban centres that surround the floodplain are growing, and in some areas of the floodplain agriculture has expanded by reducing natural flooding with permanent control structures and reservoirs. Moreover, a reduced buffer would facilitate the intrusion of humans from the settlements into the natural habitats, thus increasing the vulnerability of wildlife

to hunting. In short, on-going and future hydrological disruptions, together with increased human intervention, are likely to have a significant effect on the ecosystem and will probably impose even greater challenges to conservation and management.

6.4.3 Need for prioritizing habitat conservation

Although habitat heterogeneity is essential to maintain species diversity, specific habitats with "keystone structures" enhance animal diversity (Tews et al., 2004). This is certainly true in the Tonle Sap, where the greatest number of animal species is found in gallery forests and flooded shrublands, which provide the tallest and densest canopy among all habitats. Early succession habitats in this wetland – grasslands, abandoned fields, and rice paddies – occur primarily as a result of human-driven disturbances such as fire, cattle grazing and ploughing (see Chapter 4). These disturbance factors are dynamic in time and space, and have been occurring in the Tonle Sap for centuries. Although highly feasible, restoration of these disturbed habitats into forests and shrublands has not been carried out in the Tonle Sap at any substantial scale. Implementation of a reforestation program, including protection and planting should focus in those areas where the environmental conditions (flooding regime in particular) will be optimal in the long term, following the concept of assisted colonization (Hoegh-Guldberg et al., 2008; McLachlan et al., 2007) and taking into consideration predicted changes to the system and the consequent habitat shifts. Regardless of whether or not replanting is undertaken, it is essential that authorities and conservationists ensure that a balance between agricultural and natural habitats is maintained by securing those areas that will be feasible for gallery forests and shrublands in the future.

6.4.4 Implications for conservation planning

How can authorities and conservationist use the information provided in this chapter? It is implicitly suggested that a bottom-up approach would increase the chances of successful conservation programs in wetland ecosystems. The first step to guarantee the survival of a species is to ensure that adequate habitat is provided. This study suggests that the optimal area for seasonally flooded habitats could be smaller in upcoming decades. Identifying areas of feasible habitat in the future is a major step for conservation, because current conservation areas or reserves might not be the locations for optimal conservation in the future. The UNESCO Biosphere Reserve, for example, was planned with 3 core conservation areas (Figure 4.1), but as Kummu & Sarkkula (2008) pointed out, a large fraction of these areas will probably be permanently inundated. One step further from that analysis suggests that the habitat cover might change in the near future within the Biosphere Reserve core areas (Table 6.3). A large fraction (75-98%) of the flooded grasslands and flooded forests (13-97%) are expected to either become permanently flooded or transition into flooded shrublands. These drastic changes are likely to shift optimal habitat for certain species beyond the current boundaries of the protected areas, and therefore, it may be best to remap the conservation core zones to incorporate additional floodplain areas that are at least equivalent to the fraction that will be permanently flooded.

Conservation planning needs to consider mitigating these losses and ensuring habitat connectivity for those species moving throughout the wetland. Nevertheless, spatial planning is only a first step towards an effective conservation program; other key activities such as, reforestation, wildlife protection, and species monitoring, concurrent with education and outreach, are equally important to the maintenance of a diverse and healthy ecosystem.

Table 6.3. Changes in potential habitat area (in km^2) caused by hydrological disruptions from future hydropower scenario within the Tonle Sap's Biosphere Reserve Core Conservation Zones. See Fig. 1 for location of each zone.

	Prek Toal			Boeng Chmar			Stung Sen		
Habitat	Baseline	Definite future	Maximum hydropower	Baseline	Definite future	Maximum hydropower	Baseline	Definite future	Maximum hydropower
Flooded grassland	124	30	27	70	1	0	39	17	8
Flooded shrubland	30	124	26	1	70	31	17	38	25
Gallery forest	59	33	52	46	5	32	5	2	21
Open water	0	27	108	28	69	83	0	4	8

6.5 Chapter conclusions

This chapter introduced a modelling framework to quantify changes in the fauna of the Tonle Sap as a result of hydrological disruptions in the Mekong Basin. Maps of historical and future habitat changes as a function of hydrology – developed primarily in Chapters 3 and 5 – were used in this chapter in combination with key characteristics of ecology and life-history. A list of animal species with particular ecological, conservation, and nutrition value was then compiled and species were assigned to specific habitats by considering their likely seasonal movements through the wetland, as well as their feeding and reproduction habits. Species richness was found to be greatest in those natural habitats that experience long seasonal inundation, namely gallery forests, flooded shrublands, and flooded grasslands. These habitats will experience the most significant changes in area and location due to the predicted future flooding patterns and resulting human activities; hence animal groups who are permanent residents or reliant on these habitats to complete essential life-history stages will be negatively impacted. Even though abrupt losses of natural vegetation could occur in upcoming recent decades –in particular in the gallery forest– these results show that sufficient areas will exhibit conditions suitable for this habitat type to exist under future hydrological scenarios.

This chapter presents a tool to be used in the Tonle Sap and other large wetlands to overcome limited information on biophysical-fauna interactions. The modelling framework, however, should be refined as research progresses and new fauna and biophysical datasets become available. Some of the current limitations to this study is that there is very little known about habitat succession and fauna adaptation in the Tonle Sap. This impedes the development of dynamic habitat models that can be coupled with hydrological models, and it also limits the consideration of fauna resilience to habitat shifts. Another aspect that needs

further investigation is the habitat-species link. This has been mainly documented for species that remain in one habitat, but habitat use of species whose life histories are dependent on the flood regime is much less known. Moreover, prey-predator interactions play an important role in determining when and where a particular species could be found. There are, however, no studies of multi-species interactions in the Tonle Sap. This study did not consider other non-hydrological factors (aka., temperature) that could also have an impact on future fauna populations. Future hydrological disruptions, however, seem imminent and distinct, and could arguably overrule any other factors of change in future decades. Hence, the application of the modelling framework presented in this chapter offers an important tool for prospective ecosystem management.

This chapter concludes that if the Tonle Sap is to continue providing habitat to a diverse community of animal species, there are four essential steps that should be followed in spatial conservation planning: (1) recognizing upcoming biophysical shifts, (2) identifying suitable areas for habitats that maximize species richness, (3) protecting these areas from agricultural conversion, and (4) assisting reforestation/colonization.

CHAPTER 7: SUMMARY, CONCLUSIONS, AND RECOMMENDATIONS

7.1 Summary

The Mekong and the Tonle Sap comprise a unique hydro-ecological system of global significance. The hydrology driving this system, however, is changing at a faster rate than ever in its geological history, and therefore is crucial to understand the link between the hydrology and the ecology to be able to project the future fate of this system. Hence, a research question was postulated: *How could hydrological alterations caused by hydropower and climate change affect the Tonle Sap ecosystem?* This question generated a two-fold hypothesis. First, it implied that there is a direct and fundamental relationship between the hydrology and the ecology of the Tonle Sap. Second, it implied that ongoing and future disruptions caused by hydropower and climate change will be substantial and will therefore modify the current condition of the Tonle Sap ecosystem.

An overview of the scientific literature related to the Tonle Sap hydrology and ecology revealed two major points. First, there is evidence of contemporary changes in the Mekong's hydrology, mostly reflected in an increased frequency of extreme floods. Even though changes to the average seasonal water fluctuations have not been documented yet, ongoing hydropower development throughout the Mekong Basin is expected to bring drastic disruptions in the upcoming decades. Furthermore, the literature review highlighted multiple knowledge gaps that must be considered in order to achieve a good scientific understanding of the Tonle Sap as an ecosystem. Some of these included: analysis of inter-annual variation of hydrological and land cover data, assessment of vegetation shifts as a response to

hydrological changes, field measurements with appropriate spatial coverage, statistical inference of field measurements, and incorporation of calibration, validation and sensitivity procedures in hydro-ecological models.

A distinct relationship between large-scale patterns of inundation and vegetation was revealed through a GIS and remote sensing analysis. This assessment involved field verification of GIS and remote sensing data, and analysis of historical and inter-annual variation in landscape inundation and vegetation patterns. These procedures decreased the uncertainty associated with this type of spatial analysis and subsequent projections. Based on the maximum likelihood of their presence according to the annual flood duration, as well as physiognomic patterns and human activity, the vegetation patterns were divided into five distinct habitat groups: (1) Open water, flooded for 12 months in an average hydrological year; (2) Gallery forest, with flood duration of 9 months annually; (3) Seasonally flooded habitats, flooded 5-8 months and dominated by shrublands and grasslands; (4) Transitional habitats, flooded 1-5 months and dominated by abandoned agricultural fields, receding rice/floating rice, and lowland grasslands; and (5) Rainfed habitats, flooded up to 1 month and consisting mainly of wet season rice fields and village crops. Water infrastructure development is likely to increase the area of open water (+18 to +21%) and the area of rainfed habitats (+10 to +14%), while reducing the area of seasonally flooded habitats (-13 to -22%) and gallery forest (-75 to -83%). Expected habitat cover shifts as a result of climate change include a net increase of open water (2-21%), as well as a reduction of rainfed habitats by 2-5% and seasonally flooded habitats by 5-11%.

Field investigations were carried out to establish relationships among habitat biophysical characteristics, including inundation patterns, water quality, vegetation, and soils. Field measurements were made with extensive spatial coverage, and these measurements were subject to statistical inference, which permitted the integration of water quality, soils,

and human impacts into the hydrology-habitat relationship. These results showed that despite the complexity and intense human use of this ecosystem, the flood-pulse is the underlying driver of habitat characteristics by determining the depth and duration of inundation, creating the main gradient of soils, limiting the area cleared for agriculture, influencing vegetation structure and water quality, and shaping the composition of plant species.

A numerical model was used to quantify sedimentation, primary productivity, and subsequent potential future changes. This model incorporated calibration, validation, and sensitivity procedures which resulted in a good level of reliability in its results. The estimated annual net sedimentation was 3.28 ± 0.93 million tons for baseline conditions, projected to decrease by 35-53% with climate change and hydropower. Annual average NPP in the open water and in the floodplain was 1.07 ± 0.06 and 3.67 ± 0.61 million tons C, respectively, and a reduction of 9-39% is expected for future scenarios. It was concluded that hydropower development could bring more imminent disruptions than climate change, but when both factors are analyzed together, the cumulative impact will be of similar magnitude as the hydropower scenario alone, save for a range of uncertainty that is added to the overall reduction of natural habitats, sedimentation, and NPP.

A spatial modelling framework was presented in which information from the flood duration-habitat relationships was linked to fauna species in order to quantify future impacts. The direct impacts on 61 animal species with documented nutritional, conservation, or ecological value were examined. Species richness was greatest in those natural habitats that experience long seasonal inundation, namely gallery forests, flooded shrublands, and flooded grasslands. In general, animals that permanently reside in, or that rely on these habitats to complete essential life-history stages will probably be the most affected by future changes. This modelling framework and its results are crucial for research and conservation of the Tonle Sap as one of the last remaining wetland wildlife refuges in Asia.

7.2 Conclusions

7.2.1 The Mekong's flood-pulse is the major driver of floodplain vegetation and habitat characteristics in the Tonle Sap

The flood-pulse hydrology controls large-scale patterns of vegetation, primarily by creating groups of natural, transitional and agricultural habitats that are delimited by the hydrological gradient. The flood-pulse is highly influential in habitat field characteristics, by determining the depth and duration of inundation, creating the main gradient of soils, delimiting the area cleared for agriculture, influencing vegetation structure and water quality characteristics, and by shaping the composition of plant species. Even though other aspects are partially influential in floodplain vegetation, including agricultural practices, cattle herding, and fire, these are themselves constrained by the intensity of flooding. According to the Flood-Pulse Concept, plant community structure of large river floodplains is dictated by the gradient of annual flooding (Junk et al., 1989). Through the study of landscape patterns and field measurements, this thesis has demonstrated that the Tonle Sap fits indeed this concept. Even though this finding is not surprising, the corroboration of this first hypothesis is an important outcome because it provides a comprehensive and quantitative formulation that directly links fundamental components of the Tonle Sap ecosystem to its flood-pulse hydrology; consequently, this formulation can be used to project ecosystem changes based on systematic disruptions to its hydrology. This formulation is also a fundamental step in determining the potential impacts that these alterations could bring to the fisheries that rely on the Tonle Sap's habitats and primary production for their subsistence.

7.2.2 Modifications to the Mekong's hydrology caused by hydropower and climate change could bring significant disruptions to the ecological structure and function of the Tonle Sap

There is an escalating effect of impacts to the Tonle Sap ecosystem as a result of hydrological modifications, starting first with small changes in water levels, and leading to significant and distinct shifts in habitat, sedimentation and productivity. The seasonal water level fluctuation is expected to be dampened, primarily as a result of increased water levels during the dry season, but also as a minor decrease in water levels during the wet season. As a response to water level changes, habitats are expected to shift; the extent of the open water and rainfed habitats is expected to increase, while the extent of the gallery forest is expected to decrease considerably. These shifts will jeopardize the habitat of fauna species that are restricted to the gallery forests, and it will probably also elevate the pressures that surrounding human settlements impose on fauna. As a combined effect of water level, habitat, and sediment loading changes, a net reduction in the sedimentation and net primary production – processes of great importance to the overall ecosystem productivity – are expected. In general, hydropower is a more immediate threat to the Tonle Sap ecosystem than climate change, mainly because of the more distinct disruptions to seasonal fluctuations that have been projected to date. Changes to the primary production and the other environmental drivers could bring significant disruptions to the ecosystem services that the Tonle Sap provides to local livelihoods and the Lower Mekong region, which include flood retention, water supply, wildlife refugia, and fisheries, among others. The impact to fisheries, in particular, is a factor of potentially large consequences to Cambodia's food security, and the reduction of basal resources projected in this thesis could play a large detrimental role in the long term sustainability of this fishery.

7.3 Contribution to the scientific understanding of floodplain wetlands

Research findings from this thesis focused on the Tonle Sap, but given the fundamental commonalities between this system and other large floodplains, the information presented is highly informative to other large flood-pulse driven systems around the globe. In particular, there are three outcomes from this thesis that have important implications to the general understanding of hydrological-ecological interactions in floodplains that will be described in more detail in the following sections.

7.3.1 A modelling framework to assess impacts of hydrological alterations in floodplain ecosystems

Vast floodplain areas are being subjected to hydrological alterations in the tropics, but in seldom occasions sufficient data exist to characterize pre-impact, long-term hydrological and ecological characteristics. Impact assessments become a real challenge in data-deprived basins, and consequently, there is a great need for a framework and modelling tools to quantify impacts to floodplain ecosystems with the use of widely available datasets and rapid assessment tools. The methodology presented in this thesis encompasses a feasible and replicable framework that can and should be tested in other floodplains facing a similar problematic to the Tonle Sap. The landscape and the fauna habitat assessments, in particular, demonstrated how simple GIS datasets can be used to establish relationships between hydrology, LULC, and fauna that can then provide estimates of habitat changes. Even though they were only partially used in this thesis, there are worldwide datasets of terrain elevation (SRTM), LULC and vegetation indices (both derived from satellite observations like MODIS and Landsat), as well as wildlife species distributions (from the International Union for Conservation of Nature [IUCN]) that could be used in other systems with little local

information. The use of these worldwide datasets could also help standardizing this kind of landscape assessments so that estimates can be compared across the planet.

7.3.2 A flood-pulse driven numerical model of aquatic primary production

The ecosystem function modelling approach used in this thesis also demonstrated an important tool that can be applied to large floodplain wetlands elsewhere in order to provide floodplain-wide estimates of sedimentation and NPP as well as potential changes to these components under future scenarios. Estimates of primary production in aquatic ecosystems have been traditionally estimated through multiple field measurements (Hall and Moll, 1975), including aquatic metabolism and/or primary producers biomass growth. These measurements, however, are typically taken at a limited number of locations and for short periods of time; consequently, ecosystem-wide primary production estimates can yield large errors when extrapolated from localized measurements. The 3D EIA model presents an spatially explicit numerical approach to estimate daily NPP that was demonstrated to provide similar estimates to field measurements in the Tonle Sap (Holtgrieve et al., 2013). The 3D EIA model was developed based on fundamental hydrodynamics and ecological principles derived from the Flood-Pulse Concept, and therefore, this model could in theory be used to quantify NPP in other large tropical floodplains. Obviously, the accuracy of this model's estimates depend on appropriate parametization and calibration; yet, several of the parameters required for this model are not available for most large floodplain wetlands. Nevertheless, gathering these data can be on its own the focus of field campaigns that can be carried out within a reasonable time-frame and that can elucidate additional knowledge on multiple ecosystem properties.

7.3.3 Flood-pulse hydrology as driver of vegetation patterns in large floodplains: a case of intermediate disturbance?

Observations of vegetation structure, species composition, soils, and water quality in the Tonle Sap are predominantly driven by the flood-pulse hydrology. This corroborates observations throughout other large (sub-) tropical floodplain wetlands around the world, including the Central Amazon in Brazil, the Okavango Delta in Botswana, and the Wet-dry Tropics in Australia. Most of the studies in these other floodplains, however, have focused on the naturally-vegetated areas and have excluded agricultural practices, which are an essential component of most large floodplains. This thesis incorporated observations and analysis of agricultural fields in the floodplain, highlighting the role of human activities in shaping the floodplain landscape and how the intensity of unregulated flooding actually delimits the boundary between natural and agricultural habitats. The constraint that hydrology places on human activities is determined by the depth and duration of flooding, as well as by specific crop water limits and requirements. The coupling of the hydrological gradient with agricultural practices resulted in distinct unimodal distributions of plant species occurrence and richness, as well as structure characteristics such as canopy cover and vegetation height. Such spatial distributions along the hydrological gradient are remarkably similar to those following the "Intermediate Disturbance Hypothesis" (Connell, 1978). These patterns have been observed in multiple types of organisms and ecosystems (Shea et al., 2004), but direct associations with flood-pulse driven floodplains have not been made. The observations made in this thesis (Chapter 4 in particular) provide good empirical evidence of how floodplain vegetation patterns can be explained by the Intermediate Disturbance Hypothesis, and it is further hypothesized that hydrology is responsible of the main mechanisms underlying this disturbance gradient. Validation of the Intermediate Disturbance Hypothesis in flood-pulse

driven systems would provide a critical element to the fundamental understanding of floodplain ecosystems and their response to hydrological alterations.

7.4 Recommendations for future research

7.4.1 Climate change modelling

The finding that hydropower will probably bring the most imminent changes to the seasonal trends in the Tonle Sap ecosystem properties should not undermine the need for further research on impacts from climate change. To advance in this field, there needs to be a better understanding of how biological components respond to inter-annual variation, since this is the temporal scale – as opposed to seasonal variation – at which climate change is expected to bring the most dramatic changes. Moreover, most current climate change projections for the Mekong basin are based on GCMs, but these have shown to produce a wide range of inconclusive future scenarios. Further work on climate change in the Mekong should be done with projections from regional scale models that can more accurately simulate the monsoon-driven climate.

7.4.2 Environmental change monitoring

Observations of past and ongoing environmental changes are needed throughout the wetland. To study past and contemporary vegetation dynamics as a result of hydrological change, remote sensing analysis and dendrochronology (that is, the study of tree rings) are promising techniques. Vegetation dynamics also need to be directly studied in the field, where permanent stations should to be established to monitor hydrology-driven or natural succession-driven changes. Field observations demonstrated that a few parameters can be measured at these permanent stations to effectively monitor vegetation patterns, including species composition, canopy height, canopy cover, and litter cover. In addition, there are soil

and water quality parameters that should be periodically monitored, including: water electrical conductivity, water temperature, DO, water pH, soils clay and sand content, soils electrical conductivity, and soils pH. Permanent monitoring stations should cover a range of habitats and flooding patterns, and should include, of course, frequent water depth measurements.

7.4.3 Sedimentology studies

The EIA model was used to demonstrate that wetland sedimentation and primary production are particularly sensitive to upstream suspended sediment loading, which hydropower development is expected to reduce. In addition to continuing monitoring suspended sediments in the Mekong and Tonle Sap rivers, it is recommended that estimates of net seasonal sedimentation in different locations of the floodplain are undertaken. These estimates should be accompanied with estimates of nutrient composition and water column visibility.

7.4.4 Ecohydrology studies

Although the influence of hydrology on vegetation has been explained, nothing is known about the feedback that vegetation has on hydrology by means of root intake and transpiration. Floodplain vegetation could be responsible for cycling a significant fraction of the water in the Tonle Sap, but so far this contribution has been ignored. Since vegetation processes are limited both by flooding and drought, it is likely that field and modelling studies in the ecohydrology of the Tonle Sap will lead to a more mechanistic formulation of the interaction between the flood-pulse hydrology and vegetation.

7.4.5 Foodweb and fish ecology studies

A relationship was established between habitats and fauna based on feeding and reproduction information that was primarily inferred from biodiversity reviews found in the literature.

However, little scientific information exists on the actual role that these habitats provide to specific fauna species. Information on what the source of food is, and whether or not this varies with space and time, is extremely valuable, yet unknown aspects that would elaborate on the modelling framework proposed in Chapter 6. Foodweb ecology studies are particularly important to understand how changes in primary production could affect the aquatic organisms that support the productive fisheries that the Tonle Sap is well known for.

7.5 Recommendations for ecosystem management

7.5.1 Minimizing hydropower disruptions

It is feasible to develop hydropower projects that fulfil the electricity and financial needs of the Mekong countries while minimizing their impacts downstream. This can be achieved, for instance, by constructing dams at remote locations where alterations to basinwide hydrology are minimal. Other alternatives are incorporating sediment release mechanisms in dam designs, and operating dam water discharges to emulate the natural seasonal flow fluctuation. The operation alternative, of course, comes with an electricity generation penalty, but given the significance of the tradeoff at hand, it is crucial to encourage hydropower developers to implement these mitigation mechanisms in order to ease the need for further adaptation strategies.

7.5.2 Establish environmental change monitoring and social adaptation programs

Implementing hydropower mitigation strategies in the Mekong might be a complicated political affair at the national and regional level with little consultation to local stakeholders. Local authorities and non-governmental organizations should therefore ensure that disruptions are detected promptly as they occur and also prepare the ecosystem and human communities to deal with the changes. Specifically, these institutions should coordinate and

ensure technical and financial support to embark on monitoring activities like the ones mentioned in section 7.4.2. Moreover, they should also develop and implement adaptation programs within the region to ensure that the ecosystem and human communities can cope with the expected disruptions to habitat and primary production.

7.5.3 Conservation of natural habitats in areas that are likely to remain hydrologically undisturbed

Despite large shifts in habitat cover, there is likely to be a fraction of the gallery forests and seasonally flooded habitats that would continue to have their optimal hydroperiod. The agricultural boundary, however, could expand closer towards these areas, making them more vulnerable to human intervention. Therefore, it is crucial that these areas that are likely to be hydrologically undisturbed are also protected against human disturbance to ensure their future ecological functionality.

7.5.4 Restoration of natural habitats where optimal growth conditions will probably occur

Some of the areas that are currently covered with transitional habitats will probably become feasible for seasonally flooded vegetation. If nothing is done, natural succession will occur at a slow pace and pioneer and invasive plants such as *Mimosa pigra* will possibly dominate these areas. As an alternative, conscious restoration plans will accelerate succession and it will promote plant diversity. To ensure successful restoration programs, the current and future hydrological conditions of the area to be restored should be known, and plant species should be carefully selected according to their hydrological preference.

7.5.5 Control and optimization of agricultural practices in the floodplain

The flood-pulse places a limit on agricultural practices, in particular conventional rice paddies that do not tolerate deep and long inundation. However, agricultural intensification may introduce water infrastructure (that is, reservoirs and dams) to control water in a way that is more favourable for agriculture. Efforts to improve rice productivity are certainly needed in the region, but these should be emphasized in the current rainfed habitats without reclaiming any additional floodplain area by means of hard infrastructure. Moreover, traditional rice practices follow the flood regime and can infiltrate far into the floodplain. Even though these practices are an important aspect of the region's cultural heritage, it is recommended that their current extent is monitored and maintained to avoid further loss of natural seasonally flooded vegetation.

The primary drivers of the Tonle Sap's ecological productivity are changing, and a decline of its ecosystem's services should be expected if appropriate measures are not implemented. The Tonle Sap should continue to be as valuable as it has always been to Cambodia, its biodiversity, and its people.

REFERENCES

Abrams, P.A., Menge, B.A., Mittelbach, G.G., Spiller, D.A., Yodzis, P., 1996. The Role of Indirect Effects in Food Webs, in: Polis, G., Winemiller, K. (Eds.), Food Webs. Springer US, pp. 371–395.

ADB, 2004. Cumulative Impact Analysis and Nam Theun 2 Contributions (Final Report). Prepared by NORPLAN and EcoLao.

Ahmed, M., Hap, N., Ly, V., Tiongco, M., 1998. Socio-economic assessment of freshwater capture fisheries in Cambodia. Report on a household survey. Danish International Development Assistance and Mekong River Comission, Phnom Penh, Cambodia.

Angelini, R., Agostinho, A.A., 2005. Food web model of the Upper Paraná River Floodplain: description and aggregation effects. Ecological Modelling 181, 109–121.

Anthony, S.K., Hiroshi, I., Hapuarachchige, P.H., Maichun, C.Z., Yukiko, H., Kuniyoshi, T., 2008. Future hydroclimatology of the Mekong River basin simulated using the high-resolution Japan Meteorological Agency (JMA) AGCM. Hydrological Processes 22, 1382–1394.

APHA/AWWA/WEF, 2005. Standard methods for the examination of water and wastewater, 21st ed. Baltimore, USA.

Araki, Y., Hirabuki, Y., Powkhy, D., 2007. Influence of large seasonal water level fluctuations and human impact on the vegetation of the Lake Tonle Sap, Cambodia, in: Forest Environments in the Mekong River Basin. Springer, pp. 281–294.

Arias, M.E., Cochrane, T.A., Kummu, M., Killeen, T.J., Piman, T., Caruso, B.S., 2012. Quantifying changes in flooding and habitats in the Tonle Sap Lake (Cambodia) caused by water infrastructure development and climate change in the Mekong Basin. Journal of Environmental Management 112, 53–66.

Arias, M.E., Cochrane, T.A., Kummu, M., Lauri, H., Koponen, J., Holtgrieve, G.W., Piman, T., 2014. Impacts of hydropower and climate change on drivers of ecological productivity of Southeast Asia's most important wetland. Ecological Modelling 272, 252–263.

Arias, M.E., Cochrane, T.A., Lawrence, K., Killeen, T.J., Farrell, T.A., 2011. Paying the forest for electricity: a modelling framework to market forest conservation as payment for ecosystem services benefiting hydropower generation. Environmental Conservation 38, 473–484.

Ashfaq, M., Shi, Y., Tung, W., Trapp, R.J., Gao, X., Pal, J.S., Diffenbaugh, N.S., 2009. Suppression of south Asian summer monsoon precipitation in the 21st century. Geophys. Res. Lett. 36, L01704.

Baran, E., Myschowoda, C., 2009. Dams and fisheries in the Mekong Basin. Aquatic Ecosystem Health & Management 12, 227–234.

Bartlett, M.S., 1937. Properties of Sufficiency and Statistical Tests. Proceedings of the Royal Society of London. Series A, Mathematical and Physical Sciences 160, 268–282.

Benger, S.N., 2007. Remote sensing of ecological responses to changes in the hydrological cycles of the tonle sap, Cambodia, in: Geoscience and Remote Sensing Symposium,

2007. IGARSS 2007. IEEE International. Presented at the Geoscience and Remote Sensing Symposium, 2007. IGARSS 2007. IEEE International, pp. 5028–5031.

Benger, S.N., 2009. Remote Sensing of the Ecology and Functioning of the Mekong River Basin with Special Reference to the Tonle Sap, in: Geoscience and Remote Sensing. InTech, p. 598.

Bonheur, N., Lane, B.D., 2002. Natural resources management for human security in Cambodia's Tonle Sap Biosphere Reserve. Environmental Science & Policy 5, 33–41.

Bowman, D.M.J.S., McDonough, L., 1991. Tree Species Distribution Across a Seasonally Flooded Elevation Gradient in the Australian Monsoon Tropics. Journal of Biogeography 18, 203–212.

Breda, N.J.J., 2003. Ground-based measurements of leaf area index: a review of methods, instruments and current controversies. J. Exp. Bot. 54, 2403–2417.

Brooks, S.E., Allison, E.H., Gill, J.A., Reynolds, J.D., 2009. Reproductive and Trophic Ecology of an Assemblage of Aquatic and Semi-Aquatic Snakes in Tonle Sap, Cambodia. Copeia 7–20.

Brown, M.T., Cohen, M.J., Bardi, E., Ingwersen, W.W., 2006. Species diversity in the Florida Everglades, USA: A systems approach to calculating biodiversity. Aquatic Sciences 68, 254–277.

Buckley, B.M., Anchukaitis, K.J., Penny, D., Fletcher, R., Cook, E.R., Sano, M., Nam, L.C., Wichienkeeo, A., Minh, T.T., Hong, T.M., 2010. Climate as a contributing factor in the demise of Angkor, Cambodia. Proceedings of the National Academy of Sciences 107, 6748.

Campbell, I., 2009. The Challenges for Mekong River Management, in: The Mekong. Academic Press, San Diego, pp. 403–419.

Campbell, I., Poole, C., Giesen, W., Valbo-Jorgensen, J., 2006. Species diversity and ecology of Tonle Sap Great Lake, Cambodia. Aquatic Sciences - Research Across Boundaries 68, 355–373.

Campbell, I.C., 2007. Perceptions, data, and river management: Lessons from the Mekong River. Water Resources Research 43.

Campbell, I.C., Say, S., Beardall, J., 2009. Tonle Sap Lake, the Heart of the Lower Mekong, in: The Mekong. Academic Press, San Diego, pp. 251–272.

Carbonnel, J.P., Guiscafre, J., 1963. Grand Lac du Cambodge:Sedimentologie et Hydrologie (Final Report). Paris.

Chave, J., Andalo, C., Brown, S., Cairns, M.A., Chambers, J.Q., Eamus, D., Fölster, H., Fromard, F., Higuchi, N., Kira, T., Lescure, J.-P., Nelson, B.W., Ogawa, H., Puig, H., Riéra, B., Yamakura, T., 2005. Tree allometry and improved estimation of carbon stocks and balance in tropical forests. Oecologia 145, 87–99.

Cochrane, T.T., Cochrane, T.A., 2010. Amazon Forest and Savanna Lands: A guide to the climates, vegetation, landscapes and soils of central tropical South America. Scotts Valley: CreateSpace.

Connell, J.H., 1978. Diversity in Tropical Rain Forests and Coral Reefs. Science 199, 1302–1310.

Costa-Cabral, M.C., Richey, J.E., Goteti, G., Lettenmaier, D.P., Feldkötter, C., Snidvongs, A., 2007. Landscape structure and use, climate, and water movement in the Mekong River basin. Hydrol. Process. 22, 1731–1746.

Darby, S.E., Trieu, H.Q., Carling, P.A., Sarkkula, J., Koponen, J., Kummu, M., Conlan, I., Leyland, J., 2010. A physically based model to predict hydraulic erosion of fine-grained riverbanks: The role of form roughness in limiting erosion. J. Geophys. Res. 115, F04003.

Davidson, P.J.., 2006. The biodiversity of the Tonle Sap Biosphere Reserve: 2005 status review.

Day, M.B., Hodell, D.A., Brenner, M., Chapman, H.J., Curtis, J.H., Kenney, W.F., Kolata, A.L., Peterson, L.C., 2012. Paleoenvironmental history of the West Baray, Angkor (Cambodia). Proceedings of the National Academy of Sciences.

Day, M.D., Hodell, D.A., Brenner, M., Curtis, J.H., 2011. Middle to late Holocene initiation of the annual flood pulse in Tonle Sap Lake, Cambodia. J Paleolimnol 85–99.

DeAngelis, D.L., Gross, L.J., Huston, M.A., Wolff, W.F., Fleming, D.M., Comiskey, E.J., Sylvester, S.M., 1998. Landscape Modeling for Everglades Ecosystem Restoration. Ecosystems 1, 64–75.

Delgado, J.M., Apel, H., Merz, B., 2010. Flood trends and variability in the Mekong river. Hydrology and Earth System Sciences 14, 407–418.

Delgado, J.M., Merz, B., Apel, H., 2012. A climate-flood link for the lower Mekong River. Hydrology and Earth System Sciences 16, 1533–1541.

Dudgeon, P., 2000. The Ecology of Tropical Asian Rivers and Streams in Relation to Biodiversity Conservation. Annual Review of Ecology and Systematics 31, 239–263.

Dy Phon, P., 2000. Dictionary of Plants used in Cambodia, 1st ed. Imprimerie Olympic, Phnom Penh, Cambodia.

Eastham, J., Mpelasoka, F., Mainuddin, M., Ticehurst, C., Dyce, P., Hodgson, G., Ali, R., Kirby, M., 2008. Mekong River Basin water resources assessment: impacts of climate change. CSIRO: Water for a Healthy Country National Research Flagship.

Eloheimo, K., Hellsten, S., Jantunen, T., Jozsa, J., Kiirikki, M., Lauri, H., Koponen, J., Sarkkula, J., Varis, O., Virtanen, M., 2002. Water Utilization Program - Modelling of the Flow Regime and Water Quality of the Tonle Sap: Data Report. MRCS/WUP-FIN.

Eng, C., Ouch, V., 2006. TSBR Land Cover Map Derived from the Orthophoto Map.

Evans, D., Pottier, C., Fletcher, R., Hensley, S., Tapley, I., Milne, A., Barbetti, M., 2007. A comprehensive archaeological map of the world's largest preindustrial settlement complex at Angkor, Cambodia. Proceedings of the National Academy of Sciences 104, 14277–14282.

FAO, 2006. Guidelines for Soil Description. FAO, Rome.

Ferreira, L.V., Stohlgren, T.J., 1999. Effects of river level fluctuation on plant species richness, diversity, and distribution in a floodplain forest in Central Amazonia. Oecologia 120, 582–587.

Finlayson, C.M., 2005. Plant Ecology of Australia's Tropical Floodplain Wetlands: A Review. Annals of Botany 96, 541 –555.

Fitz, H.C., Trimble, B., 2006. Documentation of the Everglades Landscape Model: ELM v2. 5. South Florida Water Management District, West Palm Beach (USA).

Foti, R., del Jesus, M., Rinaldo, A., Rodriguez-Iturbe, I., 2012. Hydroperiod regime controls the organization of plant species in wetlands. Proceedings of the National Academy of Sciences.

Fujii, H., Garsdal, H., Ward, P., Ishii, M., Morishita, K., Boivin, T., 2003. Hydrological roles of the Cambodian Floodplain of the Mekong River. International Journal of River Basin Management 1, 1–14.

Furch, K., 1997. Chemistry of Varzea and Igapo soils and nutrient inventory of their floodplain forest, in: The Central Amazon Floodplain. Ecology of a Pulsing System. pp. 47–67.

Furch, K.., Junk, W.J., 1997a. Physicochemical conditions in the floodplains, in: The Central Amazon Floodplain. Ecology of a Pulsing System. Springer-Verlag, Berlin, pp. 69–108.

Furch, K.., Junk, W.J.., 1997b. Chemical composition, food value, and decomposition of herbaceous plants, leaves, and leaf littler of the floodplain forest, in: The Central Amazon Floodplain. Ecology of a Pulsing System. Springer-Verlag, Berlin, pp. 187–206.

Gaff, H., DeAngelis, D.L., Gross, L.J., Salinas, R., Shorrosh, M., 2000. A dynamic landscape model for fish in the Everglades and its application to restoration. Ecological Modelling 127, 33–52.

Goes, F., Hong, C., 2002. The status and significance of large waterbirds of the Tonle Sap, Cambodia 2000-2001. Cambodia Bird News 8, 3–19.

Gray, T.N.E., Borey, R., Hout, S.K., Chamnan, H., Collar, N., Dolman, P.M., 2009. Generality of Models that Predict the Distribution of Species: Conservation Activity and Reduction of Model Transferability for a Threatened Bustard. Conservation Biology 23, 433–439.

Grumbine, R.E., Dore, J., Xu, J., 2012. Mekong hydropower: drivers of change and governance challenges. Frontiers in Ecology and the Environment 10, 91–98.

Grumbine, R.E., Xu, J., 2011. Mekong Hydropower Development. Science 332, 178.

HACH, 2003. Water analysis handbook, 4th ed. Loveland, Colorado, USA.

Hai, P.T., Takao, M., Katsuyuki, S., 2008. Development of a two-dimensional finite element model for inundation processes in the Tonle Sap and its environs. Hydrological Processes 22, 1329–1336.

Hall, C.S., Moll, R., 1975. Methods of Assessing Aquatic Primary Productivity, in: Lieth, H., Whittaker, R. (Eds.), Primary Productivity of the Biosphere, Ecological Studies. Springer Berlin Heidelberg, pp. 19–53.

Hamilton, S.K., Sippel, S.J., Melack, J.M., 2002. Comparison of inundation patterns among major South American floodplains. J. Geophys. Res. 107, 8038.

Hamilton, S.K., Sippel, S.J., Melack, J.M., 2004. Seasonal inundation patterns in two large savanna floodplains of South America: the Llanos de Moxos (Bolivia) and the Llanos del Orinoco (Venezuela and Colombia). Hydrol. Process. 18, 2103–2116.

Hand, R.T., 2002. System Structure, Natural History, Dynamic Modeling and Adaptive Management of the Mekong Watershed's Tonle Sap-Great Lake, Cambodia (PhD thesis). University of Maryland, College Park, MA (USA).

Harvey, K.R., Hill, G.J.E., 2001. Vegetation mapping of a tropical freshwater swamp in the Northern Territory, Australia: A comparison of aerial photography, Landsat TM and SPOT satellite imagery. International Journal of Remote Sensing 22, 2911–2925.

Hellsten, S., Jarvenpaa, E., Dubrorin, T., 2003. Preliminary observations of floodplain habitats and their relations to hydrology and human impact, Modelling of the Flow Regime and Water Quality of the Tonle Sap. MRCS/WUP-FIN.

Hoegh-Guldberg, O., Hughes, L., McIntyre, S., Lindenmayer, D.B., Parmesan, C., Possingham, H.P., Thomas, C.D., 2008. Assisted Colonization and Rapid Climate Change. Science 321, 345–346.

Holtgrieve, G.W., Arias, M.E., Irvine, K.N., Ward, E.J., Kummu, M., Koponen, J., Richey, J.E., Lamberts, D., 2013. Ecosystem metabolism and support of freshwater capture fisheries in the Tonle Sap Lake, Cambodia. PLoS ONE 8, e71395.

Holtgrieve, G.W., Schindler, D.E., Branch, T.A., Teresa A'mar, Z., 2010. Simultaneous quantification of aquatic ecosystem metabolism and reaeration using a Bayesian statistical model of oxygen dynamics. Limnology and Oceanography 55, 1047.

Hortle, K.G., 2007. Consumption and the yield of fish and other aquatic animals from the Lower Mekong Basin (No. MRC Technical Paper No. 16). Mekong River Commission, Vientiane, Lao PDR.

Inomata, H., Fukami, K., 2008. Restoration of historical hydrological data of Tonle Sap Lake and its surrounding areas. Hydrological Processes 22, 1337–1350.

Intergovernmental Panel on Climate Change (IPCC), 2007. Climate Change 2007: The Physical Science Basis. Contribution of Working Group I to the Fourth Assessment Report of the Intergovernmental Panel on Climate Change. Cambridge Univ. Press, Cambridge. U. K.

Irvine, K.N., Richey, J.E., Holtgrieve, G.W., Sarkkula, J., Sampson, M., 2011. Spatial and temporal variability of turbidity, dissolved oxygen, conductivity, temperature, and fluorescence in the lower Mekong River–Tonle Sap system identified using continuous monitoring. International Journal of River Basin Management 9, 151–168.

JICA, 1999. Cambodia reconnaissance survey digital data.

Johnston, R., Kummu, M., 2011. Water Resource Models in the Mekong Basin: A Review. Water Resources Management 1–27.

Jørgensen, S.E., Bendoricchio, G., 2001. Fundamentals of Ecological Modelling, Third. ed, Developments in Environmental Modelling. Elsevier, Oxford (UK).

Junk, W.J., Bayley, P.B., Sparks, R.E., 1989. The flood pulse concept in river-floodplain systems, in: International Large River Symposium, Canadian Special Publication of Fisheries and Aquatic Sciences. pp. 110–127.

Junk, W.J., Brown, M.T., Campbell, I.C., Finlayson, C.M., Gopal, B., Ramberg, L., Warner, B.G., 2006. The comparative biodiversity of seven globally important wetlands: a synthesis. Aquatic Sciences - Research Across Boundaries 68, 400–414.

Junk, W.J., Piedade, M.T.F., 1997. Plant life in the floodplain with special reference to herbaceous plants, in: The Central Amazon Floodplain. Ecology of a Pulsing System. Springer-Verlag, Berlin, pp. 147–186.

Keskinen, M., 2006. The Lake with Floating Villages: Socio-economic Analysis of the Tonle Sap Lake. International Journal of Water Resources Development 22, 463–480.

Keskinen, M., Kummu, M., Salmivaara, A., Paradis, S., Lauri, H., de Moel, H., Ward, P., Sokhem, P., 2011. Exploring Tonle Sap Futures. Baseline results from hydrological and livelihood analyses. Aalto University and 100Gen Ltd. with Hatfield Consultants Partnership, VU University Amsterdam, EIA Ltd. and Institute of Technology of Cambodia.

Keskinen, M., Varis, O., 2012. Institutional cooperation at a basin level: For what, by whom? Lessons learned from Cambodia's Tonle Sap Lake, in: Natural Resources Forum. pp. 50–60.

King, P., Bird, J., Haas, L., 2007. The Current Status of Environmental Criteria for Hydropower Development in the Mekong Region: A Literature Compilation. ADB/MRC/WWF, Vientiane, Lao PDR.

Kingston, D., Thompson, J., Kite, G., 2011. Uncertainty in climate change projections of discharge for the Mekong River Basin. Hydrol. Earth Syst. Sci 15, 1459–1471.

Kite, G., 2001. Modelling the Mekong: hydrological simulation for environmental impact studies. Journal of Hydrology 1–13.

Koehnken, L., 2012. IKMP Discharge and Sediment Monitoring Program Review, Recommendations and Data Analysis (No. Part 2: Data analysis of preliminary results). Information and Knowledge Management Programme, Mekong River Commission, Vientiane, Lao PDR.

Koponen, J., Kummu, M., Lauri, H., Virtanen, M., Inkala, A., Sarkkula, J., 2010a. 3D Modelling User Guide (Final Report), DMS - Detailed Modelling Support Project. MRC Information Knowledge Management Programme/ Finnish Environment Institute (SYKE)/ EIA Centre of Finland Ltd.

Koponen, J., Lamberts, D., Sarkkula, J., Inkala, A., Junk, W.J., Halls, A.S., Kshatriya, M., 2010b. Primary and Fish Production Report (Final Report), DMS - Detailed Modelling Support Project. MRC Information Knowledge Management Programme/ Finnish Environment Institute (SYKE)/ EIA Centre of Finland Ltd.

Kum, V., 2012. The bioeconomic impact of altering Mekong water flow on Tonle Sap fisheries of Cambodia: a system dynamic study (PhD thesis). University of Hawaii, Manoa, HI (USA).

Kummu, M., 2009. Water management in Angkor: Human impacts on hydrology and sediment transportation. Journal of Environmental Management 90, 1413–1421.

Kummu, M., Lu, X.X., Wang, J.J., Varis, O., 2010. Basin-wide sediment trapping efficiency of emerging reservoirs along the Mekong. Geomorphology 119, 181–197.

Kummu, M., Penny, D., Sarkkula, J., Koponen, J., 2008. Sediment: Curse or Blessing for Tonle Sap Lake? AMBIO: A Journal of the Human Environment 37, 158–163.

Kummu, M., Sarkkula, J., 2008. Impact of the Mekong River flow alteration on the Tonle Sap flood pulse. Ambio 37, 185–192.

Kummu, M., Sarkkula, J., Koponen, J., Nikula, J., 2006. Ecosystem Management of the Tonle Sap Lake: An Integrated Modelling Approach. International Journal of Water Resources Development 22, 497 – 519.

Kummu, M., Tes, S., Yin, S., Adamson, P., Józsa, J., Koponen, J., Richey, J., Sarkkula, J., 2013. Water balance analysis for the Tonle Sap lake - floodplain system. Hydrol. Process. n/a–n/a.

Kuper, M., Mullon, C., Poncet, Y., Benga, E., 2003. Integrated modelling of the ecosystem of the Niger river inland delta in Mali. Ecological Modelling 164, 83–102.

Lamberts, D., 2001. Tonle Sap fisheries: a case study on floodplain gillnet fisheries in Siem Reap, Cambodia (RAP No. 2001/11). FAO, Bangkok.

Lamberts, D., 2006. The Tonle Sap Lake as a Productive Ecosystem. International Journal of Water Resources Development 22, 481–495.

Lamberts, D., Koponen, J., 2008. Flood pulse alterations and productivity of the Tonle Sap ecosystem: A model for impact assessment. Ambio 37, 178–184.

Lauri, H., de Moel, H., Ward, P.J., Räsänen, T.A., Keskinen, M., Kummu, M., 2012. Future changes in Mekong River hydrology: impact of climate change and reservoir operation on discharge. Hydrol. Earth Syst. Sci. 16, 4603–4619.

Lepš, J., Šmilauer, P., 2003. Multivariate Analysis of Ecological Data using CANOCO. Cambridge University Press, Cambridge, UK.

Li, S.J., He, D.M., 2008. Water level response to hydropower development in the upper Mekong River. Ambio 37, 170–177.

Lim, P., Lek, S., Touch, S.T., Mao, S., Chhouk, 1999. Diversity and spatial distribution of freshwater fish in Great Lake and Tonle Sap River. Aquat. Living Resour. 12, 379–386.

Linhoss, A.C., Muñoz-Carpena, R., Allen, M.S., Kiker, G., Mosepele, K., 2012. A flood pulse driven fish population model for the Okavango Delta, Botswana. Ecological Modelling 228, 27–38.

MacAlister, C., Mahaxay, M., 2009. Mapping wetlands in the Lower Mekong Basin for wetland resource and conservation management using Landsat ETM images and field survey data. Journal of Environmental Management 90, 2130–2137.

Mackay, A.W., Davidson, T., Wolski, P., Mazebedi, R., Masamba, W.R.L., Huntsman-Mapila, P., Todd, M., 2011. Spatial and Seasonal Variability in Surface Water Chemistry in the Okavango Delta, Botswana: A Multivariate Approach. Wetlands 31, 815–829.

McDonald, J.A., Bunnat, P., Virak, P., Bunton, L., 1997. Plant communities of the Tonle Sap floodplain. UNESCO/IUCN/WI.

McLachlan, J.S., Hellmann, J.J., Schwartz, M.W., 2007. A framework for debate of assisted migration in an era of climate change. Conservation Biology 21, 297–302.

Melack, J.M., 1976. Primary Productivity and Fish Yields in Tropical Lakes. Transactions of the American Fisheries Society 105, 575–580.

Milne, T., Tapley, I., 2004. Mapping and assessment of wetland ecosystems in the northwestern Tonle Sap Basin with AIRSAR data. Mekong River Commission and the University of New South Wales, Phnom Penh, Cambodia.

Milzow, C., Burg, V., Kinzelbach, W., 2010. Estimating future ecoregion distributions within the Okavango Delta Wetlands based on hydrological simulations and future climate and development scenarios. Journal of Hydrology 381, 89–100.

MRC, 2005. Overview of the hydrology of the Mekong Basin. MRC, Vientiane, Lao PDR.

MRC, 2009a. Hydropower Project Database. Mekong River Commission, Vientiane, Lao PDR.

MRC, 2009b. Mekong River Commission Spatial Database. Mekong River Commission, Vientiane, Lao PDR.

MRC, 2010a. State of the Basin Report 2010. Mekong River Commission, Vientiane, Lao PDR.

MRC, 2010b. Impacts on the Tonle Sap Ecosystem (No. Technical Note 10), Assessment of basin-wide development scenarios. Basin Development Plan Programme, Phase 2. Mekong River Commission, Vientiane, Lao PDR.

MRC, 2011. Assessment of Basin-wide Development Scenarios (Main Report). Basin Development Plan Programme, Phase 2. Mekong River Commission, Vientiane, Lao PDR.

Mubyana, T., Krah, M., Totolo, O., Bonyongo, M., 2003. Influence of seasonal flooding on soil total nitrogen, organic phosphorus and microbial populations in the Okavango Delta, Botswana. Journal of Arid Environments 54, 359–369.

Murray-Hudson, M., 2009. Floodplain vegetation responses to flood regime in the seasonal Okavango Delta, Botswana (PhD thesis). University of Florida, Environmental Engineering Sciences, Gainesville, FL (USA).

Murray-Hudson, M., Combs, F., Wolski, P., Brown, M.T., 2011. A vegetation-based hierarchical classification for seasonally pulsed floodplains in the Okavango Delta, Botswana. African Journal of Aquatic Science 36, 223–234.

Myers, N., Mittermeier, R.A., Mittermeier, C.G., da Fonseca, G.A.B., Kent, J., 2000. Biodiversity hotspots for conservation priorities. Nature 403, 853–858.

Nesbitt, H.J., 1997. Rice production in Cambodia. International Rice Research Institute, Manila, Philippines.

Odum, H.T., 1956. Primary Production in Flowing Waters. Limnology and Oceanography 1, 102–117.

Odunuga, S., Oyebande, L., 2007. Change detection and hydrological implications in the Lower Ogun flood plain, SW Nigeria, in: Remote Sensing for Environmental Monitoring and Change Detection. Presented at the IAHS Symposium on Remote Sensing for Environmental Monitoring and Change Detection, IAHS Press, Perugia, p. 358.

Ohtaka, A., Watanabe, R., Im, S., Chhay, R., Tsukawaki, S., 2010. Spatial and seasonal changes of net plankton and zoobenthos in Lake Tonle Sap, Cambodia. Limnology 11, 85–94.

Orr, S., Pittock, J., Chapagain, A., Dumaresq, D., 2012. Dams on the Mekong River: Lost fish protein and the implications for land and water resources. Global Environmental Change 22, 925–932.

Parolin, P., Ferreira, L.V., Albernaz, A.L.K.M., Almeida, S.S., 2004. Tree species distribution in Várzea forests of Brazilian Amazonia. Folia Geobotanica 39, 371–383.

Parolin, P., Wittmann, F., 2010. Struggle in the flood: tree responses to flooding stress in four tropical floodplain systems. AoB Plants 2010.

PASCO-FINNMAP CONSORTIUM, 2005. Purchase of Aerial Photography and Digital Orthophotos for the Tonle Sap Environmental Management Project. Cambodia Department of Fisheries.

Penny, D., 2006. The Holocene history and development of the Tonle Sap, Cambodia. Quaternary Science Reviews 25, 310–322.

Penny, D., Cook, G., Im, S.S., 2005. Long-term rates of sediment accumulation in the Tonle Sap, Cambodia: a threat to ecosystem health? Journal of Paleolimnology 33, 95–103.

Piman, T., Cochrane, T.A., Arias, M.E., Green, A., Dat, N.D., 2012. Assessment of Flow Changes from Hydropower Development and Operations in Sekong, Sesan and Srepok Rivers of the Mekong Basin. Journal of Water Resources Planning and Management.

Piman, T., Lennaerts, T., Southalack, P., 2013. Assessment of hydrological changes in the lower Mekong basin from basin-wide development scenarios. Hydrol. Process. 27, 2115–2125.

Porter, K.G., 1996. Integrating the Microhial Loop and the Classic Food Chain Into a Realistic Planktonic Food Web, in: Polis, G., Winemiller, K. (Eds.), Food Webs. Springer US, pp. 51–60.

Räsänen, T.A., Koponen, J., Lauri, H., Kummu, M., 2012. Downstream Hydrological Impacts of Hydropower Development in the Upper Mekong Basin. Water Resources Management 26, 3495–3513.

Räsänen, T.A., Kummu, M., 2013. Spatiotemporal influences of ENSO on precipitation and flood pulse in the Mekong River Basin. Journal of Hydrology 476, 154–168.

Räsänen, T.A., Lehr, C., Mellin, I., Ward, P.J., Kummu, M., 2013. Palaeoclimatological perspective on river basin hydrometeorology: case of the Mekong Basin. Hydrol. Earth Syst. Sci. 17, 2069–2081.

Reyes, E., White, M.L., Martin, J.F., Kemp, G.P., Day, J.W., Aravamuthan, V., 2000. Landscape modeling of coastal habitat change in the Mississippi Delta. Ecology 81, 2331–2349.

Rodríguez, J.P., 2003. Challenges and opportunities for surveying and monitoring tropical biodiversity – a response to Danielsen et al. Oryx 37, 411–411.

Rollet, B., 1972. La vegetation du Cambodge. Rev. Bois et For. des Trop. 3–16.

Sarkkula, J., Koponen, J., 2010. DMS - Detailed Modelling Support Project (Final Report). MRC Information Knowledge Management Programme/ Finnish Environment Institute (SYKE)/ EIA Centre of Finland Ltd.

Sarkkula, J., Koponen, J., Lauri, H., Virtanen, M., 2010. Origin, fate and role of Mekong sediments (Final Report), DMS - Detailed Modelling Support Project. MRC Information Knowledge Management Programme/ Finnish Environment Institute (SYKE)/ EIA Centre of Finland Ltd.

Sarkkula, Koponen, J., Hellesten, S., Keskinen, M., Kiirikki, M., Lauri, H., Varis, O., Virtanen, M., Dubrorin, T., Eloheimo, K., Haapala, U., Jozsa, J., Jarvenpaa, E., Kummu, M., 2003a. Modelling Tonle Sap for Environmental Impact Assessment and Management Support (Draft final report). MRCS/WUP-FIN.

Sarkkula, Koponen, J., Hellsten, S., Keskinen, M., Kiirikki, M., 2003b. MRCS/WUP-FIN Model Report: Modelling Tonle Sap watershed and lake processes for environmental change assessment. MRC/WUP-FIN.

Seng, K.H., Pech, B., Poole, C.M., Tordoff, A.W., Davidson, P., 2002. Directory of Important Bird Areas in Cambodia: key sites for conservation. Department of Forestry and Wildlife, Department of Nature Conservation and Protection, Birdlife International in Indochina and the Wildlife Conservation Society, Phnom Penh, Cambodia.

Shea, K., Roxburgh, S.H., Rauschert, E.S.J., 2004. Moving from pattern to process: coexistence mechanisms under intermediate disturbance regimes. Ecology Letters 7, 491–508.

Simard, M., Zhang, K., Rivera-Monroy, V.H., Ross, M.S., Ruiz, P.L., Castaneda-Moya, E., Twilley, R.R., Rodriguez, E., 2006. Mapping height and biomass of mangrove forests in Everglades National Park with SRTM elevation data. Photogrammetric engineering and remote sensing 72, 299–311.

Takeuchi, 2008. Studies on the Mekong River Basin-Modelling of hydrology and water resouces. Hydrological Processes 22, 1243–1245.

Tanaka, S., Ohtaka, A., 2009. Freshwater Cladocera (Crustacea, Branchiopoda) in Lake Tonle Sap and its adjacent waters in Cambodia. Limnology.

Ter Braak, C.J.F., 1986. Canonical Correspondence Analysis: A New Eigenvector Technique for Multivariate Direct Gradient Analysis. Ecology 67, 1167–1179.

Tews, J., Brose, U., Grimm, V., Tielbörger, K., Wichmann, M.C., Schwager, M., Jeltsch, F., 2004. Animal species diversity driven by habitat heterogeneity/diversity: the importance of keystone structures. Journal of Biogeography 31, 79–92.

Thompson, J.R., Green, A.J., Kingston, D.G., Gosling, S.N., n.d. Assessment of uncertainty in river flow projections for the Mekong River using multiple GCMs and hydrological models. Journal of Hydrology.

Tingay, R.E., Nicoll, M.A.C., Whitfield, D.P., Visal, S., McLeod, D.R.A., 2010. Nesting Ecology of the Grey-Headed Fish-Eagle At Prek Toal, Tonle Sap Lake, Cambodia. Journal of Raptor Research 44, 165–174.

Todd, M.J., Muneepeerakul, R., Miralles-Wilhelm, F., Rinaldo, A., Rodriguez-Iturbe, I., 2011. Possible climate change impacts on the hydrological and vegetative character of Everglades National Park, Florida. Ecohydrol. 5, 326–336.

Todd, M.J., Muneepeerakul, R., Pumo, D., Azaele, S., Miralles-Wilhelm, F., Rinaldo, A., Rodriguez-Iturbe, I., 2010. Hydrological drivers of wetland vegetation community distribution within Everglades National Park, Florida. Advances in Water Resources 33, 1279–1289.

UNESCO, 2010. Biosphere Reserves - World Network [WWW Document]. UNESCO-MAB (Man and the Biosphere) Secretariat, Paris, France. URL http://www.unesco.org/mab/ (accessed 11.24.10).

Valbo-Jørgensen, J., Coates, D., Hortle, K., 2009. Fish Diversity in the Mekong River Basin, in: The Mekong. Academic Press, San Diego, pp. 161–196.

Van Griensven, A., Meixner, T., Grunwald, S., Bishop, T., Diluzio, M., Srinivasan, R., 2006. A global sensitivity analysis tool for the parameters of multi-variable catchment models. Journal of Hydrology 324, 10–23.

Van Trung, N., Choi, J.-H., Won, J.-S., 2012. A Land Cover Variation Model of Water Level for the Floodplain of Tonle Sap, Cambodia, Derived From ALOS PALSAR and MODIS Data. IEEE Journal of Selected Topics in Applied Earth Observations and Remote Sensing 1–16.

Västilä, K., Kummu, M., Sangmanee, C., Chinvanno, S., 2010. Modelling climate change impacts on the flood pulse in the Lower Mekong floodplains. Journal of Water and Climate Change 01, 67–86.

Walling, D.E., 2009. The Sediment Load of the Mekong River, in: The Mekong. Academic Press, San Diego, pp. 113–142.

Ward, D.P., Hamilton, S.K., Jardine, T.D., Pettit, N.E., Tews, E.K., Olley, J.M., Bunn, S.E., 2012. Assessing the seasonal dynamics of inundation, turbidity, and aquatic vegetation in the Australian wet–dry tropics using optical remote sensing. Ecohydrol. n/a–n/a.

Warfe, D.M., Pettit, N.E., Davies, P.M., Pusey, B.J., Hamilton, S.K., Kennard, M.J., Townsend, S.A., Bayliss, P., Ward, D.P., Douglas, M.M., Burford, M.A., Finn, M., Bunn, S.E., Halliday, I.A., 2011. The "wet–dry" in the wet–dry tropics drives river ecosystem structure and processes in northern Australia. Freshwater Biology 56, 2169–2195.

WB, 2004. Modelled Observations on Development Scenarios in the Lower Mekong Basin. World Bank, Vientiane, Lao PDR.

WCD, 2000. Dams and development. A new framework for decision-making. The report of the World Commission on Dams. Earthscan Publications Ltd, London and Sterling, VA.

Weber, G.E., Furch, K., Junk, W.J., 1996. A simple modelling approach towards hydrochemical seasonality of major cations in a Central Amazonian floodplain lake. Ecological Modelling 91, 39–56.

Wilson, J.W., 1963. Estimation of foliage denseness and foliage angle by inclined point quadrats. Australian journal of botany 11, 95–105.

Wittmann, F., Anhuf, D., Junk, W.J., 2002. Tree species distribution and community structure of central Amazonian várzea forests by remote-sensing techniques. J. Trop. Ecol. 18.

Wittmann, F., Junk, W.J., Piedade, M.T.F., 2004. The varzea forests in Amazonia: flooding and the highly dynamic geomorphology interact with natural forest succession. Forest Ecology and Management 196, 199–212.

Wittmann, F., Schongart, J., Montero, J.C., Motzer, T., Junk, W.J., Piedade, M.T.F., Queiroz, H.L., Worbes, M., 2006. Tree species composition and diversity gradients in white-water forests across the Amazon Basin. Journal of Biogeography 33, 1334–1347.

Worbes, M., 1997. The forest ecosystem of the floodplains, in: The Central Amazon Floodplain. Ecology of a Pulsing System. Springer-Verlag, Berlin, pp. 223–266.

Yoshimura, C., Zhou, M., Kiem, A.S., Fukami, K., Prasantha, H.H.A., Ishidaira, H., Takeuchi, K., 2009. 2020s scenario analysis of nutrient load in the Mekong River Basin using a distributed hydrological model. Science of The Total Environment 407, 5356–5366.

Ziv, G., Baran, E., Nam, S., Rodriguez-Iturbe, I., Levin, S.A., 2012. Trading-off fish biodiversity, food security, and hydropower in the Mekong River Basin. Proceedings of the National Academy of Sciences 109, 5609–5614.

Appendix A. Chapter 3

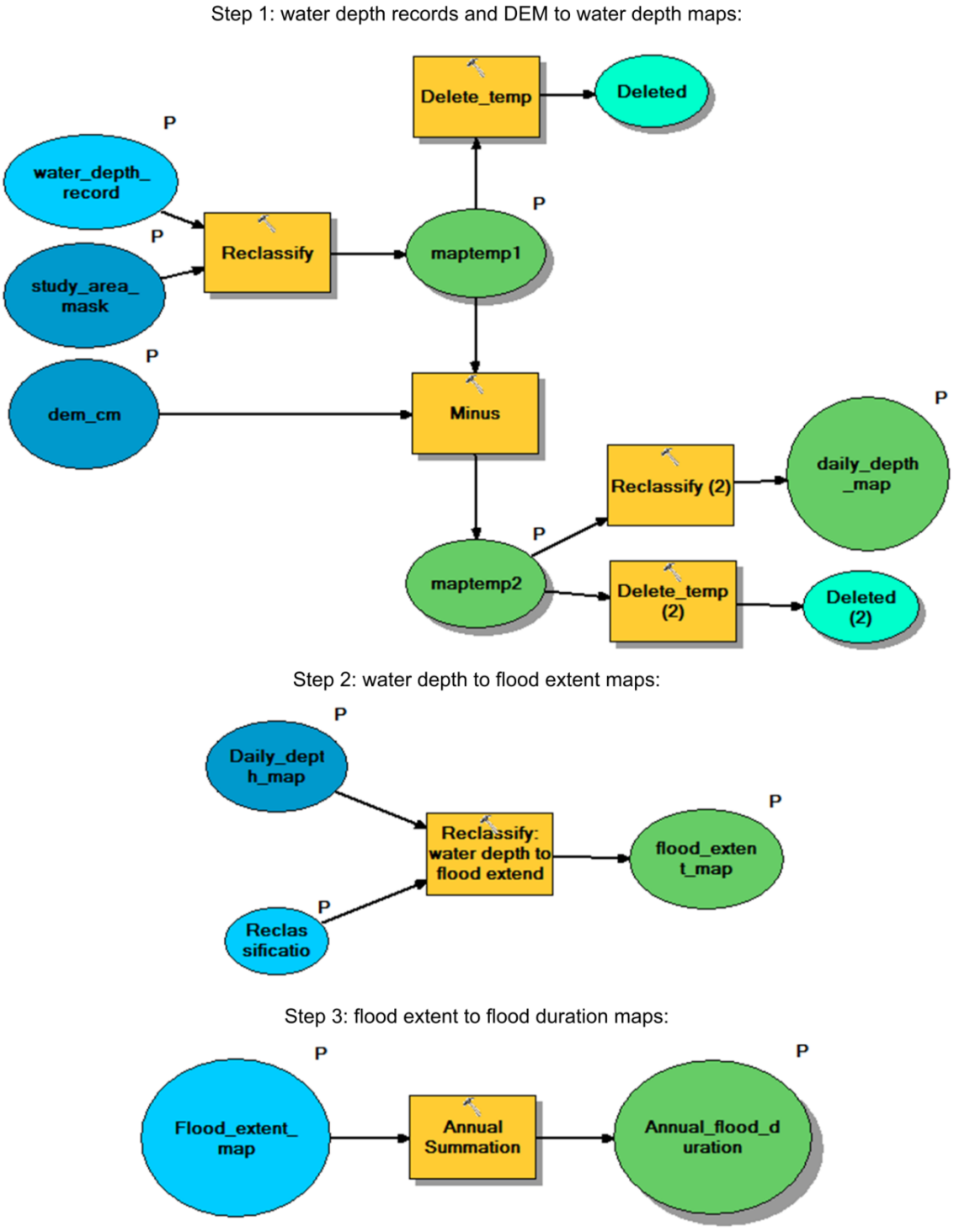

Figure A1. ArcGIS model builder procedures used for flood mapping.

Appendix B. Chapter 4

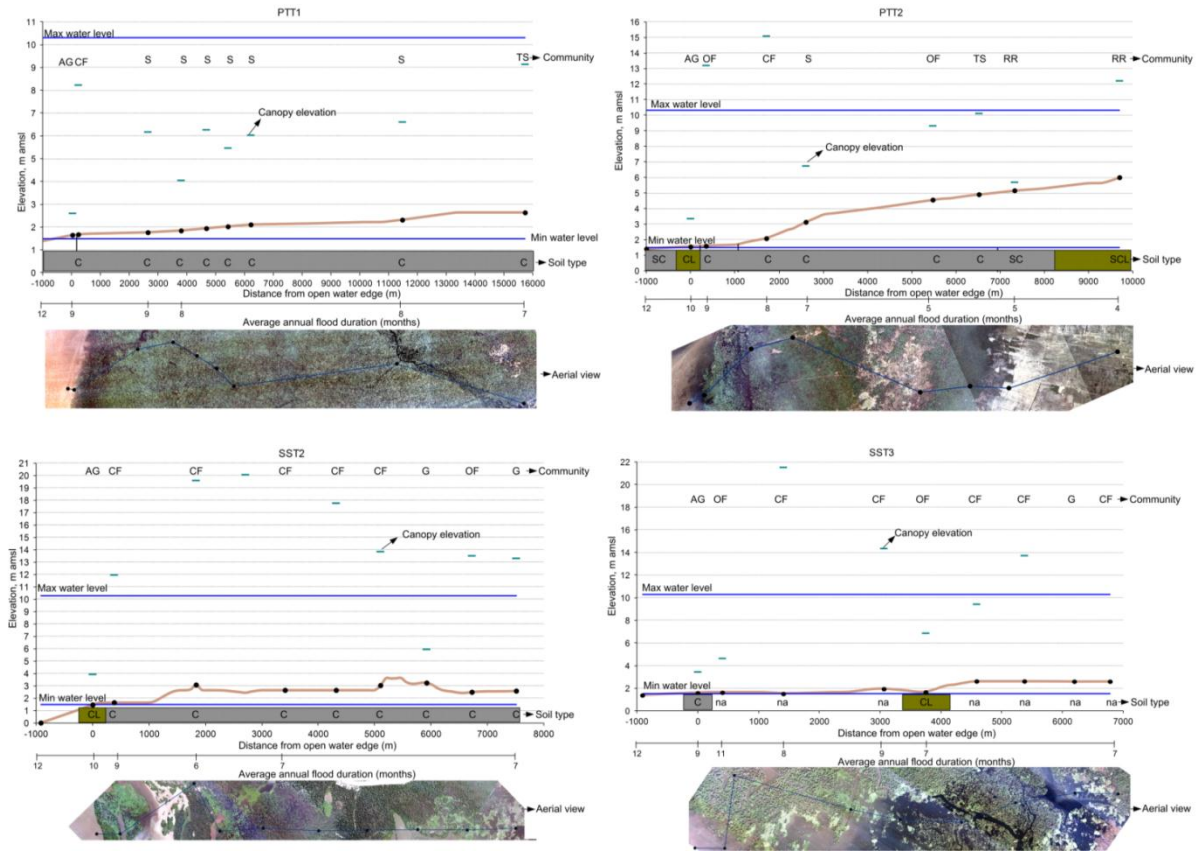

Figure B1. Elevation profiles and aerial view of "flat transects". Brown line is terrain elevation, blue lines are minimum and maximum water elevations above sea level (asl), black dots are sampling plot locations, and capital letters represent habitat or soil types. C = clay; SC = sandy clay; SCL = sandy clay loam; OF = open forest; CF = closed forest; S = flooded shrubland; TS = tall shrubland; FR = floating rice; AF = abandoned field; VC = village crop; R = wet season rice. Aerial imagery from February 2006 (PASCO-FINNMAP CONSORTIUM, 2005).

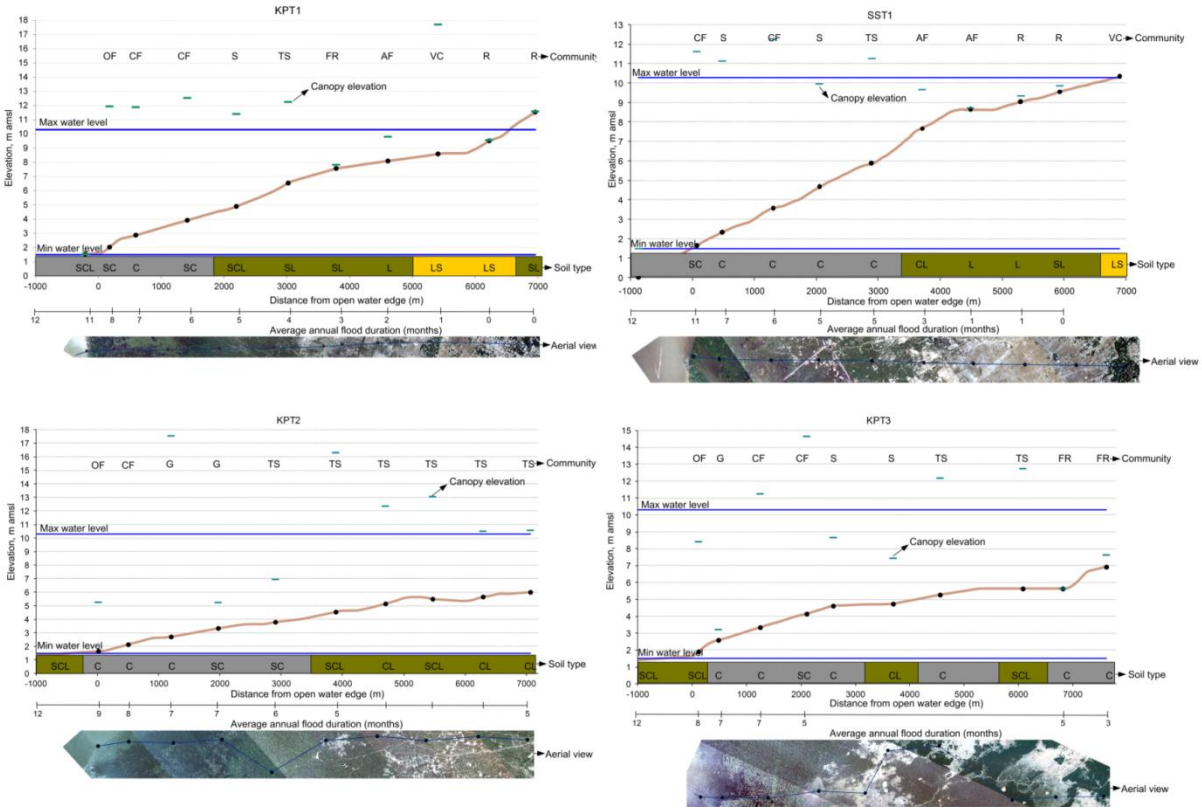

Figure B2. Elevation profile and aerial view of "steep transects. Brown line is terrain elevation, blue lines are minimum and maximum water elevations above sea level (asl), black dots are sampling plot locations, and capital letters represent habitat or soil types. C = clay; SC = sandy clay; SCL = sandy clay loam; OF = open forest; CF = closed forest; S = flooded shrubland; TS = tall shrubland; FR = floating rice; AF = abandoned field; VC = village crop; R = wet season rice.

Table B3. Sampling point locations (projection WGS 1984 UTM Zone 48N), landscape hydrological indicators, and human use status.

Point code	Coordinates	Habitat type	Average annual flood duration (days)	Flood frequency 1986-2010	Deforestation evidence	Fire evidence	Cattle grazing	Plant species present
KP LAKE SED	N12.58766 E104.20005	open water	304	1.00	NA	NA	NA	NA
KPT1P1	N12.58587 E104.19703	open forest	232	1.00	1	0	1	*Barringtonia acutangula*, *Brachiaria mutica*, *Cyperus cyperoides*, *Scirpus ternatanus*, *Vitex holoadenon*
KPT1P10	N12.53609 E104.16070	wet season rice	0	0.00	1	1	1	*Oryza sativa*
KPT1P2	N12.58294 E104.19462	closed forest	207	1.00	0	0	0	*Acacia caesia*, *Barringtonia acutangula*, *Combretum trifoliatum*, *Crateca adansani*, *Derris elliptica*, *Ficus heterophylla*, *Mimosa pigra*, *Morinda persicaefolia*, *Passiflora foetida*, unknown_22 Gramineae, *Vitex holoadenon*
KPT1P3	N12.57683 E104.19034	flooded shrubland	180	1.00	1	0	0	*Antidesma ghaesembilla*, *Ardisia rigida*, *Barringtonia acutangula*, *Combretum trifoliatum*, *Cratoxylum cochinchimense*, *Croton caudatus*, *Dalbergia horrida*, *Derris elliptica*, *Morinda persicaefolia*, *Terminalia cambodiana*, unk_15, *Vitex holoadenon*
KPT1P4	N12.57110 E104.18612	flooded shrubland	154	1.00	0	0	0	*Ardisia rigida*, *Croton caudatus*, *Dalbergia horrida*, *Derris elliptica*, *Gmelina asiatica*, *Hymenocardia wallichii*, *Morinda persicaefolia*, *Parameria loevigata*, *Rotula aquatica*, *Terminalia cambodiana*, unk_15, unknown_9 Fabaceae-papilionoideae

KPT1P5	N12.56505 E104.18168	tall shrubland	114	1.00	0	0	0	*Ardisia rigida, Cratoxylum cochinchimense, Croton caudatus, Dalbergia horrida, Derris elliptica, Gmelina asiatica, Hymenocardia wallichii, Morinda persicaefolia, Parameria loevigata, Paspalum commersonii, Quisqualis indica, Rotula aquatica, Terminalia cambodiana,* unk_15, unknown_8 Fabaceae-Mimosideae
KPT1P6	N12.55948 E104.17751	floating rice	90	0.96	1	1	0	*Aeschynomene indica, Fimbristylis argentea, Gmelina asiatica, Hymenocardia wallichii, Oldenlandia praecox, Oryza sativa,* unk_15, unknown_24 Gramineae, unknown_25 Labialeae
KPT1P7	N12.55365 E104.17280	abandoned field	74	0.84	1	0	0	*Aeschynomene indica, Calamus salicifolius, Hymenocardia wallichii, Merremia hederacea, Oldenlandia praecox,* unk_15
KPT1P8	N12.54782 E104.16847	village crop	48	0.72	1	1	0	*Anacardium occidentale, Borassus flabellifer, Carallia brachiata, Streblus asper*
KPT1P9	N12.54171 E104.16427	wet season rice	2	0.28	1	1	0	*Oryza sativa*
KPT2P1	N12.62113 E104.18174	open forest	279	1.00	0	0	0	*Alternanthera sessili, Barringtonia acutangula, Brachiaria mutica, Combretum trifoliatum, Croton caudatus, Diospyros cambodiana, Eichhornia crassipes, Ficus heterophylla*
KPT2P10	N12.57988 E104.14622	tall shrubland	130	1.00	0	0	0	*Cratoxylum cochinchimense, Cyperus esculentus, Gardenia angkorensis, Madhuca elliptica, Morinda persicaefolia, Parameria loevigata, Terminalia cambodiana,* unk_15
KPT2P2	N12.61744 E104.17928	closed forest	230	1.00	1	1	0	*Acacia concinna, Barringtonia acutangula, Cratoxylum cochinchimense, Derris elliptica, Ficus heterophylla, Mallotus anisopodus, Stireia obtusifolia, Vitex holoadenon*

KPT2P3	N12.61285 E104.17485	Flooded grassland	213	1.00	0	1	0	*Alternanthera sessili, Mimosa pigra,* unknown_22 Gramineae, *Vitex holoadenon*
KPT2P4	N12.60736 E104.17052	flooded grassland	195	1.00	1	1	0	*Alternanthera sessili, Anogeissus rivularis, Ardisia rigida, Mimosa pigra, Morinda persicaefolia, Passiflora foetida,* unknown_19 Araliaceae, unknown_22 Gramineae, *Vitex holoadenon*
KPT2P5	N12.60517 E104.16222	tall shrubland	182	1.00	0	0	0	*Antidesma ghaesembilla, Croton caudatus, Derris elliptica, Hymenocardia wallichii, Lophopetalum wightianum, Morinda persicaefolia, Oxyceras longiflora, Terminalia cambodiana,* unk_15, *Vitex holoadenon*
KPT2P6	N12.59643 E104.16044	tall shrubland	162	1.00	1	1	0	*Ardisia rigida, Croton caudatus, Derris elliptica, Gmelina asiatica, Hymenocardia wallichii, Morinda persicaefolia, Oxyceras longiflora, Terminalia cambodiana, Vitex holoadenon*
KPT2P7	N12.59055 E104.15596	tall shrubland	149	1.00	1	1	0	*Croton caudatus, Derris elliptica, Gmelina asiatica, Hymenocardia wallichii, Morinda persicaefolia, Oxyceras longiflora, Parameria loevigata, Rotula aquatica, Terminalia cambodiana,* unk_15, *Xanthophyllum glaucum*
KPT2P8	N12.58579 E104.15081	tall shrubland	138	1.00	0	0	0	*Croton caudatus, Gmelina asiatica, Hymenocardia wallichii, Oxyceras longiflora, Terminalia cambodiana,* unk_15, unknown_8 Fabaceae-Mimosideae, *Xanthophyllum glaucum*
KPT2P9	N12.57988 E104.14622	tall shrubland	138	1.00	1	0	0	*Cratoxylum cochinchimense, Croton caudatus, Derris elliptica, Gmelina asiatica, Hymenocardia wallichii, Madhuca elliptica, Morinda persicaefolia, Morinda tomentosa, Oxyceras longiflora, Schoenoplectus mucronatus, Terminalia cambodiana,* unk_15, *Phyllantus reticulatus,* unknown_8 Fabaceae-Mimosideae

KPT3P1	N12.64960 E104.15170	open forest	251	1.00	1	0	1	*Barringtonia acutangula, Combretum trifoliatum, Cyperus esculentus, Eichhornia crassipes*
KPT3P10	N12.62347 E104.09545	floating rice	106	0.96	1	1	0	*Mimosa pigra, Oryza sativa*
KPT3P2	N12.64829 E104.14861	open forest	223	1.00	1	1	1	*Barringtonia acutangula, Brachiaria mutica, Diospyros cambodiana, Mimosa pigra, Morinda persicaefolia*
KPT3P3	N12.64536 E104.14219	closed forest	195	1.00	1	1	0	*Barringtonia acutangula, Vitex holoadenon*
KPT3P4	N12.64116 E104.13558	closed forest	170	1.00	0	0	0	*Barringtonia acutangula, Combretum trifoliatum, Croton caudatus, Cynometra ramiflora, Morinda persicaefolia, Vitex holoadenon*
KPT3P5	N12.63842 E104.12895	closed forest	159	1.00	1	1	0	*Acacia concinna, Anogeissus rivularis, Mimosa pigra, Morinda persicaefolia, Vitex holoadenon*
KPT3P6	N12.63110 E104.12859	open forest	158	1.00	1	1	0	*Mimosa pigra*
KPT3P7	N12.62714 E104.12173	flooded shrubland	144	1.00	0	0	0	*Antidesma ghaesembilla, Ardisia rigida, Croton caudatus, Cynometra ramiflora, Derris elliptica, Hymenocardia wallichii, Madhuca elliptica, Morinda persicaefolia, Oxyceras longiflora*
KPT3P8	N12.62988 E104.10799	flooded shrubland	136	1.00	1	0	0	*Cynometra ramiflora, Dalbergia horrida, Hymenocardia wallichii, Oxyceras longiflora, Terminalia cambodiana*
KPT3P9	N12.62664 E104.10208	floating rice	136	1.00	1	1	0	*Oryza sativa*
PTT1P1	N13.18373 E103.70146	grassland	273	1.00	0	0	0	*Aeschynomene indica, Brachiaria mutica, Cyperus dubius, Fimbristylis gracilenta, Oryza rufipagon, Sphenoclea zeylanica,* unknown_23 Gramineae

PTT1P10	N13.16724 E103.56785	flooded shrubland	214	1.00	1	0	0	*Barringtonia acutangula, Combretum trifoliatum, Cratoxylum cochinchimense, Croton caudatus, Ficus heterophylla, Hymenocardia wallichii, Morinda persicaefolia, Vitex holoadenon*
PTT1P2	N13.18321 E103.69966	open forest	270	1.00	1	0	0	*Barringtonia acutangula, Brachiaria mutica, Combretum trifoliatum, Merremia hederacea, Oryza rufipagon*
PTT1P3	N13.19319 E103.67986	closed forest	261	1.00	0	0	0	*Acacia concinna, Cratoxylum cochinchimense, Ficus heterophylla, Vitex holoadenon*
PTT1P4	N13.19428 E103.66928	closed forest	253	1.00	0	0	0	*Cratoxylum cochinchimense, Ficus heterophylla, Morinda persicaefolia, Vitex holoadenon*
PTT1P5	N13.18972 E103.66265	closed forest	241	1.00	1	0	0	*Cratoxylum cochinchimense, Ficus heterophylla, Vitex holoadenon*
PTT1P6	N13.18554 E103.65720	closed forest	232	1.00	1	0	0	*Cratoxylum cochinchimense, Ficus heterophylla, Morinda persicaefolia, Vitex holoadenon*
PTT1P7	N13.17993 E103.65263	closed forest	230	1.00	1	0	0	*Barringtonia acutangula, Cratoxylum cochinchimense, Vitex holoadenon*
PTT1P8	N13.18207 E103.60414	closed forest	225	1.00	0	0	0	*Cratoxylum cochinchimense, Derris elliptica, Ficus heterophylla, Vitex holoadenon*
PTT2P1	N13.25855 E103.71791	grassland	304	1.00	0	0	0	*Scirpus ternatanus*
PTT2P10	N13.33601 E103.74150	receding rice	127	1.00	1	1	0	*Actinoscirpus grossus, Barringtonia acutangula, Cyperus tenuiculmis, Fuirema ciliaris, Lindernia crustaceae, Ludwigia adscendens, Mazus japonicus, Oryza sativa, Scirpus ternatanus*
PTT2P2	N13.26172 E103.71764	open forest	292	1.00	0	0	0	*Barringtonia acutangula, Eichhornia crassipes*
PTT2P3	N13.27323 E103.71310	closed forest	230	1.00	0	0	0	*Barringtonia acutangula, Ficus heterophylla, Ipomoea aquatica, Morinda persicaefolia, Vitex holoadenon*

PTT2P4	N13.28122 E103.71427	closed forest	199	1.00	1	1	0	*Cratoxylum cochinchimense, Ficus heterophylla, Vitex holoadenon*
PTT2P7	N13.29904 E103.73356	closed forest	141	1.00	1	1	1	*Alternanthera sessili, Barringtonia acutangula, Brachiaria mutica, Combretum trifoliatum, Ludwigia adscendens, Morinda persicaefolia, Polygonum barbatum, Vitex holoadenon*
PTT2P8	N13.30810 E103.73630	flooded shrubland	153	1.00	1	1	0	*Barringtonia acutangula, Croton caudatus, Derris elliptica, Gmelina asiatica, Hymenocardia wallichii, Morinda persicaefolia,* unk_15
PTT2P9	N13.31462 E103.73960	receding rice fields	146	1.00	1	1	0	*Actinoscirpus grossus, Brachiaria mutica, Cyperus tenuiculmis, Fuirema ciliaris, Mazus japonicus, Oldenlandia praecox, Oryza sativa, Schoenoplectus mucronatus*
SST1P1	N12.51019 E104.48372	closed forest	329	1.00	0	0	0	*Crateva religiosa, Croton caudatus, Ficus heterophylla, Mallotus anisopodus, Quisqualis indica, Vitex holoadenon*
SST1P10	N12.46042 E104.44674	Village crop	0	0.04	1	1	0	*Citrus reticulata, Cocos nucifera, Dendrocalamus asper, Psidium guajava*
SST1P2	N12.50739 E104.48124	closed forest	228	1.00	1	0	0	*Barringtonia acutangula, Combretum trifoliatum, Croton caudatus, Mimosa pigra, Morinda persicaefolia, Vitex holoadenon*
SST1P3	N12.50143 E104.47682	closed forest	188	1.00	1	1	0	*Barringtonia acutangula, Brachiaria mutica, Combretum trifoliatum, Cratoxylum cochinchimense, Diospyros cambodiana, Mimosa pigra, Morinda persicaefolia, Vitex holoadenon*
SST1P4	N12.49585 E104.47293	flooded shrubland	**160**	1.00	1	1	0	*Barringtonia acutangula, Cratoxylum cochinchimense, Derris elliptica, Hymenocardia wallichii, Morinda persicaefolia, Parameria loevigata, Vitex holoadenon*

SST1P5	N12.48966 E104.46839	tall shubland	131	1.00	1	0	0	*Acacia spp, Cratoxylum pruniflorum, Croton caudatus, Derris elliptica, Gmelina asiatica, Hymenocardia wallichii, Parameria loevigata,* unk_15, *Vetiveria giganioides*
SST1P6	N12.48377 E104.46389	abandoned field	88	0.96	0	0	0	*Cynodon dactylon, Parameria loevigata,* unk_15
SST1P7	N12.47807 E104.45967	abandoned field	47	0.72	1	0	0	*Cynodon dactylon*
SST1P8	N12.47210 E104.45527	wet season rice	36	0.64	1	1	0	*Oryza sativa*
SST1P9	N12.46612 E104.45096	wet season rice	0	0.20	1	1	0	*Oryza sativa,* unknown_20 Gramineae
SST2P1	N12.52630 E104.48107	aquatic grassland	304	1.00	1	0	1	*Barringtonia acutangula, Brachiaria mutica*
SST2P10	N12.57123 E104.52381	flooded grassland	217	1.00	1	0	0	*Barringtonia acutangula, Cyperus esculentus, Ipomoea aquatica, Ludwigia adscendens, Ludwigia hyssiopifolia, Polygonum barbatum,* unknown_22 Gramineae
SST2P2	N12.52878 E104.48350	closed forest	279	1.00	1	0	0	*Barringtonia acutangula, Combretum trifoliatum, Dalbergia horrida, Derris alborubra, Morinda persicaefolia*
SST2P3	N12.54173 E104.48573	closed forest	187	1.00	1	0	0	*Barringtonia acutangula, Combretum trifoliatum, Derris alborubra, Ficus heterophylla, Ichnocarpus oxypetalus, Mallotus anisopodus, Morinda persicaefolia, Vitex holoadenon*
SST2P5	N12.54450 E104.49766	closed forest	214	1.00	1	1	0	*Barringtonia acutangula, Derris alborubra, Ficus heterophylla, Maclura cochinchimensis, Mallotus anisopodus, Morinda persicaefolia, Vitex holoadenon*
SST2P6	N12.55012 E104.50372	closed forest	214	1.00	1	1	0	*Barringtonia acutangula, Combretum trifoliatum, Ficus heterophylla, Garcina cochinchinensis, Lophopetalum wightianum, Morinda persicaefolia, Vitex holoadenon*

SST2P7	N12.55532 E104.50866	closed forest	195	1.00	0	0	0	*Barringtonia acutangula, Combretum trifoliatum, Cratoxylum cochinchimense, Morinda persicaefolia, Parameria loevigata, Terminalia Cambodiana, Vitex holoadenon*
SST2P8	N12.56073 E104.51382	flooded grassland	195	1.00	0	1	1	unknown_22 Gramineae
SST2P9	N12.56593 E104.51898	open forest	217	1.00	1	1	0	*Barringtonia acutangula, Eichhornia crassipes*
SST3P1	N12.59370 E104.45117	open forest	228	1.00	0	0	0	*Brachiaria mutica, Combretum trifoliatum, sesbania javanica*
SST3P2	N12.59573 E104.45428	open forest	279	1.00	0	0	0	*Barringtonia acutangula, Brachiaria mutica, Diospyros cambodiana, Vitex holoadenon*
SST3P3	N12.60385 E104.45016	closed forest	329	1.00	0	0	0	*Diospyros cambodiana, Morinda persicaefolia*
SST3P4	N12.60845 E104.46466	closed forest	251	1.00	0	0	0	*Barringtonia acutangula, Ficus heterophylla, Ipomoea aquatica, Morinda persicaefolia*
SST3P5	N12.61083 E104.47052	open forest	267	1.00	1	0	0	*Barringtonia acutangula, Eichhornia crassipes, Polygonum barbatum, Vitex holoadenon*
SST3P6	N12.61481 E104.47709	closed forest	214	1.00	0	0	0	*Barringtonia acutangula, Combretum trifoliatum, Ficus heterophylla, Vitex holoadenon*
SST3P7	N12.62058 E104.48133	closed forest	214	1.00	0	0	0	*Barringtonia acutangula, Combretum trifoliatum, Mallotus anisopodus, Morinda persicaefolia, Vitex holoadenon*
SST3P8	N12.62567 E104.48683	grassland	217	1.00	0	1	1	*Brachiaria mutica, Eichhornia crassipes, Ipomoea aquatica, Polygonum barbatum, Vetiveria giganioides*
SST3P9	N12.62856 E104.49137	closed forest	217	1.00	0	0	0	*Barringtonia acutangula, Combretum trifoliatum, Cratoxylum cochinchimense, Croton caudatus, Derris alborubra, Morinda persicaefolia, Terminalia cambodiana, Vitex holoadenon*
PTWL	N13.18060 E103.71501	open water	365	1.00	NA	NA	NA	NA

Table B4. Detailed soil parameters characterized.

Point code	Organic layer depth (cm)	A-horizon depth (cm)	Mottles abundance (%)	Organic matter content (%)	Moisture (%)	N (mg/kg)	K (mg/kg)	P (mg/kg)	pH	Wet soil color	Clay (%)	Silt (%)	Sand (%)	plant available water (m^3 water/m^3 soil)	Electrical conductivity ($\mu s/m^2$)
KP LAKE SED				1.7	48.0	7.5	12.4	5.5	6.12	Yellowish Brown	30	10	60	0.09	80.4
KPT1P1	0	17	10	8.8	21.1	7.5	12.4	5.5	5.23	Brown	37.5	12.5	50	0.1	161.2
KPT1P10	0	30	0	0.9	5.2	7	24.9	5.5	5.68	Brown	15	17.5	67.5	0.1	16.6
KPT1P2	6	13	20	4.5	13.3	7.5	12.4	5.5	4.43	Dark Gray	42.5	15	42.5	0.11	199.1
KPT1P3	6	10	30	7.0	19.0	7	12.4	5.5	4.13	Very Dark Grayish Brown	37.5	10	52.5	0.1	116.4
KPT1P4	0	13	0	2.6	11.0	7.5	29.0	5.5	5.25	Brown	22.5	15	62.5	0.1	63.1
KPT1P5	0.5	23.5	10	9.4	5.5	7.5	45.6	5.5	4.71	Brown	12.5	25	62.5	0.11	62.6
KPT1P6	0	16	0	2.3	9.6	7.5	12.4	5.5	4.98	Brown	16.25	21.25	62.5	0.1	71.6
KPT1P7	0	14	15	1.7	6.1	7.5	12.4	5.5	5.11	Brown	20	35	45	0.13	41.6
KPT1P8	0	20	0	0.4	4.7	7.5	24.9	5.5	6.02	Brown	5	15	80	0.09	33.2
KPT1P9	0	19	0	0.9	4.5	7	24.9	5.5	5.99	Brown	7.5	12.5	80	0.09	42.7
KPT2P1	0	9	0	5.9	26.2	7	18.7	5.5	6.43	Brown	45	12.5	42.5	0.11	365
KPT2P10	1	22	0	8.3	9.8	7	12.4	5.5	4.56	Brown	33.75	43.75	22.5	0.16	36
KPT2P2	3.5	12.5	30	7.3	24.9	7	18.7	5.5	4.75	Brown	48.75	17.5	33.75	0.12	280
KPT2P3	2	9	34	9.3	18.3	7	15.6	5.5	4.33	Grayish Brown	61.25	8.75	30	0.11	253
KPT2P4	1	6	10	3.8	12.9	7	12.4	5.5	4.05	Very Dark Gray	37.5	7.5	55	0.09	193
KPT2P5	3	10	50	7.3	17.7	7	39.4	5.5	4.22	Dark Grayish Brown	40	13.75	46.25	0.11	157
KPT2P6	0	17	28	8.1	26.8	7	66.4	5.5	4.80	Dark Grayish Brown	33.75	20	46.25	0.11	119

KPT2P7	3	15	25	6.4	15.7	7	66.4	5.5	4.11	Brown	38.75	31.25	30	0.14	86
KPT2P8	2	11	0	12.0	12.3	7	66.4	5.5	3.99	Brown	27.5	25	47.5	0.12	65
KPT2P9	2	14	40	10.7	24.6	7	66.4	5.5	3.94	Dark Grayish Brown	28.75	35	36.25	0.14	52
KPT3P1	0	26	0	21.8	33.9	7.5	12.4	5.5	5.30	Dark Yellowish Brown	32.5	15	52.5	0.1	180
KPT3P10	0	17	30	10.0	22.6	7	24.9	5.5	4.49	Dark Grayish Brown	52.5	13.75	33.75	0.12	145
KPT3P2	0	22	20	9.9	23.6	7.5	12.4	5.5	4.37	Brown	57.5	15	27.5	0.12	233
KPT3P3	2.5	18.5	57.8	10.6	18.6	7.5	12.4	5.5	4.41	Grayish Brown	52.5	5	42.5	0.1	165
KPT3P4	5	8	30	11.6	17.9	7.5	12.4	5.5	4.46	Dark Grayish Brown	45	5	50	0.09	113
KPT3P5	1	11	20	10.0	19.1	7	12.4	5.5	4.67	Brown	42.5	12.5	45	0.11	83
KPT3P6	1	9	15	11.1	16.5	7.5	12.4	5.5	4.82	Brown	37.5	17.5	45	0.12	81
KPT3P7	4	16	20	8.7	14.4	7.5	12.4	5.5	4.19	Brown	40	22.5	37.5	0.12	71
KPT3P8	2	6	30	13.9	14.1	7	24.9	5.5	4.38	Brown	33.75	13.75	52.5	0.1	108
KPT3P9	0	13	20	4.3	10.7	7	24.9	5.5	4.53	Brown	41.25	13.75	45	0.11	146
PTT1P1	0	22	10	15	44	7.5	24.9	5.5	7.06	Brown	45	21.25	33.75	0.12	535
PTT1P10	9	5	20	13.8	20.3	7.5	12.4	5.5	4.45	Brown	55	5	40	0.1	288
PTT1P2	3	33	30	13.2	21.4	7.5	24.9	5.5	6.01	Brown	52.5	16.25	31.25	0.12	365
PTT1P3	2	13	40	17.6	22.9	7.5	24.9	5.5	6.00	Brown	65	10	25	0.12	230
PTT1P4	3	11	20	12.8	33.0	7.5	24.9	5.5	4.86	Brown	70	8.75	21.25	0.13	317
PTT1P5	3	9	40	12.8	28.3	7.5	24.9	5.5	4.73	Brown	70	7.5	22.5	0.13	383
PTT1P6	3.5	14.5	40	13.8	24.6	7.5	18.7	5.5	4.81	Brown	62.5	10	27.5	0.12	431
PTT1P7	3.5	17	30	14.1	23.6	7.5	12.4	5.5	5.28	Brown	62.5	5	32.5	0.11	291
PTT1P8	3	11	33.3	15.4	19.5	7.5	12.4	5.5	4.01	Yellowish Brown	63.75	6.25	30	0.11	252
PTT2P1	3	8	80		23	7.5	24.9	5.5	6.96	Brown	37.5	20	42.5	0.12	335
PTT2P10	0.7	16.3	10	2.5	26.5	7	12.4	5.5	4.56	Brown	21.25	13.75	65	0.09	65

PTT2P2	2	11	50	8.3	35.0	7.5	45.6	5.5	4.16	Brown	42.5	15	42.5	0.11	369
PTT2P3	6	12	50	7.7	29.3	7.5	12.4	5.5	4.73	Brown	60	11.25	28.75	0.12	450
PTT2P4	3	10	30	9.5	28.3	7.5	45.6	5.5	4.11	Brown	62.5	12.5	25	0.12	340
PTT2P7	3	10	30	12.1	28.1	7.5	12.4	5.5	4.32	Dark Grayish Brown	45	15	40	0.11	242
PTT2P8	2	11	25	9.3	23.1	7	12.4	5.5	4.21	Brown	46.25	8.75	45	0.1	133
PTT2P9	3	13	20	9.3	25.6	7.5	18.7	5.5	4.02	Very Dark Gray	40	12.5	47.5	0.1	185
SST1P1	0	24	20	7.1	16.4	7	45.6	5.5	5.13	Brown	40	45	15	0.16	443
SST1P10	0	16	0	4.1	4.3	30.0	83.0	21.8	6.16	Black	5	15	80	0.09	
SST1P2	0	12	40	7.0	12.8	7	83.0	5.5	4.91	Brown	50	32.5	17.5	0.15	646.5
SST1P3	3	12	30	9.7	20.8	7.5	45.6	5.5	4.90	Light Brownish Gray	62.5	10	27.5	0.12	396
SST1P4	2	16	40	9.6	14.9	7	66.4	5.5	4.49	Brown	45	21.25	33.75	0.12	112
SST1P5	0	13		6.0	10.6	7	66.4	5.5	4.52	Dark Grayish Brown	20	18.75	61.25	0.1	63
SST1P6	0	8	0	6.7	5.5	7.5	45.6	5.5	5.36	Brown	27.5	40	32.5	0.14	97
SST1P7	0	7	29	4.6	6.8	7.5	45.6	5.5	5.32	Brown	17.5	26.25	56.25	0.11	52
SST1P8	0	17	29	4.8	3.3	7	45.6	5.5	4.78	Light Brownish Gray	15	47.5	37.5	0.15	84
SST1P9	0	7	0	2.6	4.4	7.5	66.4	5.5	4.98	Pale Brown	12.5	50	37.5	0.15	
SST2P1	2	30	30	7.5	22.2	7.5	12.4	5.5	4.61	Brown	37.5	36.25	26.25	0.15	107
SST2P10	3.5	8.5	40	8.4	31.5	7.5	12.4	5.5	5.37	Brown	45.16	37.63	17.21	0.15	209
SST2P2	4	18	30	7.5	25.6	7.5	12.4	5.5	4.49	Brown	52.5	25	22.5	0.14	156
SST2P3	6	13	20	6.6	17.0	7.5	12.4	5.5	5.24	Brown	50	28.75	21.25	0.14	184
SST2P5	7	14	40	10.1	17.5	7.5	12.4	5.5	5.06	Brown	45	23.75	31.25	0.13	183
SST2P6	5	10	30	5.9	20.5	7.5	12.4	5.5	5.17	Brown	52.5	30	17.5	0.14	146
SST2P7	4	9	20	7.4	23.0	7.5	12.4	5.5	5.29	Brown	50	37.5	12.5	0.15	170
SST2P8	3	6	20	9.0	27.1	7.5	12.4	5.5	5.08	Brown	57.5	20	22.5	0.13	280

SST2P9	3	9	30	9.1	30.2	7.5	12.4	5.5	5.40	Brown	62.5	20	17.5	0.13	708
SST3P1	0	12	0	8.5	46.5	7.5	12.4	5.5	5.72	Brown	46.25	31.25	22.5	0.14	182
SST3P2	5	13	10	8.0	43.5	15.0	12.4	5.5	6.34	Brown	55	17.5	27.5	0.12	153
SST3P3	7	14	32	7.8	30.5	15.0	12.4	5.5	4.57	Brown	50	25	25	0.13	150.5
SST3P4	3	11	40	8.6	30.1	15.0	12.4	5.5	5.83	Brown	65	16.25	18.75	0.13	310
SST3P5	2	17	20	9.8	45.0	22.5	12.4	5.5	4.22	Brown	33.57	25.83	40.6	0.12	123
SST3P6	5	11	20	8.7	43.5	7.5	12.4	5.5	4.67	Dark Yellowish Brown	51.25	13.75	35	0.12	154
SST3P7	5	8	40	10.9	42.0	7.5	12.4	5.5	4.51	Dark Yellowish Brown	45	12.5	42.5	0.11	179
SST3P8	3	9	40	13.5	34.7	7.5	12.4	5.5	5.74	Brown	46.25	12.5	41.25	0.11	269
SST3P9	3	13	60	7.3	13.9	7.5	12.4	5.5	4.66	Yellowish Brown	57.5	12.5	30	0.12	170
PTWL					49.0	7	12.4	5.5	6.81	Brown	36.25	11.25	52.5	0.1	519

Table B5. Detailed vegetation characteristics. AGB = Above-ground biomass.

Point code	Litter cover (%)	Ground cover (%)	Sub-canopy cover (%)	Canopy cover (%)	AGB canopy (kg/m^2)	AGB subcanopy shrubs (kg/m^2)	AGB subcanopy herbs (kg/m^2)	Canopy height (m)	Plant species richness
KP LAKE SED	0	0	0	0	0	0	0	0	0
KPT1P1	2	87	36	22	0.96	0.35	0.23	9.9	5
KPT1P10	0.7	13	0	0	0.00	0.00	0.03	0.1	1
KPT1P2	28.3	52	77	60	0.88	0.83	0.02	9.0	11
KPT1P3	85	12	71	68	0.76	0.91	0.00	8.6	12
KPT1P4	63.3	23	73	74	0.05	4.20	0.00	6.5	12
KPT1P5	60	30	68	73	0.06	0.34	0.07	5.7	15
KPT1P6	5.7	15	4	0	0.00	0.00	0.10	0.3	9
KPT1P7	6.7	47	74	0	0.00	0.04	1.03	1.7	6
KPT1P8	0	46	0	0	24.64	0.00	0.05	9.1	4
KPT1P9	7.7	10	3	7	0.00	0.00	0.08	0.1	1
KPT2P1	8.3	20	70	19	0.01	2.04	0.03	3.6	8
KPT2P10	15.7	38	64	27	0.05	0.66	0.10	4.6	8
KPT2P2	81.7	15	85	90	5.03	0.94	0.00	15.4	8
KPT2P3	17	33	75	28	0.00	0.81	0.06	2.5	4
KPT2P4	18.3	27	52	14	0.01	1.07	0.03	3.6	9
KPT2P5	63.3	23	83	65	1.05	1.12	0.00	12.5	10
KPT2P6	50	20	84	59	0.17	1.43	0.00	7.8	9
KPT2P7	81.7	14	68	55	0.31	2.18	0.00	7.9	11
KPT2P8	63.3	15	61	61	0.11	0.46	0.00	5.0	8
KPT2P9	65	15	77	51	0.04	2.91	0.00	4.9	14
KPT3P1	2.3	10	12	9	0.48	0.01	0.03	6.5	4
KPT3P10	3.3	1	1	0	0.00	0.01	0.03	0.7	2
KPT3P2	0	80	2	0	0.00	0.02	0.10	0.6	5
KPT3P3	40	13	86	27	0.22	0.81	0.00	7.9	2
KPT3P4	30	13	90	61	0.25	1.27	0.00	10.5	6
KPT3P5	10	17	84	38	0.00	2.11	0.00	4.0	5
KPT3P6	28.3	18	62	34	0.00	0.03	0.00	2.7	1
KPT3P7	80	13	86	81	0.07	1.45	0.00	6.9	9
KPT3P8	80	10	72	79	0.25	1.31	0.00	7.1	5
KPT3P9	1.7	0	0	0	0.00	0.00	0.02	0.0	1
PTT1P1	2	63	51	0	0.00	0.00	0.39	1.0	7
PTT1P10	56.7	23	76	67	0.05	0.65	0.00	6.5	8
PTT1P2	11.7	20	58	75	1.12	0.01	0.02	6.6	5
PTT1P3	48.3	30	64	62	0.00	0.48	0.00	4.4	4
PTT1P4	27.5	40	76	33	0.00	0.20	0.00	2.2	4
PTT1P5	65	18	86	71	0.00	0.52	0.00	4.3	3
PTT1P6	65	22	65	58	0.00	0.19	0.00	3.4	4
PTT1P7	60	28	68	76	0.00	1.34	0.00	3.9	3
PTT1P8	51.7	17	72	65	0.00	0.48	0.00	4.3	4
PTT2P1	5	72	80	12	0.00	0.00	1.03	1.8	1
PTT2P10	4.3	55	29	0	0.29	0.08	0.48	6.2	9
PTT2P2	40	37	59	63	3.57	0.00	0.42	11.6	2
PTT2P3	63.3	33	67	58	9.48	0.09	0.07	13.0	5
PTT2P4	28.3	43	82	80	0.00	0.26	0.00	3.6	3
PTT2P7	6.7	67	42	32	0.18	1.20	0.29	4.8	8
PTT2P8	80	13	71	61	0.10	4.04	0.00	5.2	7
PTT2P9	15	57	27	0	0.00	0.00	0.66	0.5	8
SST1P1	40	20	88	33	0.40	1.18	0.00	10.0	6

SST1P10	0	0	0	74	4.73	0.00	0.00	18.0	4
SST1P2	33.3	12	76	43	0.30	0.39	0.01	8.8	6
SST1P3	41.7	8	34	30	0.06	0.11	0.02	8.7	8
SST1P4	90	10	92	67	0.02	6.48	0.00	5.3	7
SST1P5	78.3	22	76	57	0.03	5.17	0.05	5.4	9
SST1P6	0	12	6	0	0.00	0.18	0.04	1.7	3
SST1P7	0	25	0	0	0.00	0.00	0.02	0.1	1
SST1P8	28.3	0	0	0	0.00	0.00	0.25	0.0	1
SST1P9	26.7	2	0	0	0.00	0.00	0.03	0.1	2
SST2P1	0	77	43	0	0.00	0.48	0.65	2.5	2
SST2P10	35	53	59	20	0.35	0.00	0.55	10.7	7
SST2P2	33.3	8	83	87	2.35	0.18	0.00	10.3	5
SST2P3	76.7	17	88	80	2.89	0.95	0.00	16.5	8
SST2P5	73.3	15	83	67	4.08	1.10	0.00	17.4	7
SST2P6	75	19	84	82	2.70	0.40	0.00	15.1	7
SST2P7	65	33	86	74	1.29	0.41	0.00	10.8	7
SST2P8	10	15	88	22	0.00	0.00	0.33	2.7	1
SST2P9	43.3	10	50	4	1.02	0.00	0.31	11.0	2
SST3P1	0	70	50	1	0.00	0.51	0.57	1.9	3
SST3P2	0	33	40	0	0.00	1.32	0.18	3.0	4
SST3P3	-	17	93	75	10.30	2.55	0.00	20.0	2
SST3P4	55	8	37	92	2.06	0.18	0.00	12.4	4
SST3P5	0	33	66	5	0.05	0.31	0.27	5.2	4
SST3P6	-	9	88	82	0.11	4.29	0.00	6.8	4
SST3P7	90	12	89	77	1.13	0.69	0.00	11.1	5
SST3P8	0	70	7	0	0.00	0.00	0.32	0.5	5
SST3P9	-	40	94	72	0.88	2.71	0.00	13.7	8
PTWL	0	0	0	0	0.00	0.00	0.00	0.0	0

Table B6. List of plant species used in the ordination analyses.

Scientific name/unique ID	Khmer name	Family	Growth form	6 digit code
Acacia caesia (L) Willd. Var. subnuda (craib) I.C. Neilsen	Kampriem	Fabaceae-Mimosideae	Shrub	Acacea
Acacia		Fabaceae-Mimosideae	Shrub	Acacia
Acacia concinna (Willden)	bânla sâ:ot	Fabaceae-Mimosideae	Liana	Acacon
Actinoscirpus grossus (L.f.) Goetgh l. P. A. Simpson	unknown	Cyperaceae	Gramminoid	Actino
Aeschynomene indica L.	snaô ach mon	Fabaceae-papilionoideae	Herb	Aeschy
Alternanthera sessili (L.) DC	Chëng bänhâhg	Amaranthaceae	Herb	Altern
Anacardium occidentale L.	svaay chantii	Anacardiaceae	Tree	Anacar
Anogeissus rivularis (Gagnep.) Lecomte	Rei	Combretaceae	Shrub	Anogei
Antidesma ghaesembilla Gaertn.	Dangkiep k'dame	Euphorbiaceae	Shrub	Antide
Ardisia rigida	Saku	Myrsinaceae	Shrub	Ardisi
Barringtonia acutangula Gaertm.	reang tük	Lecythidaceae	Tree/Shrub	Barrin
Borassus flabellifer L.	thnaôt	Arecaceae	Tree	Borass
Brachiaria mutica Stapf.	smau barang/smau koo	Gramineae	Gramminoid	Brachi
Calamus salicifolius Becc	Ropeak	Palmae	Shrub	Calsal
Carallia brachiata (Lour.) Merr.	tromêng	Rhizophoraceae	Tree	Carall
Citrus reticulata		Rutaceae	Tree	Citrus
Cocos nucifera L.	daung	Palmae/Arecaceae	Tree	Cocos
Combretum trifoliatum Vent.	(voër) trâhs	Combretaceae	Shrub, Liana	Combre
Crateca adansani subs. Odorata	thngan'	Capparidaceae	Shrub	Cratec
Crateva religiosa G. Forest	Tunlië	Capparidaceae	Shrub	Cratev
Cratoxylum cochinchimense Blume (Lour)	lo'ngieng tük	Guttiferae	Tree	Cracoc
Cratoxylum pruniflorum Dyer	longieng ach' ko:n		Tree/Shrub	Crapru
Croton caudatus Griseb	Prâbuëy	Euphorbiaceae	Tree/Shrub	Croton
Cynodon dactylon (L) Pers.	smau chénchién	Gramineae	Gramminoid	Cyndac
Cynometra ramiflora Limme	Chôm'prinh	Fabaeae cesalpimioideae	Tree	Cynram
Cyperus cyperoides (L) kuntze	Kok	Cyperaceae	Gramminoid	Cypcyp
Cyperus dubius Rottb.		Cyperaceae	Gramminoid	Cypdub
Cyperus esculentus	moemphlang	Cyperaceae	Gramminoid	Cypesc
Cyperus tenuiculmis Boeck		Cyperaceae	Gramminoid	Cypten
Dalbergia horrida (Demsted) Malbberley var. glabrescens (Prain)	Khna:y moan	Fabaceae-Papilionoideae	Liana	Dalber
Dendrocalamus asper			Tree	Dendro
Derris alborubra var. alborubra Hemseley		Fabaceae-papilionoideae	Liana	Deralb
Derris elliptica (Sweet) Benth	Voer Khbiehs	Fabaceae-papilionoideae	Liana	Derell

Diospyros cambodiana H. Lec.	Phtol	Ebenaceae	Tree/Shrub	Diospy
Eichhornia crassipes (Martius) Solms	Kamplau	Pontederiaceae	Herb	Eichho
Ficus heterophylla var.	Slâ	Moraceae	Shrub	Ficus
Fimbristylis argentea (Rottb. Vahl)		Cyperaceae	Gramminoid	Fimarg
Fimbristylis gracilenta Hance		Cyperaceae	Gramminoid	Fimgra
Fuirema ciliaris (L.) Rorb.		Cyperaceae	Gramminoid	Fuirem
Garcina cochinchinensis (Low) Choisy	Sândán	Guttiferae	Tree	Garcin
Gardenia angkorensis Pit.	Dai khla	Rubiaceae	Shrub	Garang
Gmelina asiatica L.	ânneha:nh	Verbenaceae	Tree/Shrub	Gmelin
Hymenocardia wallichii Tul.	Phnom Phnaèng	Euphorbiaceae	Tree/Shrub	Hymeno
Ichnocarpus oxypetalus Pit.	thmē:nh trei voër	Apocynaceae	Liana	Ichnoc
Ipomoea aquatica Forssk	trakuen	Convolvulaceae	Herb	Ipomoe
Lindernia crustaceae (L.) F. Muell	Smau cheng kok	Scrophulariace	Herb	Linder
Lophopetalum wightianum Arn.	Saeda sa	Celastraceae	Tree/Shrub	Lophop
Ludwigia adscendens (L.) Hara.	Kâmping puey kok	Apocynaceae	Herb	Ludads
Ludwigia hyssiopifolia (G. Don) Exell	smau smach tuk	Onagraceae	Herb	Ludhys
Maclura cochinchimensis (Low) Corner	nhô kla:y , khê	Moraceae	Liana	Maclur
Madhuca elliptica (Dubard) H.J. Lam		Sapotaceae	Tree/Shrub	Madhuc
Mallotus anisopodus (Gagnep)/Coccoceras anisopodum Gagnep.	Chhkaéng	Euphobiaceae	Tree	Mallot
Mazus japonicus (Thunb.) Kuntze	Pramat dei	Scrophulariace	Herb	Mazus
Merremia hederacea (Burn. F.) Hallier f.	(voër) ta aek	Convolvulaceae	Liana	Merrem
Mimosa pigra	Bonla yuon	Fabaceae-Mimosideae	Shrub	Mimosa
Morinda persicaefolia	nhô sba:tb	Rubiaceae	Shrub	Morper
Morinda tomentosa Roth	nhô prei	Rubiaceae	Shrub	Mortom
Oldenlandia praecox Pierre erepit.	prâmat dei chén	Rubiaceae	Gramminoid	Oldenl
Oryza sativa L.	srow	Poaceae	Gramminoid	Orysat
Oryza rufipagon Griffith	Srā gnaē	Poaceae	Gramminoid	Oryruf
Oxyceras longiflora	Thmueng Kam chôhs	Rubiaceae	Tree/Shrub	Oxycer
Parameria loevigata (Juss) Moldenke/Parameria glandulifera Benth.	Chuch, angkat, (voër) kôômuey	Apocynaceae	Liana	Parame
Paspalum commersonii Lam	smau chenh chien	Gramineae	Gramminoid	Paspal
Passiflora foetida L.	vor sau maw	Passifloraceae	Herb	Passif
Polygonum barbatum	kanteang hae phlae chrung	Polygonaceae	Herb	Polygo
Psidium guajava L.		Myrtaceae	Tree	Psidiu
Quisqualis indica L.		Combretaceae	Liana	Quisqu
Rotula aquatica Lour.	rei tük	Boraginaceae	Shrub	Rotula
Schoenoplectus mucronatus (L.) Palla		Cyperaceae	Gramminoid	Schoen
Scirpus ternatanus Reimu ex Miq.		Cyperaceae	Gramminoid	Scirpu

sesbania javanica Miquel	Snaô	Fabaceae-Papilionoideae	Shrub	sesban
Sphenoclea zeylanica	Kanndieng-Krapen tuk	Sphenocleaceae	Herb	Spheno
Stireia obtusifolia Hook. F. of Thom	au krâpe	Capparidaceae	Tree	Stirei
Streblus asper Lour		Moraceae	Tree	Strebl
Terminalia cambodiana	ta_our	Combretaceae	Tree/Shrub	Termin
unknown_14			Tree	unk_14
unknown_15			Shrub	unk_15
Phyllantus reticulatus Poir.	Propenh chmool	Euphorbiaceae	Shrub	Phylla
unknown_19 Araliaceae		Araliaceae	Herb	unk_19
unknown_20 Gramineae		Gramineae	Gramminoid	unk_20
unknown_22 Gramineae		Gramineae	Gramminoid	unk_22
unknown_23 Gramineae		Gramineae	Gramminoid	unk_23
unknown_24 Gramineae		Gramineae	Gramminoid	unk_24
unknown_25 Labialeae		Labialeae	Herb	unk_25
unknown_8 Fabaceae-Mimosideae		Fabaceae-Mimosideae	Tree/Shrub	unk_8
unknown_9 Fabaceae-papilionoideae		Fabaceae-papilionoideae	Shrub	unk_9
Vetiveria giganioides (L.) Nash	sbaur rônndahs	Gramineae	Gramminoid	Vetive
Vitex holoadenon D. Dop		Vevenaceae	Shrub	Vitex
Xanthophyllum glaucum wall	Kansaeng	Xanthophylaceae	Tree/Shrub	Xantho

Table B7. Water quality parameters at average depth.

Plot code	Max depth (m)	Specific conduc (µS/cm)	Temp (°C)	DO (%)	DO (mg/L)	pH	TSS (mg/L)	TP (mg/L)	NO_3-N (mg/L)	NH_3-N (mg/L)
KPSEDSAMPLE	8.9	89.8	28.35	75.38	5.84	6.99	2.67	0.6	0.06	0.14
KPT1P1	8.2	91.7	29.53	105.7	8.06	7.49	7	0.55	0	0.06
KPT1P2	7.4	93.2	28.71	77.90	5.92	7.05	5.9	1.12	0.09	0.01
KPT1P3	6.2	93.0	29.12	63.38	4.78	7.04	2.95	0.64	0	0.02
KPT1P4	5.1	89.7	29.55	66.38	4.99	7.02	6.33	0.58	0	0.15
KPT1P5	4.2	86.5	29.18	45.46	3.46	6.65	4	0.69	0	0.09
KPT1P6	3.1	76.0	29.72	64.75	4.91	6.74	9.51	0.66	0	0.11
KPT1P7	1.4	27.0	31.73	78.01	5.82	5.93	9.51	0.77	0	0.12
KPT2P1	8.2	92.5	28.38	54.82	6.24	7.30	9.74	0.72	0.09	0.06
KPT2P10	2.7	23.2	28.66	38.87	2.94	5.89	9.24	0.77	0	0.06
KPT2P2	7.4	92.9	28.47	80.52	6.19	7.21	6.56	0.62	0	0.14
KPT2P3	7.4	94.4	28.55	72.63	5.80	7.12	3	0.99	0	0.04
KPT2P4	6.9	94.9	28.56	39.96	3.03	6.83	2.24	0.54	0	0.36
KPT2P5	5.9	91.8	28.72	17.14	1.30	6.47	4.89	0.74	0	0.14
KPT2P6	5.3	90.9	28.71	21.88	1.68	6.48	4	1.01	0	0.04
KPT2P7	4.8	92.0	28.55	23.49	1.79	6.39	2.86	0.91	0	0.23
KPT2P8	4.2	83.8	28.69	26.30	2.01	6.38	3.49	0.71	0	0.24
KPT2P9	3.4	63.3	28.39	24.91	1.88	6.33	17.7	0.89	0	0.13
KPT3P1	8.5	94.9	28.31	72.55	5.67	6.86	3.61	0.59	1.14	0.04
KPT3P10	4.4	47.9	28.59	43.28	3.30	6.40	11.22	0.87	0	0.05
KPT3P2	7.4	94.0	28.38	52.33	4.01	6.78	4.56	0.56	0.15	0.06
KPT3P3	7.4	98.2	28.52	12.02	0.90	6.42	3.67	0.96	0	0.09
KPT3P4	6.5	85.5	28.55	15.66	1.18	6.26	9.84	0.64	0	0.09
KPT3P5	5.6	56.2	28.26	17.03	1.29	6.23	10.96	0.97	0	0.3
KPT3P6	5.6	44.0	28.19	30.89	2.36	6.48	14.9	0.64	0	0.06
KPT3P7	5.3	36.1	28.11	43.29	3.34	6.42	6.91	0.86	0	0.05
KPT3P8	4.7	35.9	28.33	42.18	3.23	6.32	11.44	0.74	0	0.06
KPT3P9	4.4	40.2	28.36	40.99	3.19	6.26	8.88	0.88	0	0.04
PTT1P1	9	88.8	29.50	74.76	5.70	7.32	15	0.71	0	0.16
PTT1P10	7.8	104.1	29.48	46.14	3.41	7.08	12.87	1.32	0.47	0.09
PTT1P2	8.6	89.1	29.50	77.32	5.89	7.32	13	1.16	0.48	0.08
PTT1P3	7.4	90.8	29.70	87.08	6.63	7.34	22.8	1.13	0.46	0.09
PTT1P4	7.7	91.9	29.71	82.92	6.30	7.45	13.7	1.13	0.5	0.11
PTT1P5	7.7	94.2	29.75	92.52	7.01	7.64	11.6	1.09	0.5	0.12
PTT1P6	7.2	96.3	29.72	97.59	7.38	7.73	11.84	1.18	0.67	0.06
PTT1P7	7.3	98.4	29.74	99.82	7.54	7.85	15.25	1.01	0.67	0.05
PTT1P8	7.4	104.6	29.68	85.08	6.38	7.72	14.43	1.49	0.56	0.1
PTT2P1	8.9	98.8	29.67	45.65	3.32	6.98	9.65	1.23	0.48	0.16
PTT2P10	5	20.3	29.02	71.75	5.41	5.84	20	1.45	0.37	0.18

PTT2P2	8.7	97.4	29.52	51.49	3.88	6.87	12.33	1.02	0.54	0.15
PTT2P3	8.1	84.7	29.22	69.77	5.28	7.04	14.7	0.74	0.5	0.2
PTT2P4	7.4	75.3	29.10	65.43	5.02	6.88	14	0.9	0.45	0.15
PTT2P7	7	57.5	28.76	53.67	4.12	6.57	21.38	1.16	0.51	0.14
PTT2P8	5.9	33.0	28.84	65.79	5.06	5.94	18.24	1.03	0.41	0.11
PTT2P9	5.5	26.9	28.85	67.26	5.18	6.07	15.67	0.9	0.38	0.24
PTWL	9.7	88.8	29.20	84.41	6.46	7.46	10.33	0.92	0.45	0.08
SST1P1	7	86.5	28.81	71.83	5.53	7.19	3.33	0.72	0	0.05
SST1P2	7.3	86.8	28.92	78.48	6.02	7.19	2.3	0.85	0	0.06
SST1P3	6.6	86.8	29.26	82.33	6.26	7.61	0.94	0.76	0	0.05
SST1P4	5.1	76.3	29.56	82.16	6.25	7.55	2.67	0.97	0	0.06
SST1P5	3.3	53.1	29.38	51.68	3.91	6.68	2.32	0.82	0	0.03
SST1P6	3.3	30.8	28.91	48.94	3.74	NA	3.3	0.96	0	0.06
SST1P7	2.1	20.3	29.57	71.76	5.65	6.04	8.14	0.32	0	0.06
SST1P8	1.6	20.2	29.89	76.69	5.81	5.88	11	0.73	0	0.07
SST1P9	1	17.3	31.00	85.40	6.41	5.95	10.16	0.38	0	0.04
SST2P1	8.2	88.6	28.16	57.29	4.43	6.90	15.38	0.39	0.89	0.02
SST2P10	7.8	96.1	28.55	27.33	2.10	6.70	1.67	0.91	0	0.07
SST2P2	7.4	92.2	28.41	37.11	2.89	6.76	2.56	0.34	0.15	0.06
SST2P3	7.4	95.4	28.38	13.86	1.08	6.68	2.96	0.8	0	0.09
SST2P4	8	94.9	28.38	11.32	1.30	6.66	1.98	0.83	0	0.09
SST2P5	6.6	94.2	28.68	37.31	2.85	6.94	1.32	0.8	0	0.07
SST2P6	6.2	95.0	28.38	23.47	1.83	6.90	4.56	1.1	0	0.1
SST2P7	6.5	95.4	28.46	22.94	1.76	6.69	1.98	0.9	0	0.12
SST2P8	8.1	97.4	28.34	11.34	0.87	6.66	4.61	0.95	0	0.06
SST2P9	8.1	96.1	28.42	18.24	1.42	6.64	4.71	0.88	0	0.13
SST3P1	9	89.2	28.34	74.09	5.78	7.24	7.62	1.13	0	0.08
SST3P2	8.4	89.8	28.48	36.70	2.80	6.98	5.65	1.02	0	0.02
SST3P3	7.6	89.6	28.49	38.15	2.92	6.87	4.61	1.04	0	0.07
SST3P4	7.9	92.0	28.47	25.30	1.96	6.78	3.47	0.87	0	0.08
SST3P5	8.4	93.7	28.49	23.21	1.80	6.75	3	0.77	0	0.04
SST3P6	8.6	92.2	28.47	25.14	1.94	6.74	2.67	1.21	0	0.08
SST3P7	7.9	91.6	28.46	24.90	1.92	6.76	2	0.77	0	0.03
SST3P8	8.3	93.5	28.55	20.03	1.54	6.68	4	0.96	0	0.01
SST3P9	7.3	93.2	28.65	23.30	1.78	6.69	2.33	0.92	0	0.04
SSWQT1-2 (N12.51847 E104.4840)	12.1	88.0	28.25	62.84	4.88	6.98	5.57	0.89	0.81	0.03
CIHOUSE DRY (N12.64483 E104.18473)	9.7	91.0	28.39	81.70	6.36	7.52	5.44	0.81	0.04	0.07

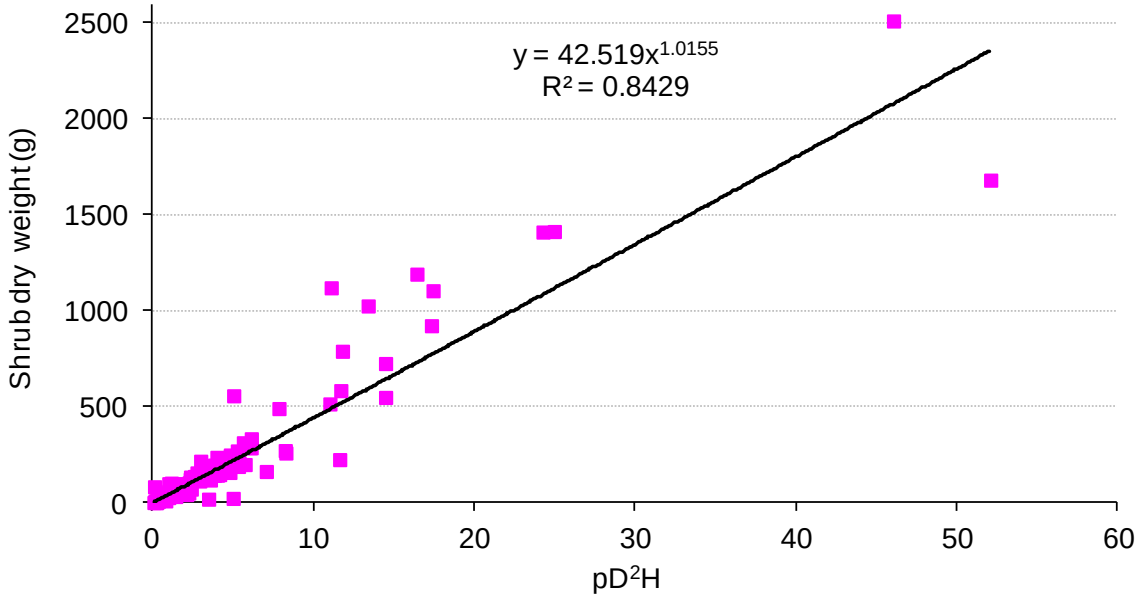

Figure B8. Allometric relationship between shrub dry weight and the product of wood density (p), the square of stem diameter (D^2), and stem height (H).

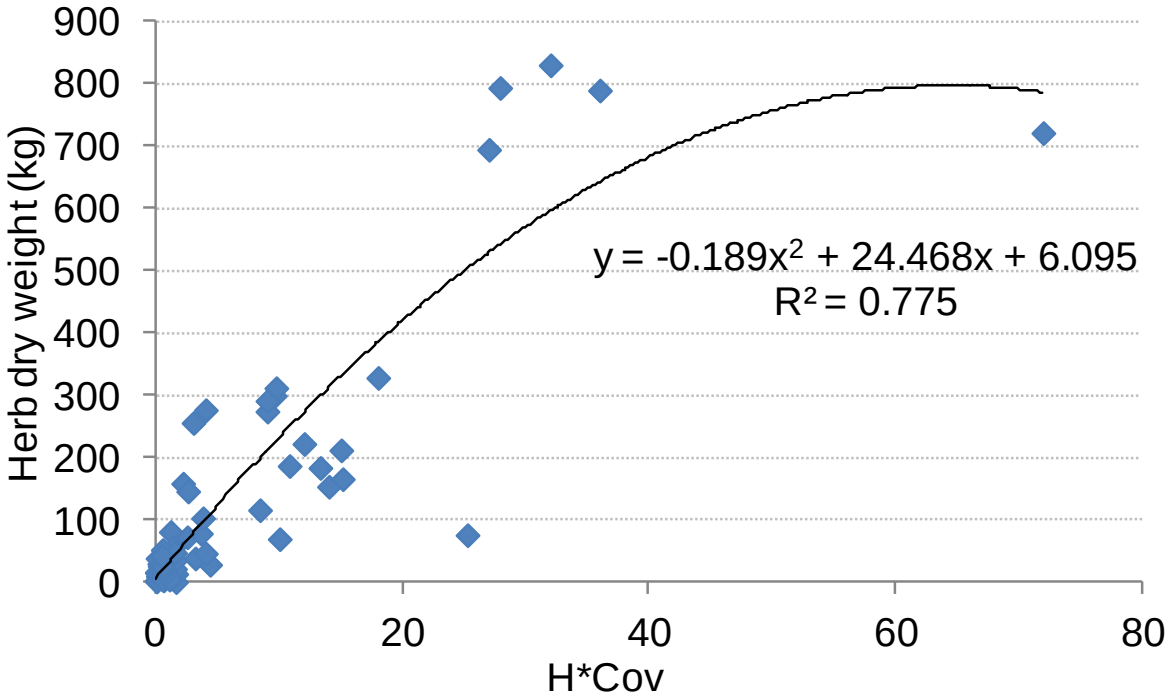

Figure B9. Allometric relationship between herbaceous vegetation dry weight and the product of stem height (H) and vegetation coverage (Cov).

Appendix C. Chapter 6

Table C1. Tonle sap fauna and habitat seasonal associations. OW = open water, GF = gallery forest, FG = seasonally flooded grasslands, FS = seasonally flooded shrublands, LG = lowland grasslands, AF = abandoned fields, TR = transitional zone rice (floating and recession rice), VC = village crops, LS = lowland shrublands, and R = rainfed/irrigated rice.

Common name	Species	Diet	Breeding time	Breeding location	Rising season (Jun-Aug)	Wet season (Sept-Nov)	Receding season (Nov-Feb)	Dry season (Mar-May)	Nutri-tional value	Conser-vation value	Ecolo-gical value	Source
Cyprinid	*Cirrhinus microlepis*	Plankton, plants, insects	May-June	Mekong	OW, GF, FG, FS	OW, GF, FG, FS, TR, AF	OW, GF, FG, FS,	OW	1	0	0	Lim et al. (1999); Lamberts (2001)
Cyprinid	*Cyclocheilichthys apogon*	plankton, zoobenthos, crustaceans	Sept-Oct	floodplain	OW, GF, FG, FS	GF, FS, FG, TR, AF	OW, GF,	OW	1	0	0	Lamberts (2001)
Cyprinid	*Cyclocheilichthys enoplos*	zooplankton, insects, fish, benthic community	Jun	inundated land	OW, GF, FS, FG	OW, GF, FS, FG, LG, AF, TR	OW, GF	OW	1	0	0	Lim et al. (1999); Lamberts (2001)
Cyprinid	*Henicorhynchus siamensis*	Plankton, plants	May-June	river-floodplain	OW, GF, FG, FS	OW, GF, FG, FS, T	OW, GF, FG, FS	OW	1	0	0	Lim et al. (1999); Lamberts (2001)
Cyprinid	*Osteochilus melanopleurus*	plankton, plants, detritus	May-June	Floodplain	OW, GF, FG, FS	OW, GF, FG, FS, T	OW	OW	1	0	0	Lim et al. (1999); Lamberts (2001)
Cyprinid	*Dangila spp.*	phytoplankton, zooplankton	May-June	Floodplain	OW, GF, FG, FS	OW, GF, FG, FS, T	OW, GF, FG, FS	OW	1	0	0	Lim et al. (1999); Lamberts (2001)
Snakehead	*Channa striata*	fish	Jun-Jul	Floodplain	OW, GF, FG, FS	OW, GF, FG, FS, T	OW, GF, FG, FS	OW, GF, FG, FS	1	0	0	Lim et al. (1999)

Giant Snakehead	*Channa micropeltes*	fish, crustaceans	Jun-Jul	Floodplain	OW, GF, FG, FS	OW, GF, FG, FS, T	OW, GF, FG, FS	OW, GF, FG, FS	1	0	0	Lim et al. (1999)
Snakehead	*Channa lucius*	fish, prawns, crabs	Jun-Jul	Floodplain	OW, GF, FG, FS	OW, GF, FG, FS, T	OW, GF, FG, FS	OW, GF, FG, FS	1	0	0	Lim et al. (1999)
Walking Catfish	*Clarias batrachus*	fish-molluscs	Jun-Jul	Floodplain	OW, GF, FG, FS	OW, GF, FG, FS, TR, AF, LG	OW, GF, FG, FS	OW, GF, FG, FS	1	0	0	Lim et al. (1999) ; Campbell et al. (2006)
Climbling perch	*Anabas testudineus*	fish	Wet season	Floodplain	OW, GF, FG, FS	OW, GF, FG, FS, TR, AF, LG	OW, GF, FG, FS	OW, GF, FG, FS	1	0	0	Lim et al. (1999); Campbell et al. (2006); Valbo-Jørgensen et al. (2009)
Pangasius	*Pangasius larnaudieri*	fish, crustaceans, plant matter	May-Jun	Floodplain /Mekong	OW, GF, FG, FS	OW, GF, FG, FS, TR, AF, LG	Mekong	Mekong	1	1	0	Lim et al. (1999) ; Campbell et al. (2006)
Pangasius	*Pangasius siamensis*	insects	May-Jun	Floodplain /Mekong	OW, GF, FG, FS	OW, GF, FG, FS, TR, AF, LG	Mekong	Mekong	1	1	0	Lim et al. (1999)
Homalopsidae water snake	*Enhyndris Enhydris*	Fish	Apr-Jun	GF, FG, FS	GF, FG, FS	GF, FG, FS	GF, FG, FS	GF, FG, FS	1	1	0	Brooks et al. (2009)
Homalopsidae water snake	*Enhyndris longicaude*	Fish	Apr-Jun	GF, FG, FS	GF, FG, FS	GF, FG, FS	GF, FG, FS	GF, FG, FS	1	1	0	Brooks et al. (2009)
Homalopsidae water snake	*Homalopsis buccata*	Fish	Apr-Jun	GF, FG, FS	GF, FG, FS	GF, FG, FS	GF, FG, FS	GF, FG, FS	1	1	0	Brooks et al. (2009)
Homalopsidae water snake	*Enhyndris bocourti*	Fish	Apr-Jun	GF, FG, FS	GF, FG, FS	GF, FG, FS	GF, FG, FS	GF, FG, FS	1	1	0	Brooks et al. (2009)

Homalopsidae water snake	*Enhyndris tentaculatus*	Fish	Apr-Jun	GF, FG, FS	GF, FG, FS	GF, FG, FS	GF, FG, FS	GF, FG, FS	1	1	0	Brooks et al. (2009)
Checkered keelback Water Snake	*Xenochrophis piscator*	Fish and frogs	Apr-Jun	GF, FG, FS	GF, FG, FS	GF, FG, FS	GF, FG, FS	GF, FG, FS	1	1	0	Brooks et al. (2009)
Red-tailed Pipe Water Snake	*Cylindrophis ruffus*	eels , other snakes	Aug-Oct	GF, FG, FS	GF, FG, FS	GF, FG, FS	GF, FG, FS	GF, FG, FS	1	1	1	Brooks et al. (2009)
Malayan Snail-eating Turtle	*Malayemys subtrijuga*	Snails, benthis onvertebrates	dry season	FS	GF, FS	FR	FR	GF, FS	1	1	0	Davidson (2006)
Burmese Python	*Python molurus*	small mammals, amphibians, invertebrates	dry season	FS	-	-	-	FS	0	0	1	Davidson (2006)
Grey-headed fish-eagle	*Ichthyophaga ichthyaetus*	Water snakes, fish	Oct-Dec	GF, FG, FS	GF, FG, FS	GF, FG, FS	GF, FG, FS	GF, FG, FS	0	1	1	Tingay et al. (2010)
Spot-billed Pelican	*Pelecanus philippensis*	Fish	Jan-May	GF, FS	GF, FS, FG	GF, FS, FG	GF, FS, FG	GF, FS, FG	0	1	0	Campbell et al. (2006) after Seng et al. (2002)
Greater Adjutant	*Leptoptilos dubius*	Omnivore, scavenger	Dec-May	GF, FS	GF, FS, FG	GF, FS, FG	GF, FS, FG	GF, FS, FG	0	1	0	Campbell et al. (2006) after Seng et al. (2002)
Darter	*Anhinga melanogaster*	Fish	Sept-Nov	GF, FS	GF, FS	GF, FS	GF, FS	GF, FS	0	1	0	Campbell et al. (2006) after (Seng et al. 2002)

Masked Finfoot	*Heliopais personata*	Insects, amphibians, benthic invertebrates, fish	Nov - Jan	GF, FS	GF, FS	GF, FS	GF, FS	GF, FS	0	1	0	Campbell et al. (2006) after Seng et al. (2002)
Black-headed Ibis	*Threskiornis melanocephalus*	Fish, frogs	Oct-Jan	GF, FS	GF, FS, FG	GF, FS, FG	GF, FS, FG	GF, FS, FG	0	1	0	Campbell et al. (2006) after Seng et al. (2002)
Milky Stork	*Mycteria cineria*	Fish, amphibians, insects	Oct-Dec	GF, FS	GF, FS, FG	GF, FS, FG	GF, FS, FG	GF, FS, FG	0	1	0	Campbell et al. (2006) after Seng et al. (2002)
Painted Stork	*Mycteria leucocephala*	Fish, benthic invertebrates	Sept-Nov	GF, FS	GF, FS, FG	GF, FS, FG	GF, FS, FG	GF, FS, FG	0	1	0	Campbell et al. (2006) after Seng et al. (2002)
Lesser Adjutant	*Leptoptilos javanicus*	omnivorous: fish, mammals, herpetofauna	Nov-Jan	GF, FS	GF, FS, FG	GF, FS, FG	GF, FS, FG	GF, FS, FG	0	1	0	Campbell et al. (2006) after Seng et al. (2002)
Bengal Florican	*Houbaropsis bengalensis*	Invertebrates,	Jan-May	FG, LG	FG, LG	FG, LG	FG, LG	FG, LG	0	1	0	Gray et al. (2009); Davidson (2006)
Manchurian Reed Warbler	*Acrocephalus tangorum*	Seeds and nuts		FS, FG		migrating	migrating	FG, LG, AF, TR	0	1	1	Davidson (2006)
Greater Spotted Eagle	*Aquila clanga*	Carnivorous:herpetofanua, small mammals		GF	migrating	migrating	FG	migrating	0	1	1	Campbell et al. (2006) after Seng et al. (2002)
Sarus Crane	*Grus antigone*	invertebrates, eggs	Jul-Oct	GF	migrating	migrating	FG	migrating	0	1	1	Campbell et al. (2006) after Seng et al. (2002)

White-shouldered Ibis	*Pseidibis davisoni*	grains, invertebrates	Feb-Jul	FG, LG	FG, LG	FG, LG	FG, LG	FG, LG	0	1	0	Campbell et al. (2006) after Seng et al. (2002) ; Davidson et al (2006)
Black-necked Stork	*Ephippiorhynchus asiaticus*	Carnivorous: small birds, fish	Oct-Jan	GF	migrating	migrating	FG	migrating	0	1	0	Campbell et al. (2006) after Seng et al. (2002)
Asian Golden Weaver	*Ploceus hypoxanthus*	Seeds and nuts		FG, LG	FG, LG	FG, LG	FG, LG	FG, LG	0	1	0	Campbell et al. (2006) after Seng et al. (2002) ; Davidson et al (2006)
Hairy-nosed Otter	*Lutra sumatrana*	Fish, water snakes	Nov-Feb	GF, FS	GF	GF	GF	FG, FS	0	1	1	Davidson (2006): Campbell et al (2006)
Smooth Otter	*Lutrogale perspicillata*	Fish, water snakes		GF, FS	GF	GF	GF	FG, FS	0	1	1	Davidson (2006)
Loris sp.	*Nycticebus coucang*	omnivorous: small mammals, leaves, fruit	?	GF	?	?	?	?	0	1	0	Campbell et al. (2006) after Seng et al. (2002)
Loris sp.	*Nycticebus bengalensis*	omnivorous: small mammals, leaves, fruit	?	GF	?	?	?	?	0	1	0	Campbell et al. (2006) after (Goes and Hong, 2002); Davidson (2006)

Long-tailed Macaque	*Macaca fascicularis*	Frigivorous: fruit, leaves	Jun-Sept	GF	GF	GF	GF	GF	0	1	0	Campbell et al. (2006) and Davidson (2006) after Goes and Hong (2002)
Silvered Langus	*Semnopithicus cristatus*	herbivore: leaves, fruit	None	GF	GF	GF	GF	GF	0	1	0	Campbell et al (2006) and Davidson (2006) after Goes and Hong (2002)
Flying Foxes	*Pteropus sp.*	Fruit, seeds, blossoms	Feb-Apr	GF		GF, FS			0	1	0	Campbell et al. (2009) after Goes and Hong (2002)
Small Asia Mongoose	*Herpetes javanicus*	small mammals, amphibians	?	?	GF, FS, FG, LG, AF, TR	GF, FS, FG, LG, AF, TR	GF, FS, FG, LG, AF, TR	GF, FS, FG, LG, AF, TR	0	0	1	Campbell et al. (2006) and Davidson (2006) after Goes and Hong (2002)
Asiatic Jackal	*Canis aureus*	Small mammals, amphibians, fish	None	FG, FS, AF	GF, FS, FG	GF, FS, FG	GF, FS, FG	GF, FS, FG	1	1	1	Campbell et al. (2006) and Davidson (2006)
Zooplankton	Protozoans and rotifers	?	?	?	?	OW, GF, FG, FS		OW	0	0	1	Ohtaka et al. (2010)
Zoobenthos	Macrozoobenthos, mollusks, oligochaetes, chironomids	?	?	?	?	OW, FG, FS	OW, FG, FS	OW	0	0	1	(Ohtaka et al., 2010)
Freshwater Cladocera	*Crustacea* (21 species)	?	?	?	FG, FS	FG, FS	FG, FS	-	0	0	1	Tanaka and Ohtaka (2009)

Freshwater Cladocera	*Pseudosida bidentata*	?	?	?	OW, FG, FS	OW, FG, FS	OW, FG, FS	-	0	0	1	Tanaka and Ohtaka (2009)
Freshwater Cladocera	*Diaphanosoma excisum*	?	?	?	-	OW, GF	OW	FG, FS (ponds)	0	0	1	Tanaka and Ohtaka (2009)
Freshwater Cladocera	*Ceriodaphnia laticaudata, Bosmina meridionalis, Bosminopsis deitersi*	?	?	?	OW, FG, FS	GF, OW, FG, FS	OW, FG, FS	-	0	0	1	Tanaka and Ohtaka (2009)
Freshwater Cladocera	*Moina micrura*	?	?	?	-	OW, GF	OW	OW, FG, FS (ponds)	0	0	1	Tanaka and Ohtaka (2009)
Freshwater Cladocera	*Ilyocryptus spinifer, Macrothrix flabelligera, Macrothrix spinosa, Karualona karua*	?	?	?	FG, FS	FG, FS	FG, FS	FG, FS (ponds)	0	0	1	Tanaka and Ohtaka (2009)
Freshwater Cladocera	*Camptocercus rectirostris, Oxyurella singalensis*	?	?	?	FG, FS	GF, FG, FS	FG, FS	-	0	0	1	Tanaka and Ohtaka (2009)
Freshwater Cladocera	*Diaphanosoma sp., Bosmina fatalis, Alona costata, Nicsminovius eximius*	?	?	?	-	OW	OW	-	0	0	1	Tanaka and Ohtaka (2009)
Freshwater Cladocera	*Euryalona orientalis, Chydorus eurynotus*	?	?	?	FG, FS	GF, FG, FS	FG, FS	FG, FS (ponds)	0	0	1	Tanaka and Ohtaka (2009)

Freshwater Cladocera	*Disparalona caudata*, *Pseudochydorus globosus*	?	?	?	-	GF	-	-				Tanaka and Ohtaka (2009)